STUDIES ON THE MOLECULAR REGULATION OF EPICARDIAL CELL MOVEMENT

By

Emily Elizabeth Cross

Dissertation

Submitted to the Faculty of the

Graduate School of Vanderbilt University

in partial fulfillment of the requirements

for the degree of

DOCTOR OF PHILOSOPHY

in

Cell and Developmental Biology

May, 2012

Nashville, Tennessee

Approved:

Professor David M. Bader

Professor H. Scott Baldwin

Associate Professor Alissa M. Weaver

Associate Professor Matthew J. Tyska

Assistant Professor Sandra S. Zinkel

I dedicate this to my family.

It all started with "Skunks".

ACKNOWLEDGEMENTS

This work was made possible by the financial support of the Vanderbilt University Cancer Biology and Cardiovascular Mechanisms Training Grants. I am additionally grateful for the Cell and Developmental Biology Department and Program in Developmental Biology leadership and support staff. These standout programs have developed hugely successful mechanisms to groom and grow students into scientists, and I am appreciative of my training.

The scientific goals that I have reached are due to the untiring efforts of two individuals. Dr. Robert Rawding at Gannon University was my scientific inspiration. Before I met Dr. R, I was an aimless undergraduate "pre-med" major. He recognized in me an innate curiosity for questions beyond the facts listed in the textbooks, and he was an endlessly patient teacher. His mentorship helped me to realize that I was searching for this career.

The second important individual to whom I will be ever grateful is my graduate mentor Dr. David Bader. The lessons I have learned from the environment David fosters in the Bader lab, and from David himself, will serve me for the rest of my life. Because of David's influence I have become: widely inquisitive but experimentally focused, a good listener but unafraid to contribute, a devoted and efficient worker that knows the benefit of an afternoon away. David taught me how to think carefully and logically, how to write with both clarity and a compelling turn of phrase, and how to engage a diverse audience in

settings ranging from formal lectures to relaxed conversations over drinks. David, I have appreciated your patience as I learned and grew.

I thank my committee. Each of my committee members has gone beyond the expectations to suggest and teach me methodologies, to help broaden my evaluation of results and outcomes, and to support me as I move forward to a post doctoral position. I was very fortunate to collaborate with two of my committee members, Drs. Alissa Weaver and Scott Baldwin. I am so excited about the work that we have done together!

Likewise, I would like to thank Dr. Charles Hong for his assistance as a collaborator. Thank you too, Bong Hwan Sung, Xianghu Qu, Joe Roland, Bob Matthews, and Carol Ann Bonner for collaborating, sharing and teaching.

To the Bader Lab: I couldn't have done this without you! I can't imagine a better environment than ours. Thank you Becca Thomason, Niki Winters, Hillary Hager, Kt Moynihan, Paul Miller, Sam Reddy, Elaine Shelton, Tong Wang, Pierre Hunt and Ryan Roberts. You were endlessly supportive as I went through the growing pains of this experience. A special thank you to Paul Miller for teaching me how to analyze data and for letting me run to him in an experimental panic. Thank you to all my graduate school friends, and especially to the Bader Babes, Jess Mazerik and Billy Carver. Bec, Nik, Kt and Hill: I will really miss the 4PM funny video breaks, the basketball games, and going to Sportsmans. I can't wait for Sunrise Village.

Thank you to my families old and new. Mom and dad, I love you! You have the highest expectations for all of us and your example taught me how to be

a success and a good person. You made this experience so much easier for me and for that I will always be grateful. To my sister, her family and my brother: I couldn't have done this without your humor and listening ears. To Grandpa Knapp: thank you for all of your support, and for Italy! You took care of me when I needed it most. Thank you also Aunt Roberta, Uncle Buck, Aunt Judy and Blim. I have appreciated your interest in my journey. Thank you Benesh family for opening your arms so widely to me.

Finally, thank you Andy (and Sweetie, too, of course!). You have been endlessly supportive and patient through all of this, even when I was (frequently) extra difficult. Andy, I really admire you scientifically. You are an inspiration. I love you and I'm so excited about our future.

TABLE OF CONTENTS

LIST OF TABLES

LIST OF FIGURES

CHAPTER I

INTRODUCTION

Epicardial mesothelium (epicardium) is a progenitor tissue critical for coronary vessel development. Epicardial researchers aim to understand the signaling cascade regulation of epicardial development with the goal of reawakening this progenitor function in human adults after myocardial infarction (MI). Still, the cooperative signaling relationships and cellular mechanisms facilitating this program are largely undefined. This dissertation seeks to identify cooperative signaling cascade relationships regulating epicardial behaviors, cellular mechanisms imparting epicardial behaviors and regulators of these mechanisms.

This chapter will first introduce epicardium, the principle tissue utilized in these studies. Epicardial *ex vivo* and cell line models were studied here because the tissue participates in a myriad of cellular behaviors that occur concurrently. Studying epicardial cells afforded the opportunity to develop a novel Small Organic Molecule (SOM) screening methodology to identify regulators of epicardial behaviors and describe their coordination. Additionally, epicardial cells are highly migratory during development and injury repair (Mikawa and Gourdie 1996; Lepilina et al, 2006), and epicardial cell lines can recapitulate migratory behaviors in culture (Wada et al, 2003; Pae et al, 2008). Using these assays elucidated an interaction between Blood vessel epicardial substance (Bves) and

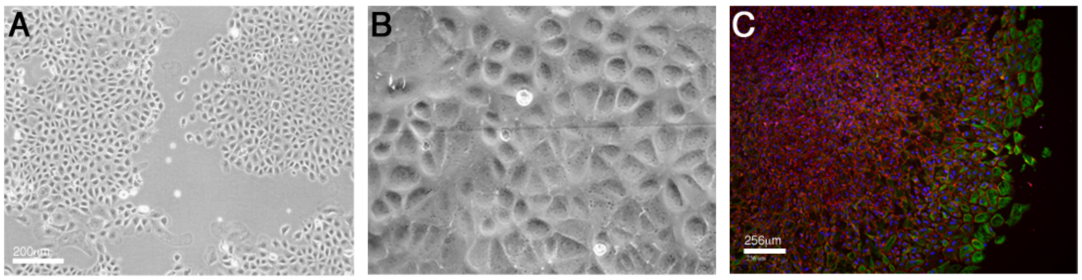

Figure 1.1 Epicardial cells form simple squamous sheets. (A-B) Rat epicardial cell lines grown in culture form islands of cells that grow together with cobblestone morphology. (C) Epicardial cell sheets isolate from developing chick hearts also form simple squamous sheets in which zona occludens-1 (ZO-1; red) marks the intercellular junctions and a-Smooth Muscle Actin (SMA; green) marks the differentiating peripheral edge.

N-myc Downstream Regulatory Gene 4 (NDRG4) in epicardial movement. Bves/NDRG4 interaction regulates migration through trafficking of fibronectin in the newly identified autocrine ECM production mechanism. Additionally, data presented here demonstrate that Bves interacts with VAMP3 to regulate cell adhesion through recycling endosome trafficking of the transmembrane adhesion molecule, β1-integrin. Taken together, these studies elucidate regulation of epicardial cell behaviors, reveal a novel epicardial behavior, and suggest a global mechanism for Bves diverse effects on cell-cell adhesion and cellular movement.

Epicardial Mesothelium Development

A mesothelium is a specialized epithelial layer derived from the embryonic mesoderm (Mutsaers and Wilkosz 2007). Morphologically, a mesothelium is a cobblestone-shaped simple squamous layer of cells (Figure 1.1) that lines the pericardial, pleural and peritoneal body cavities and covers the internal organs. Juxtaposed mesothelia are protective structures for the body cavities, which elaborate fluids to facilitate the movement of organs against compartment walls

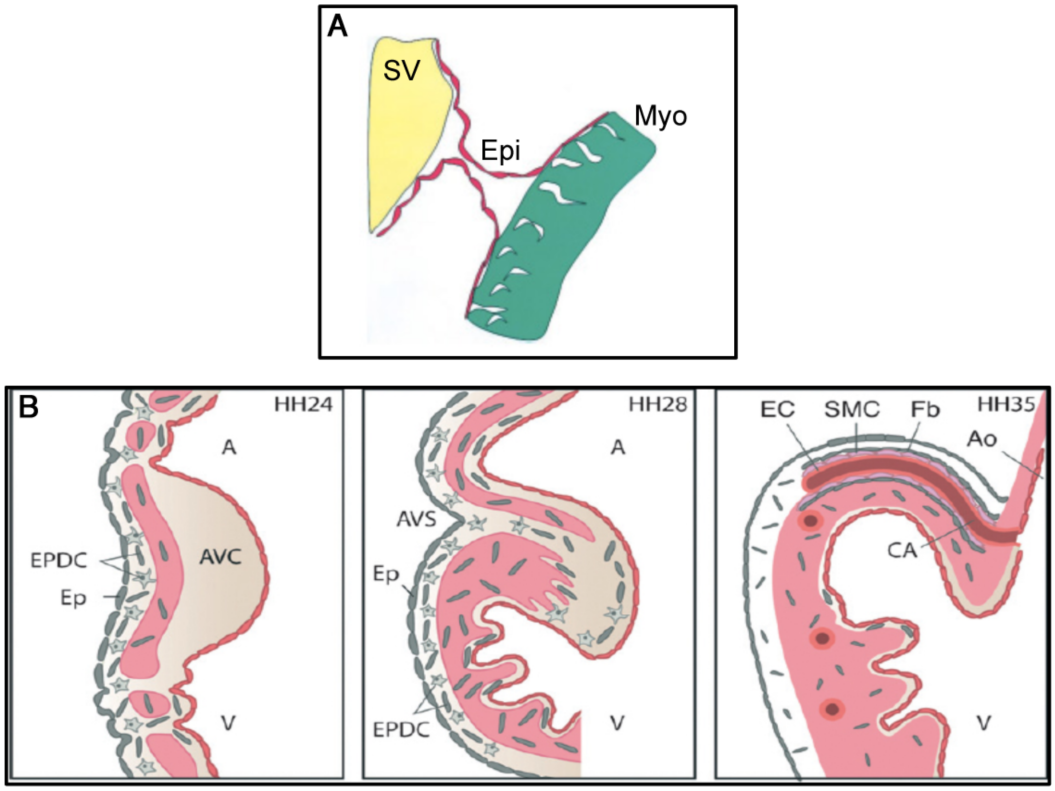

Figure 1.2 Epicardial cell development supports coronary vasculature formation. (A) Proepicardial cells protrude from the sinus venosus and migrate as an epithelial sheet to and over the apical surface of the myocardium; adapted from Wada et al. 2003. (B) While covering the myocardium, some epicardial cells delaminate, undergo epithelial to mesenchymal transition and invasively move into and throughout the myocardium. Epicadial derived cells then differentiate into multiple cell types and are essential for coronary vessel formation; adapted from Ratajska et al. 2008.

and neighboring organs (Koss and Melamed 2006; Mutsaers and Wilkosz 2007).

The epicardial mesothelium covering the heart is also a progenitor population that contributes cells to the underlying myocardium in a variety of developmental model systems (Manasek 1969; Mikawa and Fischman 1992; Muñoz-Chápuli et al, 1994; Mikawa and Gourdie 1996; Männer et al, 2001; Poss et al, 2002; Winter and Gittenberger-de Groot 2007; Duan et al, 2011; Riley and Smart 2011).

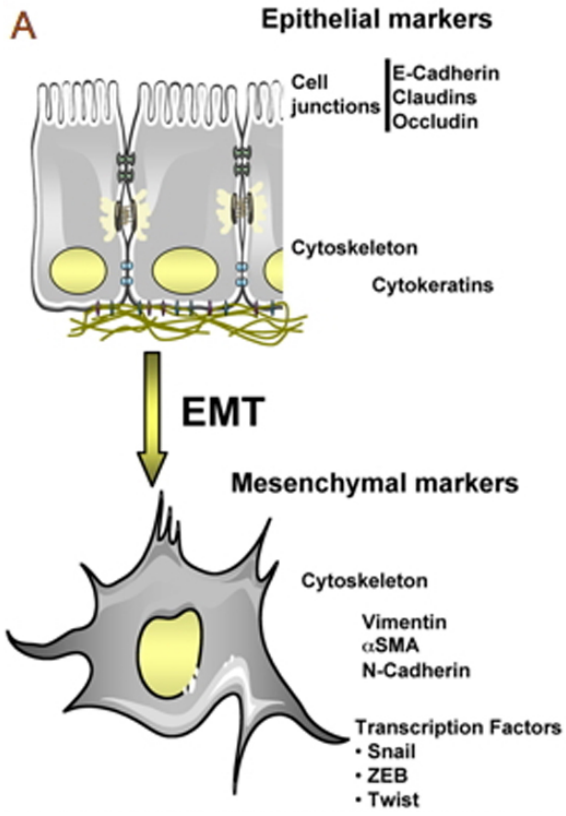

Figure 1.3 Epithelial to mesenchymal transition (EMT) drastically shifts epithelial cell character. Epithelial cells that undergo EMT, such as the epicardium, alter many characteristics including: apicobasal polarity, cytoskeletal organization, gene expression patterning, and cellular behaviors (e.g. proliferation or migration); image adapted from Deshire et al. 2011.

This development program is driven by two forms of migration: lateral movement as an epithelial sheet from the embryonic proepicardium (PE) to and over the heart, and, after epithelial-to-mesenchymal transition, single cell invasive migration from the epicardial sheet into/throughout the underlying myocardium for subsequent differentiation (Reese et al, 2002).

At murine embryonic day 8.5 (E8.5) or Hamburger and Hamilton stage 14 (HH14) in the chick, the PE arises from the region of the sinus venosus (Ho and Shimada 1978; Virágh and Challice 1981). From murine E9-12.5 and HH16-27

(E3-5) in the chick, the epicardium migrates from the sinus venosus to the dorsal surface of the heart where it covers the apical myocardium for the life of the organism [Figure 1.2A; (Komiyama et al, 1987; Männer 1992; Winter and Gittenberger-de Groot 2007)]. In the chick, PE villus protrusions migrating over an extracellular matrix bridge to the developing heart (Männer 1992; Männer 1993; Kramer et al, 1999; Nahirney et al, 2003) while in mammalian and fish embryos epicardial cell clusters detach from the sinus venosus, float to the myocardium, and fuse to form an epicardial sheet (Virágh and Challice 1981; Komiyama et al, 1987; Muñoz-Chápuli et al, 1994). In all known animal models of PE development, cells travel to the heart and laterally spread across it as an epithelial sheet with apicobasal polarity and intercellular junctions (Ho and Shimada 1978; Komiyama et al, 1987; Männer 1992; Vrancken Peeters et al, 1995; Nahirney et al, 2003; Lie-Venema et al, 2005).

After lateral migration commences some epicardial cells undergo epithelial-to-mesenchymal transition (EMT) and delaminate into the subepicardial space [Figure 1.2B; (Mikawa and Gourdie 1996; Dettman et al, 1998)]. These cells, termed Epicardial-derived cells (EPDCs), individually spread throughout the heart and are found in the compact and trabecular myocardium, the endocardial cushions, and abundantly surrounding the coronary arteries [Figure 1.2B; (Mikawa and Gourdie 1996; Dettman et al, 1998; Gittenberger-de Groot et al, 1998; Lie-Venema et al, 2005)]. EMT and delamination is a dramatic shift in epicardial cell morphology characterized by: asymmetric proliferation into the underlying myocardium, enriched EMT/EPDC gene expression, loss of

apicobasal polarity and intercellular junctions, with actin/intermediate filament reorganization to facilitate cell mobility [Figure 1.3; (Vrancken Peeters et al, 1995; Morabito et al, 2001; Winter and Gittenberger-de Groot 2007; Wu et al, 2010; Smith et al, 2011). After EMT, EPDCs have the capacity to differentiate into the smooth muscle, cardiac fibroblasts and endocardial cells of the coronary vasculature, as well as a small population of cardiomyocytes (Vrancken Peeters et al, 1995; Mikawa and Gourdie 1996; Dettman et al, 1998; Pérez-Pomares et al, 1998; Männer 1999; Cai et al, 2008; Zhou et al, 2008; Smith et al, 2011). While the developmental programs and cell fates of PE and EPDCs are largely resolved, the signaling paradigms that facilitate this developmental program require further study.

General Signaling During Epicardial Development

Specification of the proepicardium is a complex process that relies on coordinated activity of multiple transcription and growth factors (Svensson 2009). Progenitor cells arise from the lateral plate mesoderm and express Islet-1 and Nkx2.5 transcription factors, but a detailed description of PE formation requires further study (Zhou et al, 2008). Common markers of PE cells include: T-box factor-18 (Tbx-18), Wilms Tumor-1 (WT1) and Transcription factor-21 [Tcf21; (Svensson 2009)]. The effect of hormone signaling on PE specification and differentiation may be time/spatially dependent. Bone Morphogenetic Protein (BMP)-stimulated hormone signaling is required for initial PE marker expression in chick and zebrafish model systems (Schlueter et al, 2006; Liu and Stainier

2010), yet lineage specification of PE tissue into epicardial and myocardial tissue depends on BMP-stimulates myocardial differentiation which is inhibited by Fibroblast Growth Factor (FGF) signaling (van Wijk et al, 2009). Thus, PE specification and early lineage differentiation entails complex crosstalk, overlapping uses for growth factors, and is still unresolved.

Adherence of epicardium to myocardium requires focal adhesions and extracellular matrix (ECM) substrates for proper binding (Kwee et al, 1995; Yang et al, 1995; Sengbusch et al, 2002; Pae et al, 2008). In murine models, knockout of the cell surface focal adhesion component α4-integrin and its matrix substrate VCAM-1 causes detached epicardium, failure to produce subepicardial mesenchymal and coronary plexus, and embryonic lethality (Kwee et al, 1995; Yang et al, 1995; Sengbusch et al, 2002). It is important to emphasize that many integrin subtypes are expressed in the PE, and integrin adherence to substrates on the heart is a driving force behind epicardial development (Pae et al, 2008). Additionally, global or epicardial-specific knockout mice for erythropoietin receptor (EpoR), Transforming Growth Factor β Receptor III (TGFβR3), Activin-Like Kinase receptor 5 (ALK-5) and Retinoid X Receptor α (RXRα) exhibit partial loss of epicardial adherence with developmental consequences (Compton et al, 2005; Merki et al, 2005; Sridurongrit et al, 2008; Olivey and Svensson 2010). Furthermore, WT1 knockout epicardia fail to adhere and downregulate α4-integrin expression, suggesting that integrin adhesion is the molecular framework through where WT1 transcription exerts its effects (Kirschner et al, 2006). While

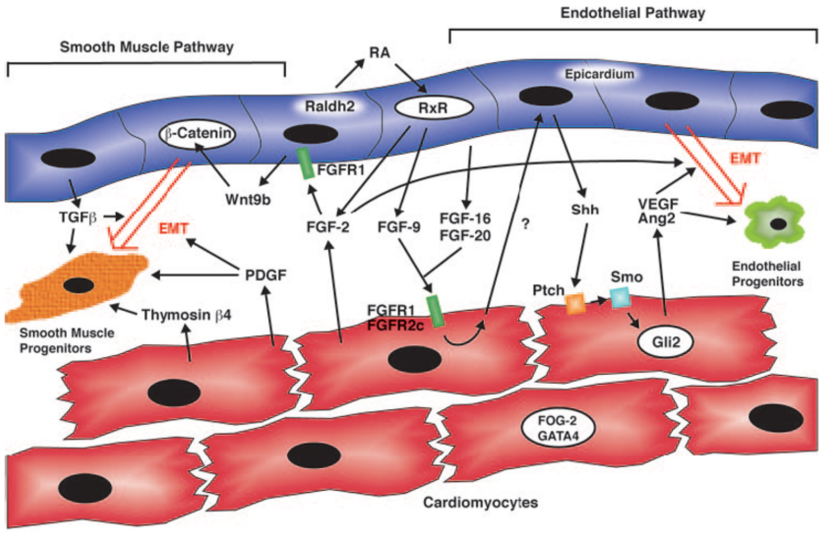

Figure 1.4 Epicardial EMT involves complex signaling events. Many hormones have been identified that originate from epicardial and myocardial cells to stimulate EMT. Some signals have paracrine effects on the adjacent tissue while others have autocrine effects on the secretory tissue, or both. Furthermore, single signals ilicit widely varied responses from the two tissues. How signaling cascades coordinate their effects to collectively stimulate a particular behavior requires further elucidation; adapted from Olivey and Svensson 2010.

many signaling cascades have been identified to regulate epicardial adherence, subcellular mechanisms conferring and maintaining adherence are unresolved.

Extrinsic growth factors that initiate and regulate epicardial EMT and coronary vascular development include: TGF$\beta_{1\text{-}3}$, FGF1,2 and 7, Vascular Endothelial Growth Factor (VEGF), Platelet Derived Growth Factor (PDGF), Wnt/β-Catenin and Sonic Hedgehog [Shh; (Morabito et al, 2001; Molin et al, 2003; Compton et al, 2005; Merki et al, 2005; Tomanek 2005; Lavine et al, 2006; Zamora et al, 2007; Mellgren et al, 2008; Pennisi and Mikawa 2009)]. The mechanisms through which these signals cooperatively regulate EMT are complicated by extensive crosstalk that occurs between the epicardium

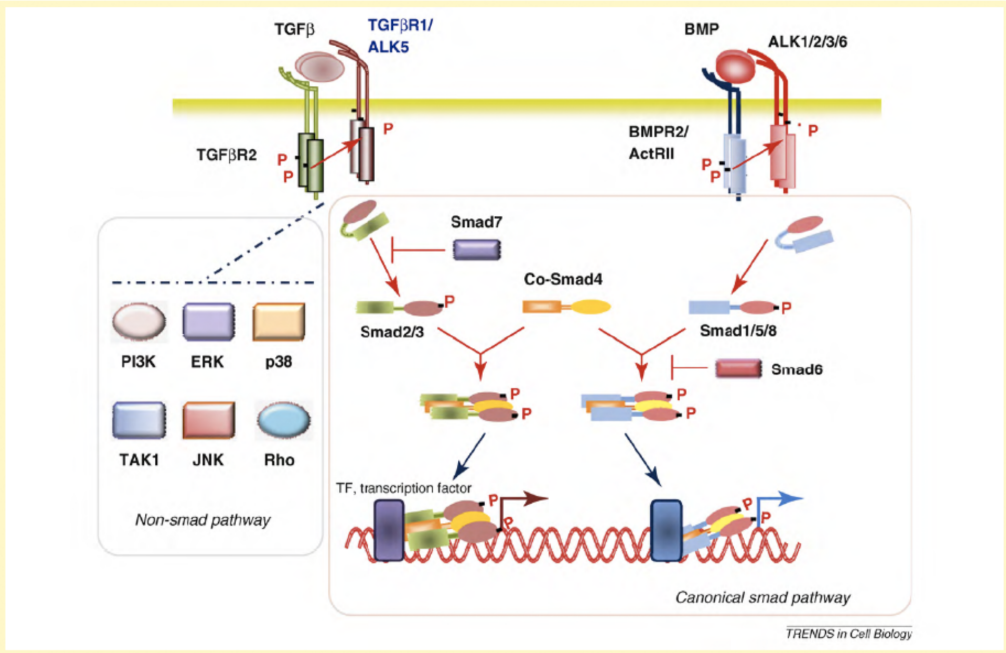

Figure 1.5 TGFβ superfamily signaling occurs through a common mechanism with unique players. Both TGFβ and BMP peptide hormones signal by binding to specific heterotetrameric complexes of Type-I and Type-II receptors (R-II/R-I). Once activated by ligand binding, these receptors phosphorylate pathway specific cytoplamic transduction proteins, Smads. After binding with a common mediator Smad protein, the cytoplasmic complexes translocate to the nucleus and stimulate expression of hormone-specific target genes; adapted from Pardali et al. 2010.

(influencing myocardial growth) and the myocardium (stimulating epicardial EMT) as well as autocrine activation [Figure 1.4; (Olivey and Svensson 2010)]. To add complexity, epicardium and myocardium use overlapping growth factors to influence each tissue independently (Figure 1.4). For example, FGFR1/2 on cardiomyocyte membranes respond to epicardial-produced FGF hormones to promote a wave of Shh signaling that activates VEGFA-C and angiopoietin-2 expression to induce proliferative expansion (Lavine et al, 2006). At the same time, epicardial FGFR1 responds to FGF hormone to complete invasion into the

underlying myocardium (Pennisi and Mikawa 2009). FGFR1 dual signal transduction is likely a prototypical example of the tightly coordinated signaling that occurs during epicardial development. While reporting the functions of all the molecules that influence epicardial development is outside the scope of this introduction, it is relevant to discuss two regulators investigated in this dissertation: TGFβ and BMP.

TGFβ and BMP Signaling in the Epicardium

The TGFβ superfamily of signaling peptides encompasses many protein ligand families including: TGFβ, activin/inhibin, Growth Differentiation Factor (GDF) and (Heldin et al, 1997; Schmierer and Hill 2007). These molecules each elicit unique subcellular signaling cascade responses to influence cellular behaviors. TGFβ superfamily peptides can stimulate independent functions in tissues, or can work antagonistically against other hormones, including other TGFβ superfamily members (Guo and Wang 2009). Despite the variable responses elicited by TGFβ superfamily molecules, signaling proceeds through similarly structured signaling cascades [Figure 1.5; (Pardali et al, 2010)]. Canonical TGFβ signaling occurs when hormones stimulate heterotetrameric complexes of type-I and type-II signaling receptors, the Activin-Like Kinases [ALK; (Guo and Wang 2009)]. The type-II receptors phosphorylate serine/threonine residues on ligand-specific type-I receptors, which transduce signal to the nucleus via ligand-specific receptor-mediated SMAD molecules (Pardali et al, 2010). TGFβ ligand-stimulated ALKs 4,5 and 7 activate SMADs 2/3

to transduce signals, while BMP ligand-stimulated ALKs 1,2,3 and 6 mediate signal through SMADs 1,5 and 8 [Figure 1.5; (Pardali et al, 2010)]. Through a common mediate SMAD molecule, SMAD 4, activated ligand-specific SMADs enter the nucleus where they stimulate expression of downstream genes (Figure 1.5).

Previous studies suggest that TGFβ signaling potently regulates epicardial development. In a Gata4-driven (epicardial-specific) deletion of the TGFβ receptor ALK5 epicardial cells failed to undergo EMT *in vitro* and displayed impaired myocardial attachment *in vivo* (Sridurongrit et al, 2008). Additionally, ALK5 is necessary for loss of epithelial morphology in initial stages of EMT and smooth muscle differentiation (Austin et al, 2008; Olivey and Svensson 2010), TGFβ type-III receptors are necessary for coronary vessel development in the mouse (Compton et al, 2005), and TGF$\beta_{1/2}$ ligands stimulate epicardial cell migration (Austin et al, 2010). Together, *in vitro* data suggest that TGFβ signaling stimulates multiple epicardial behaviors to facilitate migration, EMT and/or cell differentiation.

BMP signals are vital for specification of PE tissue and downstream epicardial/myocardial cell fate decisions (van Wijk et al, 2009; Liu and Stainier 2010). Additionally, studies have demonstrated that BMP signaling facilitates PE villi lateral migration (Austin et al, 2010; Ishii et al, 2010), as BMP2/4 recruit PE villi to the atrioventricular junction of the heart via sheet movement (Ishii et al, 2010). Ectopic expression of BMP2 aberrantly targets epicardial sheet migration to the heart, which can be suppressed by the BMP inhibitor, noggin (Ishii et al,

2010). Together, these data demonstrate that BMP signaling plays multiple roles in early epicardial specification and development. The exact interplay of TGFβ and BMP signaling is elucidated in Chapter II of this dissertation.

Epicardium in Injury Repair

Epicardium may provide a therapeutic tool to improve injury repair after myocardial infarction (MI). Heart disease is a leading cause of mortality in humans. After MI, cardiomyocyte death is followed by fibrotic scar formation at the lesion. Fibrosis increases stress on the remaining living cardiac muscle leading to dilated cardiac chambers, declined contractility and eventual heart failure (Segers and Lee 2008; Vieira and Riley 2011). Epicardium contributes to scar formation and may be a progenitor population that could be manipulated to support cardiac regeneration (Vieira and Riley 2011). In some lower organisms epicardial cells rapidly proliferate and induce growth or differentiation of newly-formed cardiomyocytes to regenerate heart tissue after injury (Poss et al, 2002). While mammalian heart tissue has poor regenerative capacity, recent studies been developed with the aim of: a) driving epicardial progenitors to differentiation into nascent cardiomyocytes, or b) exogenously initiating epicardial behaviors that support myocardial regrowth (Ausoni and Sartore 2009; Duan et al, 2011).

Murine lineage tracing studies suggested that a small population of epicardial cells might differentiate into cardiomyocytes during development, but the findings remain controversial (Cai et al, 2008; Zhou et al, 2008). Adult epicardial cells express cardiomyocyte progenitor markers, and epicardial cells

can be driven to express differentiated cardiomyocyte markers *in vitro* after addition of growth factors (Kruithof et al, 2006). However, the effectiveness of such treatments *in vivo* is questionable. For example, Thymosin β4 peptide has been shown to initiate cardiomyocyte differentiation from epicardial explants *in vitro,* and priming the tissue with this hormone may support *de novo* cardiomyocyte differentiation after MI *in vivo* (Smart et al, 2010). However*,* followup lineage tracing studies demonstrate that Thymosin β4 does not stimulate cardiomyocyte differentiation *in vivo,* although epicardial thickness and coronary vessel density improves (Zhou et al, 2012). Due to conflicting studies such as these, epicardial cell differentiation into cardiac muscle with a drug or hormone treatment currently seems an unlikely therapeutic tool that requires breakthrough studies before effective treatments can be developed.

Another, perhaps more immediately promising, therapeutic tool could take advantage of EPDC modulatory effects on myocardial development (Winter and Gittenberger-de Groot 2007). For example, retinoic acid receptor signaling on epicardial cells elicits trophic factors that stimulate cardiomyocyte proliferation *in vitro* (Chen et al, 2002). Additionally, as discussed above, EPDCs signal through FGFR1 and FGFR2 on cardiomyocytes to stimulate proliferation (Lavine et al, 2006; Pennisi and Mikawa 2009). Adult human EPDCs injected into infarcted murine heart tissue preserved some cardiac function and diminished ventricle remodeling (Winter and Gittenberger-de Groot 2007). EPDCs secrete paracrine factors to support angiogenesis after MI, and injection of EPDC-conditioned medium improves heart function (Zhou et al, 2011). Recent literature indicates

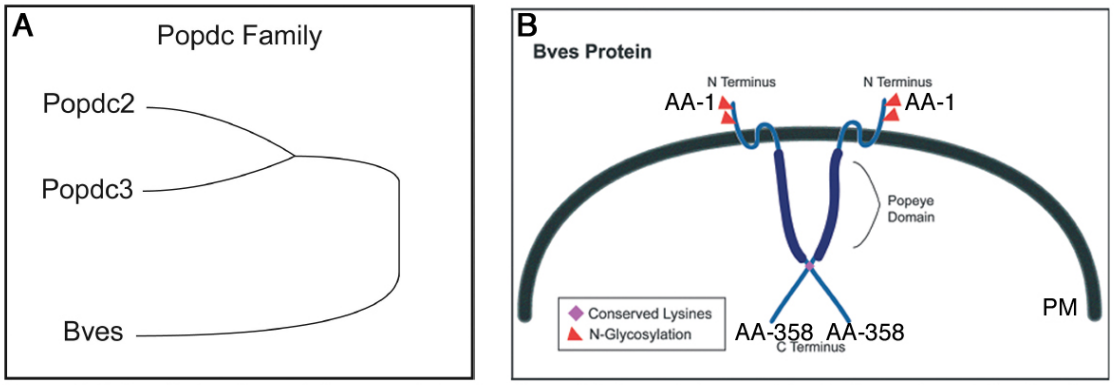

Figure 1.6 Popdc family and Bves protein structure. (A) Bves is the prototypical member of the Popdc family of which there are three genes. (B) Bves is a 358 amino acid a triple-pass transmembrane protein that localizes at plasma membranes and on cytoplasmic vesicles, shown here is a putative conformation of Bves dimers at the plasma membrane (PM); adapted from Hager and Bader 2009.

that epicardial cells activated through notch signaling contribute to fibrotic scar formation after infarct, which is both essential for initial healing, and detrimental in the long term (Russell et al, 2011). Thus, epicardium and EPDCs have critical supportive influence on adult heart tissue during repair after MI, which could be therapeutically manipulated.

Improvements in these therapeutic strategies will be gained from better understanding of epicardial cell biology. Subcellular regulators of migration, adhesion, differentiation and secretion remain to be identified. Additionally, by elucidating the known regulatory relationships coordinating these behaviors it may be possible to recapitulate local factor stimulation and drive cellular behaviors *in vivo.* This dissertation seeks to explicate these regulatory questions for future development of novel tools to manipulate this tissue. One epicardial enriched protein, Bves, could regulate a variety of epicardial behaviors.

Bves Structure and Tissue Distribution

Bves, [Popeye domain containing 1 (Popdc1)], is a heart-enriched gene identified using subtractive screening methods (Reese et al, 1999; Andrée et al, 2000). Bves is the prototypical member of the three-gene Popdc family, which share a conserved region (*popeye domain*) of unknown function (Andrée et al, 2000; Wada et al, 2001). Bves is highly conserved among all eukaryote species, while Popdc2 and Popdc3 are only expressed in vertebrates, but these molecules may provide redundancy in the case of Bves disruption [Figure 1.6A; (Andrée et al, 2002; Hager and Bader 2009)]. Popdc family members share no significant homology with other protein families based on structure, which is barrier in elucidating Bves function (Andrée et al, 2000; Brand 2005).

Bves (358 aa in mouse) is a triple-pass trans-membrane protein with a short extracellular N-terminal domain (AA 1-42) that contains two N-glycosylation sites [Figure 1.6B; (Andrée et al, 2000; Knight et al, 2003)]. The function of the N-terminal domain is unstudied, but may involve targeting to subcellular trafficking compartments (Roth 2002). The C-Terminal domain begins after the third trans-membrane pass from AA 118 to 358; the Popeye domain comprises AA 91-266 [Figure 1.7; (Osler et al, 2005; Smith et al, 2008)]. Multiple Bves-binding proteins interact within the conserved Popeye domain (Kawaguchi et al, 2008; Smith et al, 2008; Hager et al, 2010), and binding partner association is important for Bves function (discussed in detail below).

Cell types expressing Bves are widely varied. Initial studies suggested that expression was limited to heart and skeletal muscle

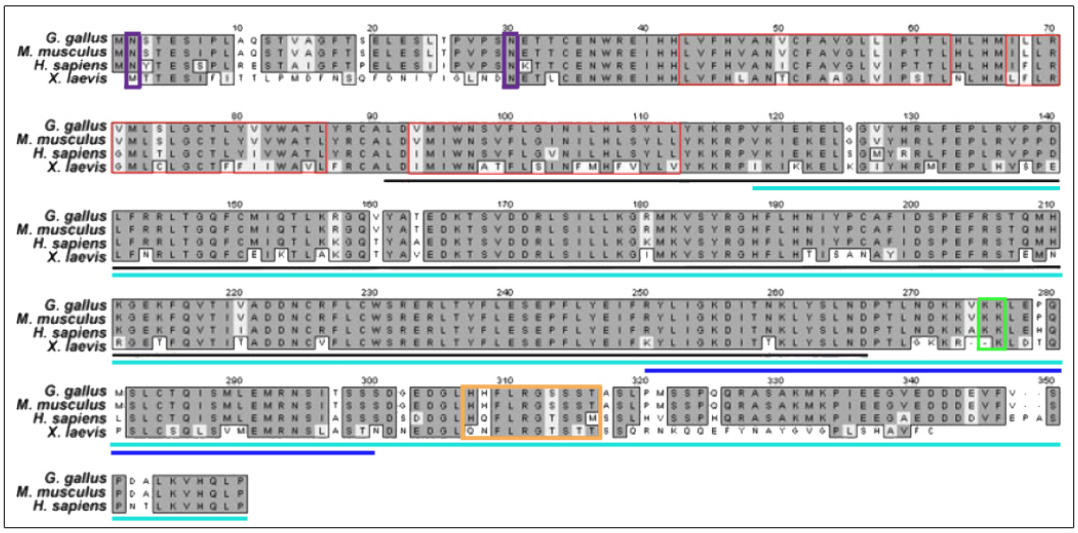

Figure 1.7 Bves amino acid sequence. Bves protein is 358 amino acids with conserved transmembrane domains (red boxes), n-glycosylation sites (purple boxes) and the Popeye domain (black line). The function of this domain is unknown, but it partially contains the minimal binding domain residues required for the GEFT binding domain (blue line). The conserved KK domain is the site of Bves homodimerization (green box). NDRG4 minimal binding sequence is from residues 307-316 (orange box), and VAMP3 is within the C-terminus but requires further definition (teal line denotes C-terminal construct domain); adapted from Osler et al. 2006.

(Reese et al, 1999; Andrée et al, 2000). However, RT-PCR studies and expression databases indicate that Bves is additionally expressed in a range of tissues from lung to thymus (Hager and Bader 2009). Antibody labeling has indicated that Bves is robustly expressed in the epicardium and cardiomyocytes of the heart as well as in smooth and skeletal muscle (Reese et al, 1999; Andrée et al, 2000; DiAngelo et al, 2001; Andrée et al, 2002; Hitz et al, 2002; Osler and Bader 2004; Vasavada et al, 2004; Smith and Bader 2006; Torlopp et al, 2006). Additionally, Bves has been visually identified in epithelial tissues such as the endoderm of the gut and cornea of the eye, and also in the brain [Figure 1.8;

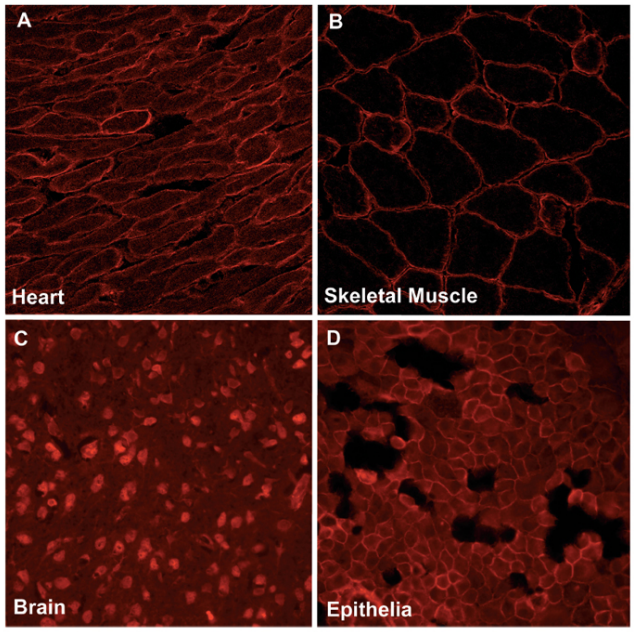

Figure 1.8 Bves tissue expression. Bves protein is found in adherent tissues ranging from (A) cardiomyocytes to (B) skeletal muscle, to (C) brain, to (D) various epithelial including MDCK (kidney epithelial cells) shown here; from Hager and Bader 2009.

(Osler and Bader 2004; Ripley et al, 2004; McCarthy 2006; Smith and Bader 2006; Russ et al, 2010; Russ et al, 2011; Williams et al, 2011)]. Hager and Bader (2009) recognized that Bves-enriched tissues have adherent properties, suggesting that Bves facilitates cellular adhesion.

Bves expression has been characterized in several model organisms. Bves is expressed in early stages of chick development: in Henson's Node at HH4, and in the developing germ layers at HH stages 8 and 11 (Osler and Bader 2004; Torlopp et al, 2006). In later chick development Bves is expressed in the retina, cornea and lens of the eye, the heart and the endoderm of the gut (Wada et al, 2001; Osler and Bader 2004; Ripley et al, 2004). Bves has also been identified in follicle and nurse cells of the *Drosophila melanogaster* oocyte

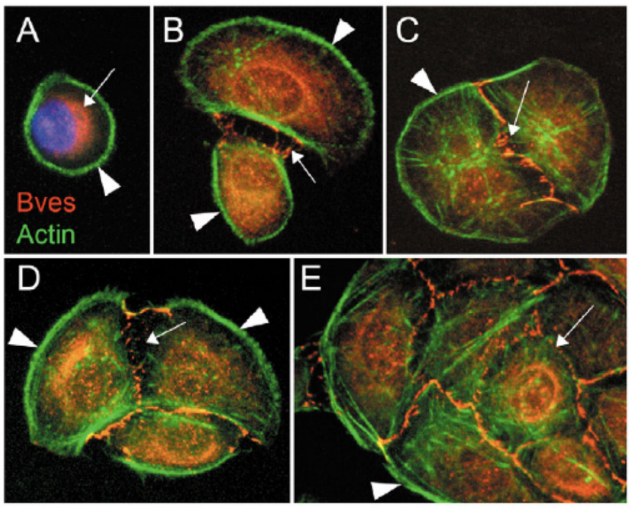

Figure 1.9 Bves subcellular localization pattern. Single cells have cytoplasmic pools of Bves (red) that translocates to the cell surface at putative points of contact, preceding classic junction proteins. Bves then remains at the plasma membrane in epithelial sheets. Actin cytoskeleton detected in green; from Olser et al. 2005.

(Lin et al, 2007). During murine embryonic development (E12.5) Bves is found in muscle, heart, epidermis, digestive and respiratory tracts, and epithelium of the developing eye (Smith and Bader 2006; Russ et al, 2010), but Bves knockout mice have normal development (Andrée et al, 2002). Similarly, initial studies in the rat indicate heart and skeletal muscle enrichments (Parnes et al, 2007). Finally, identification of Bves gene in humans indicates enriched expression in adult/fetal heart, and skeletal muscle (Reese and Bader 1999), and more recent data additionally indicate expression in the cornea, lens and trabecular meshwork cells of the eye (Russ et al, 2010). Importantly, Williams et al. (2011) demonstrated that intact Bves expression is a metastasis suppressor in human colonic epithelium. Thus, Bves is widely expressed early in development in many model organisms, continued expression occurs in the adult in a variety of

muscle/epithelial tissues, and this expression must be maintained to prevent colorectal, lung and gastric cancers.

The *Xenopus laevis (X. laevis)* model system was utilized in this dissertation to determine Bves (named Xbves in this system) function on cell surface adhesion during gastrulation. Initial studies identified Xbves as 60-65% identical to human Bves (Hitz et al, 2002). Bves is expressed in the heart, and in the surface epithelium and involuting cells of gastrulation stage embryos (11.5) (Hitz et al, 2002; Ripley et al, 2006). At stage 19, Xbves is found in all three germ layers, and specifically is identified in epithelial of the neural tube, developing eye and surface ectoderm (Ripley et al, 2006). It is important to note that Morpholino interference of Xbves function is an extremely effective knockdown technique as: a) Popdc2 and Popdc3 are not expressed in this organism, diminishing redundancy issues, and b) knockdown effects can be fully rescued (Ripley et al, 2006). Morpholino knockdown of Xbves has drastic effects on embryonic development: the epithelial movements epiboly and involution are disrupted and gastrulation is halted (Ripley et al, 2006).

Bves has dynamic subcellular localization depending on cell morphology *in vivo* and *in vitro* (Wada et al, 2001). In the developing AV junction, Bves localizes to intercellular junctions between adjacent epicardial cells, while in delaminated subepicardial cells Bves is cytoplasmic (Wada et al, 2001; Osler et al, 2005). This phenomenon has also been characterized in human corneal epithelial (HCE) sheet biogenesis and EMT, in which Bves has cytoplasmic localization when cells are singular, but as cell-cell junctions form Bves precedes

classic junction markers (E-cadherin, ZO-1) and is maintained at cell-cell interfaces [Figure 1.9; (Ripley et al, 2004; Osler et al, 2005; Russ et al, 2011)]. Conversely, after epithelial EMT is stimulated, Bves localization shifts from the membrane back to the cytoplasm, along with a concomitant upregulation of mesenchymal markers (Wada et al, 2001; Kawaguchi et al, 2008). Additionally, in primary cardiac muscle cultures or cardiomyocyte cell lines, Bves translocates from the cytoplasm to the intercalated disc at cell-cell junctions (Vasavada et al, 2004; Smith and Bader 2006), suggesting that this is a global Bves phenomenon.

Bves Regulates Cell-Cell Adhesion

Due to lack of homology to other molecules, determining Bves function is difficult (Hager and Bader 2009). Bves localizes to the tight junction (TJ), colocalizes with canonical TJ transmembrane proteins ZO-1 and Occludin, and indirectly interacts with ZO-1 (Osler et al, 2006; Russ et al, 2011). Overexpression studies of Bves in non-adherent L-cells conferred adhesive properties in culture, decreased epithelial sheet permeability and increased Trans Epithelial Resistance [TER; (Wada et al, 2001; Russ et al, 2010; Russ et al, 2011)], while loss-of-function studies in HCEs and epicardial cells demonstrated that Bves is essential for maintenance of epithelial junction integrity and TER (Ripley et al, 2004; Osler et al, 2005). Importantly, the Bves C-terminus is required for intact localization of occludin, E-cadherin or β-catenin to intercellular junctions, suggesting that Bves is required for shuttling cell adhesion molecules to the cell surface (Osler et al, 2005; Kawaguchi et al, 2008). Other studies

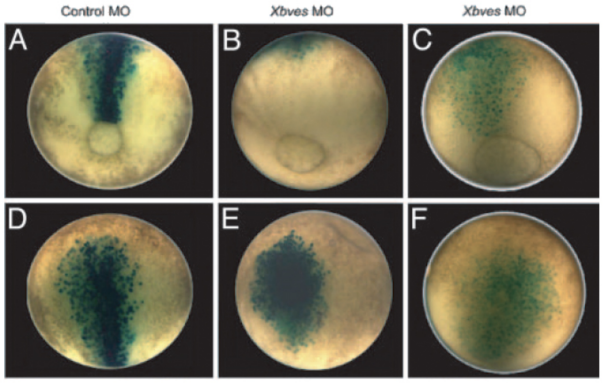

Figure 1.10 Bves disruption causes random migration. Bves depletion from *X. laevis* A1-blastomere causes random scatter migration of progeny cells (LacZ stain, B-C and E-F); from Ripley et al. 2005.

additionally suggest that Bves supports epithelial junction signaling. RhoGEFs are activators of the molecular switch enzymes, RhoGTPases, which regulate many essential cellular behaviors (Bishop and Hall 2000). RhoA signaling elevates cellular contractility and is downregulated when the RhoGEF, GEF-H1, is bound to TJs and spatially inhibited (Somlyo and Somlyo 2000; Aijaz et al, 2005). Russ et al. (2011) demonstrated that RhoA activity is modulated by Bves expression level and that GEF-H1 localization depends on Bves expression, proposing that Bves strengthens TJ integrity by spatially inhibiting GEF-H1. Thus, Bves may function as a supporting structure at cell junctions, rather than physically providing adhesion, and may shuttle adhesion proteins to the cell surface.

Bves regulates cell migration

Bves also regulates cell migration, which was first suggested by chick PE explants cultures in which Bves antibody blocked tissue outgrowth (Wada et al,

2001). Ripley et al. (2004) demonstrated in HCE-punch wound injury that Bves-depleted cells migrated faster than controls, but migration was disorganized and wound healing impaired. Wound healing was also impaired in murine knockout Bves models after skeletal muscle injury (Andrée et al, 2002). During *X. laevis* development, Bves-depleted two-cell embryos exhibited halted gastrulation due to deregulated convergence/extension movements in animal caps. Importantly, injection of Bves morpholino and a tracer into the A1-blastomere (32-cell stage) initiated rogue movements in the knockdown cells; cells moved randomly throughout the embryo and precociously invaded below the surface ectoderm [Figure 1.10; (Ripley et al, 2006)]. Lin et al. (2007) demonstrated that pole cells in oocytes laid by *Drosophila melanogaster* expressing antisense Bves RNA failed to migrate to their target destination, reflecting results obtained from frog studies. Finally, Smith et al. (2008) demonstrated that NIH-3T3 cells expressing Bves C-terminus inhibited Rho GTPases Rac1 and Cdc42, produce fewer lamellipodial protrusions with impaired movement. Collectively, these studies indicate that Bves regulates organized migration. The studies presented in Chapter III and IV use animal/cell culture models to demonstrate a Bves mechanism that influences adhesion and directional migration. These data suggest a unifying model that may explain the disparate phenotypes observed above.

Bves is a Metastasis Suppressor

Recently, Bves was identified as hypermethylated from a screen performed on cancerous versus non-cancerous lung tissue samples (Feng et al,

2008). Kim *et al.* (2010) corroborated these results in gastric cancer where Bves and Popdc3 were hypermethylated and RNA expression of Bves and Popdc3 were 70-87% silenced. Importantly, shRNA knockdown of Popdc3 in gastric cancer cell lines promoted invasion and migration, reflecting Bves influence on migration discussed above (Kim et al, 2010). A recent study by Williams *et al.* (2011) demonstrated that Bves is hypermethylated and underexpressed in human colorectal carcinoma (CRC) tissue and adenomatous polyps. Exogenous expression of Bves inhibited migration and invasion in CRC lines and growth/metastasis of orthtopic xenografts (Williams et al, 2011). Thus, Bves is required to maintain epithelial integrity of epithelial tissues and suppress metastasis of specific cancer tissues; understanding Bves molecular function is relevant to human physiology and cancer therapeutics.

Bves Function is Elucidated by Binding Partner Interactions

In an effort to place Bves in a molecular pathway, yeast-2 hybrid and split-ubiquitin screens were performed. Previous work has described Bves homodimerization and binding of Bves to GEFT [mapped in Figure 1.7; (Kawaguchi et al, 2008; Smith et al, 2008)]. This dissertation discusses binding of Bves to VAMP3 (Chapter III) and NDRG4 (Chapter IV). With the exception of homodimerization, colocalization studies of Bves with binding partners suggest that binding may be transient (Hager and Bader 2009). Bves may influence

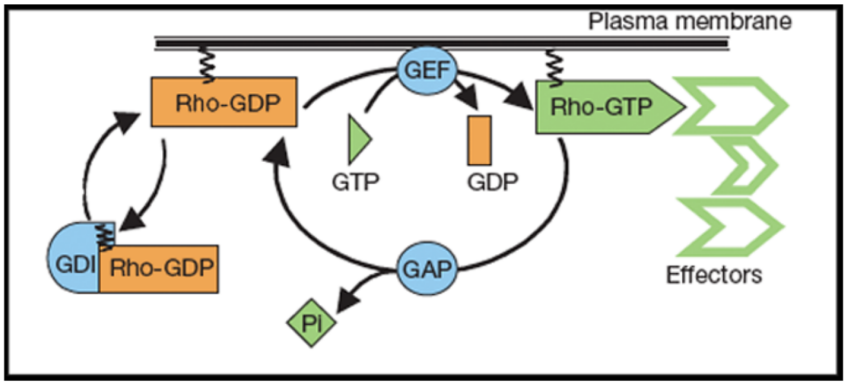

Figure 1.11 The RhoGTPase Cycle. RhoGTPase molecules cycle between active (bound to GTP) and inactive (bound to GDP). GEF proteins exchange GDP for GTP and may localize RhoGTPase to the plasma membrane. GAP proteins return RhoGTP to RhoGDP, while GDI molecules sequester RhoGDP in the cytoplasm; from Etienne-Manneville and Hall 2002.

multiple functions through context-dependent temporary binding.

Kawaguchi *et al.* (2008) were the first to examine activity of Bves protein. Lysine residues 272 and 273, (the KK domain), are essential for Bves homo-oligomerization (Figure 1.7). L-cell adhesion assays demonstrated that expression of Bves KK-mutant plasmids failed to confer adhesion, and plasma membrane localization of Bves is lost in KK-mutant expressing cells accompanied by loss of junction markers at the cell surface, and TER (Kawaguchi et al, 2008). Additionally, loss-of-Bves homodimerization stimulates EMT marker expression and, thus, is critical for epithelial sheet maintenance.

Bves and GEFT

Bves also directly binds to GEFT in the Popeye domain between residues 250-300 [Figure 1.7; (Smith et al, 2008)]. GEFT belongs to the RhoGEF family of modulators that exchange GDP for GTP to activate RhoGTPase molecular

switches and influence a variety of effector proteins and cellular behaviors [Figure 1.11; (Schmidt and Hall 2002; Guo et al, 2003). GEFT activates the RhoGTPase molecules Cdc42 and Rac1, which are canonical inducers of migration through actin polymerization to produce filopodia and lamellipodia, respectively (Schmidt and Hall 2002). Bves influences GEFT activation of Rac1/Cdc42, cell protrusion formation and migration (Smith et al, 2008). Interestingly, RhoGEFs can be spatially regulated and Bves/GEFT colocalize at cell borders in muscle tissue (Schmidt and Hall 2002; Smith et al, 2008). While actin-based protrusions drive cell migration, they also influence other cellular behaviors such as cadherin-mediated intercellular adhesion (Kuroda et al, 1999). Indeed, GEFT influences many cellular processes including cAMP-induced neurite extension, adipogenesis, myogenesis and lens differentiation through Cdc42/Rac1 activity (Bryan et al, 2004; Bryan et al, 2005; Bryan et al, 2006; Mitchell et al, 2011). Thus, the Bves/GEFT interaction could globally influence all of the developmental and disease phenotypes attributed to Bves. Bves could function to both spatially and directly regulate GEFT activity.

Bves and VAMP3

Previous studies suggest a theme in which Bves regulates activity of diverse molecules via subcellular localization (e.g. TJ/AJ components and spatial regulation of RhoGEF activity). How Bves facilitates subcellular movements is determined by studies presented in this dissertation. Our data indicate that Bves interacts with VAMP3 (cellubrevin, or synaptobrevin 3), a ubiquitous vesicular-

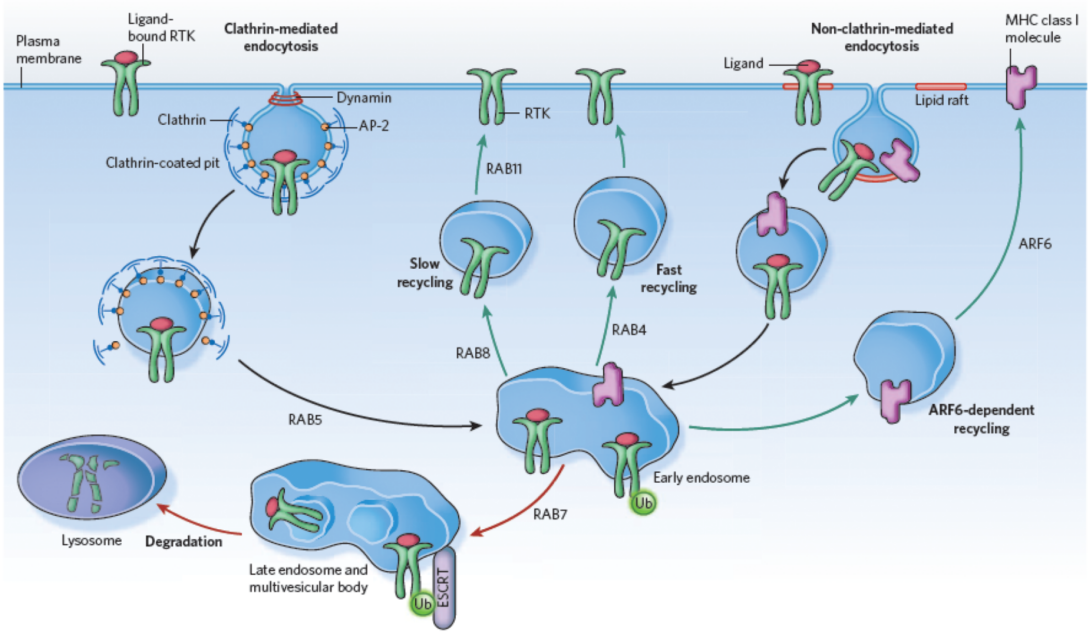

Figure 1.12 Endocytotic pathways. Internalized receptors and nutrients are endocytosed into early endosomes that sort proteins into fast or slow recycling compartments, or to late endosome/multivesicular bodies for subsequent degredation. Additionally, some multivesicular body/lysosome-like structures could be targeted for exocytosis; image from Scita and Di Flora 2010.

SNARE transport-mediating molecule (McMahon et al, 1993). This interaction provides molecular framework through which Bves could regulate transport of many cargoes. VAMP3 functions within the common eukaryotic compartmentalization process.

Intracellular membrane bound vesicles generate diverse subcellular compartments in eukaryotic cells (Alberts 2002). These compartments can function in the biosynthetic route to transport *de novo* produced immature proteins from the rough endoplasmic reticulum to the Golgi apparatus for post-translational modifications, then mature proteins are shuttled to functional compartments at the plasma membrane or outside the cell (Proux-Gillardeaux et al, 2005). Alternatively, intracellular compartmentalization also mediates

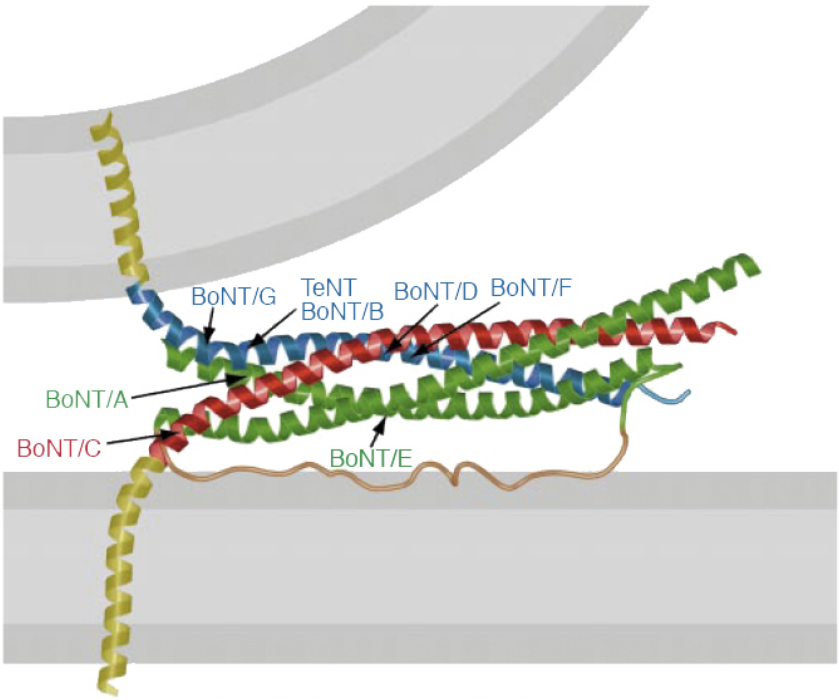

Figure 1.13 The SNARE complex. SNARE proteins have a highly specialized structure consisting of coiled-coil domains that fuse to cognate SNARE proteins extending from apposing membranes. SNAREs bring membranes together and facilitate fusion. Botulinum neurotoxins target SNARE molecules; adapted from Sutton et al. 1998.

internalization of nutrients and signaling molecules from the plasma membrane and extracellular environment through endocytosis pathways [Figure 1.12; (Proux-Gillardeaux et al, 2005; Huotari and Helenius 2011)]. In these pathways the plasma membrane invaginates to enclose extracellular particles and receptors in early endosomes (Platta and Stenmark 2011). Early endosomes are general sorting stations containing the Rab GTPase, Rab5, and its effector, EEA1 (Scita and Di Fiore 2010; Platta and Stenmark 2011). Internalized proteins are shuttled back to the membrane through either slow or fast recycling mechanisms (marked by GTPases Rab11 and Rab4, respectively), or targeted for degradation through late endosomes and multivesicular bodies (mediated by

Rab7) to lysosomes for degradation (marked by LAMP1/2) or exosomes for secretion [Figure 1.12; (Scita and Di Fiore 2010; Platta and Stenmark 2011)]. Additionally, secretion of lysosome-like multivesicular-derived compartments can be targeted for exocytosis in some cellular contexts (Izumi 2007). The general framework of endocytosis is resolved. However, endocytotic pathways are cell-specific and multifunctional, complicating identification of the pathways through which genes of interest influence cellular behaviors (Maxfield and McGraw 2004).

Subcellular shuttling of vesicular compartments entails budding from a donor compartment, movement through the cytosol on cytoskeletal tracks and SNARE-mediated fusion of the compartment with the receiving membrane (Proux-Gillardeaux et al, 2005). Structurally, a single SNARE consists of two α-helical coils (Scales et al, 2000). Donor v-SNAREs fuse with receptor t-SNAREs to bring membranes into close apposition for fusion [Figure 1.13; (Scales et al, 2000)]. SNAREs have specificity for subcellular compartments and may have cognate binding partner SNAREs to ensure specific fusion (Scales et al, 2000).

VAMP3 is a v-SNARE enriched in recycling endosomes that participates in fusion events of vesicles being shuttled to and from the plasma membrane (Borisovska et al, 2005). VAMP3, which is sensitive to inactivation through cleavage by Tetanus Toxin (TeNT; Figure 1.13), is a well-described regulator of transferrin shuttling; this tool is used to assay VAMP3 function (Daro et al, 1996). VAMP3 shuttles a diverse array of molecules, from matrix metalloproteases for secretion to myelin transport in oligodendrocytes (Kean et al, 2009; Reefman et al, 2010; Feldmann et al, 2011). Importantly, VAMP3 is required for cell

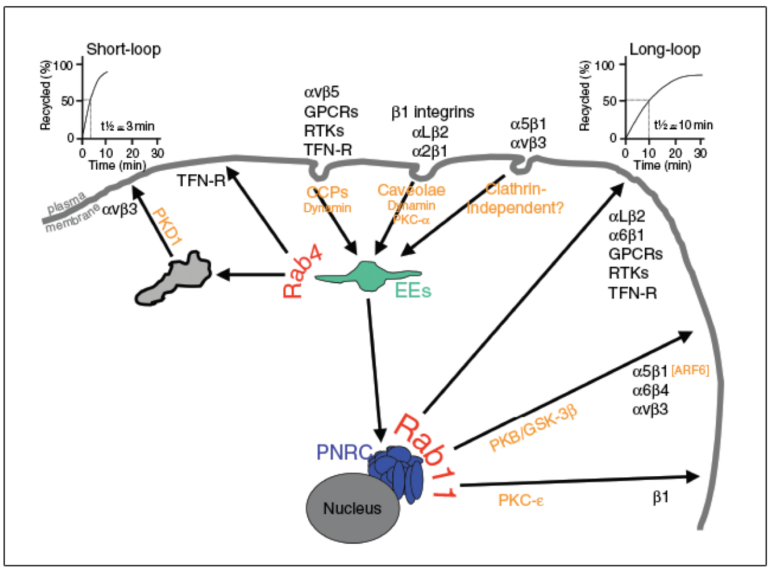

Figure 1.14 Integrin recycling. Integrin receptors are internalized into early endsosomes and either immediately returned to the plasma membrane via fast recycling, or, like $\alpha5\beta1$ integrin, sorted into a perinuclear recycling compartment (PNRC). From the PNRC, Rab11 (and VAMP3) mediate $\alpha5\beta1$ integrin return to the cell surface in the slow recycling pathway; adapted from Caswell and Norman 2006.

migration, as it mediates delivery of recycled β1-integrin to focal adhesions for lamellipodium formation (Proux-Gillardeaux et al, 2005; Skalski and Coppolino 2005). VAMP3 mediates many cellular behaviors that reflect the functions that are also attributed to its binding partner Bves. Thus, the interaction between Bves/VAMP3 elucidated in Chapter III provides a mechanistic framework to underlie the diverse phenotypes exhibited in Bves-disrupted cellular, developmental, and disease models.

Integrin trafficking

Integrin heterodimers localize in the plasma membrane where the complexes confer adherence to both the underlying surface/neighboring cells and transduce cellular signals in response to environmental stimuli (Hynes 2002).

Integrin cycling includes internalization from the plasma membrane and redeposition back to the cell surface with an average cycle time of 30 minutes (Roberts et al, 2001; Caswell and Norman 2006). The machinery for this cycling is integrin specific, and β1-integrins undergo caveolae-dependent internalization (Ng et al, 1999). After internalization β1-integrins are shuttled from early endosomes to the perinuclear recycling compartment (PNRC) for Rab11-mediated recycling [Figure 1.14; (Roberts et al, 2001; Roberts et al, 2004)]. GTPase proteins/effectors mediate movement from PNRC to Rab11 vesicles (Ng et al, 1999; Powelka et al, 2004; Skalski and Coppolino 2005). VAMP3 disruption with TeNT treatment delays β1-integrin trafficking in Rab11 vesicles from the PNRC to the membrane where it normally fuses by binding to the t-SNARE SNAP23 (Veale et al, 2011). Thus, VAMP3 functions within the canonical β1-integrin recycling mechanism to mediate cell spreading and lamellipodial extension (Proux-Gillardeaux et al, 2005). Chapter III of this dissertation details Bves regulation of β1-integrin recycling through the established VAMP3 mechanism.

Fibronectin Assembly and Trafficking

Fibronectin, a ubiquitous ECM glycoprotein that exists in a branched meshwork around cells, is a major substrate for β1-integrin adherence (Singh et al, 2010). Fibronectin has a modular structure with domains allowing for binding to other glycoproteins and cell surface molecules simultaneously, and assembly is a cell-mediated process where thin fibrils cluster together to form thick bundles

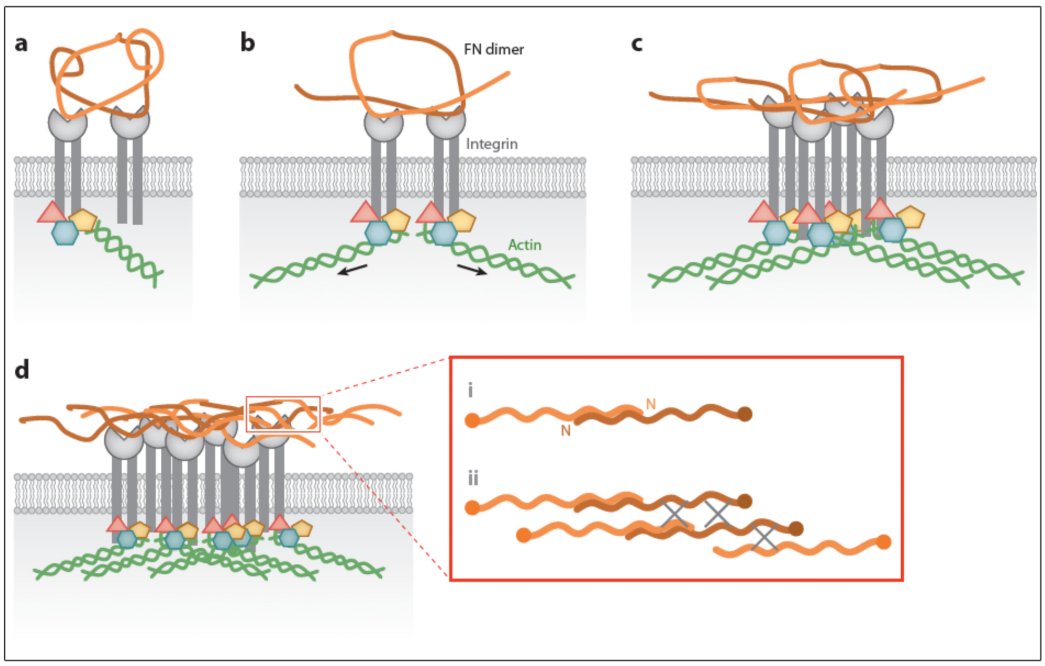

Figure 1.15 Fibronectin fibrillogenesis. (A) Fibronectin is secreted in a folded conformation. (B-D) Integrin proteins tether and change the conformation of fibronectin proteins causing oligimerization and insolubility; adapted from Singh et al. 2010.

(McDonald 1988; Mao and Schwarzbauer 2005; Singh et al, 2010). Fibronectin is secreted in a folded conformation, and cells mediate fibrillogenesis primarily through binding $\alpha 5\beta 1$-integrin to the RGD (Arg-Gly-Asp) domain on fibronectin (Ruoslahti and Obrink 1996). Tethering initiates conformational changes allowing fibronectin oligomerization in the N-terminal domain and overall matrix insolubility [Fig 1.15; (Sechler et al, 1996; Huveneers et al, 2008)]. Tethering also provides resistance to support cell contractility, and subcellular signaling through focal adhesion complexes (Singh et al, 2010). The mechanism of fibronectin matrix turnover is only now emerging, and occurs through $\beta 1$-integrin-mediated and caveolin-1-dependent endocytosis (Shi and Sottile 2008). It has recently been suggested that fibronectin and $\beta 1$-integrin are internalized and trafficked into

lysosomes for either degredation or recycling back to the basal surface of the plasma membrane to mediate cell movement (Lobert et al, 2010; Dozynkiewicz et al, 2011; Sung et al, 2011). While fibronectin turnover is essential for cell adhesion and movement, subcellular regulation of this mechanism requires further elucidation. Chapter IV of this dissertation identifies two novel regulators of fibronectin recycling and deposition, Bves and NDRG4.

NDRG4

The most frequent Bves binding partner identified in split-ubiquitin screens was NDRG4. Chapter IV will detail the interaction between Bves and NDRG4 in internalization and re-secretion of soluble fibronectin to confer directional epicardial cell migration. Elucidating this interaction provides novel information about Bves and NDRG4 influence on subcellular trafficking and secretion.

NDRG4 (Bdm1 and SMAP8) is a cytoplasmically-localized molecule of unknown function that belongs to the NDRG gene family [57-65% amino acid identity among family molecules; (Zhou et al, 2001)]. Isoforms of NDRG4 range from 339 to 371 amino acids, are highly conserved across species from plants to humans, and contain an α/β hydrolase domain predicted to be non-functional [Figure 1.16A; (Zhou et al, 2001; Qu et al, 2002; Shaw et al, 2002)]. NDRG4 is enriched in heart and brain with minor expression in a variety of other tissues such as lung, testis and skeletal muscle (Zhou et al, 2001; Nakada et al, 2002; Qu et al, 2002). NDRG4 is expressed in murine pancreatic duct epithelium and acinar cells during development, but is downregulated at 21 days

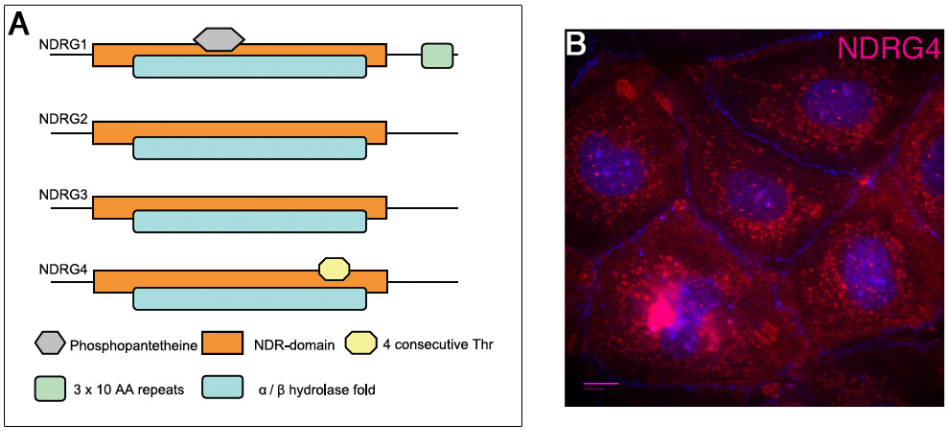

Figure 1.16 NDRG4 conserved structure and subcellular localization. (A) NDRG4 (352 AA) belongs to the NDRG protein family. These molecules share a conserved α/β hydrolase domain, but the active residues are mutated to alanines; modified from Melotte et al. 2010. (B) NDRG4 has mainly a punctate, vesicular cytoplasmic localization with some protein found at the cell surface (NDRG4 red, ZO-1/dapi blue).

(Wang and Hill 2009). In the brain, *in situ* hybridization and antibody labeling demonstrated NDRG4-enriched neurons in many areas during development and in the adult, as well as in Purkinje cells in the cerebellum (Okuda et al, 2008; Yamamoto et al, 2011). NDRG4 is also enriched in the spinal cord and peripheral nerves (Zhou et al, 2001). In the zebrafish, NDRG4 is first expressed in the central nervous system at the 10-somite stage, and this expression is enriched throughout the nervous system at 72 hpf (Qu et al, 2008). This study was additionally the first to demonstrate expression patterns of NDRG4 during heart development. NDRG4 is expressed at 24 hpf in the developing heart tube and by 36 hpf it is expressed in both atrial and ventricular tissues. In epicardial cells, NDRG4 is generally cytoplasmic and vesicular, although some protein also localizes to cell surfaces (Figure 1.16B). Cellular fractionation of rat brain homogenate suggests that NDRG4 is mitochondrial- and endoplamic reticular-

enriched and lumenally oriented, as determined through protease protection assays (Nakada et al, 2002). Generally, NDRG4 is enriched in heart and brain and expression grows progressively stronger from embryonic development to adulthood in expressing tissues (Melotte et al, 2010).

Gain- and loss-of-function studies demonstrated that NDRG4 influences a variety of cellular behaviors. Studies in PC12 neurons indicate that neurite protrusion is impair with NDRG4 disruption and, conversely, enhanced with overexpression (Ohki et al, 2002). Followup studies demonstrated that MEK/ERK signaling cascade activities needed for neuronal differentiation are enhanced with NDRG4 overexpression, while activity of Elk-1, a transcription factor target of ERK needed for cell growth is attenuated (Hongo et al, 2006). Microtubule transport is required for this attenuation, suggesting that subcellular transport of cargoes is affected by NDRG4 expression. NDRG4 has also been demonstrated to regulate cell proliferation, although the exact effect may be context dependent. In rat aortic smooth muscle cell lines (A10) overexpression of NDRG4 reduced basal proliferation rate, while overexpression of proliferation stimulated by Platelet-Derived Growth Factor (PDGF) was enhanced (Nishimoto et al, 2003). Nishimoto *et al.* (2003) similarly demonstrated enhanced MEK/ERK phosphorylation in NDRG4 overexpressing cells. Qu *et al.* (2008) demonstrated during zebrafish development that NDRG4-depletion impairs cardiac myocyte proliferation leading to cardiac growth and morphogenesis defects with overall weak contractility. Conversely, NDRG4-depleted pancreatic cells fail to repress DNA synthesis, a marker of proliferation, during differentiation (Wang and Hill

2009). Importantly, overexpression of NDRG4 in A10 cells inhibits cell migration (Nishimoto et al, 2003). Finally, NDRG4, like its binding partner Bves, is a tumor suppressor in multiple cancer cell types. Melotte *et al.* (2009) were the first to identify hypermethylation of the NDRG4 promoter in colorectal cancer cell lines and tissue. This study demonstrated that overexpression of NDRG4 in CRC lines inhibited invasion and proliferation, indicating that loss-of-NDRG4 is a biomarker for premalignant colorectal tissue (Melotte et al, 2009). Additionally, NDRG4 expression is elevated in Glioblastoma Multiform (GBM) cells where it is required for cell cycle progression and proliferation (Schilling et al, 2009). Thus, NDRG4, like Bves, influences varied behaviors in multiple cell, developmental and disease models.

NDRG4 subcellular protein activity requires elucidation. However, the molecular function of the other NDRG family members provides clues as NDRG proteins may exhibit redundancy. All of the NDRG family proteins are involved in similar cellular processes including differentiation of developing tissues, regulated cell proliferation and cellular responses to stress (Melotte et al, 2010). Additionally, all NDRG molecules have tumor suppressive functions; Kachhap et al. (2007) suggests that NDRG molecules influence later tumor changes, such as metastasis, rather than tumor initiation. NDRG1 is the best-studied NDRG molecule and is mutated in a form of human Charcot-Marie-Tooth syndrome, the degenerative peripheral neuropathy, Hereditary Sensory and Motor Neuropathy-Lom [CMT4D; (Kalaydjieva et al, 2000)]. NDRG1 expression is elevated in the cytoplasm of Schwann cells that ensheath axons of the peripheral nervous

system and oligodendrocytes of the central nervous system (Berger et al, 2004; Okuda et al, 2008). NDRG1 transfected into COS7s is cytoplasmic, diffuse and some colocalization occurs with ubiquitin (Berger et al, 2004). Two murine NDRG1$^{-/-}$ models recapitulated CMT4D with axon degeneration due to demyelination, and subsequent loss of motor function (Okuda et al, 2004). King *et al.* (2011), using *stretcher (str)* mutant NDRG1$^{-/-}$ mice, suggested that NDRG1 influences trafficking of myelin sheath components. NDRG1 interacts through yeast-2-hybrid screening with multiple trafficking proteins including Prenylated Rab Acceptor 1, a regulator of transport between endosomal compartments (Hunter et al, 2005; King et al, 2011). NDRG1 is involved in lipid transport of Apolipoprotein binding partners, ApoA-I and II (Hunter et al, 2005). Additionally, NDRG1 is a Rab4a effector that regulates shuttling E-Cadherin to/from the plasma membrane in prostate cancer cell lines (Kachhap et al, 2007), while the Alzheimers Disease associated-NDRG2 regulates secretion of the cytokine IL-10 (Mitchelmore et al, 2004; Choi et al, 2010). The molecular function of NDRG4 elucidated here in Chapter IV is consistent with functions ascribed to other NDRG family molecules, suggesting that regulation of subcellular trafficking is the global function for NDRG proteins.

Summary

Epicardial development is a complex process and its coordination requires elucidation. Chapter II of this dissertation presents a novel experimental mechanism to identify signaling cascade relationships regulating this

developmental program. Additionally, Chapters III and IV study epicardial-enriched Bves protein and reveal two new binding partners, VAMP3 and NDRG4. These studies suggest a novel global role for Bves: regulation of cell surface trafficking of multiple components. Through this function Bves facilitates cell-cell and cell-surface adhesion and supports epithelial integrity and cell movement.

CHAPTER II

APPLICATION OF SMALL ORGANIC MOLECULES REVEALS COOPERATIVE TGFβ AND BMP REGULATION OF MESOTHELIAL CELL BEHAVIORS

This chapter was published under this title in *American Chemical Society Chemical Biology* on July, 8 2011 (Cross *et al.* 2011).

Abstract

Epicardial development is a process during which epithelial sheet movement, single cell migration and differentiation are coordinated to generate coronary arteries. Signaling cascades regulate the concurrent and complex nature of these three events. Through simple and highly reproducible assays, we identified small organic molecules that impact signaling pathways regulating these epicardial behaviors. Subsequent biochemical analyses confirmed the specificity of these reagents and revealed novel targets for the widely used Dorsomorphin (DM) and LDN-193189 molecules. Using these newly characterized reagents, we show the broad regulation of epicardial cell differentiation, sheet movement and single cell migration by Transforming Growth Factor β (TGFβ). With the DM analog, DMH1, a highly specific Bone Morphogenetic Protein (BMP) inhibitor, we demonstrate the cooperative yet exclusive role for BMP signaling in regulation of sheet migration. The action of DMH1 reveals that small organic molecules (SOM) can intervene on a single

epicardial behavior while leaving other concurrent behaviors intact. All SOM data were confirmed by reciprocal experiments using growth factor addition and/or application of established non-SOM inhibitors. These compounds can be applied to cell lines or native proepicardial tissue. Taken together, these data establish the efficacy of chemical intervention for analysis of epicardial behaviors and provide novel reagents for analysis of epicardial development and repair.

Introduction

Mesothelium is the simple squamous lining of the body cavities and organs (Wilm 2005). Mesothelia are important in development, as they are essential for blood vessel formation and organogenesis in general (Mikawa and Fischman 1992; Dettman et al, 1998; Gittenberger-de Groot et al, 1998; Reese et al, 2002). Still, generation of mesothelium is complex and information on regulation of its various cell behaviors is only now emerging (Austin et al, 2008; Mellgren et al, 2008; Ishii et al, 2010). The epicardium, covering the heart, is the best-studied model of mesothelial development (Männer et al, 2001; Wada et al, 2003). During embryogenesis, the proepicardium arises independently from the heart on the sinus venosus (Mikawa et al, 1992; Gittenberger-de Groot et al, 1998; Reese et al, 2002; Nahirney et al, 2003; Cai et al, 2008). Development and differentiation of the proepicardium is dependent on multiple simultaneous cell behaviors as it migrates to the naked myocardium, adheres and spreads over the heart as an epithelial sheet (Komiyama et al, 1987; Männer et al, 2001). During this lateral migration event, selected epicardial cells undergo

epithelial/mesenchymal transition, migrate throughout the heart and differentiate into many lineages including vascular smooth muscle, fibroblasts, endothelial cells, and cardiomyocytes (Mikawa and Gourdie 1996; Dettman et al, 1998; Cai et al, 2008; Mellgren et al, 2008; Ishii et al, 2010). Epicardial development is likely to require cooperative signaling mechanisms.

The approach to understanding complex molecular interplay controlling cell behaviors has historically used gene mutation and knockdown studies to deactivate gene products (Hood et al, 2004). While these studies have been successful, they are not without caveats as they may cause secondary effects on the system, and are expensive in terms of time, effort and materials. Additionally, knockdown or knockout studies may simultaneously remove all functions performed by the gene, including regulation by non-coding microRNAs (Stockwell 2004; Poliseno et al, 2010). An emerging alternative employs organic chemical "perturbagens" that bind to proteins, alter their function, and replace or complement gene mutation or knockdown studies (Stockwell 2004). Small organic molecules (SOM) have an added advantage: when well-characterized, selected compounds have highly-specific activity on discrete residues of their target proteins and may affect only one of multiple functions performed by that molecule (Stockwell 2004).

An excellent example of this concept is Dorsomorphin (DM) and its family of analogs (Hao et al, 2008; Hao et al, 2010). These structurally-related compounds differentially target Bone Morphogenetic Protein (BMP) signaling. BMPs are part of the Transforming Growth Factor β (TGFβ) superfamily of

growth factors (Chen et al, 2004; Guo and Wang 2009) and have been implicated in regulating epicardial behaviors (Schlueter et al, 2006; van Wijk et al, 2009; Austin et al, 2010; Ishii et al, 2010). TGFβ and BMP signaling occurs through stimulation of ligand-specific type-I and type II serine/threonine kinase receptors on the effector cell membrane, where they dimerize in response to ligand (Giehl and Menke 2006). The receptor complex stimulates signal transduction in effector cells via phosphorylation of Smad family mediator molecules, which translocate to the nucleus and stimulate transcription of target genes (Giehl and Menke 2006). Identification of SOMs with broad or specific inhibitory effects on these pathways would produce versatile tools to study intricate developmental processes regulated by concurrent signaling cascade mechanisms.

Chemical biology is particularly amenable for unraveling the complexity of epicardial development, where many signaling cascades coordinately impact cell behaviors. In the present study, we conducted SOM screens of epicardial differentiation, sheet movement and single cell migration to elucidate signaling pathways regulating these independent yet concurrent events. With compounds that broadly or specifically intervene on signaling pathways, we show a dependence on TGFβ signaling in the regulation of all three activities. Conversely, using a newly characterized and highly specific BMP inhibitor, the DM analog DMH1, we show that both TGFβ and BMP signal cascades interdependently regulate epicardial sheet migration. Intervention with these perturbagens demonstrates that a single epicardial behavior can be inhibited while

simultaneous cell activities are left intact in both clonal cell lines and native tissue. Taken together, these data demonstrate the efficacy of chemical intervention to identify cooperative signaling in the regulation of epicardial behaviors. In addition, we provide the field with well-characterized reagents for intervention in both embryogenesis and wound healing.

Materials and Methods

Quantification

For the assays described below statistics and percent closure were performed in Microsoft Excel. Error bars represent the standard error of the mean; student t-tests were used to determine significance. All images being compared were adjusted equally.

Cell culture, cell and tissue processing, antibodies and immunofluorescence analysis

Epicardial cell culture conditions and processing were standard (Wada et al, 2003) as was slide preparation (Smith and Bader 2006). Commercially available antibodies included: anti-α-SMA, (Sigma 2547, 1:200), anti-ZO-1 (Zymed 61-7300, 1:200), anti-SM22, (Abcam, ab28811, 1:200), anti-cytokeratin, (Abcam, ab9377, 1:200), anti-WT-1, (Abcam, ab52933, 1:100), anti-vimentin, (Sigma, V 6630, 1:50) and anti-SM-MHC (Biomedical Technologies BT-562, 1:200) anti-Phospho-β-catenin (Cell Signaling, 9566, 1:500), Phospho-Smad1/5,

Smad5, Smad3, Phospho-Smad3 (Cell Signaling, 9516, 9517, 1:1000 WB, 1:50 IF), anti-β-Catenin (BD Transduction Laboratories, 610154, 1:500).

SMA expression and wound healing assays

Initially, 10^5 epicardial cells were seeded to 4-well glass chamber slides (NUNC Lab-Tek 154526) in standard epicardial cell medium (Wada et al, 2003). After the 18 hour incubation, the medium was changed to 2% FBS; 2% FBS/DMEM, supplemented with TGFβ_1, PDGF and EGF (Millipore GF111 & GF149, BD Biosciences 354001, respectively) at 10ng mL^{-1} each, to induce epicardial cell differentiation with simultaneous addition of SOMs at the concentrations given in Figure 2.2, panel j. For induction by TGFβ_1 alone, medium was supplemented with 20ng mL^{-1} TGFβ_1 in 2μM DMSO. The negative control consisted of medium with DMSO. For induction by BMP2, 4 and 6 (R&D Systems 355-BM, 314-BM-010, 6325-BM, respectively) growth factor was added to SFM. Noggin (R&D Systems 3344-NG) was added at 200ng mL^{-1} to the TGFβ_1-supplemented medium. In all situations, cells were incubated for 48 hours, until being processed.

To assay early differentiation and sheet migration rate, $2.5x10^5$ cells were seeded to glass 4-well chamber slides and incubated overnight in standard epicardial cell media. After 18 hours incubation, cells were equilibrated in mediums. After six-hours incubation, confluent cell sheets were scratched with a 200μL pipette tip, incubated for an additional 18 hours and then analyzed for SMA expression as above. Sheet movement was quantified at zero and six

hours after wounding. For ALK2/3 overexpression assays, 5μg of CA-ALK2/3 plasmids were expressed with the Nucleofector II Device (Amaxa Biosystems) using Solution L, program A-020. $2.5x10^5$ cells were added to each well of 4-well slide and after 48 hours incubation sheets were wounded and analyzed. This work was conducted at the Vanderbilt CISR.

Smad Phosphorylation Assays

For analysis by western blot, cells were grown to confluence, serum starved and stimulated with TGFβ as above. Lysates were collected, total protein measured, and immunoblotted as previously reported (Smith and Bader 2006) AP detection of immunoreactive bands was standard (Smith and Bader 2006). For analysis by IF, cells were seeded, treated and injured as above for western blot analysis. Cells were processed for Phospho-Smad1/5 antibody as per Cell Signaling (9516). Z-series were captured at VUMC CISR and two 0.6μm Z-planes were projected with LSM Image Browser.

IC_{50} Determination

Kinase binding and confirmatory in vitro kinase assays were performed by KinomeScan at www.kinomescan.com.

RNA collection, cDNA synthesis and Quantitative RT-PCR

18 hours preceding experimental intervention, $2x10^5$ cells were seeded in triplicate to a 6-well plastic culture dish (Falcon 353502). Next, cells were

stimulated with the TGFβ_1-induction conditions described above. After 24 hours incubation, cells were lysed (Qiashredder, Qiagen 79654), and RNA was purified as described (Shelton and Yutzey 2008). Specific primers with a melting temperature of 59^{o}C were designed from the Rattus norvegicus cDNA database using PrimerBlast (NCBI) and are listed in Supplementary Table S4. QRT-PCR was performed on the 7900HT Fast Real-Time PCR System [ABI; (using the VUMC DNA resources core)]. Gene expression was compared using TaqMan Gene Expression assays: BMP2-Rn01484736_M1, BMP4-Rn00432087_m1, BMP6-Rn00432095_m1, GAPDH-Rn99999916_s1, 18s-HS99999901_s1. Data was managed in RQ Manager 1.2 software. All statistics were performed on the DCT values.

Modified Boyden Chamber Migration Assay

3.0x10^5 cells per experiment were pelleted for 10 minutes at 1500 RPM in a desktop microcentrifuge and resuspended in 400uL of control and experimental media described above. The cells were seeded to the basket of an 8.0μM cell culture insert (Millicell P18P01250) and placed in 600μL of the same media in a 24-well plastic culture dish (Falcon). Cells were incubated for 4 hours, and processed with standard methods (Shelton and Yutzey 2008). Fifteen phase images were captured on an Olympus BX60 microscope and Olympus Camera.

Chicken Proepicardium Explant Differentiation and Migration Assay

Gallus gallus 16.5 Proepicaria were dissected from embryos and placed on 4-well glass chamber slides coated with 5ug $(cm^2)^{-1}$ Fibronectin (Sigma F4759). Proepicardia were incubated for 24 hours in TGFβ_1-induced culture conditions (above) and processed for immunochemistry with standard methods (Pennisi and Mikawa 2009). Images were captured and processed at VUMC EBC. Proepicardial explant size was ascertained with phase-contrast imaging and by total-protein content measurement (Figure 2.1).

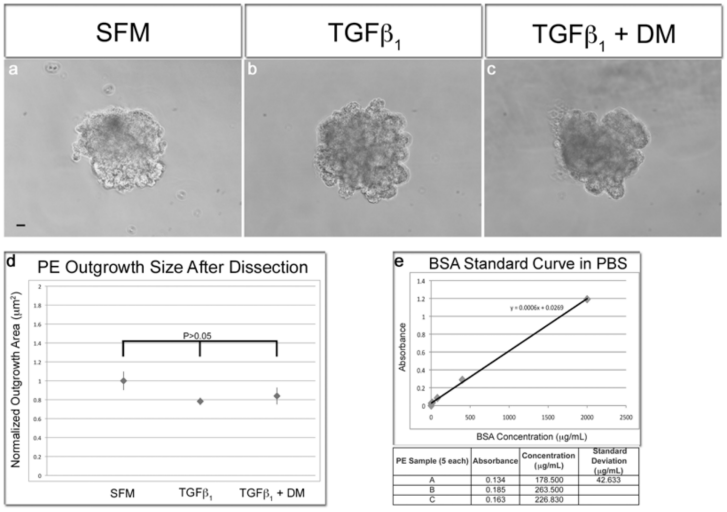

Figure 2.1 PE explants are comparable in size. Two methods were used to ensure that equally sized PE explants were used for analysis. First the size of select isolates was measured after two hours incubation from phase contrast images. Next, total protein in PE isolates was determined as a measure of explant size. (a-d) PEs were imaged and measured for total area after two hours incubation to allow PEs to settle on the slides. PEs were not statistically different in total area after culturing (P>0.05). (e) Total protein content of unincubated PEs was also calculated and three groups of PEs were found to have similar concentration, with standard deviation of 42.5 μg/mL. For PE imaging and total protein content 5 PEs were measured for each condition or group, respectively.

Results and Discussion

Specific Small Molecules Intervene in Epicardial Smooth Muscle Differentiation

In an effort to establish a broadly applicable approach to analyze regulation of specific epicardial cell behaviors, a panel of SOMs was tested for effects on early smooth muscle differentiation. Previous work from our laboratory and others determined that expression of smooth muscle α-actin (SMA) in epicardial cells is a hallmark of epithelial/mesenchymal transition, an initial step in smooth muscle differentiation, and can be stimulated by multiple growth factors (Wada et al, 2003; Olivey et al, 2005; Mellgren et al, 2008). Treatment of epicardial cell lines with a combination of known SMA-stimulating growth factors for 48 hours in serum-free medium (hereafter termed medium) evoked a robust and highly replicable SMA response (Figure 2.2, panel a versus b). Representative results of selected SOMs are presented in Figure 2.2, panels a-i. The characteristics and structures of representative molecules are listed in Figure 2.2, panels j-k. Most compounds had no or minimal effect on the number of cultured cells expressing SMA. One exception was the TGFβ inhibitor, SB-431542 (Inman et al, 2002), which completely ablated SMA expression (Figure 2.2, panel c). This is a valuable internal control, as TGFβ is known to stimulate SMA expression in epicardium. Interestingly, Dorsomorphin (DM), an inhibitor of BMP signaling cascade receptors along with other signaling pathways including vascular endothelial growth factor (VEGF)

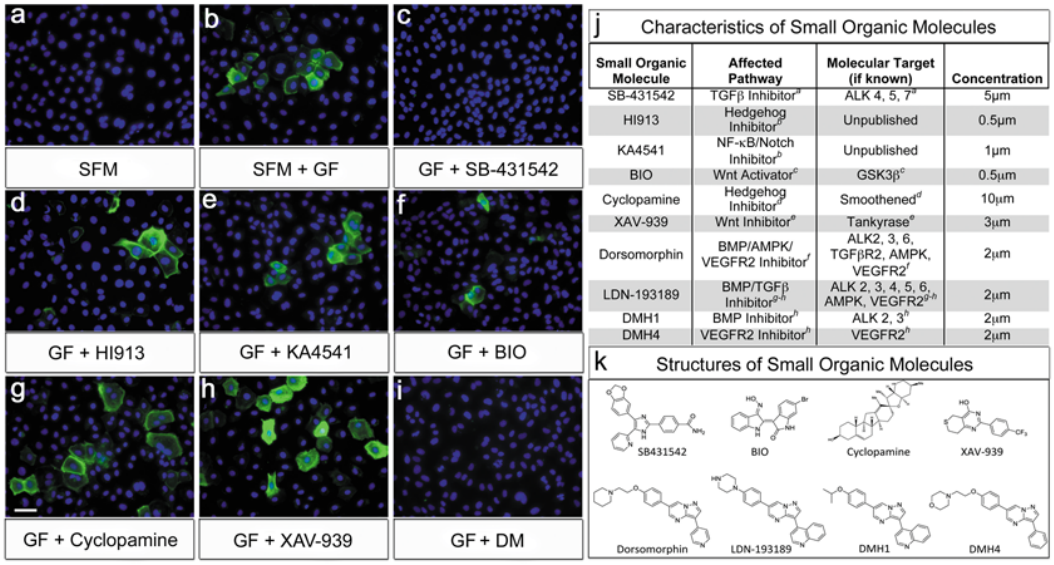

Figure 2.2. Dorsomorphin and SB-431542 inhibit epicardial α-smooth muscle actin (SMA) expression. (a-b) Epicardial/mesothelial cells (hereafter termed 'epicardial cells') treated with serum-free medium (hereafter termed 'medium') plus or minus growth factors serve as negative and positive controls for SMA expression. (c) Epicardial cells stimulated with growth factors and treated with SB-431542 ablated SMA expression. (d-h) Growth factor-stimulated cells treated with KA4541, BIO, Cyclopamine or XAV had no effect on SMA expression. (i) Growth factor-stimulated cells treated with Dorsomorphin (DM) also strongly inhibited SMA expression. (j) This information panel provides details about the SOMs tested in these studies. (k) The structures of the small molecules tested in this study are presented here. [(Scale bar=50μm; Footnotes: A-*(Inman et al, 2002)*, B-*unpublished data*, C-(Moon et al, 2004) , D-*(Chen et al, 2002)*, E-(Peterson 2009), F-(Yu et al, 2008), G-(Cuny et al, 2008), H-(Hao et al, 2010) SFM=Medium; GF=Growth Factor Medium].

(Zhou et al, 2001; Hao et al, 2008; Hao et al, 2010), also ablated SMA expression (Figure 2.2, panel i). This is an unexpected result, as BMP signaling is thought to only regulate myocardial differentiation in the heart, but is not a well-described activator of smooth muscle differentiation (Olivey et al, 2005; Giehl and Menke 2006; Schlueter et al, 2006; Svensson 2009; van Wijk et al, 2009). Thus, these surprising results raised the possibility that BMP signaling may be involved in epicardial cell smooth muscle differentiation.

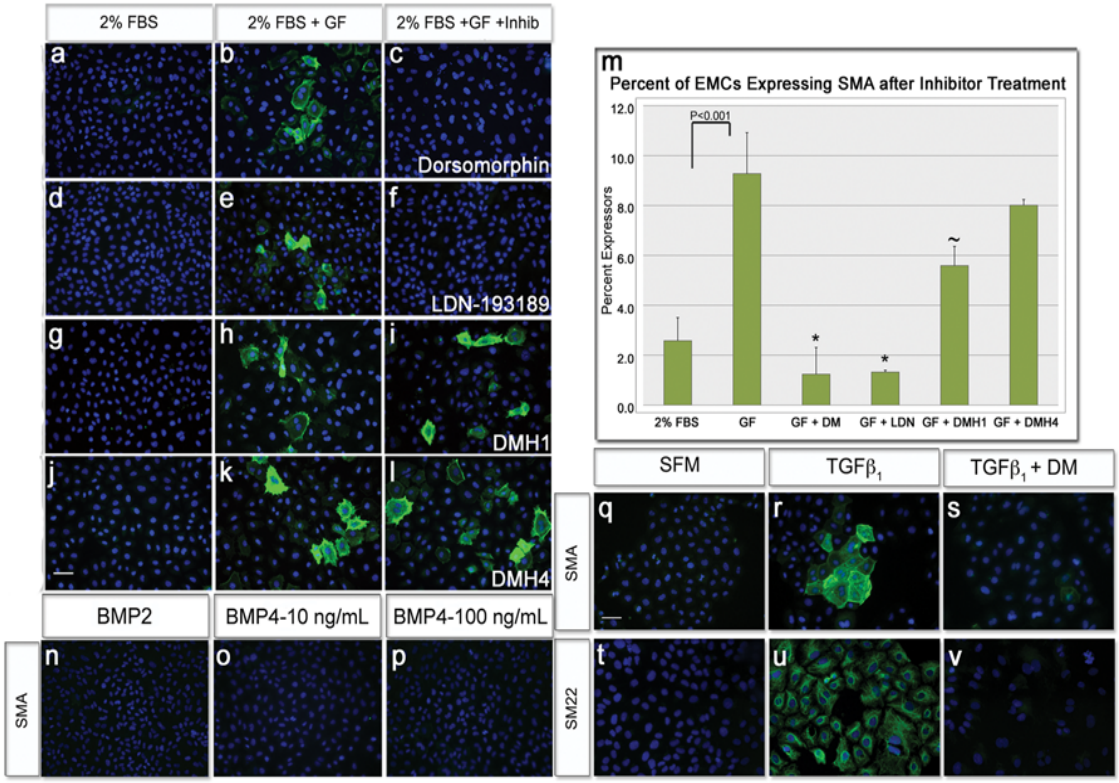

Figure 2.3 Analysis of growth factor regulation of SMA expression in epicardial cells. (a,d,g,j) Epicardial cells cultured in low-serum medium did not express SMA. (b,e,h,k) Growth factors added to low-serum medium induced high levels of epicardial SMA expression. (c,f,m) Epicardial cells cultured with growth factors and treated with DM/LDN-193189 significantly inhibited SMA expression compared to untreated cells. (i,m) Epicardial cells cultured with growth factors and treated with the BMP-specific inhibitor DMH1 marginally inhibited SMA expression. (l,m) Epicardial cells cultured with growth factors and treated with DMH4 were unaffected (from growth factor p=0.237). (n-p) Epicardial cells cultured in BMP2, or 4 did not stimulate SMA expression, at low or high concentrations. (q-r, t-u) Conversely, TGFβ_1 treatment stimulated expression of the early differentiation markers, SMA and SM22. s,v) TGFβ_1–induced SMA and SM22 expression was ablated by addition of DM. [n=≥20 images; Scale bar=50μm; (*p<0.01; ~p<0.05) TGFβ=Transforming Growth Factor β; BMP=Bone Morphogenetic Protein].

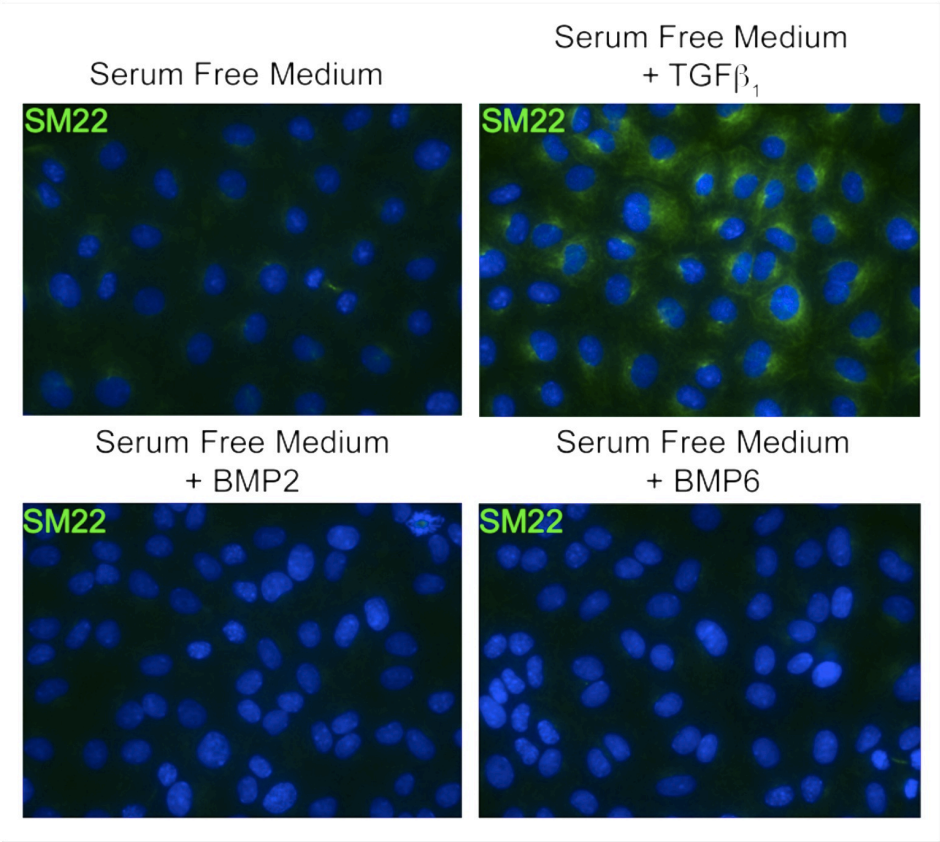

Figure 2.4 BMP2 and 6 do not stimulate SM22 expression. (a) Epicardial cell cultures maintained in serum free medium did not express SM22 protein, (b) while those treated with TGFβ_1 had a strong induction in SM22 expression. Conversely, 20ng/mL of (c) BMP2 or (d) BMP6 did not induce SM22 expression in epicardial cells.

Application of DM Analogs Elucidates Differential Requirements for TGFβ and BMP Signaling for Epicardial Differentiation

We next determined whether the previous results revealed a novel role for BMP signaling in epicardial differentiation, an effect of DM on an alternate pathway, or both. To examine these possibilities, SMA expression was assayed following treatment with 63 structural analogs of DM that have greater selectivity for individual pathways than the parent compound (Cuny et al, 2008; Hao et al, 2010). Treatment of cells with LDN-193189, an inhibitor of BMP and VEGF

pathways (Cuny et al, 2008; Hao et al, 2010), eliminated SMA expression (Figure 2.3, panels d-f, and m). Conversely DMH1, an extremely selective inhibitor of the BMP type-I receptors Activin receptor-like kinases 2 and 3 (ALK2 and ALK3) had minimal effect (Figure 2.3, panels g-i, m). Additionally, DMH4, a selective inhibitor of VEGF receptor-2 [VEGFR2; (Hao et al, 2010)], had no impact on epicardial SMA expression (Figure 2.3, panels j-m). Thus, use of these more selective inhibitors suggests that BMP signaling is not responsible for epicardial differentiation and that DM and LDN-193189 act on a previously unidentified target regulating this behavior.

To explore these unanticipated results, we conducted the inverse experiment adding specific growth factors to epicardial cultures and determining their effects on SMA expression. Addition of BMP2 and 4, both canonical stimulators of the BMP receptors ALK2/3 (Sieber et al, 2009; Mitchell et al, 2010) and highly expressed in epicardial progenitors (Schlueter et al, 2006; Ishii et al, 2010), had no effect on SMA or SM22 expression at multiple concentrations (Figure 2.3, panels n-p, Figure 2.4). TGFβ_1 was the only growth factor to induce expression of these early smooth muscle differentiation markers in epicardial cells (Figure 2.3, panels q-r, t-u), reflecting results obtained from other groups (Olivey et al, 2005; Giehl and Menke 2006; Austin et al, 2008). Interestingly and consistent with our previous data, this stimulation was completely ablated by addition of DM, identical to the inhibitory effects of SB-431542 (Figure 2.3, panels s, v). Corroborating our previous results in which the BMP inhibitor, DMH1, had little or no effect on TGFβ stimulation of epicardial differentiation (Figure 2.3,

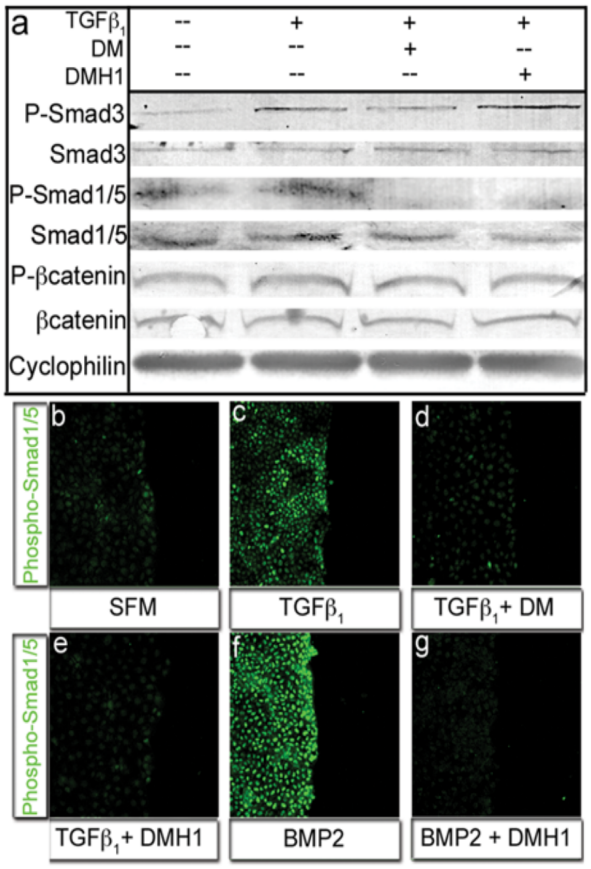

Figure 2.5 DMH1, but not Dorsomorphin, specifically inhibits Smad1/5 activity. (a) The TGFβ responsive Smad3 molecule was activated in the presence of TGFβ_1 and inhibited with addition of Dorsomorphin, but not DMH1 (row: P-Smad3). Alternatively the phosphorylation of the BMP-responsive Smad1/5 molecules was lost when cells were treated with DM or DMH1 (row: P-Smad1/5). Lysates from epicardial cells in all treatments expressed equal amounts of Cyclophilin (loading control), Smad1/5, and β-Catenin total proteins (rows: Cyclophilin, Smad3, Smad1/5, and βCatenin, respectively). β-Catenin phosphorylation was unchanged, conferring specific activity to DM and DMH1 on Smad transduction molecules (row: P-βCatenin). (b-c) Phospho-Smad1/5 nuclear localization was minimal in serum free medium and was marginally upregulated by TGFβ_1. (f) Alternatively, BMP2 treatment greatly increased activated Smad1/5 nuclear localization. (e,g) TGFβ-stimulated cells wounded, treated with DM and DMH1 did not localize Smad1/5 to the nucleus. [n=3 P-Smad3=Phosphorylated Smad3, P-Smad1/5=Phosphorylated Smad1/5 Protein, P-βCatenin=Phosphorylated βCatenin.]

panel i). These results support the data presented above, that BMP has no effect on this epicardial differentiation and that DM and LDN-193189 may affect this particular behavior in epicardial cells via inhibition of TGFβ signaling.

Identification of Novel DM Analog Targets Reveals Differential Regulation of Epicardial Receptors

To precisely determine the signal cascades inhibited by DM and its analogs, in vitro kinase inhibitory activities (as assessed by IC_{50}, concentration causing 50% inhibition) against potential BMP and TGFβ receptors were performed. As expected, all DM analogs tested strongly inhibited ALK1 and ALK2, both type-I receptors selective for BMP ligands [Table 1;(Sieber et al, 2009; Mitchell et al, 2010)]. Our previous work has shown that DM analogs also potently inhibited ALK3, another BMP type-I receptor (Hao et al, 2010). Importantly, DMH1 had minimal activity on any of the TGFβ receptors tested (Table 1: ALK4, ALK5 and TGFβR2; (Hao et al, 2010)). Conversely and unexpectedly, our data revealed for the first time that the widely-used DM and LDN-193189 inhibited TGFβR2, a type-II receptor for TGFβ (Giehl and Menke 2006).

We next examined whether the apparent differential effects of DM and DMH1 on BMP and TGFβ receptors in biochemical analyses extended to epicardial cells. Since BMP and TGFβ signaling occur via distinct receptors to trigger Smad1/5/8 and Smad2/3 phosphorylation, respectively (Chen et al, 2004; Guo and Wang 2009), we utilized pathway-specific Smad phosphorylation to

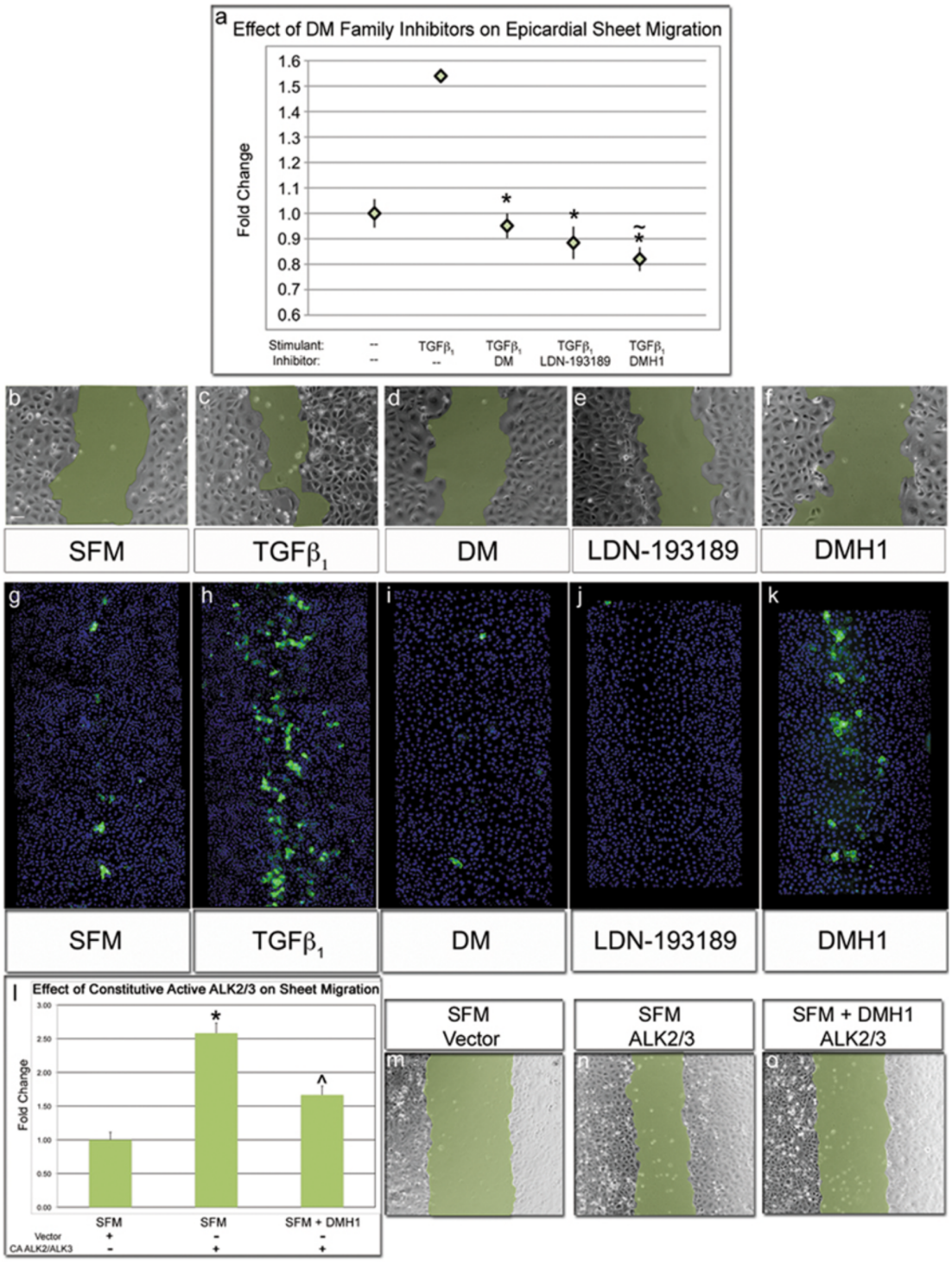
a
Effect of DM Family Inhibitors on Epicardial Sheet Migration
Fold Change
1.6
1.5
1.4
1.3
1.2
1.1
1.0
0.9
0.8
0.7
0.6
Stimulant: -- TGFβ1 TGFβ1 TGFβ1 TGFβ1
Inhibitor: -- -- DM LDN-193189 DMH1
b
c
d
e
f
SFM
TGFβ1
DM
LDN-193189
DMH1
g
h
i
j
k
SFM
TGFβ1
DM
LDN-193189
DMH1
l
Effect of Constitutive Active ALK2/3 on Sheet Migration
Fold Change
3.00
2.50
2.00
1.50
1.00
0.50
0.00
SFM
SFM
SFM + DMH1
Vector + - -
CA ALK2/ALK3 - + +
SFM Vector
SFM ALK2/3
SFM + DMH1 ALK2/3
m
n
o

Figure 2.6 DMH1 strongly inhibits epicardial sheet movement, but not SMA expression. Epicardial sheet migration rate was assessed by wound healing assays with representative images of wounds at six hours in b-f. (a,c) Wounding epicardial sheets in the presence of TGFβ_1 significantly increased sheet migration rate in comparison cells wounded in medium. (a,d-e) Epicardial wounds cultured with TGFβ_1 and concurrently treated with DM/LDN-193189 healed at medium-equivalent rates. (a,f) Interestingly, sheets wounded with TGFβ_1-and the BMP inhibitor, DMH1, healed at a rate significantly slower than unstimulated sheets. (g) Epicardial sheets wounded in medium spontaneously expressed SMA after an 18-hour incubation. (h) When wounds were cultured with TGFβ_1, SMA expression was strongly increased. (i-j) Conversly when sheets cultured with TGFβ_1 and treated with DM/LDN-193189, SMA expression was inhibited. (e) DMH1 marginally inhibited TGFβ_1-stimulated SMA expression. (l, n) Epicardial sheet migration was strongly stimulated by constitutively active ALK2/3. (l,o) Migration was modestly inhibited by treatment of constitutively active-ALK2/3 cells with DMH1, which differs from the significant inhibition that DMH1 exerts on sheet migration in Wildtype cells. [n≥8 wounds; Scale bar=50μm; (*$p<0.001$ from TGFβ_1 stimulated cells; ~$p<0.001$ from untreated cells; ^~$p<0.001$ from untreated CA-ALK2/3); CA-ALK2/3=Constitutively Active-ALK2/3].

determine the inhibitory precision of DM and DMH1 in epicardial cells. TGFβ_1 administration induced Smad3 phosphorylation, and consistent with our in vitro kinase assay data, DM, but not DMH1, inhibited TGFβ_1-dependent Smad3 phosphorylation (Figure 2.5, panel a). Conversely, both DM and DMH1 ablated Smad1/5 phosphorylation below baseline (Figure 2.5, panel a). Total Smad3, Smad1/5, and housekeeping gene (cyclophilin) protein levels were unchanged in all conditions. Additionally, the Wnt signaling cascade was unaffected under all conditions, further conferring specificity to the DM analogs (Figure 2.5, panel a). Immunofluorescence analysis demonstrated that BMP2 stimulated high levels of phospho-Smad1/5 nuclear localization, which was completely inhibited by both DM and DMH1 (Figure 2.5 f-g and data not shown). TGFβ had minor stimulatory effect on nuclear localization, which was also inhibited by DM and DMH1 (Figure 2.5, panel c-e). Collectively, our data confirm that TGFβ, but not BMP, signaling is critical for epicardial cell differentiation and identify new targets of the widely used DM and LDN-193189 molecules. With a precise understanding of the activities of the DM analogs in epicardial cells it was now possible to examine the concurrent regulation of additional behaviors by the two signaling pathways.

Elimination of BMP Signaling Inhibits Epicardial Sheet Movement, but not Differentiation

A more precise understanding of DM and DMH1 activities at the level of BMP and TGFβ receptors enabled us to use these reagents to explore whether TGFβ and/or BMP signaling regulate epicardial cell behaviors other than SMA

Table 1. *In vitro* kinase assay

Confirmatory in vitro kinase assay: IC50 (nM)	DM	LDN	DMH1	DMH2	DMH3
ALK1/ACVRL1	484	13.3	27	12	5
ALK2/ACVR1	**148**	**41**	**108**	**43**	**27**
ALK4/ACVR1B	NONE (>30K)	1825	9,622	1,407	643
ALK5/TGFβR1	NONE (>30K)	565	NONE (>30K)	2,418	2,062
TGFβR2	178	140	NONE (>30K)	86	246
AMPK	235	1,122	NONE (>30K)	3,527	1,940
VEGFR2	22	215	NONE (>30K)	2,418	2,062
PDGFRβ			NONE (>30K)		

expression. Epithelial sheet migration is a function basic to epicardial cells and can be analyzed after scratch injury (Gittenberger-de Groot et al, 1998; Reese et al, 2002; Ishii et al, 2010). In the presence of TGFβ_1, epicardial wounds incubated for six hours exhibited significantly increased regrowth rate (Figure 2.6, panels a-c). Application of DM and LDN-193189 inhibited sheet migration to control rate, indicating that elimination of TGFβ and/or BMP signaling disrupts this function (Figure 2.6, panel d-e). Interestingly, DMH1, the exquisitely selective BMP inhibitor, intervened in TGFβ-induced sheet migration; having the strongest inhibitory effect of all DM analogs (Figure 2.6, panel f compared to a). In fact, DMH1 significantly decreased migration rate below the negative control, similar to the strong TGFβ inhibitor SB-431542 (Figure 2.7, panels a-c). Because of this surprising result, we determined whether activated BMP receptors might overcome the requirement for TGFβ_1 ligand. Thus, we overexpressed constitutively active ALK2/3 and assayed sheet movement in the absence of TGFβ_1. Overexpression of these receptors strongly enhanced epicardial sheet migration, which was again inhibited upon application of DMH1 (Figure 2.6, panels l-o). Further in subsequent experiments, we will demonstrate that

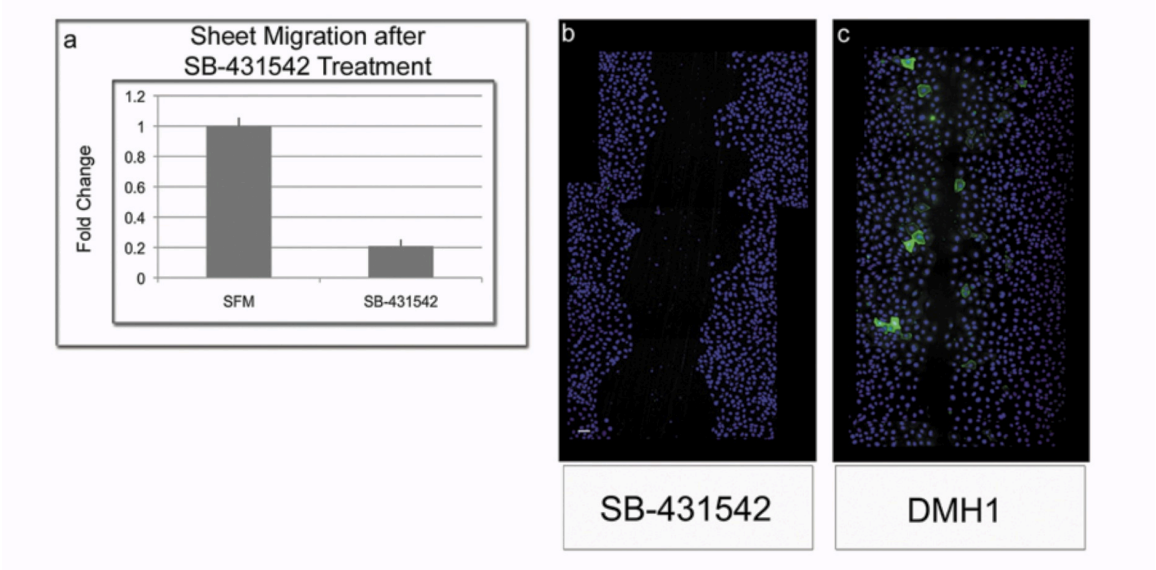

Figure 2.7. SB-431542 treatment strongly inhibits epicardial sheet migration and SMA expression at the leading edge, while DMH1 inhibits only sheet migration.(a) Treatment of epicardial sheets with SB-431542 strongly inhibited wound closure rate when compared to the SFM control. (b) Additionally, all wounds failed to close after 18 hours in culture and did not exhibit expression of SMA at the leading edge with SB-431542 treatment. (c) Similarly, sheets treated with DMH1 frequently failed to close, but maintained SMA expression at the leading edge, illustrating a similarity in ALK2/3 and TGFβ regulation of sheet migration, but a divergence in regulatory responsibilities of these cascades on SMA expression. [(*p≤0.001 from SFM); n=4 wounds.]

exogenous application of BMP ligands can also stimulate sheet movement in the absence of TGFβ (Figure 2.11, panel f-g). Thus, activated BMP signaling in the absence of TGFβ is sufficient to elicit this response, complementing the strong loss-of-migration phenotype observed with DMH1. Because addition of TGFβ is the only exogenously applied growth factor in this context, it is possible that an endogenous source of BMPs exists or that the BMP targets ALK1-3, may be directly activated by $TGF\beta_1$ ligand. We perform experiments outlined below which resolve this question (Figure 2.11). Taken together, these data illustrate the

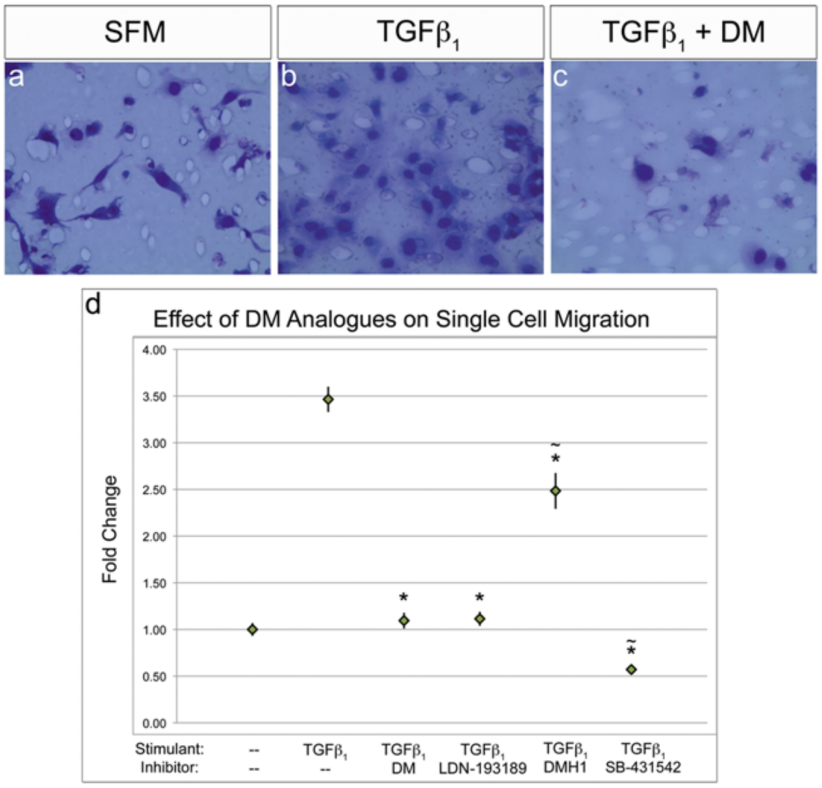

Figure 2.8 DMH1 does not ablate single cell migration. (a) Epicardial cells cultured in medium have minimal single cell migration in Boyden chamber assays. (b,d) Single cell migration is significantly enhanced by stimulation with TGFβ_1. (c,d) TGFβ_1 stimulation was inhibited by DM/LDN-193189 to a migration rate equivalent with medium, ($p=0.056$). (d) TGFβ_1 stimulation was only marginally inhibited by DMH1, unlike the TGFβ inhibitor SB-431542, which ablated this behavior. [n=30 images; (*$p<0.001$ from TGFβ_1 ~$p<0.001$ from SFM)].

concurrent requirement for TGFβ and BMP signaling in the regulation of epicardial sheet movement.

Simultaneous with migration of a wounded epithelial sheet is the expression of SMA in cells on its leading edge (Darby et al, 1990). Analysis of SMA expression during sheet migration afforded us the opportunity to examine two distinct epicardial cell behaviors at the same time, and to explore whether specific perturbagens reveal differential regulation of these events. Sheets

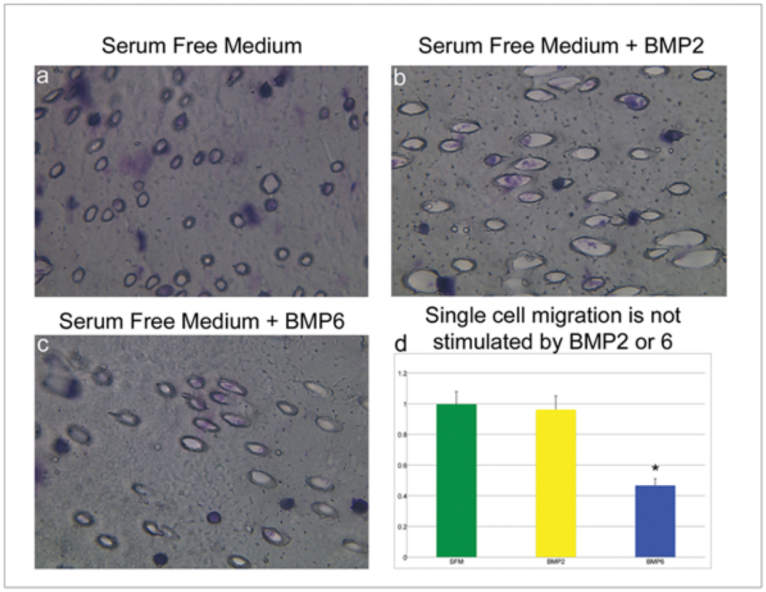

Figure 2.9. BMP2 and 6 do not stimulate epicardial cell single cell migration. (a) Epicardial cells maintained in serum free medium did not undergo significant single cell, random migration through filter membranes. Addition of (b) BMP2 or (c) BMP6 was insufficient to stimulate epicardial single cell migration. d) Single cell migration of BMP2 and 6 treated epicardial cells was quantified and normalized to the negative control. BMP2 treatment was statistically similar to untreated epicardial cultures (p=0.777). BMP6 treatment significantly decreased single cell migration rate compared to the negative control [(*p<0.0001); n=45 images from 3 experiments.]

incubated with TGFβ_1 exhibited a marked increase in SMA expression, along with robust sheet migration (Figure 2.6, panel h). Application of DM, LDN-193189 or SB-431542, all shown to inhibit TGFβ/Smad2/3 signaling in this system, strongly blocked both behaviors (Figure 2.6, panels i-j, Figure 2.7, panel b). Interestingly, while DMH1 had the greatest inhibitory effect on sheet migration, SMA expression was untouched (Figure 2.6, panel k). These data demonstrate that inhibition of TGFβ has broad inhibitory effects on epicardial behaviors, while BMP disruption is highly selective for sheet migration. Application of DM and DMH1 to epicardial cells allowed the simultaneous analysis of multiple cell

behaviors, and revealed specific intervention in only one behavior while leaving the other concurrent behaviors intact.

DMH1 does not Ablate Epicardial Single Cell Migration

Our current data suggest that BMP signaling regulates sheet movement, only, in epicardial cells. However, single cell migration is also a critical behavior for epicardial-derived cells (Reese et al, 2002) and, as such, we analyzed the impact of BMP signaling on this activity. It has been previously noted that TGFβ stimulates single cell invasive migration (Dokic and Dettman 2006), thus we used TGFβ as an activator of single cell migration and perturbed the behavior with the DM analogs. When epicardial cells were stimulated with $TGF\beta_1$ a significant increase in single cell migration rate occurred compared to controls (Figure 2.8, panels a versus b and d). Interestingly, application of DMH1 did not interfere with single cell migration (Figure 2.8, panel d). Conversely, DM, LDN-193189 and SB-431542 all strongly inhibited single cell migration, (Figure 2.8, panels c and d). BMP2 and 6 were tested for their influence on single cell migration in the same assay and, as expected, did not stimulate this behavior, corroborating the DMH1 data (Figure 2.9, panels b-d). Taken together, these data indicate that BMP signaling specifically regulates epicardial sheet migration, having little influence on other behaviors in epicardial cell lines.

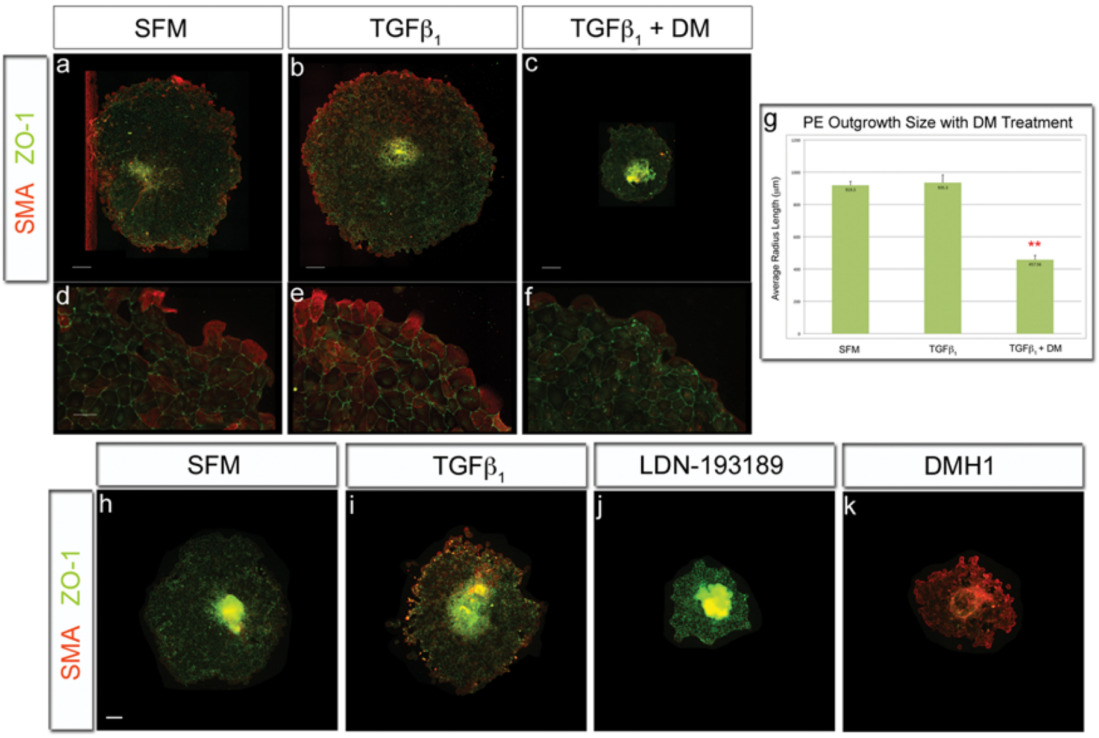

Figure 2.10 DMH1 inhibits sheet migration, but not SMA expression, in proepicardial explants. HH stage 16 proepicardia were excised from chick embryos and incubated for 24 hours. (a,d) Proepicardia incubated in medium exhibited a uniformly spread epicardial cell sheet with SMA expression at the distal edge and ZO-1, marking epithelial cells, in the interior of the sheet. (b,e,g) Proepicardia cultured in TGFβ_1 had upregulated SMA expression centrally and peripherally in the outgrowths, but TGFβ_1 treatment did not increase outgrowth migration rate from medium controls. (c,f,g,j) Proepicaria stimulated with TGFβ_1 and treated by DM/LDN-193189 had reduced epicardial sheet migration and SMA expression. (k) Proepicardia stimulated by TGFβ_1 and treated with DMH1 inhibited outgrowth migration, but had enhanced SMA expression and diminished zonula occludins-1 protein expression throughout the epicardial sheet. [Measurements assessed per condition=40; Scale bars=200μm for A-C and 50μm for D-F; (*$p<0.001$; $n\geq5$ proepicardia); ZO-1=Zonula Occludins-1].

DMH1 Inhibits Sheet Migration, but not early Differentiation, in Proepicardial Explants

The proepicardium is the source of epicardial cells in the developing embryo (Mikawa et al, 1992; Gittenberger-de Groot et al, 1998; Reese et al, 2002; Nahirney et al, 2003). Several groups have shown that proepicardial

explants grown in vitro retain the developmental properties analyzed in this study (Reese et al, 2002; Olivey et al, 2005; Pennisi and Mikawa 2009; Ishii et al, 2010). Thus, it was essential to determine whether SOMs are effective tools to modulate specific cell behaviors in native embryonic epicardial tissues. Proepicardial explants grown in basal medium spread on fibronectin to form a radial outgrowth with the average radius of 904 μm (Figure 2.10, panel a, d, g). These outgrowths had membrane localized Zonula Occludins-1 (ZO-1; a commonly used epithelial junction marker (Willis and Borok 2007), and SMA expressing cells at their periphery. Proepicardial explants incubated in TGFβ_1 had outgrowths of approximately the same size as untreated explants (avg. radius=1,003 μm; Figure 2.10, panel g). This similarity was unsurprising given the native mobility of embryonic epicardial tissue. However, TGFβ_1 evoked increased peripheral SMA expression and stimulated expression within the epicardial sheet itself (Figure 2.10, panel b, e). In contrast, when proepicardial explants were grown in the presence of DM, there was a significant decrease in the spread of the epicardial sheet at 24 hours (avg. radius=489 μm; Fig. 2.10, panel c, f, g). Similar results occurred with LDN-1923189 treatment (Figure 2.10, panel j). Additionally, in DM and LDN-193189 treated explants, SMA expression was restricted to the peripheral cells and was greatly diminished in intensity compared to TGFβ_1-treated cultures. In contrast, treatment of proepicardial explants with DMH1 resulted in the greatest inhibition of epithelial sheet migration. At the same time, DMH1 treated outgrowths displayed the highest level of SMA expression, with abundant numbers of positive cells at the periphery

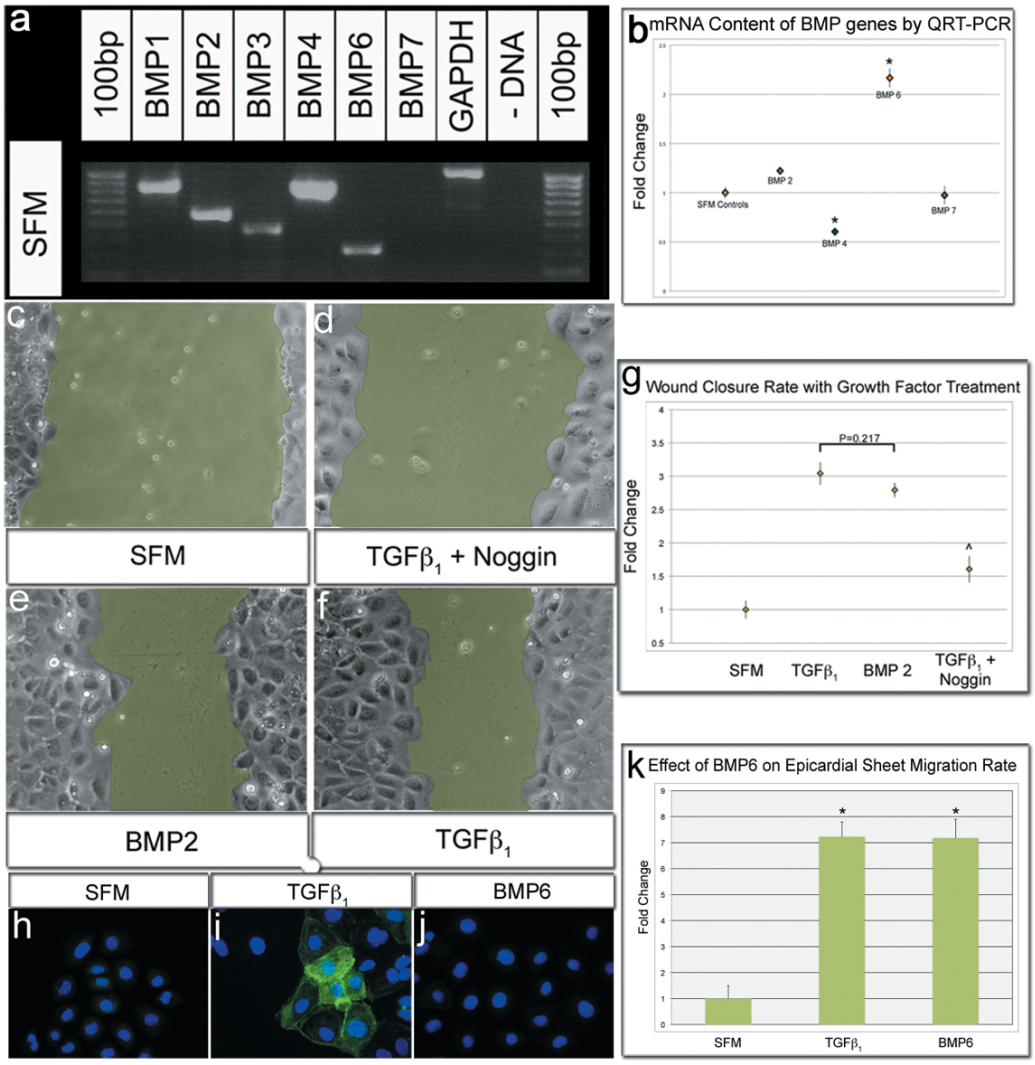

Figure 2.11 Epicardial cells express BMP factors that regulate epicardial behaviors. (a) Epicardial cells express a multitude of BMP mRNAs when assayed by RT-PCR. (b) Only BMP6 expression level was significantly increased after TGFβ_1 treatment when assayed by QRT-PCR. (c,d,f,g) Epicardial cells treated with TGFβ_1 and noggin (200ng/mL) inhibited epicardial sheet migration significantly when compared to untreated, TGFβ_1-stimulated epicardial sheets. (e) Epicardial cells treated with BMP2, only, stimulated sheet migration with a rate equivalent to TGFβ_1 stimulated sheets. (f-h) Similar to BMP2, Epicardial cells stimulated with BMP6 in medium did not express SMA when compared to TGFβ_1 stimulated cells. However, BMP6 treatment enhanced sheet migration to a rate equivalent to TGFβ_1 stimulated sheets. [(p=0.92). n=40 images; Scale bar=50μm; *p≤0.001; ^p≤0.001 from TGFβ_1 treated].

and within the sheet itself (Figure 2.10, panel k). These data corroborate our previous studies using adult epicardial cell lines and suggest that BMP signaling is required for epicardial sheet migration while having minimal, or even perhaps a permissive effect on SMA expression. The specific inhibition of sheet migration from both clonal epicardial cells and native embryonic tissue further demonstrates the efficacy of DMH1 in perturbation of a single behavior while leaving other functions unaffected.

BMPs are Expressed by Epicardial Cells and Regulate Cellular Behaviors

The present study suggests that TGFβ and BMP signaling cascades have both interdependent and independent roles governing epicardial development. While TGFβ and BMP signaling could display some cross-talk amongst transduction molecules after receptor activation, the most parsimonious explanation of this result is that BMPs are made by epicardial cells, and work together with exogenously applied TGFβ to regulate sheet migration. Indeed, previous work has shown that both epicardium and compact myocardium produce TGFβ ligands and BMPs (van Wijk et al, 2009; Ishii et al, 2010; Olivey and Svensson 2010). To determine whether epicardial cells express BMPs, cultures were incubated in medium for 24 hours and assessed by RT-PCR. As seen in Figure 2.11, panel a, a myriad of BMPs were detected under basal conditions. In subsequent studies to quantify BMP expression using QRT-PCR, $TGF\beta_1$ treatment enhanced expression of BMP6 only (Figure 2.11, panel b).

Finally, although epicardial cells make BMP growth factors, it is possible, due to effector cross-talk between TGFβ ligand and BMP signal receptors, that BMP ligands are not required to stimulate sheet migration. Previous studies indicate that while TGFβ and BMP-induced signaling cascades are often independent, TGFβ may activate BMP receptors (Olivey et al, 2005; Guo and Wang 2009). To test whether BMP itself is a stimulating ligand, the classic BMP extracellular sequestering molecule, Noggin (Zimmerman et al, 1996), was used to remove any endogenously produced BMP ligands. Wounded epicardial sheets stimulated by $TGF\beta_1$ and treated with Noggin had a significant reduction in sheet migration when compared to $TGF\beta_1$ treatment alone (Figure 2.11, panel d, g). This result was similar to, but not as pronounced as, the reduction observed with DMH1 treatment (Compare Figure 2.11, panel g with Figure 2.6, panel a). Thus, Noggin and DMH1 both inhibit extracellular stimulation of BMP receptors, but DMH1 has greater efficacy and specificity for sheet migration. In a complementary experiment, application of the canonical BMP pathway-activating protein, BMP2, enhanced epicardial sheet migration rate beyond that observed with endogenous levels of BMP (Figure 2.11, panels e, g). This differs from the effect of BMP2 on SMA expression, where addition of the growth factor had no stimulatory effect (Figure 2.3, panel n). Finally, as $TGF\beta_1$ treatment enhanced BMP6 expression, this molecule was tested for effects on SMA expression and sheet migration. As observed with BMP2 treatment, BMP6 had no effect on smooth muscle differentiation (Figure 2.11, panels h-j), but strongly enhanced sheet migration (Figure 2.11, panel k), suggesting that BMP2 and 6 have similar stimulatory

functions in this system. Interestingly as shown above, BMP2 and 6 have no effect on single cell migration (Figure 2.9, panels b-d). Taken together, these data indicate that extracellular BMP growth factors are required to stimulate epicardial sheet migration in conjunction with TGFβ.

Conclusion

Here, we present simple, highly reproducible screens to identify SOM perturbagens of epicardial behaviors. Further, we have characterized selected compounds to precisely detail their molecular specificity and have identified important new targets of the widely used DM and LDN-193189 molecules. With these reagents, it was possible to determine their potential intervention in three concurrent epicardial behaviors. Specifically, we demonstrate the broad requirement for TGFβ in epicardial differentiation, sheet movement and single cell migration, while determining that BMP signaling is essential for only sheet movement, with little to no impact on the two other functions. Together, these data illustrate that well-characterized analog families of SOMs are valuable tools to intervene on specific behaviors in multi-faceted systems. Additionally, we are the first to show cooperative regulation of epicardial sheet migration by the TGFβ and BMP signaling cascades. Using the DM analog family permitted a co-analysis of multiple signaling factor contributions to this epicardial behavior. During development, cells respond concurrently to a myriad of signals. It is highly probable that multiple signal cascades can and do contribute to the regulation of a single behavior. Developing tools like the DM analog family will permit the

identification of cooperative regulation of epicardial development, which might have been overlooked using less sensitive perturbation techniques.

CHAPTER III

IDENTIFICATION OF A NOVEL BVES FUNCTION: REGULATION OF VESICULAR TRANSPORT

This chapter was published under this title in *EMBO Journal* on January 7th, 2010 (Hager et al, 2010).

Abstract

Blood vessel/epicardial substance (Bves) is a transmembrane protein that influences cell adhesion and motility through unknown mechanisms. We have discovered that Bves directly interacts with VAMP3, a SNARE protein that facilitates vesicular transport and specifically recycles transferrin and β-1 integrin. Two independent assays document that cells expressing a mutated form of Bves are severely impaired in the recycling of these molecules, a phenotype consistent with disruption of VAMP3 function. Using Morpholino knockdown in *Xenopus laevis,* we demonstrate that elimination of Bves function specifically inhibits transferrin receptor recycling, and results in gastrulation defects previously reported with impaired integrin-dependent cell movements. Kymographic analysis of Bves-depleted primary and cultured cells reveals severe impairment of cell spreading and adhesion on fibronectin, indicative of disruption of integrin-mediated adhesion. Taken together, these data demonstrate that Bves interacts with VAMP3 and facilitates receptor recycling both *in vitro* and during early

development. Thus, this study establishes a newly identified role for Bves in vesicular transport and reveals a novel, broadly applied mechanism governing SNARE protein function.

Introduction

Vesicular transport is a conserved process where membrane bound vesicles transfer material within the cell and to the cell surface. Protein trafficking and recycling through vesicles is crucial for a myriad of processes including membrane receptor localization and cell motility. Membrane trafficking consists of both the endocytic and exocytic pathways that modulate receptors, ligands, and molecules that are present on the cell surface. While much is known about this process, identification of novel regulators is essential for a comprehensive understanding of the role vesicular transport plays in a broad spectrum of cell functions.

There are four essential steps of membrane trafficking: vesicle budding, transport, tethering, and fusion (Grosshans et al, 2006; Cai et al, 2007). Coat proteins and adaptor proteins select vesicle cargo and facilitate the initial step of vesicle budding (Cai et al, 2007; Mellman and Nelson 2008). Rab GTPases and motor proteins primarily transport vesicles to the target membrane; however there is accumulating evidence that Rab GTPases participate in every aspect of protein trafficking from budding to docking. (Segev 2001; Grosshans et al, 2006; Pfeffer 2007). Vesicle tethering is carried out by a diverse set of multi-subunit proteins (Grosshans et al, 2006). The final step in membrane trafficking is carried

out by SNARE proteins, which facilitate fusion of intracellular vesicles to the membrane (Brunger 2005; Jahn and Scheller 2006; Leabu 2006). There are three families of SNARE proteins: vesicle-associated membrane proteins (VAMPs); membrane proteins located on the target membrane (syntaxins); and target membrane localized synaptosomal associated proteins (SNAPs) (Brunger 2005; Jahn and Scheller 2006; Leabu 2006). These proteins interact to form a SNARE complex via their coiled-coil SNARE domains (Brunger 2005; Leabu 2006).

Vesicle-associated membrane protein 3 (VAMP3) is a ubiquitously expressed vesicular SNARE protein that binds syntaxin 4 in the basolateral region of epithelial cells to tether vesicular cargo to the membrane (Fields et al, 2007). VAMP3 recycles specific receptors to and from the plasma membrane through the recycling endosome (RE) (Galli et al, 1994; Breton et al, 2000; Polgar et al, 2002; Borisovska et al, 2005). VAMP3 has an established role in the recycling of transferrin and low-density lipoprotein receptor (LDLR), and is required for specific sorting through Adaptor Protein, 1B (McMahon et al, 1993; Fields et al, 2007). Disruption of VAMP3 results in the aberrant localization of both transferrin and LDLR. Overall, VAMP3 is necessary for efficient transport of cargos, which subsequently act to mediate distinct cellular functions. Several studies have shown that VAMP3 is also required for cellular movement through the trafficking of β-1 integrins. Disruption of VAMP3 results in reduced migration rate in wounded epithelial cells and slower cellular spreading on different substrates, as β-1 integrin recycling is impaired (Proux-Gillardeaux et al, 2005;

Skalski and Coppolino 2005; Tayeb et al, 2005; Luftman et al, 2009). Integrins stabilize lamellar protrusions through interactions with the ECM, and thus must be trafficked to the leading edge of the cell during migration (Caswell and Norman 2006; Caswell and Norman 2008). In development, integrin-based cell motility is imperative for proper morphogenesis. This is evident in gastrulation of *Xenopus laevis* (*X. laevis*), where integrin adhesion to fibronectin (FN) underlies mesodermal migration and subsequent formation of the head and trunk (Ramos and DeSimone 1996).

Blood vessel/epicardial substance (Bves) is a highly conserved member of the Popdc family of proteins (Hager and Bader 2009). Bves exists as a dimerized three-pass transmembrane protein with an extracellular glycosylated N-terminus and an intracellular self-associating C-terminal tail (Knight et al, 2003; Kawaguchi et al, 2008). Within the C-terminus is the highly conserved Popeye domain, although no specific function has been linked to this motif (Brand 2005; Osler et al, 2006). A wide variety of adherent tissues express Bves including all three muscle types and various epithelia (Andrée et al, 2000; Osler and Bader 2004; Ripley et al, 2004; Vasavada et al, 2004; McCarthy 2006; Osler et al, 2006; Smith and Bader 2006; Torlopp et al, 2006). Bves localizes to the lateral region of the plasma membrane of epithelial cells, overlapping the distribution of junctional molecules such as E-cadherin, ZO-1, and Occludin (Osler et al, 2005; Osler et al, 2006). In smooth, skeletal, and cardiac muscle Bves is observed around the circumference of cells (Smith et al, 2008). Intracellular punctate

distribution is also observed in both polarized monolayers and unpolarized individual cells *in vitro*.

Disruption of Bves leads to a wide range of cell phenotypes in both vertebrates and invertebrates, the majority of which remain poorly understood at the molecular level. The trans-epithelial resistance of polarized epithelial cells is significantly decreased when Bves protein is knocked down, and junctional proteins such as E-cadherin, ZO-1, and β-catenin fail to traffic to points of cell-cell contact (Osler et al, 2005). Although Bves may play a role in localizing or stabilizing proteins at the membrane, the mechanism by which Bves functions in epithelial biogenesis remains completely unknown.

Most recently, Bves has been shown to interact with a Rho GEF, Guanine Nucleotide Exchange Factor T (GEFT) (Smith et al, 2008). GEFT specifically activates Rac1 and Cdc42 to initiate filopodia and lamellipodia extension through rearrangement of the actin cortical network (Guo et al, 2003; Bryan et al, 2004; Bryan et al, 2006). Disruption of Bves function results in increased cell roundness coupled with decreased activity of Rac1 and Cdc42, indicating decreased protrusion extension. Bves disruption also results in decreased cell movement, which is consistent with decreased Rac1 and Cdc42 activity (Smith et al, 2008). However, the exact mechanism by which Bves regulates GEFT remains unexplained.

Finally, Bves has been studied in the context of *X. laevis* gastrulation, where Bves is the only Popdc family member expressed (Ripley et al, 2006; Hager and Bader 2009). Frog gastrulation is highly dependent upon cellular

migration via integrin recycling (Ramos and DeSimone 1996; Ramos et al, 1996; Marsden and DeSimone 2001; Davidson et al, 2006), and protein knockdown suggests that Bves is necessary for cell movement (Ripley et al, 2006). Again, no prior data demonstrate the precise molecular and cellular mechanism underlying Bves function in *X. laevis*.

An emerging theme is that vesicular transport may underlie the essential biological processes in which Bves is involved: cell-cell adhesion, movement, and epithelial biogenesis. However, little is known about the mechanism by which Bves functions in these diverse yet fundamental processes. As inhibition of Bves function disrupts vital membrane functions and possibly vesicular transport, we conducted a split-ubiquitin screen to identify potential protein-protein interactions at the cell membrane. Here we report that Bves interacts with the SNARE protein, VAMP3, and that disruption or depletion of Bves results in impaired VAMP3-mediated vesicular transport. From these data, we hypothesize that Bves influences VAMP3 function to affect multiple cellular behaviors and suggest that a role for Bves in the general process of vesicular transport may explain the varied nature of previously reported phenotypes.

Materials and Methods

For all assays below data was analyzed with Microsoft Excel and error bars indicate standard deviation (SD); student t-tests were standard.

Antibodies, Constructs, Cell Lines, Tissue Processing, and Protein Harvest

VAMP3-GFP and VAMP2-GFP were generous gifts from Dr. W Trimble (University of Toronto) (Bajno et al, 2000). Rescue RNA that is mutated in the MO binding site was used for *X. laevis* experiments as reported (Ripley et al, 2006). Rat VAMP3 was cloned into pCMV-3tag-4A, and RNA synthesized with mMESSAGE mMACHINE (Ambion). Bves antibodies SB1 and B846 were reported (Wada et al, 2001; Smith and Bader 2006). All other antibodies and reagents were obtained commercially as follows: Anti-VAMP3 (Novus Biologicals, NB300-510 and Santa Cruz, sc-18208, clone N-12); Anti- β-1-FITC (BD Pharmingen, clone Ha 2/5 555005); Anti-CD29 (BD Transduction Laboratories, clone 18, 610468); Anti-CD29 (BD Transduction Laboratories, clone Ha 2/5, 555003); Anti-8C8 supernatant (*X. laevis* β-1 integrin) (Developmental Studies Hybridoma Bank); Anti-GFP (Clonetech, JL8); Anti-myc (Sigma, M4439 and C3956); Anti-GST (GE Healthcare); and Phalloidin-488 and 568 (Molecular Probes). MDCK cells were obtained from ATCC. Tissue processing and western blotting followed standard protocols (Ripley et al, 2006).

Split-Ubiquitin Screen

A split-ubiquitin screen was conducted by Dualsystems (Zurich, Switzerland). Full-length mouse Bves was cloned into pCCW-Ste and screened against a mouse adult heart library cloned into pDSL-Nx. VAMP3 passed all selection tests.

GST-pulldown and Co-IP

Lysates were prepared as follows: COS-7 cells were transfected with either VAMP3-GFP alone or both VAMP3-GFP and Bves-myc and confluent monolayers harvested by rocking at 4° for one hour in CHAPS buffer (50mM Tris HCl pH 8.0, 150mM NaCl, 10mM EDTA, 1% CHAPS) plus protease inhibitors (Roche, 11697498001). Lysates were collected and spun down at 18,000 x g for 30 minutes at 4° C. Co-IPs were conducted using Protein G Magnetic Dynabeads and a Dynal MPC Magnet as per manufacturer's instructions (Invitrogen). Bves-GST-Pulldowns of VAMP-GFP proteins were conducted as previously published (Smith et al, 2008); western blots were standard.

Generation of Stable Cell Lines

The extracellular and transmembrane domains of mouse Bves (amino acids 1-118; referred to as Bves118) were cloned in frame into pCMV-3myc-4A (Stratagene). Bves118 was nucleofected into MDCK cells according to manufacturer's specifications (Amaxa). Three individual clones were selected and then maintained in 400µg/mL of G418. RT-PCR and immunofluorescence confirmed the expression of stably transfected tagged proteins (Figure 4.18). Cell lines expressing wildtype or mutant Tetanus toxin, WT TeNT and mut-TeNT, respectively have been described (Proux-Gillardeaux et al, 2005).

Transferrin Assays

MDCK cells: Uptake of Alexa-633 or Alexa-488 labeled transferrin (Invitrogen, T23362, T13342) was assessed using flow cytometry. Briefly, cells that had been passaged three times were incubated in DMEM and 0.2% BSA for 2 hours at 37° C and then incubated for 30 minutes with 50ug/mL of labeled transferrin at 4° C in the dark. Cells were allowed to internalize labeled transferrin at 37°C for the indicated times, and then washed 4X with ice cold PBS on ice. Cells were probed for Mean Fluorescence Intensity (MFI) using a BD FACS Canto II; data were acquired with Diva 6.0, analyzed with WinList, and are reported as the average MFI from four different experiments.

Animal Caps: Internalization of labeled transferrin-633 (Invitrogen T23362) in animal caps was measured in a T-format spectrofluorometer (PTI Quantamaster 2000-7SE). Animal caps were dissected at stage 9-10 in 1X Modified Barth's saline (MBS) and 0.1% BSA and then serum starved in agar-coated dishes for 2 hours in 1X MBS. Caps were incubated with 50µg/mL of transferrin-633 for 30 minutes at 4° C in the dark, and then allowed to uptake transferrin-633 for 25 minutes (first five minutes at 37° C; last 20 minutes at room temperature with gentle agitation). Caps were washed 5X with cold 1X MBS on ice, briefly spun down at 8,000 x g at 4° C, and then 4 caps/well were solubilized by vortexing for 15 seconds in 0.2 mL of 0.25% Triton X-100 in PBS. Protein was harvested by centrifuging at 15,000 x g for 5 minutes, and the supernatant was analyzed for fluorescence (excitation = 488; emission = 633). Protein concentration of the animal caps was determined using a BCA assay (Thermo

Scientific 23227) and fluorescent units/μg of protein determined. For side by side comparison of control and experimental models, Bves MO, Bves MOR, VAMP3 MO and VAMP3 MOR data are reported as a percentage of the control (COMO).

Scratch Assay

A scratch assay was performed and scored for the amount of internalized β-1 integrin according to Proux-Gillardeaux et al. For scratch assays that directly compared TeNT cells and Bves118 cells, CD29 was conjugated to Alexa-564 (Molecular Probes) and conducted in triplicate.

Cell Spreading Assay in MDCK Cells

Cell spreading was defined as the increase of cell area over time prior to polarized cell movement. One day before cell spreading analysis, cells were plated at single cell density so that they would be contact naïve at the time of the assay. On the day of image acquisition, cells were trypsinized and plated at single cell density on MatTek dishes (MatTek Corporation) coated with 25μg/mL of FN Sigma (F4759). Attached yet rounded cells were chosen 45 minutes after plating and DIC images acquired with a temperature and CO_2-controlled WeatherStation as part of a DeltaVision platform (Precision Control). Images were obtained with an Olympus IX71 inverted microscope and a CoolSNAP-HQ2 CCD camera using the 40X objective at intervals of one minute for one hour. Image deconvolution was carried out with the SoftWorx software. Metamorph 6.0

was used to determine cell area and construct kymographs from DIC images every tenth minute.

X. laevis Embryos

Female *X. laevis* were obtained from Nasco, primed, and fertilized by standard methods (Ripley et al, 2006). Images of appropriately staged embryos (Nieuwkoop and Faber 1994) were captured with Magnafire (Olympus America Diagnostics).

Microinjection and Morpholino Treatment

Embryos were microinjected with 5nL into both cells at stage 2; embryos were injected in 5% Ficoll in 1X Steinberg's Solution (SS), then switched to 0.1X SS before gastrulation. Bves MO, VAMP3 MO, or COMO were injected into sister embryos along with mGFP or mRFP (1.5ng) as a tracer at a concentration of 20ng (stage 35-42 analysis only) or 40ng/embryo (Gene Tools, LLC) (Wallingford et al, 2000; Ripley et al, 2006). For transferrin assays, 100pg of Rescue RNA (described above) was co-injected along with Bves MO or VAMP3 MO. Xbves Rescue RNA has been reported previously (Ripley et al, 2006) and is mutated in the MO binding sequence, thus not recognized by Bves MO. The most successful MO for knockdown of *X. laevis* VAMP3 was designed against the 5' UTR, approximately 20 base pairs upstream from the ATG site: GGACACCGGTCCGACTTTACTC (Gene Tools, LLC). Note this sequence is

perfectly conserved with *Xenpus tropicalis*, but has no conservation with rat VAMP3 (EST databases).

SEM

Embryos were fixed and processed for SEM with standard methods and HM was dissected out (the overlying BCR was peeled away from this region to expose cells that are attached to FN) with eyebrow knives. SEM images were quantified as follows: cells were chosen from random fields from ten different embryos and measured for cellular overlap and polarity using the leading edge as a reference point. Overlap was defined as the number of overlapping cell bodies or lamellipodia for each selected cell. Polarity was determined by defining the length/width axis (longest axis of the cell intersected perpendicularly by the widest part of the cell), measuring the deviation of this axis from a set point, and then averaging the standard deviations from the defined point.

***X. laevis* Microdissections, Adhesion Assays, and Spreading Assays**

Microdissections of *X. laevis* embryos were carried out according to (Ren et al, 2006). Explants were disassociated in Ca^{2}+ Mg^{2}+ free MBS and single cells were plated in MBS on slides (for adhesion assays; LabTek) or on Mat Tek dishes (for spreading assays) coated with 200µg/mL of FN (Sigma F4759). Explants from several embryos (control or experimental) were pooled and plated for either adhesion or spreading assays.

Adhesion assays on FN were conducted and scored as described (Ramos et al, 1996). Cells were cultured for two hours, washed three times in MBS to remove non-adhered cells, fixed in PFA overnight at 4° C, labeled with Phalloidin, and imaged with a Zeiss Inverted LSM 510 Confocal Microscope using a 40X objective. Round cells are attached to the plate and spherical, while spread cells are elongated and had two or more lamellipodia as previously defined (Ramos et al, 1996).

For spreading analysis, time-lapse images were obtained with the DeltaVision platform. Movies of mGFP or mRFP labeled cells were imaged over a 35 minute timeframe with fluorescent and DIC images being collected every minute. The point of cell/matrix interaction was used as the focal point in obtaining these images. Quantification of lamellipodia and cell spreading are as follows: for at least 12 different cells, the average number of lamellipodia (defined here as 10 μm extensions devoid of yolk granules with distinct matrix attachment sites) was determined for ten time points at three minute intervals over the period of culture for both control and experimental groups. Metamorph 6.0 was used to analyze every third frame to determine the cell area and construct kymographs.

Results

Bves interacts with VAMP3

Given the protein distribution of Bves, and previously reported phenotypes, we conducted a split-ubiquitin screen to detect Bves-interacting membrane proteins with characterized functions in cell movement (Dünnwald et al, 1999).

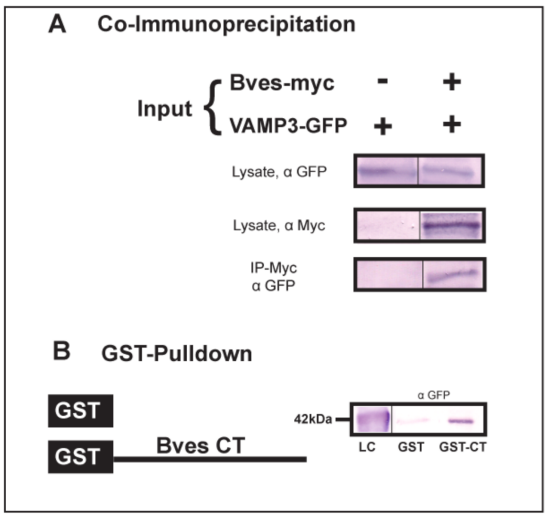

Figure 3.1 Bves and VAMP3 interact. For Co-IP (A), COS-7 cells were transfected with tagged proteins: VAMP3-GFP alone, or VAMP3-GFP and full length Bves-myc. Cell lysates were pulled down with myc and blotted for GFP. In GST pulldown assays (B), the C-terminus of Bves fused to GST (GST-CT) was sufficient to pulldown transfected VAMP3-GFP from COS-7 cell lysate. Loading controls (lysate in A and LC in B) are shown for comparison.

VAMP3, a SNARE protein that facilitates the fusion of apposing membranes during vesicular transport (McMahon et al, 1993), was identified as a binding partner in this screen. Importantly, VAMP3 transports membrane proteins, and is required for the vesicular transport underlying cell motility (Galli et al, 1994; Proux-Gillardeaux et al, 2005; Skalski and Coppolino 2005; Tayeb et al, 2005). As Bves is also required for cell motility, and VAMP3 has a known function in this process, we chose to probe this interaction further.

To confirm this result, we determined if Bves and VAMP3 proteins interact biochemically using co-immunoprecipitation (co-IP) and GST-pulldown assays. As seen in Figure 3.1A, VAMP3 was precipitated with Bves. Additionally, GST-pulldown assays demonstrated a specific interaction between Bves and VAMP3, localized to the intracellular C-terminal Popeye domain (Figure 3.1B).

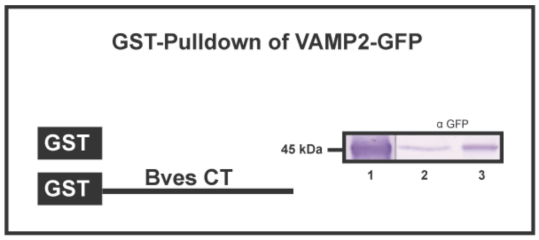

Figure 3.2 GST pulldown demonstrates Bves and VAMP2-GFP interact biochemically. Loading control (Lane 1) detects the mobility of VAMP2 by immunoblotting. GST alone does not interact with VAMP2 above background (Lane 2). The C-terminus of Bves fused to GST was sufficient to pulldown transfected VAMP2-GFP from COS-7 cell lysate (Lane 3), demonstrating this intracellular portion of the protein binds VAMP2-GFP, in addition to VAMP3-GFP. Lane 1. VAMP2-GFP Loading Control ; Lane 2. GST/VAMP2-GFP; Lane 3. GST-CT/VAMP2-GFP.

Interestingly, Bves also interacts with VAMP2 via GST-pulldown (Figure 3.2) VAMP2 and VAMP3 are highly homologous, with only one amino acid difference in their SNARE binding domain (McMahon et al, 1993), suggesting a conserved interaction between Bves and SNARE proteins. Taken together, these data confirm the direct interaction of Bves through its cytoplasmic tail with VAMP3.

Bves and VAMP3 co-localize

Bves and VAMP3 exhibit similar dynamic distributions that are both at the cell periphery and in intracellular compartments (Osler et al, 2005; Hager and Bader 2009). Co-localization in Madin-Darby Canine Kidney (MDCK) cells of endogenous Bves (Figure 3.3A) and exogenously expressed VAMP3-GFP (Figure 3.3B) is readily observed both at the cell periphery and in intracellular vesicles (merge in Figure 3.3C, arrows). While overlap is extensive, it is not complete, as some intracellular vesicles labeled with Bves are not co-labeled with VAMP3. Examining endogenous localization in confluent epithelial sheets,

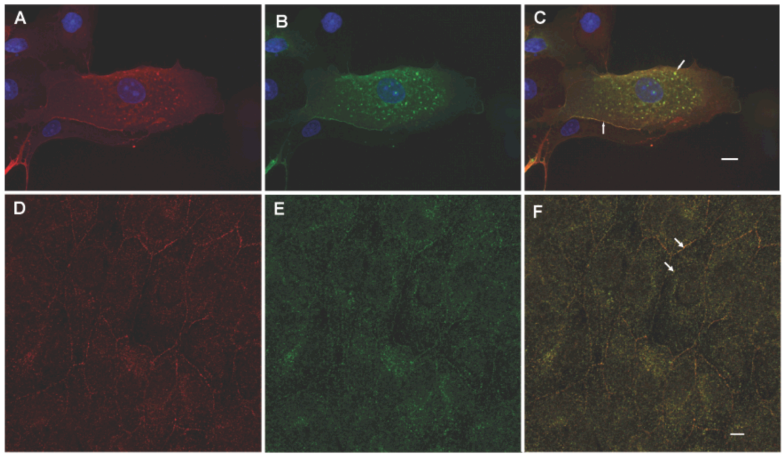

Figure 3.3 Bves and VAMP3 co-localize in MDCK cells. Both endogenous Bves (A) and transfected VAMP3-GFP (B) are observed at the membrane and in vesicles. The endogenous distribution of both proteins also demonstrates this same localization pattern (Bves, D; VAMP3, E), and Bves and VAMP3 co-localize at both of these subcellular locations (arrows, C, F). Scale bars are 5μm.

Bves (Figure 3.3D) and VAMP3 (Figure 3.3E) co-localized in the lateral portion of MDCK cells and staining is also observed in intracellular vesicles (merge in Figure 3.3F, arrows). These data confirm that overlap of these two proteins is consistent with their previously reported endogenous distribution profile (Osler et al, 2005; Fields et al, 2007). Disruption of VAMP3 function (detailed below) resulted in a significant decrease in the presence of Bves at the cell membrane (Figure 3.4) while expression of a truncated Bves lacking the VAMP3 binding domain (also detailed below) produced only minor changes in protein distribution.

While VAMP3 is ubiquitously expressed across all non-neuronal tissue types, Bves is present at high levels in muscle as well as in other adherent or excitable tissues (McMahon et al, 1993; Hager and Bader 2009). Thus, we characterized endogenous protein distribution in mouse heart and skeletal muscle to probe for colocalization. Significant co-localization was observed in

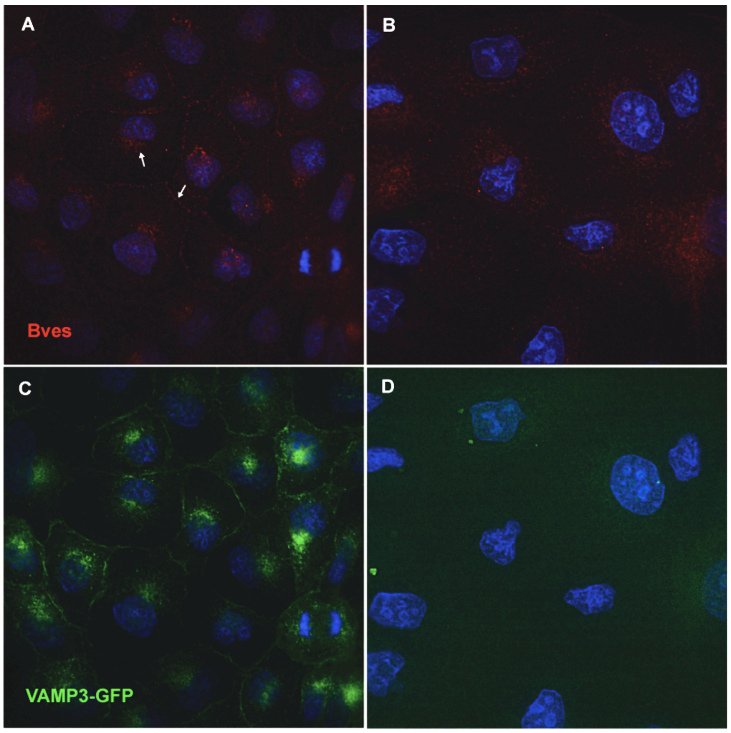

Figure 3.4 Bves localization in TeNT cell lines. In mut-TeNT cells, which express VAMP3-GFP (C), Bves (red) localization is seen intracellularly and at the membrane in confluent epithelial sheets (A, arrows). However, whenVAMP3-GFP is cleaved by wildtype Tetanus toxin (D), Bves localization is reduced at the membrane, although intracellular labeling is still visible (B).

both muscle types, although overlap was not absolute (Figure 3.5). Co-localization was seen primarily at the circumference of the myocytes, with certain muscle cells demonstrating more intense labeling (Figure 3.5C, G, white arrows). Intensity profiles (Figure 3.5D, H) of both Bves and VAMP3 signal demonstrate the high degree of co-localization (Figure 3.5C, G; red arrows indicate area of intensity profile). As Bves and VAMP3 both interact and co-localize, we next focused on functional assays to determine the potential importance of this interaction.

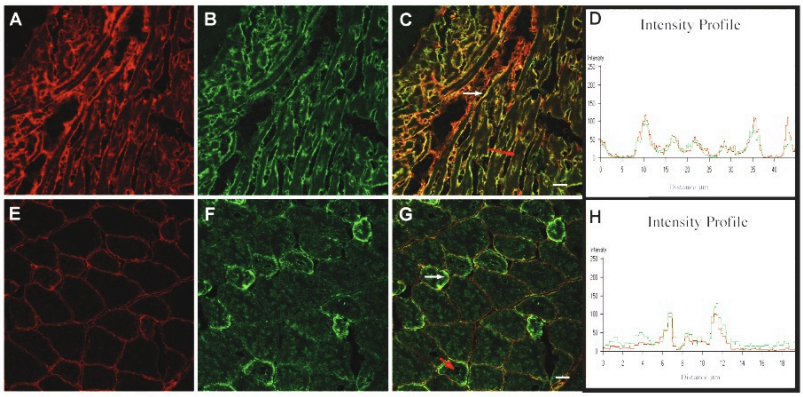

Figure 3.5 Endogenous Bves and VAMP3 co-localize in muscle. Bves (A, E) and VAMP3 (B, F) are seen at the cell periphery in adult cardiac (A-C) and skeletal muscle (E-G). Areas of intense co-localization are denoted by the white arrows (C, G). Red arrows indicate the area of the fluorescent intensity profile for cardiac (D) and skeletal muscle (H). Scale bars are 20μm.

Transferrin recycling is attenuated in cells with disrupted Bves function

VAMP3 is required for recycling of transferrin, as cleavage of VAMP3 disrupts vesicular transport of this receptor (McMahon et al, 1993; Galli et al, 1994). To identify the potential role of Bves in VAMP3-dependent recycling using a standard transferrin uptake assay, we developed an MDCK cell line that stably expresses only the first 118 amino acids of Bves (Bves118). Bves118 lacks the intracellular VAMP3-binding domain and contains only the short extracellular and transmembrane domains. Transferrin endocytosis was analyzed at 5, 10, and 20 minutes (Figure 3.6A), and the mean fluorescence intensity (MFI) was analyzed in MDCK and Bves118 cells. At 5 minutes internalization, average MFI (which directly correlates to the amount of endocytosed transferrin) for MDCK cells was 46.53, whereas Bves118 cells had an average MFI of 16.41, demonstrating decreased uptake of labeled transferrin. This trend continued at 10 and 20 minutes internalization with Bves118 cells having severely decreased

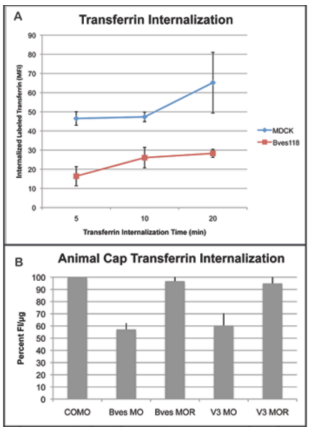

Figure 3.6 Transferrin uptake is attenuated when Bves is disrupted. (A) MDCK and Bves118 cells internalized labeled transferrin for 5, 10, or 20 minutes. Transferrin uptake, as measured by the MFI, was significantly decreased in Bves118 cells at all time points. (B) When normalized with Control values (100%), Bves MO and VAMP3 (V3) MO treated caps were impaired in internalization of labeled transferrin/µg of total protein. Transferrin uptake is restored when Bves MO or V3 MO are co-injected with rescue Bves (Bves MOR) or VAMP3 (V3 MOR) RNAs, demonstrating that this phenotype is specific to depletion of the respective proteins.

internalization of labeled transferrin relative to MDCK cells (5 minutes: $p < 0.001$; 10 minutes: $p < 0.003$; 20 minutes: $p < 0.0036$). Disruption of transferrin kinetics was also demonstrated by a recycling assay, as labeled transferrin was exocytosed from Bves118 cells more slowly compared to controls (Figure 3.7). This phenotype is consistent with disrupted VAMP3 function and supports the hypothesis that Bves-VAMP3 interaction is necessary for VAMP3-mediated vesicular transport.

To corroborate and extend these studies with an *in vivo* model and directly compare the effects of transferrin recycling between Bves- and VAMP3-depleted embryos, we used a Morpholino (MO) knockdown and rescue strategy in *X. laevis* (Ripley et al, 2006). Embryos were injected with Bves MO, VAMP3 MO, or Control MO (COMO); alternatively, sister embryos were co-injected with Bves

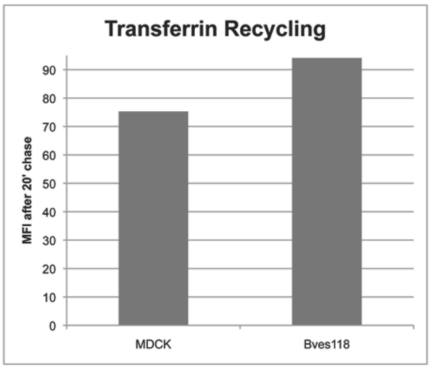

Figure 3.7 Transferrin Recycling in Bves118 cells. MDCK or Bves118 cells were serum starved for three hours in DMEM plus 0.2% BSA at 37° C, and then allowed to uptake Transferrin-633 (25µg/mL) for 60 minutes at 37° C. Cells were then washed 4X on ice with cold PBS with 0.1% BSA and incubated in DMEM plus 0.2% BSA with 5mg/mL of unlabeled APO transferrin for 20 minutes at 37° C. After the twenty minute chase with unlabeled transferrin, cells were probed for MFI using a MACSQuant flow cytometer (Miltenyi Biotech). It was found that Bves118 cells had a higher MFI (94.1±33) than MDCK cells 75.3±28, indicating that exocytosis of transferrin, a process mediated by VAMP3, was impaired in cells expressing mutated Bves.

MO or VAMP3 MO and their respective rescue RNAs (Bves MOR, VAMP3 MOR). Isolated animal caps, which express the transferrin receptor (NCBI, EST databases), were allowed to endocytose transferrin-633 for 25 minutes and the fluorescent intensity (FI)/µg of animal cap protein was determined. As seen in Figure 3.6B, recycling of labeled transferrin in Bves MO and VAMP3 MO treated animal caps is severely reduced relative to COMO treated caps. When normalized against COMO treated caps (100%), Bves MO treated animal caps display only 57.2±5.06% of FI/µg, demonstrating that recycling of labeled transferrin is inhibited when Bves is depleted (Table 2). Similarly, VAMP3 MO treated caps internalize 60.4±9.9% of labeled transferrin relative to COMO (Table 2). This reduction in recycling of labeled transferrin in animal caps is completely dependent upon knockdown of Bves or VAMP3, as these phenotypes are

Table 2.

Figure 3.6

Transferrin Internalization in Animal Caps

% FI/µg of COMO

COMO	Bves MO	Bves MOR	VAMP3 MO	VAMP3 MOR
100	57.2±5.06	96.8±4.57	60.4±9.9	94.9±12.14
P Value < 0.0001	P Value < 0.2111		P Value < 0.0002	P Value <0.4340

rescued in caps co-injected with Bves rescue RNA along with Bves MO, or VAMP3 rescue RNA along with VAMP3 MO (Bves MOR: 96.8±4.57% and VAMP3 MOR: 94.9±12.14% of FI/µg relative to COMO treated caps; Table 2). Taken together, these two independent methods demonstrate that recycling of transferrin is attenuated after Bves disruption, suggesting that VAMP3-mediated transport is dependent on Bves function.

VAMP3-mediated recycling of β-1 integrin is impaired in cells expressing mutated Bves

VAMP3 function is necessary for the recycling of β-1 integrin during cell movement (Proux-Gillardeaux et al, 2005; Skalski and Coppolino 2005; Tayeb et al, 2005; Luftman et al, 2009). Proux-Gillardeaux et al. have reported an *in vitro* scratch assay that directly tests VAMP3-mediated recycling of β-1 integrins by quantifying its recycling over time; we adapted this method by using β-1 integrin labeled with FITC. In wildtype MDCK cells, 59.6 ±5% of cells at the free edge of the wound were positive for labeled integrin (Figure 3.8A-C; Table 3). Bves118 cells showed a dramatic decrease in endocytosed FITC-labeled integrins (Figure

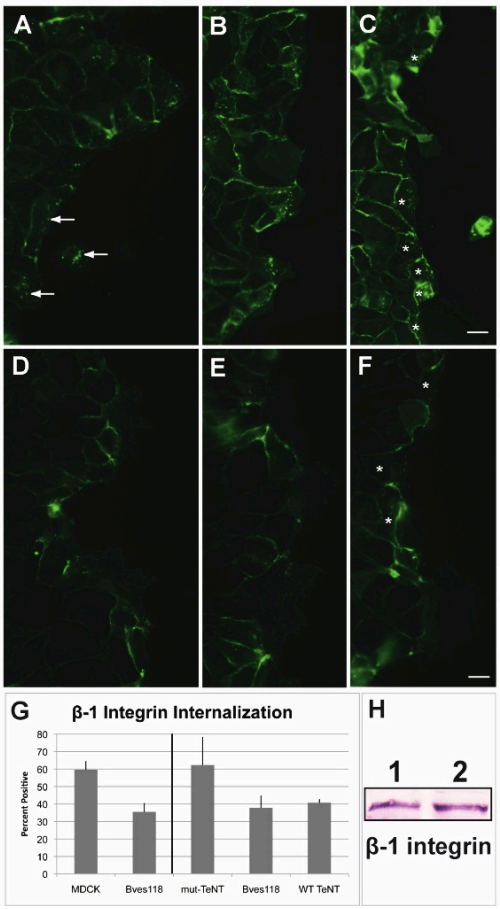

Figure 3.8 Cells stably expressing mutated Bves have decreased integrin recycling. A wounded monolayer of MDCK cells (A-C) internalized FITC labeled β-1 integrin antibody (panel A, arrows: intracellular labeling) as cells migrated to close the wound. β-1 integrin recycling is visualized by the presence of FITC-labeled protein in intracellular compartments. In Bves118 cells, integrin recycling was attenuated (D-F), as seen by decreased intracellular punctate labeling, although integrin expression levels of Bves118 cells are consistent with MDCK cells (H). This decrease in integrin internalization is also seen when directly compared to WT TeNT and mut-TeNT cells (G; SI Fig 6). Cells marked with an asterisk (C, F), were counted as integrin positive in quantification (G, Table 3). Scale bars are 20μm.

3.8D-F). Note the limited number of Bves118 cells with internalized FITC-labeled integrin (35.5±5%) as compared to wildtype MDCK cells (Figure 3.8G; Table 3, $p < 0.0001$) even though β-1 integrin protein levels remain the same (Figure 3.8H).

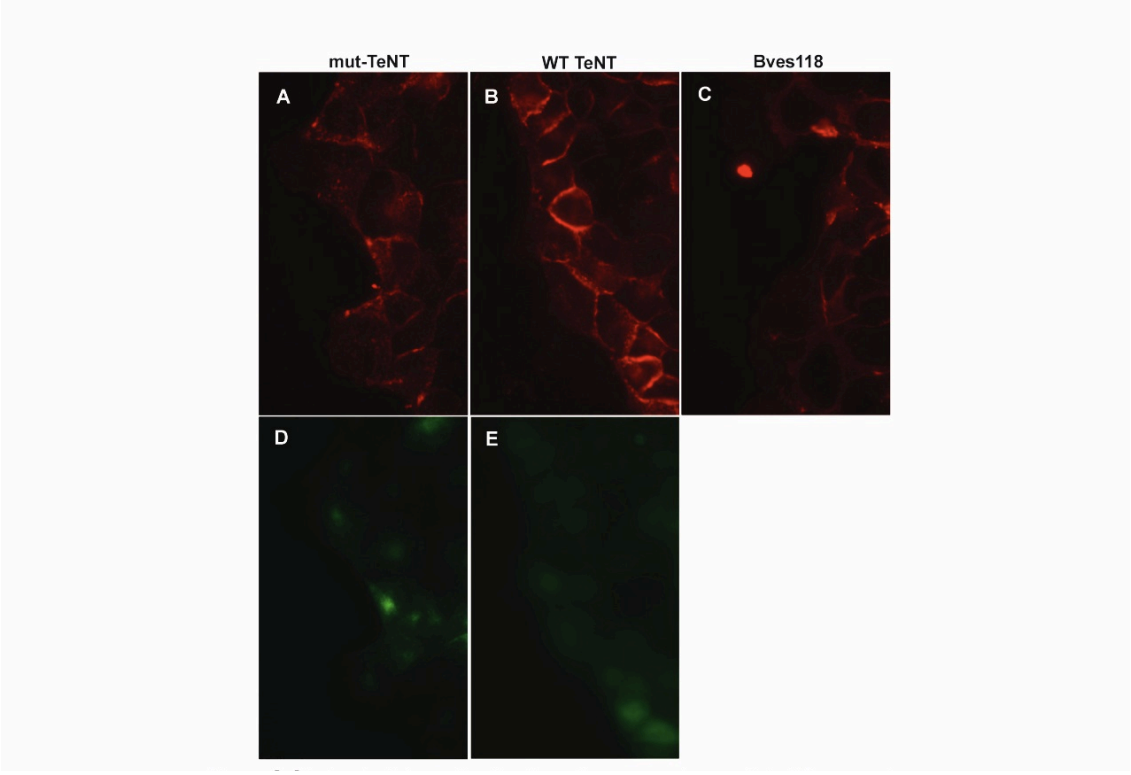

Figure 3.9 Integrin internalization in cells expressing mutated Bves and VAMP3. As demonstrated in Figure 4.8, Bves118 cells have decreased internalization of β-1 integrin-FITC when induced to migrate. To verify this result, we directly compared Bves118 cells uptake of β-1 integrin-Alexa-564 with cells without VAMP3. As Tetanus toxin selectively cleaves VAMP1-3 (McMahon et al., 2003), Proux-Gillardeaux et al., 2005 utilized this property to create cell lines without VAMP3, which we used here. In our hands, 62.4±16% of MDCK cells expressing VAMP3-GFP and mutated and inactive form Tetanus toxin (mut-TeNT were positive for internalized β-1 integrin; visualized by the punctate intracellular labeling of VAMP3-GFP, panel D). Note that the mutated toxin serves as a positive control as VAMP3 remains intact. In contrast, MDCK cells expressing VAMP3-GFP and wild type Tetanus toxin (WT TeNT) display a diffuse intracellular labeling due to the of cleavage of VAMP3-GFP (panel E). When expressing the WT TeNT, only 40.8±2% of cells were positive for internalized β-1 integrin (B). This decrease in integrin internalization was reported previously in Proux-Gillardeaux et al., 2005. In a side-by-side comparison, 37.8±7% of Bves118 cells were positive for intracellular integrin labeling (panel C), demonstrating that β-1 integrin internalization is attenuated in Bves118 cells, with similar internalization rates as cells without VAMP3. Data is quantified in Table II.

To confirm that disruption of Bves does in fact phenocopy disruption of VAMP3,

we repeated this assay using β-1 integrin antibody (CD29, clone Ha 2/5)

Table 3.

Figure 3.8

β-1 Integrin Recycling

	MDCK	Bves118
% Positive	59.6±5	35.5 ±5
Total Cells	1955	2597
		P Value < 0.0001

	mut-TeNT	Bves118	WT TeNT
% Positive	62.4±16	37.8±7	40.8±2
Total Cells	733	768	816
		P Value < 0.004	P Value < 0.008

conjugated to Alexa-564, and directly compared cells expressing wildtype Tetanus toxin (WT-TeNT, which effectively cleaves VAMP3, rendering it unable to transport integrin) with Bves118 cells. Using the exact cell line in which disrupted integrin recycling upon VAMP3 knockdown was first reported (Proux-Gillardeaux et al, 2005), along with the control cell line that expresses mutant inactive Tetanus neurotoxin (mut-TeNT), we determined that in a side-by-side comparison, 37.8±7 % of Bves118 cells and 40.8±2% WT TeNT cells internalized labeled integrins, while 62.4±16% of mut-TeNT cells were positive for integrin internalization (Figure 3.8G; Figure 3.9). Additionally, internalized β-1 integrin co-localized with both Bves and VAMP3 antibodies (Figure 3.10), supporting a role for Bves and VAMP3 in recycling of integrins. These data demonstrate that disruption of Bves and VAMP3 result in similar phenotypes and further supports the hypothesis that intact Bves function is required for proper VAMP3-mediated

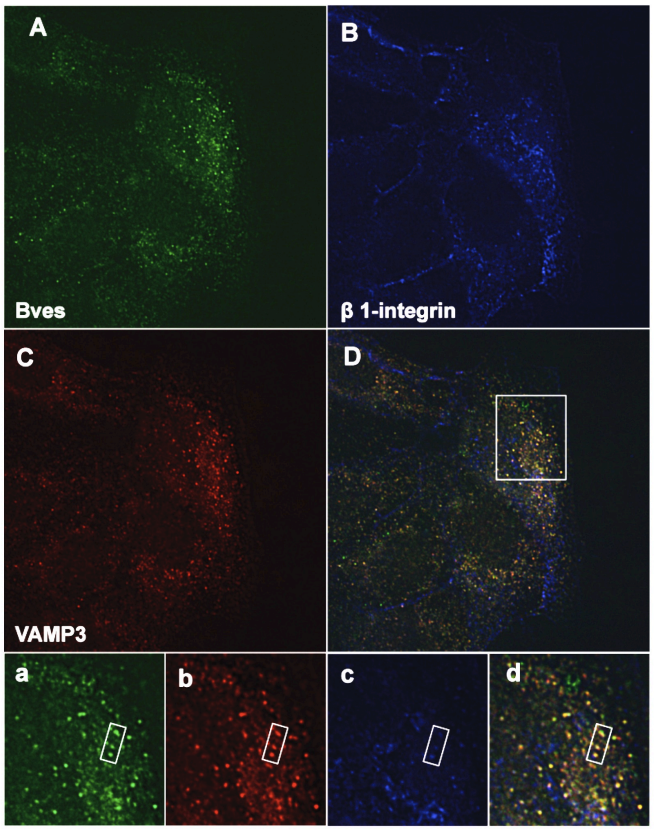

Figure 3.10 Co-localization of Bves, VAMP3 and β-1 integrin. Confluent MDCK cells were wounded via scratch and allowed to internalize β-1 integrin-FITC (B) as described in the methods. Antibody labeling of Bves (A) and VAMP3 (C) revealed these proteins co-localize with endocytosed integrins in individual vesicles as seen in the merged image (D, white vesicles). For better visualization, corresponding magnified views of panels A, B, and C of the area outlined in D are seen in panels a, b, c, and d. The white box surrounds three separate vesicles, all of which are positive for Bves, VAMP3, and β-1 integrin.

recycling of different molecules.

Expression of mutated Bves or TeNT disrupts cell spreading

As Bves118 and WT TeNT cells have impaired integrin uptake during cell movement, we determined if another integrin dependent function, cell spreading, was also disrupted. Cells were plated on FN at single cell density and allowed to adhere for 45 minutes prior to time-lapse analysis. At time 0, all four cell types, MDCK (Figure 3.11A), Bves118 (Figure 3.11C), mut-TeNT (Figure 3.11E), and

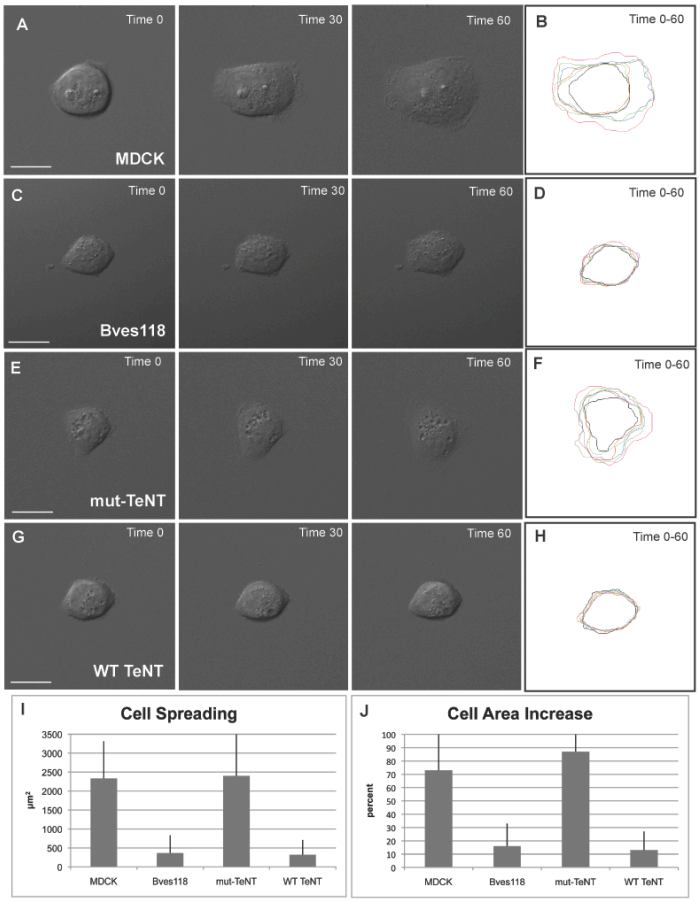

Figure 3.11 Cell Spreading is attenuated with disruption of Bves or VAMP3 function. Time-lapse analysis indicates that cell spreading, or the increase of area prior to polarized cell movement, is decreased in Bves118 cells (C) compared to MDCK cells (A). Similarly, WT TeNT (G) cells have less cell spreading than mut-TeNT cells (E). Kymographs of cell spreading over time demonstrate the difference in the degree of cell spreading between control and experimental groups (MDCK, panel B vs Bves118, panel D; and mut-TeNT, panel F vs WT TeNT, panel H). Note the similarity in cell areas (I) and percent increase of cell area (J) between experimental groups and control groups as determined from composite kymographs (B, D, F, H). Scale bars are 20µm.

WT TeNT (Figure 3.11G) displayed similar areas and it was evident that cell protrusions were beginning to form. However, after one hour of image acquisition, MDCK and mut-TeNT cells (Figure 3.11A, E; Time 60) greatly increased cellular areas (Figure 3.11J, Table 4), 73% and 87% respectively, while Bves118 and WT TeNT cells (Figure 3.11C, G; Time 60) only increased cell areas by 16% and

Table 4.

Figure 3.11

MDCK Cell Spreading Quantification

	MDCK	Bves118	mut-TeNT	WT TeNT
% Area Increase	73±30	16±17	87±49	13±14
P Value <		0.0001		0.0007

	MDCK	Bves118	mut-TeNT	WT TeNT
Cell Spreading (μm^2)	2,337±979	363±466	2,401±1111	318±396
P value		0.0001		0.0002

13%, respectively (Figure 3.11J; Table 4). Kymographs of cell spreading over time reveal significant differences in cell spreading between MDCK cells (Figure 3.11B) and Bves118 cells (Figure 3.11D); as well as between mut-TeNT cells (Figure 3.11F) and WT TeNT cells (Figure 3.11H; Table 4). It should be noted that in a direct comparison of the area of cell spreading (Figure 3.11I), both experimental cell lines have similar areas of cell spreading (Bves: 363μm^2; and VAMP3: 318μm^2), which are significantly reduced from the areas observed in both control cell lines (MDCK: 2,337μm^2; and mut-TeNT: 2,401μm^2). Individual frames of composite kymographs seen in Figure 3.11B, D, F and H are given in Figure 3.12. These data, which are corroborated using the *X. laevis* system (see below), demonstrate that cell spreading is significantly impaired in cells with mutated Bves or VAMP3, suggesting that interaction of these two proteins is important for integrin-mediated processes.

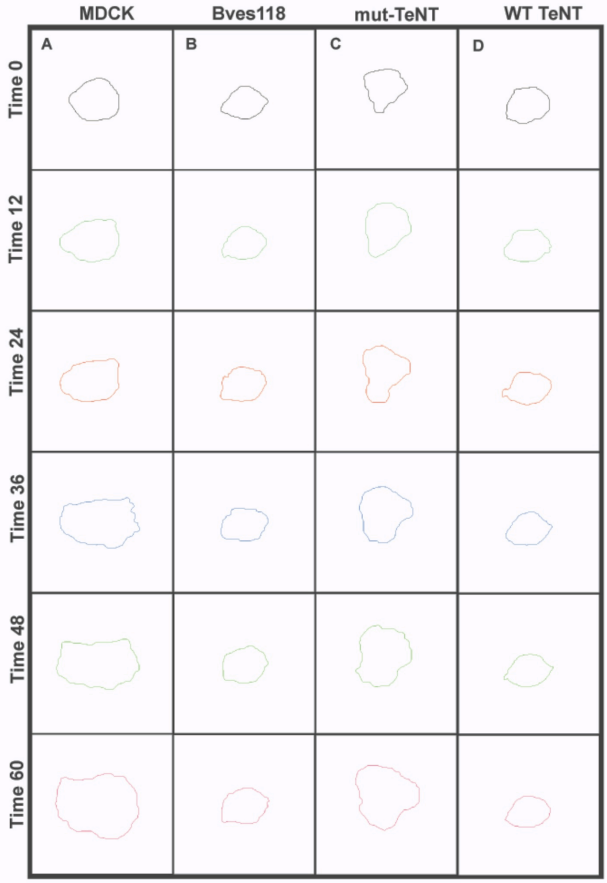

Figure 3.12 Individual frames of time-lapse imaging seen in Figure 4.11. As seen in Figure 4.11, Bves118 and WT TeNT cells have decreased cell spreading on FN. Cell tracings from different time points demonstrate that although cell area is similar in all four cell lines at the onset of image acquisition (panels A-D, Time 0), during the period of analysis, MDCK and mut-TeNT cell lines increase their cellular area more quickly than Bves118 and WT TeNT cell lines (panels A-D, Time 60). Individual cell tracings throughout time are shown here and are displayed as a composite in Figure 4.11, panels B, D, F, and H.

Morphological defects are observed in Bves- and VAMP3-depleted *X. laevis* embryos

Having established that Bves is required for VAMP3-mediated vesicular transport *in vitro*, we next determined the *in vivo* significance of this interaction. Gastrulating *X. laevis* embryos undergo extensive integrin-dependent cellular

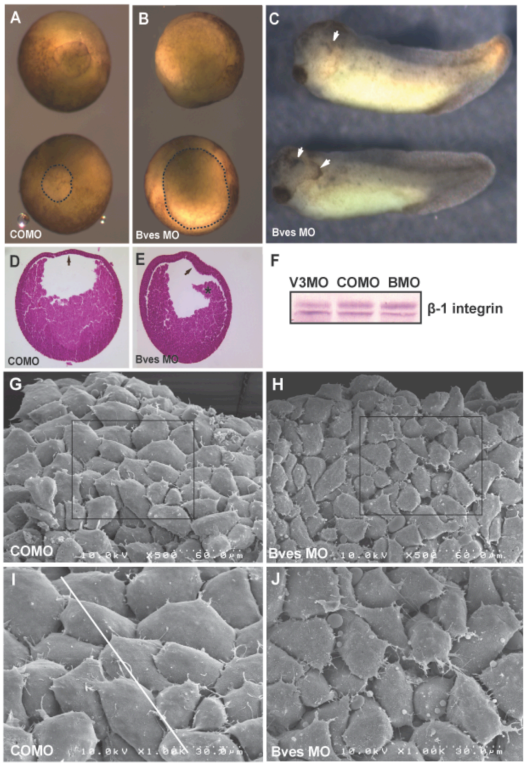

Figure 3.13 Bves depletion in *X. laevis* embryos. Blastopore closure in embryos injected with Bves MO was dramatically decreased (B) in comparison to embryos injected with COMO (A). The blastopore is outlined in the bottom embryo in panels A and B for better visualization. Anterior defects are observed in Bves-depleted stage 35 embryos (C), characterized by disrupted eye morphogenesis and ectodermal outgrowths (arrows). Histological staining demonstrates the BCR has failed to intercalate properly, and remains thickened (E, arrow), whereas the BCR of control embryos has thinned (D, arrow). Also, the involuting HM has become detached from the BCR in Bves depleted embryos (E, asterisk). Integrin levels in Bves MO treated embryos (and in VAMP3 treated embryos) are similar to COMO treated embryos (F). In SEM analysis of HM, COMO injected embryos display a distinct pattern of tightly overlapped and polarized cells (G, I, white line indicates direction of polarity), whereas Bves MO injected embryos lack directionality, have increased spaces between cells, and exhibit irregular cell shapes (H, J; quantified in Table 5). Panels I and J show magnified views of the boxed areas in panels G and H, respectively.

rearrangement, hence this is an advantageous system in which to analyze Bves function in development (Keller 1980; DeSimone et al, 2005). Bves-depleted

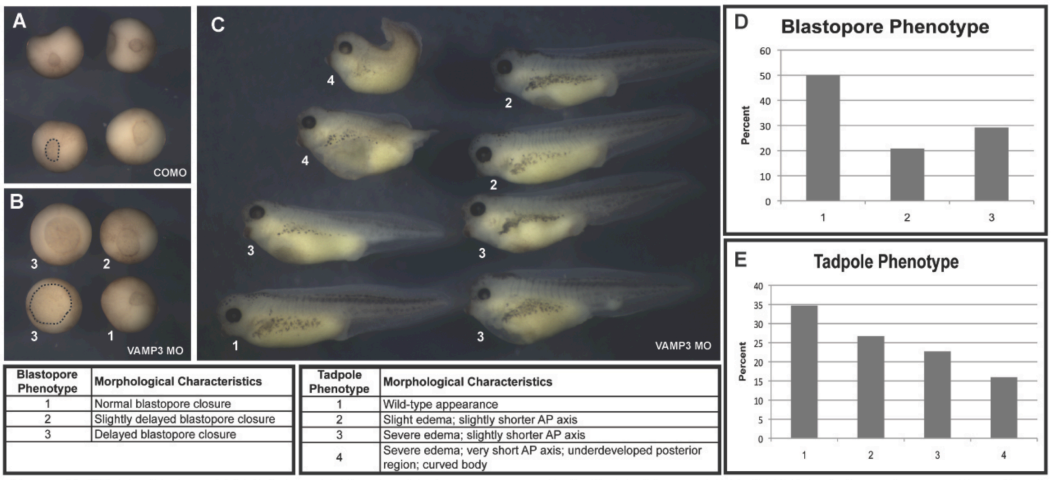

Blastopore Phenotype	Morphological Characteristics
1	Normal blastopore closure
2	Slightly delayed blastopore closure
3	Delayed blastopore closure

Tadpole Phenotype	Morphological Characteristics
1	Wild-type appearance
2	Slight edema; slightly shorter AP axis
3	Severe edema; slightly shorter AP axis
4	Severe edema; very short AP axis; underdeveloped posterior region; curved body

Figure 3.14: **Depletion of VAMP3 in *X. laevis*.** Embryos were injected with 40 ng of VAMP3 MO at stage two and then fixed at different time points. In stage 11.5 embryos, blastopore closure was delayed in 50% of embryos (Panel B, D; 2,3), while the remaining 50% of embryos had normal blastopore closure (Panel B, D; 1) relative to COMO injected embryos (Panel A). This represents a similar, yet less severe phenotype in relation to Bves MO injected embryos (see Figure 4.13B). It is interesting that similar defects are seen at this stage in both Bves- and VAMP3-depleted embryos, as this is when integrin-mediated adhesion is very important for migration across the blastocoel roof, which results in blastopore closure (Marsden et al., 2001). It should be noted that delayed blastopore closure can result from a range of defects, however, it generally is an indicator of impaired cell movement. Knockdown of VAMP3 in *X. laevis* embryos resulted in a range of phenotypes in tadpoles. The most severe embryos (Panel C; 4) displayed substantial edema, a curved body, and a drastically shortened anterior-posterior (AP) axis (16% of embryos; panel E, 4), while roughly half of the embryos (panel C; 2, 3) had a less extensive manifestation of this phenotype (49.4% of embryos, phenotypes 2 & 3; panel E, 2, 3). Approximately one third of embryos (34.7%; panel E, 1) were indistinguishable from COMO injected controls (panel C; 1).

Table 5.

Figure 3.13

SEM Quantification

Cell Overlap

	Total Cells	Overlaps/Cell
COMO	67	1.66±0.42
Bves MO	64	0.641±0.41

Cell Polarity

	COMO	Bves MO
σ Avg	12.5±3.7	50.2±9.0

embryos (via aforementioned MO knockdown) exhibited delayed closure of the blastopore during gastrulation, which is indicative of disrupted cellular movement [Figure 3.13B; (Johnson et al, 1993; Ramos and DeSimone 1996; Ramos et al, 1996; Marsden and DeSimone 2001; Marsden and DeSimone 2003)]. Similarly, embryos injected with VAMP3 MO, displayed a delay in blastopore closure (Figure 3.14B), although this phenotype was less penetrant when compared to the Bves phenotype. It is interesting that similar defects are seen at this stage, as this is when integrin-mediated adhesion is important for migration across the blastocoel roof (BCR), which results in blastopore closure (Marsden and DeSimone 2001). The BCR intercalates to become two to three cell layers thick in COMO injected embryos (Figure 3.13D, arrow), but remained thickened in Bves-depleted embryos upon histological analysis [Figure 3.13E, arrow; (Keller 1980)]. Additionally, the involuting mesoderm is disassociated from the BCR in Bves-depleted embryos, suggesting decreased cell-matrix adhesion (Figure

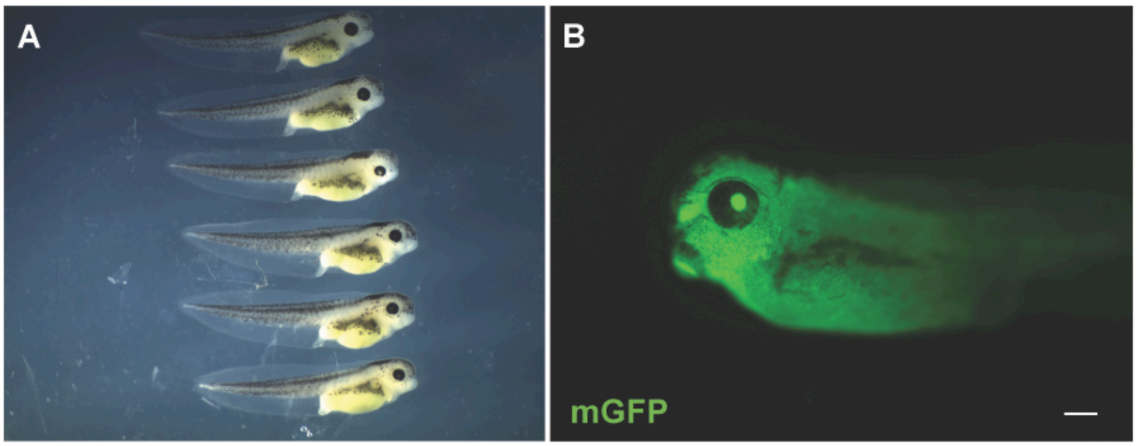

Figure 3.15 Bves Morpholino (MO) specifically knocks down Bves function. Embryos were injected into 2/2 cells with mGFP, 20ng of Bves MO, and 100pg of Xbves Rescue RNA that is mutated in the MO binding site. Stage 41 embryos (A) developed normally, with no gross defects in development, thus demonstrating full rescue. Embryos had membrane GFP labeling in the majority of cells (B), indicating the injected constructs diffused to each cell. This rescue data confirms Bves MO is specific, and off target effects are minimal.

3.13E, asterisk). Interestingly, *X. laevis* embryos injected in one of two cells with a lower dose of Bves MO (20ng), display anterior defects, characterized by disrupted morphogenesis of head structures and ectodermal outgrowths on the injected side (Figure 3.13C, arrows). These phenotypes are completely dependent upon inhibition of Bves function as total rescue is achieved by co-injecting Bves MO with 100 pg of *X. laevis* Bves mRNA (Figure 3.15). Conversely, VAMP3 MO treated embryos did not display overt defects in the anterior region at the tadpole stage and generally had a less severe phenotype compared to Bves MO treated embryos that was characterized by a shorter Anterior-Posterior (AP) axis and moderate to severe edema (Figure 3.14).

In *X. laevis*, anterior structures are the progeny of the involuting head mesoderm (HM), thus, we further analyzed the this population of cells [region

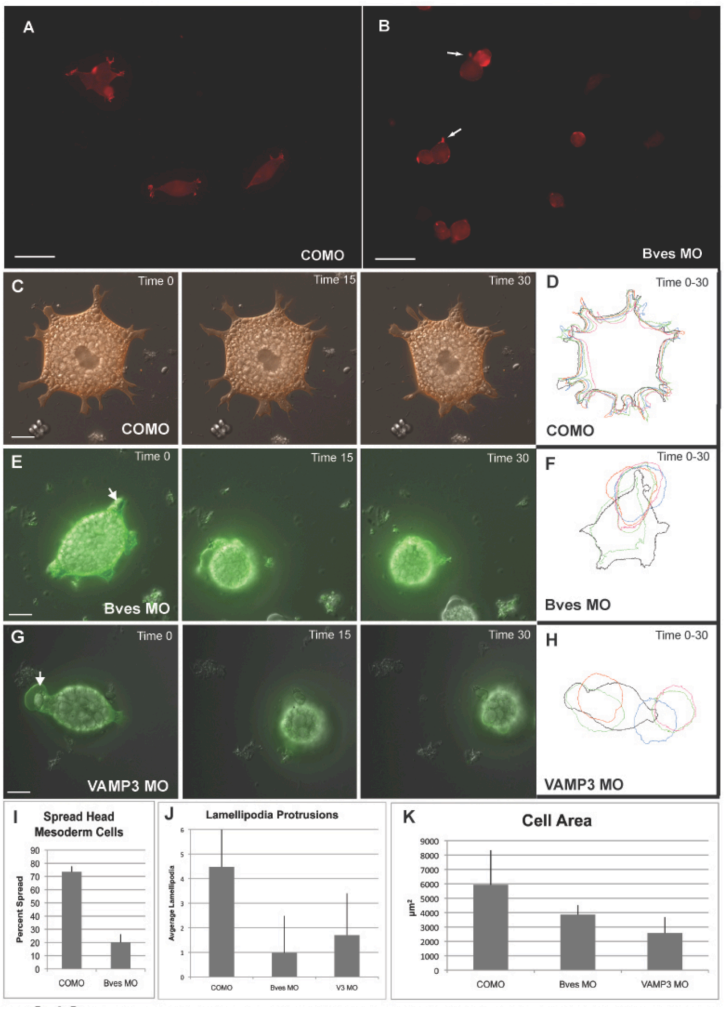

Figure 3.16 Bves- and VAMP3-depleted cells display decreased cell adhesion on FN. HM cells stained with Phalloidin-568 from COMO injected embryos (A) display distinctly spread morphologies on FN, while Bves-depleted cells (B) are round. Analysis over time (in minutes) indicates that as an mRFP labeled COMO treated cell moves (C, Time 0-30), it maintains a spread phenotype, extending several lamellipodia. Conversely, mGFP labeled Bves- (E, Time 0-30) or VAMP3- (G, Time 0-30) depleted cells are unable to maintain substrate adhesion and become rounded. Kymographs (D, F, H) depict cell morphology over time, underlining the distinct differences in cell shape, lamellipodia number, and cell area, which are quantified in graphs I, J, and K. Scale bars are 100µm (A, B) and 20µm (C, E, and G).

denoted by the asterisk in Figure 3.13E; (Kumano and Smith 2002)]. Involuting HM utilizes integrin adhesion to migrate along a FN gradient that is distributed on the BCR (Smith et al, 1990). These cells are directionally polarized towards the

Table 6.

Figure 3.16

Head Mesoderm Cell Adhesion Quantification

(a) Cell Spreading

	COMO	Bves MO
% Spread	73.6±4	20.2±6
% Round	26.4±4	79.2±6
Total Cells	557	414
P Value <	0.0002	

(b) Lamellipodia Formation

	COMO	Bves MO	VAMP3 MO
Lamellipodia/cell	4.45±2.3	0.98±1.5	1.7±1.7
P Value <		0.0001	0.0001

(c) Cell Area (μm2)

COMO	Bves MO	VAMP3 MO
5941±2401	3,872±644	2,592±1097
P Value <	0.046	0.001

leading edge and extend lamellipodia (Winklbauer and Nagel 1991). Scanning electron microscopy (SEM) and quantitative morphometrics of this region revealed significant changes in cell polarity and overlap in experimental embryos when compared to controls (Table 5). SEM of Bves-depleted embryos determined that the anterior population of HM was severely disorganized (Figure 3.13H, J) with fewer overlaps, large spaces between cells, and no detectable polarity of cell orientation (Figure 3.13H, J; Table 5). In contrast, control embryos displayed a ‘shingle-like’ pattern of overlapping cells that are all situated in a similar direction relative to the leading edge of the involuting mesoderm [Figure 3.13G, I; (Winklbauer and Nagel 1991)]. Taken together, these data suggest that gastrulation movements have been disrupted in both Bves MO and VAMP3 MO

treated embryos, and that Bves function is necessary for proper orientation, cell contact, and morphology of HM during involution. Previous studies show that inhibition of integrin function results in overt defects in cellular movement, similar to those seen in Bves-depleted embryos [Figure 3.13; (Ramos and DeSimone 1996; Marsden and DeSimone 2001; Na et al, 2003)].

Bves-depletion results in decreased *X. laevis* cell spreading on FN

Integrins are required for migration of the involuting HM over a FN gradient during gastrulation of *X. laevis* (Marsden and DeSimone 2001). As integrins are recycled by VAMP3, we next determined if this was potentially an integrin-dependent phenotype (Proux-Gillardeaux et al, 2005; Skalski and Coppolino 2005; Tayeb et al, 2005; Luftman et al, 2009). By plating primary disassociated HM cells on FN, we found that COMO cells had defined lamellipodia and displayed spread morphology *in vitro* (Figure 3.16A), as defined by previous published studies (Ramos and DeSimone 1996). Conversely, Bves-depleted cells exhibited distinctly decreased cellular spreading on FN (Figure 3.16B), with smaller cell protrusions. Previous reports have demonstrated disruption of integrin function results in round or spherical cells, phenocopying Bves depletion (Ramos and DeSimone 1996). This decrease in spread morphology was not due to a decrease in integrin expression levels, as Bves MO injected embryos expressed the same level of integrin protein as COMO treated embryos (Figure 3.13F). The majority of Bves-depleted cells remain rounded (79.2±6%), with few filopodia anchoring them to FN (Figure 3.16B, arrows; Table

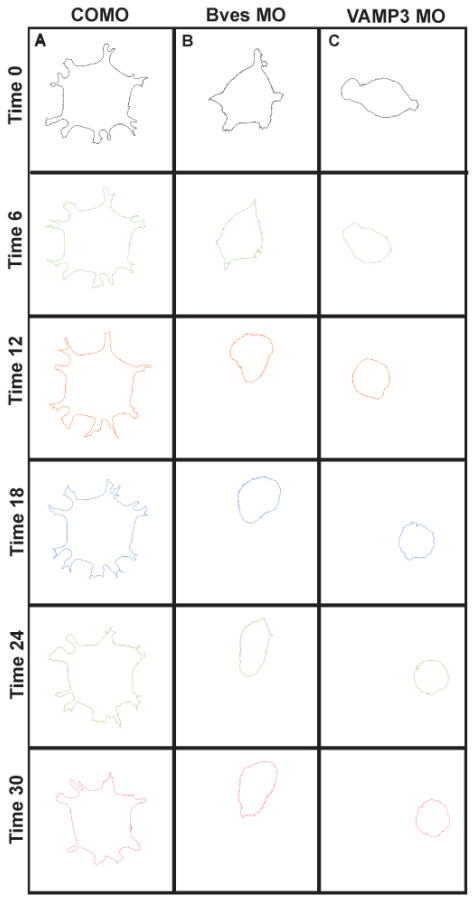

Figure 3.17: Kymographs of HM cells. Figure 4.16 demonstrates that cell adhesion to a FN substrate in Bves- and VAMP3-depleted *X. laevis* primary head mesoderm cells is disrupted over time. Individual cell tracings displayed here from COMO (panel A), Bves MO (panel B), and VAMP3 MO (panel C) demonstrate that lamellipodia protrusions and cell area are decreased in Bves- and VAMP3-depleted cells over time (Time 0-60; quantified in Table V). Overall, Bves or VAMP3 MO treated cells have distinctly different cell morphology, characterized by rounded or spherical cells which indicates decreased integrin-mediated cell adhesion, while COMO treated cells maintain cellular protrusions, as well as spread morphology.

6a). Conversely, 73.6±4% of control cells were spread in morphology. This result was significant: $p < 0.0002$.

We next used live cell imaging to determine if Bves-depleted cells displayed impaired cell spreading, morphology, or movement over time; additionally, we extended this study to examine the effect of VAMP3 MO on HM

cell morphology. HM cells injected with COMO, Bves MO, or VAMP3 MO displaying spread morphologies were chosen at the onset of image capture and were visualized by previously co-injected membrane GFP (mGFP, experimentals) or RFP [mRFP, control; (Wallingford et al, 2000)]. The behavior of individual cells was recorded over time and subjected to kymographic analysis for cell spreading and morphology. Both control and experimental cells display a heavily yolk-laden appearance (Figure 3.16C, E, G) and no cell in any group exhibited “directional” migration over the course of study. Time-lapse analysis demonstrated COMO injected cells (Figure 3.16C) displayed on average 4.45±2.3 lamellipodia per cell, while Bves or VAMP3 MO treated cells had only 0.98±1.5 and 1.7±1.7 lamellipodia/cell (Figure 3.16J, Table 6b). As previously reported (Ramos and DeSimone 1996), when integrins are non-functional, cultured HM cells remain round in appearance. This was clearly observed in both Bves- and VAMP3-depleted cells (Figure 3.16E and G). In a controlled side-by-side comparison of cells plated on the same FN coated dish, Bves-depleted cells (labeled with mGFP) became rounded over time while COMO treated cells (labeled with mRFP), remained spread. Additionally, both Bves- and VAMP3-depleted cells often exhibited large and very transient bleb-like protrusions that harbored yolk granules (Figure 3.16E, G, arrows); in control cells (Figure 3.16C), yolk granules indicate the stable boundary between the cell body and cell protrusion (Selchow and Winklbauer 1997). These membrane blebs, known as circus movements in early development (Johnson 1976) were short-lived, and are generally thought to be associated with decreased adhesion or breakdown of

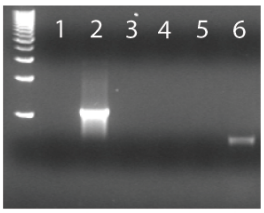

Figure 3.18 Stable Bves118 expression in MDCK cells is confirmed by RT-PCR. After selection in G418, stably transfected lines were assayed for RNA transcripts. Briefly, MDCK cell lysate was harvested using Trizol, and cDNA was made using Superscript II RT. PCR was carried out with the following primers: the forward primer began at pCMV-3Tag-4 vector nucleotide 584 (AAC CGT CAG ATC CGC TA) and the reverse primer began at nucleotide 943 (CTG GCA ACT AGA AGG CAC), thus spanning the multiple cloning site. Bves118 is 354 nucleotides, yielding a PCR product of 713 nucleotides as seen in lane 6. Lanes 1, 3-5 are negative controls, Lane 2 is a positive control.

the actin-cytoskeleton network (Shook and Keller 2003; Fackler and Grosse 2008) Kymographs of the area of attachment reveal Bves- and VAMP3-depleted cells had a significantly smaller area of interaction with the substrate (Figure 3.16D, F, H, K; see Figure 3.17 for individual frames), when compared to the COMO injected cells. These statistically significant results (Table 6c) demonstrate that cell adhesion and process extension, processes regulated by integrins (Holly et al, 2000; Caswell and Norman 2006), are impaired in Bves- and VAMP3-depleted cells. These data, which are corroborated by our current findings with MDCK cells, further support a role for Bves in cell movement through VAMP3-mediated recycling of integrins.

Discussion

In this study we present data that link Bves to the fundamental cellular process of vesicular transport. Bves has been previously reported to regulate cell

movement and cell-cell adhesion, although these functions were unexplained at the molecular level. Here we describe a mechanism that may elucidate the role Bves plays in these processes through its interaction with the vesicular transport protein, VAMP3. Our findings demonstrate that the intracellular domain of Bves interacts directly with VAMP3 and that these proteins co-localize in a variety of cell types. Furthermore, stable expression of a mutant form of Bves or elimination of Bves protein function results in a remarkably similar disruption in transport of two independent molecules, transferrin and β-1 integrin, both of which are trafficked by VAMP3 (Galli et al, 1994; Proux-Gillardeaux et al, 2005). These findings are corroborated in *X. laevis* embryos, where Bves depletion (as well as depletion of VAMP3) results in impaired transferrin recycling in animal caps and morphological defects consistent with the disruption of integrins. Furthermore, in both model systems, cells with inhibited Bves function have disrupted cell adhesion or spreading, consistent with VAMP3-dependent trafficking of integrins. Based on these data, we propose that Bves is essential for VAMP3 function in vesicular transport, and is specifically required for the recycling of VAMP3-mediated receptors. Thus, we propose that Bves functions in broad cellular processes regulated by vesicular transport, explaining previously reported phenotypes unresolved at the molecular level.

Bves as a novel regulator of vesicular transport

Bves is essential for proper cell movement, although the exact role Bves played in this process was previously unknown (Ripley et al, 2006; Smith et al,

2008). We propose that, through interaction with VAMP3, Bves is necessary for the vesicular transport of the adhesion molecule, β-1 integrin, as attenuated integrin recycling is observed during cell migration when Bves is disrupted. This retardation in integrin recycling exactly phenocopies VAMP3 disruption and directly links Bves disruption to impaired integrin recycling. These data are corroborated by attenuated cell spreading or adhesion (processes dependent upon integrin integrity) observed with Bves inhibition. Furthermore, impaired recycling of integrins is a potential mechanism explaining the gastrulation phenotype observed in the embryo.

VAMP3 transports transferrin, hence, the rate of transferrin uptake is a general indicator of the integrity of VAMP3 trafficking (Galli et al, 1994). With Bves disruption, either by expression of a mutated protein or protein depletion, endocytosis of transferrin decreases over time and phenocopies VAMP3 inhibition. These data, along with decreased recycling of β-1 integrin, demonstrate that Bves is important for VAMP3-mediated vesicular transport of receptors.

Bves is important for the generation and maintenance of epithelial junction integrity (Osler et al, 2005). In the process of epithelial biogenesis, cell-cell adhesion is initiated as specific proteins are trafficked to the forming adherens junctions (Bryant and Stow 2004; Yap et al, 2007). This process is disrupted upon Bves depletion, as the canonical adherens junction molecule, E-cadherin, is not localized to points of cell-cell contact (Osler et al, 2005). Cadherin-based cell adhesion is a dynamic process with E-cadherin constantly being replenished at

the cell surface via vesicular transport (Bryant and Stow 2004; Yap et al, 2007). Defects in the vesicular transport of E-cadherin could lead to disrupted cell adhesion or signaling, which results in pathogenic states such as metastatic cancer (Hirohashi 1998). Recently, it has been shown that efficient delivery of E-cadherin in both polarized and unpolarized cells is dependent upon functional Rab11 positive REs (Desclozeaux et al, 2008). Disruption of either Rab11 (a Rab GTPase and known player in vesicular transport) or the RE results in apical delivery of proteins. VAMP3 is a well-known member of the RE (Skalski and Coppolino 2005; Fields et al, 2007) and thus it is plausible to hypothesize that VAMP3-mediated vesicle fusion may be important for the recycling of E-cadherin, and mislocalization of E-cadherin upon Bves depletion may be explained by disrupted VAMP3-mediated vesicular transport. Thus, the current data and previous results suggest that Bves may influence vesicular transport in a broad array of cell functions.

Bves in cell adhesion, spreading, and movement

We provide conclusive evidence that Bves-depleted embryos have disrupted cell movements during gastrulation. *X. laevis* gastrulation is a well-studied system where integrin-dependent cell adhesion and movement are critical for development (Marsden and DeSimone 2003; Davidson et al, 2006). We report that HM cells in Bves-depleted embryos fail to orient properly and, when isolated, display rounded morphology and impaired process extension when plated on FN. Additionally, these cells display transient membrane blebs,

which have been associated with decreased cell adhesion during development (Shook and Keller 2003), and indicate localized breakdown of the actin-cytoskeletal network (Fackler and Grosse 2008). Evidence of this breakdown is seen in Bves-depleted cells as yolk granules, which are usually confined to the cell body, extend into lamellipodia (Selchow and Winklbauer 1997). The decreased integrin-mediated cell-substrate adhesion, coupled with actin-cytoskeletal network breakdown found in these cells is not surprising. Bves depletion influences Rac and Cdc42 activity (Smith et al, 2008), both of which are molecules that are important for actin polymerization and communicate with integrins during cell movement (DeMali et al, 2003). Additionally, actin polymerization has a well documented role in the endocytic pathway (Lanzetti 2007). Overall, these gastrulation-stage phenotypes are consistent with disrupted integrin function, as integrins are responsible for cell adhesion and spreading on FN (Marsden and DeSimone 2001). As VAMP3 is known to recycle integrins, our data suggest VAMP3 interaction with Bves is necessary for proper integrin-dependent movements during early *X. laevis* development.

In turn, several previous reports have linked Bves to the regulation of cell movement. For example, germ cell migration in the developing *Drosophila* embryo is impaired with mutation of *Dmbves* (Lin et al, 2007), while Bves/Popdc1-null mice exhibit impaired skeletal muscle regeneration due to the inhibition of myoblast movement (Andrée et al, 2002). Previous work from our own group has demonstrated impaired movement and regulation of cell shape *in vitro* and in developing organisms (Ripley et al, 2004; Ripley et al, 2006; Smith et

al, 2008). Still, until the identification of Bves-VAMP3 interaction, a molecular mechanism underlying these phenotypes was unresolved. Interestingly, the *Bves* gene is hypermethylated in specific cancer types (Feng et al, 2008), suggesting silencing of this gene may coincide with down-regulation of cell-cell adhesion. Thus, the role of Bves in the modulation of SNARE function may have broad impact on development and disease.

Bves as a moderator of diverse cellular pathways

In addition to interacting with VAMP3, we show that Bves interacts with VAMP2. It has been reported that VAMP2 and VAMP3 are promiscuous during development and *in vitro*, substituting for each other when one molecule is absent (Bhattacharya et al, 2002; Deak et al, 2006). This comes as no surprise, as rat VAMP2 and VAMP3 are highly homologous, differing by only one amino acid in their SNARE binding domain (McMahon et al, 1993). Bves interaction with VAMP2, and the potential overlapping function between different VAMP homologues, may explain the milder phenotype observed in VAMP3-depleted *X. laevis* embryos, and may suggest a broader role for Bves in influencing VAMP-mediated vesicular transport. Additionally, VAMP2 is expressed in muscle satellite cells and is up-regulated during skeletal muscle regeneration (Tajika et al, 2007); interestingly, this process is delayed in Bves knockout mice (Andrée et al, 2002). Finally, Bves is highly expressed in the brain, tissue where VAMP1 and 2 are also enriched, although Bves has never been studied in this context (Hager and Bader 2009). It would be interesting to determine if Bves interacts with

VAMP1, and if interaction with VAMP1 or 2 had any functional significance in the nervous system. Overall, Bves interaction with VAMP2 may suggest a broader role for Bves in a variety of tissue types that utilize SNARE machinery.

Current and recent studies have shown that Bves interacts with two proteins, VAMP3 and GEFT, that function through downstream targets to regulate convergent cellular processes (Smith et al, 2008). In light of the present data, it is intriguing to consider the overlapping cell operations in which GEFT and VAMP3 are involved. Although the direct functions of VAMP3 and GEFT within the cell are very different, they are nonetheless involved in a common pathway. GEFT activates Rho GTPases, which in turn regulate cell adhesion, cell motility, polarity, gene expression, and membrane trafficking (Etienne-Manneville and Hall 2002). VAMP3, through regulation of protein trafficking, modulates cell motility, polarity, and gene expression (Schwartz and Shattil 2000). Indeed, several studies have even implicated Rho GTPase activity in the regulation of vesicular transport (Ridley 2001; Symons and Rusk 2003), and integrins have been shown to recruit Rho GTPases necessary for modulation of the actin network (Holly et al, 2000; Caswell and Norman 2008). However, the interplay between integrin signaling and Rho GTPase function is not entirely understood. We hypothesize that through interaction with VAMP3 and GEFT, Bves may provide crosstalk to achieve cellular synchrony in these essential cell processes. Taken together, our data suggest that Bves may play an unexpected role in a broad spectrum of cellular functions regulated by vesicular transport.

CHAPTER IV

BVES AND NDRG4 REGULATE EPICARDIAL CELL MIGRATION THROUGH AUTOCRINE EXTRACELLULAR MATRIX DEPOSITION

This chapter is currently in submission.

Abstract

Here, we demonstrate a novel interaction between Bves and NDRG4 that is essential for directionally persistent cell migration. This activity is dependent on another novel function for these proteins identified in this study; namely, vesicular trafficking of internalized soluble fibronectin through late endosomal/lysosomal compartments for deposition into the extracellular matrix. This endocytic/recycling mechanism was recently discovered in cancer cells. Loss of Bves and NDRG4 function disrupts directional movement and decreases matrix secretion from epicardial cells. Revealing the relationship between matrix deposition and directed cell movement has important implications for heart development, as directed epicardial cell motility is essential for coronary vessel morphogenesis. Together with prior studies, the present data demonstrate that Bves traffics not only cell-cell and cell-matrix adhesion molecules but also their matrix substrates to the cell surface for adhesive and migratory events. With previously reported functions, our data suggest that Bves is a global regulator of cell-

microenvironmental interactions in a diverse set of migratory cell behaviors impacting development, repair and disease.

Introduction

Blood vessel epicardial substance (Bves) was first identified in epicardial tissue and later recognized for its dynamic distribution in a multitude of cell types (Reese et al, 1999; Andrée et al, 2000; DiAngelo et al, 2001; Wada et al, 2001; Ripley et al, 2004; Vasavada et al, 2004; Smith and Bader 2006; Kawaguchi et al, 2008; Russ et al, 2010). Bves (Popdc1) is the prototypical member of the Popdc family, which share a conserved Popeye Domain, but do not contain homologous domains with other protein families (Andrée et al, 2000). Loss of Bves function in epithelial cells results in disruption of sheet integrity and defects in epithelial morphogenesis (Osler et al, 2005; Ripley et al, 2006; Kawaguchi et al, 2008). A reoccurring theme seen with disruption of Bves is randomization of cell movement. For example, in normal *Xenopus laevis* development, individual A1 blastomeres, early embryonic cells, give rise to progeny that migrate in a highly patterned manner incorporating into anterior head and somitic structures. With morpholino knockdown of Bves in these same blastomeres, migration of resulting progeny is completely randomized with cells moving throughout the embryo (Ripley et al, 2006). Similarly, *Drosophila melanogaster* larvae expressing antisense Bves have aberrant pole cell migration (Lin et al, 2007). An *in vitro* model of wound repair demonstrates that Bves-depleted human corneal epithelial

cells move more rapidly than controls but in a disorganized manner resulting in impaired epithelial sheet closure (Ripley et al, 2004). Bves-disrupted cells have impaired lamellipodial formation and loss of adhesion (Smith et al, 2008; Hager et al, 2010). Finally, Bves is a recently-identified tumor suppressor of gastric and colorectal cancers with Bves mutations associating with epithelial-to-mesenchymal transition and metastatic behaviors (Kim et al, 2010; Williams et al, 2011). Thus, Bves regulates cell movement in a variety of settings, although the underlying mechanism is poorly understood.

Bves itself is not an adhesion molecule but is important for intracellular trafficking of adhesion molecules, such as E-Cadherin, Occludin and ZO-1, and stability of junctional complexes (Osler et al, 2005; Russ et al, 2011). Additionally, Bves is critical for the trafficking of β_1-integrin to the cell surface and subsequent lamellipodial extension through interaction with the SNARE protein Vamp3 (Hager et al, 2010). Together, previous reports suggest that Bves has an important role in trafficking integral membrane proteins to the cell surface for cell-cell and cell-matrix adhesion.

In ongoing interaction screens to identify Bves binding partners and determine protein function, the most frequent hit was N-myc Downstream Regulatory Gene 4 (NDRG4), a cytoplasmically-localized protein whose expression, similar to Bves, is enriched in heart tissue (Zhou et al, 2001; Qu et al, 2002; Qu et al, 2008). This interaction was of interest, as other NDRG family members have been implicated in trafficking adhesion molecules to the cell

surface (Okuda et al, 2004; Berger et al, 2006; Kachhap et al, 2007; Choi et al, 2010). Additionally NDRG4, like Bves, is a colorectal cancer tumor suppressor that regulates cell migration, morphology and differentiation (Zhou et al, 2001; Nishimoto et al, 2003; Melotte et al, 2009; Schilling et al, 2009; Kim et al, 2010; Williams et al, 2011). Furthermore, NDRG4 depletion impairs neurite extension, mirroring the loss of lamellipodia observed in Bves-depleted cells (Ohki et al, 2002).

Here, we demonstrate that Bves/NDRG4 interaction, through a unique binding domain, is critical for directionally persistent cell migration. Further, we identify another novel function for these proteins; namely, trafficking of internalized fibronectin for deposition into the extracellular matrix. Endocytosis and resecretion of internalized fibronectin from a late endosomal/lysosomal secretory compartment was recently shown to promote the motility of cancer cells (Sung et al, 2011). We show that this mechanism is essential for directionally persistent movement of epicardial cells and that fibronectin resecretion is dependent on Bves and NDRG4 function. This has broader implications for heart morphogenesis and coronary vessel development. Together with previous studies, the present data demonstrate that Bves traffics not only cell-cell and cell-matrix adhesion molecules but also their matrix substrates to the cell surface for adhesive and migratory events critical in development, cancer and repair.

Materials and Methods

All experiments performed with murine models followed IACAC guidelines.

Quantification

For the assays described below statistics were performed in Microsoft Excel 2011. The error bars represent the standard error of the mean; standard student t-tests were used to determine significance. All compared images were equivalently adjusted in Adobe Photoshop CS5. For intensity profile quantification, the ImageJ Straighten program was used to follow structures at a width of five pixels, these pixels were averaged for fluorescence intensity and each channel was plotted together in Excel versus distance (μm). Progressive paths of epicardial cells after gene manipulation were gathered using ImageJ Manual Tracking and were compiled in Photoshop.

Cell Culture, Antibodies, Immunocytochemistry and Immunohistochemistry

EMC maintenance and processing was standard (Wada et al, 2003). The dilutions and manufacturers of the antibodies were: anti-Bves SB3 (1:1000) (Smith and Bader 2006), anti-NDRG4 91:500, Novus, H00065009-M01), anti-Fibronectin (1:100, Santa Cruz, SC-9068), anti-GAPDH (1:500, Abcam, ab290), anti-GFP (1:500, Clonetech, 632375), anti-Myc (1:200, Clonetech, 631206), Rab4a/b (1:200, Abcam, ab13252), Rab11a (1:500, Gift from James Goldenring), EEA1 (1:200, BD Transduction, 610457), Lamp1 (1:100, BD Transduction,

555798), Lamp2 (1:100, Abcam, ab18538), Rab27a (1:200 Abcam ab55667), Alexa Fluor-488, 568, and 647 1:500 (Molecular probes), DAPI, 1:10000. Zenon IgG labeling kits were used for direct labeling (Molecular Probes). Slide preparation for immunocytochemistry was standard (Smith and Bader 2006). For immunohistochemistry, 10μm slices of E14.5 murine hearts were cryosectioned onto charged slides. Tissue processing followed standard methodologies (Osler et al, 2005; Smith and Bader 2006). Images were captured with Leica TCS-SP5 confocal microscope (Leica Microsystems), Zeiss LSM150 inverted confocal microscopes, and the DeltaVision Platform (Precision Control). All microscopy was done in conjunction with VUMC CISR and EBC.

Split-Ubiquitin Screen

A split ubiquitin screen of murine Bves (NM_024285) against a mouse heart library was performed as previously described (Hager et al, 2010). Murine NDRG4 transcript A (NM_001195006.1) was cloned into the pPR3-N vector and passed all nutrient drop-out selection tests against Bves.

Co-IP, GST pulldown and Native IP

For Co-IP, Bves, cloned into the pCMV-myc-3tag-4A vector (Stratagene), and NDRG4, cloned into the pEGFP-C1 vector (BD Biosciences), were exogenously expressed in COS-7 monkey kidney cells (ATCC) with Lipofectamine 2000 (Invitrogen). Lysates were harvested as previously

described (Hager et al, 2010) and CoIPs performed per manufacturer's instructions using Profound c-Myc Tag IP/Co-IP Application Set (Pierce). Bves-GST truncation pulldowns of NDRG4-GFP expressed in COS7 cells were performed as previously described (Smith et al, 2008). For Native-IP, lysates from three 10cm plates of EMCs were pooled in M-PER Mammalian Protein Extraction Reagent (Pierce). 20μg Bves SB3 antibody was crosslinked using BS_3 to protein G Magnetic Dynabeads (Invitrogen) as per manufacturer's protocol. Dynabeads were washed in PBS-T pH 7.4 and 250 uL of EMC lysate was applied and rocked at 4^{o}C for two hours. Binding partners were eluted per manufacturer's protocol and probed with NDRG4 antibodies via western blotting, which was exposed with standard alkaline phosphatase methodology (Hager et al, 2010).

SPOTs Analysis

A SPOTs membrane designed to the Bves C-terminus (residues 115-358) was synthesized (Sigma Genosys) with each 13-mer SPOT having 10 amino acid overlap with neighboring SPOTs. NDRG4-EGFP or EGP vector control lysates were exogenously expressed in COS7 cells, and lysates were collected using MPER buffer as described above. Standard BCA assays (Thermo Scientific) determined total protein concentration, and lysates were incubated with both monoclonal and polyclonal GFP antibodies to enhance signal, overnight at 4^{o}C. The SPOTs membrane was prepped and incubated in lysate as previously

described (Kawaguchi et al, 2008). Antibody binding was visualized using standard chemiluminescence methodology, and the membrane was regenerated using DiMethylFormamide (DMF) as previously described (Kramer and Schneider-Mergener 1998). The DNA sequence of an ~120 base pair region of Bves (BC132044.1; residues 292 to 330) was cloned into the pCMV-3tag-4a vector (Agilent Technologies #240198) with standard methods (Hager et al, 2010) and in-frame ligation was confirmed via PCR, restriction enzyme dropout of the insert and sequencing (in conjunction with the Vanderbilt University DNA Sequencing Facility). Overexpression of 10μg of two separate clones was performed with nucleofection as described below. Expression efficiency and proper localization, colocalization was ascertained by analyzing images gather with the Delta Vision platform, and confocal microscopes.

Modified Boyden Chamber Migration Assay

$3.0x10^5$ EMCs per experiment were pelleted for 10 minutes at 1500 RPM in a desktop microcentrifuge and resuspended in 400uL of 10% FBS plus P/S in DMEM. The cells were seeded to the basket of an 8.0μM cell culture insert (Millicell) and placed in 600μL of the same media in a 24-well plastic culture dish (Falcon). Cells were incubated for 4 hours, and processed with standard methods (Cross et al, 2011). Phase images were captured on an Olympus BX60 microscope and Olympus Camera.

Table 7. Bves and NDRG4 knockdown constructs

Target	siRNA Name	siRNA Oligo Seqence	Start
NM_001077590	Bves 1 sense	CAGUAGAUAUAUUAAUAUUdTdT	1301
NM_001077590	Bves 1 antisense	AAUAUUAAUAUAUCUACUGdTdT	1301
NM_001077590	Bves 2 sense	GGAGUUGUGUGCUGCCUGUdTdT	1209
NM_001077590	Bves 2 antisense	ACAGGCAGCACACAACUCCdTdT	1209
NM_001077590	Bves 3 sense	GACCUUUGGUGGUUUGCUUdTdT	1151
NM_001077590	Bves 3 antisense	AAGCAAACCACCAAAGGUCdTdT	1151
AK_090374	NDRG4 1 sense	CUUACACACUCCUGUCUCAdTdT	1365
AK_090375	NDRG4 1 antisense	UGAGACAGGAGUGUGUAAGdTdT	1365
AK_090376	NDRG4 2 sense	GAGAGAAAGCACUAAGUGUdTdT	2212
AK_090377	NDRG4 2 antisense	ACACUUAGUGCUUUCUCUCdTdT	2212
AK_090378	NDRG4 3 sense	GGUAUUGUAUGGGUGUUCUdTdT	2259
AK_090379	NDRG4 3 antisense	AGAACACCCAUACAAUACCdTdT	2259

siRNA Knockdown and Rescue

Oligos were designed against the 3' UTR of Bves and NDRG4 (Sigma Custom Oligos; sequences listed in Table 7). Nucleofection using the Nucleofector II Device (Lonza) was optimized in EMCs with a Cell Line Optimization Kit (Lonza VCO-1001N). Briefly, 5x 10^5 EMCs in solution L using program A-033 had the highest transfection efficiency of pMAX-GFP DNA (>70%) and highest viability (>80%). Using this protocol, three pooled Bves and/or NDRG4 siRNA oligos were applied to EMCs at 100nM each, as were standard control oligos (Sigma SIC001).

Cells were incubated for 48 hours in standard conditions and collected as outlined above and protein concentration was normalized to expression of the housekeeping gene cyclophilin via western blot. Rescue constructs of Bves and NDRG4 pCMV-Myc-3tag-4 vector (Stratagene) lacked the siRNA target sequences and were stably expressed in EMCs via nucleofection, followed by 3 weeks of G418 treatment. Cells were clonally sorted at the Nashville VA Medical

Center Flow Cytometry Core, expanded, and then assayed with a Boyden Chamber, as above.

Live Imaging Assays and Analysis

EMCs siRNA depleted for Standard Control, Bves and/or NDRG4 plasmid as described above were incubated for 24 hours in standard medium then split to glass-bottom 35mm dishes (MatTek) either uncoated or coated in 10μg/cm^2 Fibronectin (Sigma F4759) at 5,000 cells per dish, and incubated for another 24 hours. To monitor cell movements, DIC images were acquired with the DeltaVision Platform in a temperature, humidity and CO_2 controlled weather station. Images were taken every 60 seconds with autofocus every 30th image. The movies were analyzed for distance, velocity and directional persistence using ImageJ Cell Tracker software. These data were collected in conjunction with VUMC EBC.

Cell-Free ECM Assays

Control or Bves/NDRG4 knockdown EMCs were seeded at 1x10^6 on MatTek dishes or 5x10^5/well of a 4 well glass chamber slide (NUNC Lab-Tek) and grown to confluence (48 hours). A cell-free ECM was prepared by applying 20mM ammonium hydroxide to the cells with vigorous rocking for five minutes. The cellular debris was washed away with one application of water and three of PBS for five minutes each, again, with vigorous rocking. As a measure of

properly produced ECM, directional persistence was compared between control cells in complete medium, Bves and NDRG4 knockdown cells in complete medium, and control cells in fibronectin depleted medium, as a negative control, using the live-cell directional persistence assay described above.

Fibronectin Medium Depletion and fibronectin internalization/deposition assays

To deplete medium of fibronectin, FBS was purified over a disposable column using Gelatin Sepharose 4B beads (GE Healthcare) according to the manufacturer's protocol and assayed for FN depletion via western blot. Gene-depleted cells maintained on glass MatTek dishes were fibronectin starved for 24 hours, DyLight 550 NHS Ester (Thermo Scientific)-, or Sulfo-NHS-LC-LC-Biotin-labeled fibronectin at 10 ug/mL for times specified in the text and as previously described (Sung et al, 2011). Cells were washed twice with complete medium and 3 times with PBS for five minutes each, and then cells were processed for immunofluorescence as above. For DiI labeling experiments, EMCs seeded at very low confluence on glass or 10$\mu g/cm^2$ Fibronectin were covered with 200 μL Fast DiI (Molecular Probes; 5μL DiI per 1mL 10% FBS DMEM), incubated for 35 minutes at 37^oC, fixed with Formalin for 25 minutes and processed for antibody labeling as discussed above. For biotin labeled deposition experiments, confluent fibronectin starved cell sheets on 35mm plastic dishes (Corning) were fed biotin-FN for 48 hours, a cell-free ECM assay was performed, as below, and

conjugated to Streptavadin-HRP overnight at 4°C (Thermo Scientific). The plates were washed with TBST pH 8.0 four times for 10 minutes each. Cells were exposed to TMB substrate (Pierce) for 25 minutes. Reactions were stopped with 2M sulfuric acid and absorbance read per manufacture's protocol.

Results

Bves and NDRG4 Bind Directly Through a Novel Interaction Domain

In an effort to determine Bves function, molecular binding partners were identified with a split ubiquitin two-hybrid screen (Iyer et al, 2005) designed for membrane-associated proteins in the heart using Bves as bait. Initial results identified a direct interaction between Bves and NDRG4, the most common target from this screen. The interaction passed quadruple dropout stringency selection tests (Figure 4.1A), and was further confirmed as myc-tagged full length Bves (Bves-myc) coimmunoprecipitated GFP-tagged NDRG4 (NDRG4-GFP; Figure 4.1B) from Cos7 cell lysates. To further define this interaction domain, a series of Bves C-Terminus truncation constructs spanning intracellular sequences of the protein were produced (BCT; diagrammed in Figure 4.1C). Only the full-length construct (amino acids 115-358) interacted with NDRG4 while all other constructs (spanning amino acid residues 115 to 150, 218, 250, 275 and 300 of Bves, respectively) failed to pulldown NDRG4-GFP (Figure 4.1D).

SPOTs analysis was performed to determine the minimal Bves residues sufficient to interact with NDRG4. As diagrammed in Figure 4.1E, 13-mer

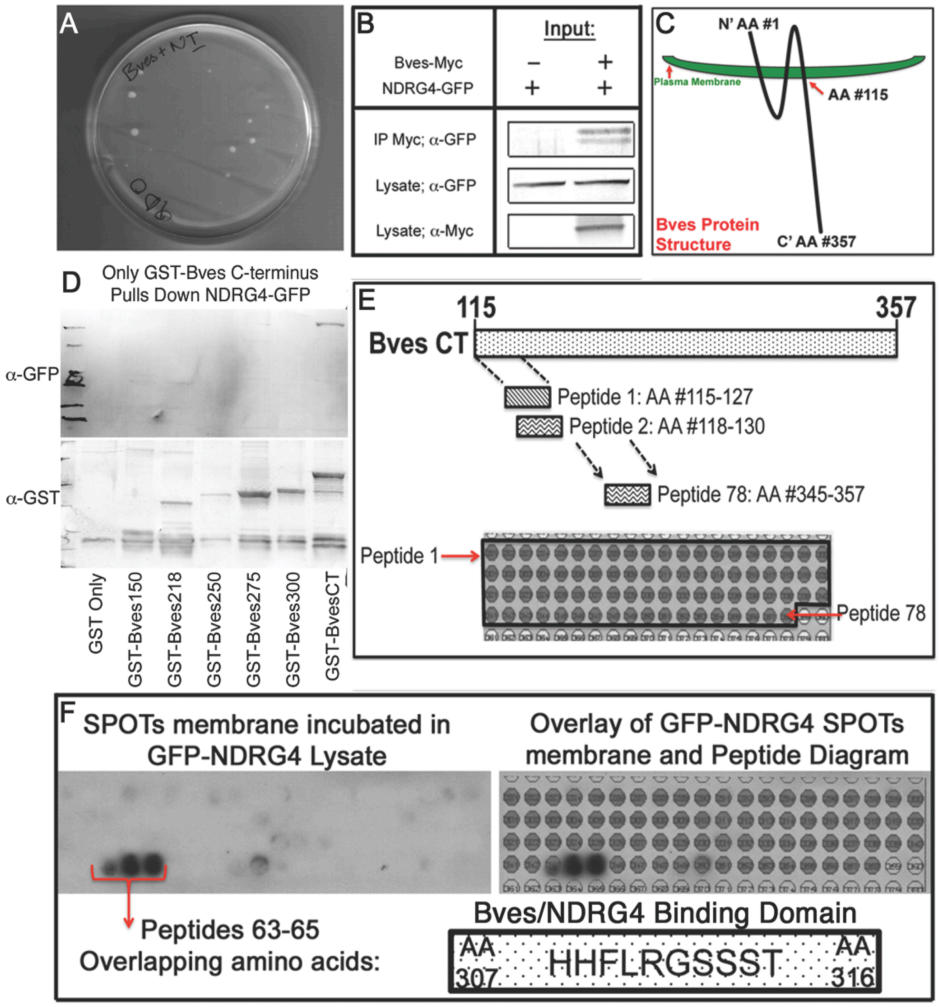

Figure 4.1 NDRG4 Protein Directly Interacts with Bves Residues 307-316. (A) Bves protein directly interacts with NDRG4 by split-ubiquitin quadruple drop-out selection test; n=3 assays. (B) Exogenously expressed Bves-Myc protein pulls down NDRG4-GFP from COS7 lysate above background lysate lacking Bves-Myc expression; n=3 assays. (C) A diagram of the Bves structure depicts the functional intracellular C-terminal domain (BCT) spanning residues 115-357. (D) Bacterial produced BCT-GST truncations indicate that only the full length BCT is sufficient to pull down NDRG4-GFP from COS7 lysate, unlike constructs truncated at residue 150, 218, 250, 275, or 300 ; n=3 assays. (E) SPOTs Assay: 13-mer synthesized peptides, from amino acid 115 to the end of the Bves protein, are fused to a cellulose membrane, with 10 amino acid consecutive overlap. (F) GFP-NDRG4 lysate binds to three Bves peptides on the cellulose membrane. The Bves-SPOTs blot overlaid on the cellulose membrane indicates that NDRG4-GFP binds to peptides 63-65. The Bves residues essential for binding NDRG4-GFP are: 307-316; HHFLRGSSST.

peptides of BCT were fused to a cellulose membrane with 10 amino acid overlap between adjacent peptides and probed with Cos7 lysate containing NDRG4-GFP. Interestingly, NDRG4-GFP bound strongly to peptides 63 through 65, which corresponded with residues 307 to 316 of the Bves protein (Figure 4.1F, Bves/NDRG4-Minimal Binding Domain). Importantly, SPOTs analysis matched our truncation pulldown experiments where Bves/NDRG4 interaction was observed only with inclusion of residues 300-358 (Figure 4.1D). These data identify a novel protein-protein interaction site within Bves that is outside of the conserved Popeye domain previously identified for Bves/Bves dimerization activity (Kawaguchi et al, 2008).

Bves and NDRG4 Colocalize and Interact in Mammalian Epicardial Cells

As Bves and NDRG4 are both enriched in the heart (Qu et al, 2002; Hager and Bader 2009), distribution patterns of the two gene products in embryonic murine cardiac tissue were determined. Bves and NDRG4 colocalized in cardiac myocytes and the epicardium in E14.5 hearts (Figure 4.2A, inset and intensity plot). As Bves has different subcellular localization in cells depending whether they are freely migrating or present in epithelial sheets (Wada et al, 2001; Osler et al, 2005), we determined the subcellular localization of Bves and NDRG4 under varying conditions. Epicardial cells plated at low confluence are motile, with a mesenchymal morphology (Wada et al, 2003). In this setting, Bves and NDRG4 colocalized at the cell cortex and in extended cell processes (Figure

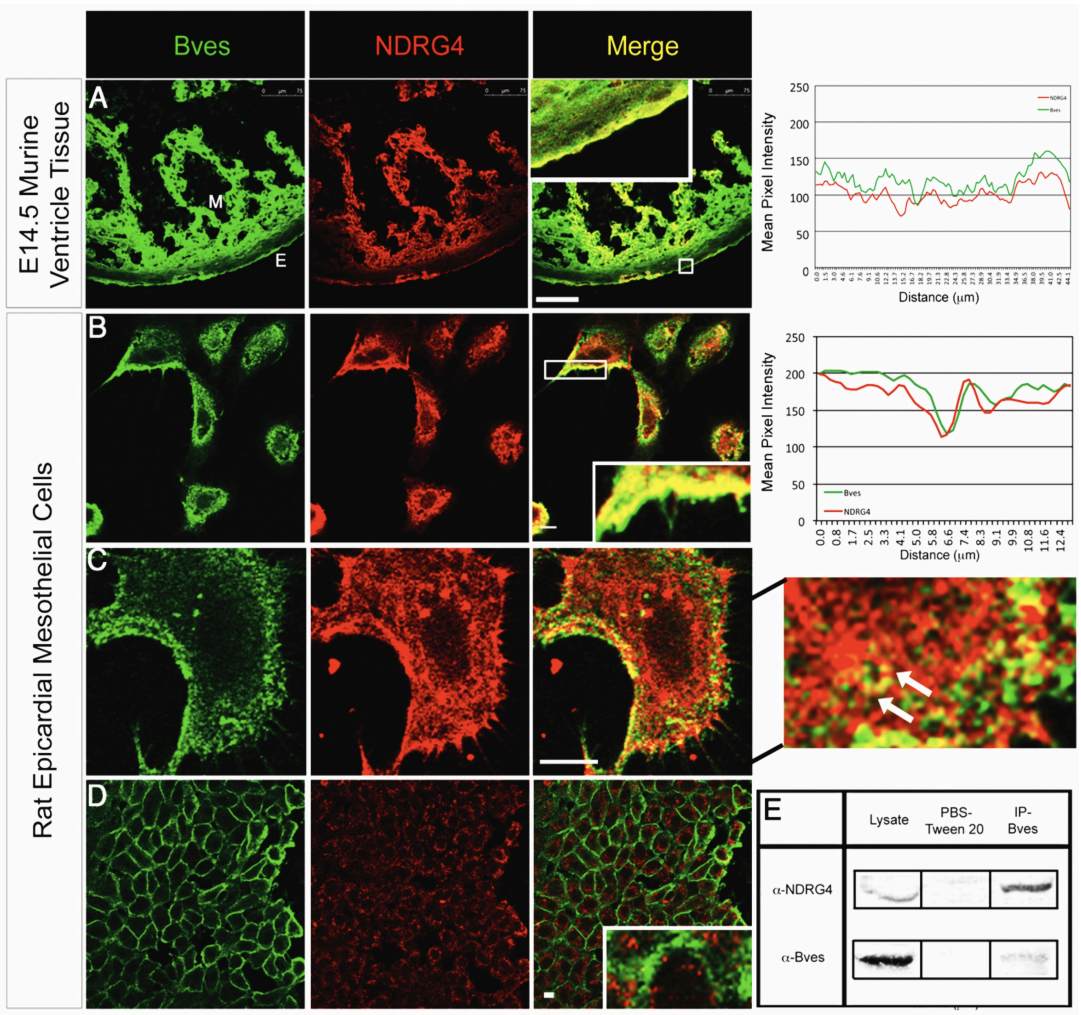

Figure 4.2 Bves and NDRG4 colocalize and interact in mammalian epicardial cells. Bves expression is visualized by green labeling, NDRG4 is red; all optical slices are 1 Airy Unit. (A) In murine E14.5 ventricle tissue, Bves and NDRG4 colocalize in cardiomyocytes (merge) and epicardial cells (inset; confocal images of transverse sections). Colocalization is quantified by ImageJ intensity profiling (box and graph). M: myocardium, E: epicardium; scale is 75μm. (B) Mesenchymal-shaped epicardial cells at low confluence exhibit Bves and NDRG4 colocalization in plasma membrane protrusions (merge and inset); colocalization in the box quantified in the intensity profile; scale is 10μm. (C) High magnification of Bves/NDRG4 subcellular position indicates that proteins have punctate, vesicular colocalization (white arrows in digital zoom demarcate colocalization); scale is 10μm. (D) Epicardial cells at high confluence do not contain areas of Bves and NDRG4 colocalization (inset shows cell borders); scale is 10μm. (E) Epicardial cell lysate run over a column cross-linked to Bves antibody pulls down and enriches for NDRG4 protein above background (PBS-Tween 20: no Bves antibody); n=3 pulldowns.

4.2B, inset and intensity profile), at points of cell contact (data not shown), and on intracellular vesicular structures (Figure 4.2C, digital zoom and white arrows). Still, in other regions of the cell, non-overlapping distribution of these proteins was also apparent and these two proteins failed to colocalize in established epicardial sheets (Figure 4.2D, inset). Interestingly, in confluent cells, NDRG4 localization was primarily vesicular whereas Bves localized to the cell cortex and plasma membrane. Additionally, co-immunoprecipitation demonstrated that Bves and NDRG4 interact in epicardial cells (Figure 4.2E). Taken together, these data indicate that Bves and NDRG4 interact in epicardial cells of mobile morphology, suggesting that they may function together in a capacity related to cell migration.

Bves and NDRG4 Interaction Regulates Epicardial Cell Movement

To ascertain whether cell motility was altered in epicardial cells with loss of Bves and/or NDRG4 protein, nucleofection of siRNA oligonucleotides was optimized in epicardial cells to disrupt protein expression. Pooling three siRNAs designed against the 3' UTRs of Bves and NDRG4 most strongly depleted epicardial cells of the respective proteins compared to standard control (SC) siRNA treatment (Figure 4.3A; siRNA sequences in Materials and Methods).

With successful depletion of protein levels, we assayed whether loss of Bves and/or NDRG4 affected epicardial cell migration with a modified Boyden Chamber system in which serum chemoattractant was placed on both sides of the filter to promote random motility. Consistent with previous reports on both

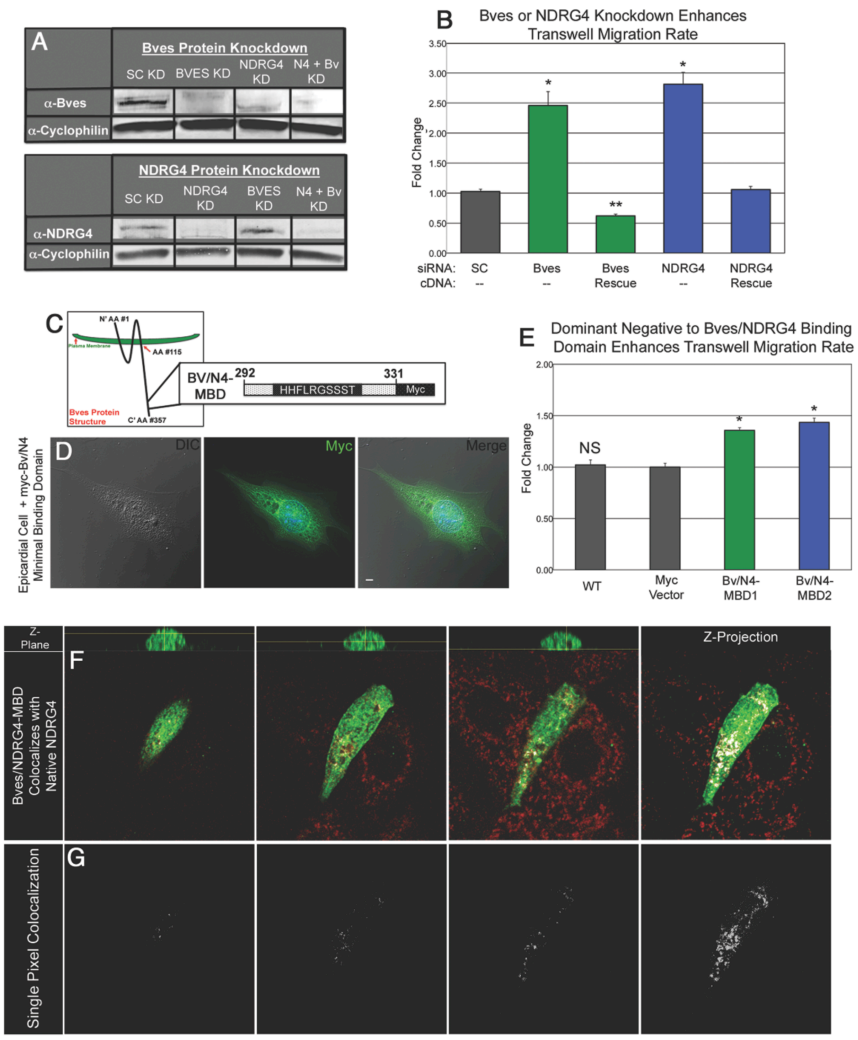

Figure 4.3 The Bves and NDRG4 interaction regulates epicardial cell movement. (A) Bves or NDRG4 siRNA oligos applied to epicardial cells via nucleofection knockdown protein levels of respective genes. Co-knockdown with Bves and NDRG4 oligos depleted expression of both proteins; n=3 blots. (B) siRNA depletion of Bves or NDRG4 elevates single cell migration through a modified Boyden Chamber which is rescued by overexpression of each respective gene; n=5 separate assays; *p≤0.0003 from standard control (SC) treated samples, **p≤0.05 from SC. (C) The structure of the Bves/NDRG4 minimal binding domain (Bv/N4-MBD) construct contains the Bves residues that bind to NDRG4 fused to a 3-myc tag, the construct should compete for binding with native NDRG4 protein. (D) Overexpression of the Bv/N4-MBD plasmid has robust cytoplasmic, punctate and membrane localization in epicardial cells, reminiscent of native NDRG4 protein localization. (E) Overexpression of two separate Bv/N4-MBD clones significantly elevate single cell migration, while vector control cell migration was unchanged compared to wildtype; n=55 images from 3 experiments *p≤0.0001 from vector treated cells, NS=not significant compared to vector. (F) Overexpression of the Bv/N4-MBD construct (green) colocalizes with native NDRG4 protein (red) in multiple planes as calculated by single pixel analysis and demarcated by white pixels. (G) The overlapping pixels from each Z-plane are displayed in the bottom panel; 0.5μm optical slices.

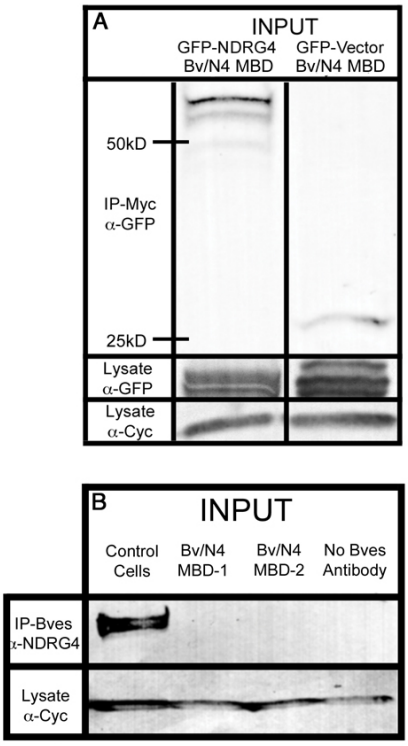

Figure 4.4 Bves/NDRG4-myc tagged dominant negative competes for NDRG4-GFP binding to Bves. (A) Co-overexpression of BvN4-DN with GFP-vector or GFP-NDRG4 plasmids indicate that BvN4-DN is sufficient to pulldown NDRG4 above vector background; cyclophilin housekeeping gene is a loading control; top GFP-NDRG4 band runs at the expected molecular weight for NDRG4 plus a GFP tag of ~26kDa. (B) Two separate BvN4-DN constructs were sufficient to interfere with endogenous Bves and NDRG4 interaction in epicardial cells.

proteins (Nishimoto et al, 2003; Ripley et al, 2006), depletion of Bves or NDRG4 significantly increased the movement of cells in this assay (Figure 4.3B). Expression of a cloned RNA lacking the 3'UTR oligonucleotide target sequences decreased the enhanced migration exerted by Bves and NDRG4 siRNA, rescuing the phenotype (Figure 4.3B).

To determine whether interaction of Bves and NDRG4 directly regulated this process, the minimal binding domain of Bves for NDRG4 (see Figure 4.1E)

was expressed in epicardial cells to interfere with native interaction (diagrammed in Figure 4.3C). Subcellular localization of the myc-tagged minimal binding domain (Bv/N4-MBD) was consistent with native Bves and NDRG4 localization in that it was cytoplasmic and primarily localized to vesicles (Figure 4.3D). Further, in apical, central and basal z-planes, Bv/N4-MBD and NDRG4 proteins colocalized in epicardial cells, as determined by single pixel analysis (Figure 4.3F cells, 4.3G single pixel colocalization per designated plane). Interaction of Bv/N4-MBD and NDRG4 proteins was confirmed by pulldown methods (Figure 4.4A), demonstrating that this domain binds NDRG4 in cells. Conversely, interference of endogenous Bves/NDRG4 protein interaction with overexpression of the binding domain was visualized by the absence of NDRG4 protein with Bves pulldown analysis (Figure 4.4B). Together these data demonstrate that the Bv/N4-MBD of Bves for NDRG4 interferes with Bves/NDRG4 interaction, and thus is a dominant negative peptide against this interaction. Using Bves/NDRG4-MBD constructs, modified Boyden Chamber analysis of random cell migration was conducted to measure migration rate in serum. In these experiments, overexpression of two different Bv/N4-MBD constructs significantly increased transwell migration rate compared to controls (Figure 4.3E), mirroring the gene depletion studies.

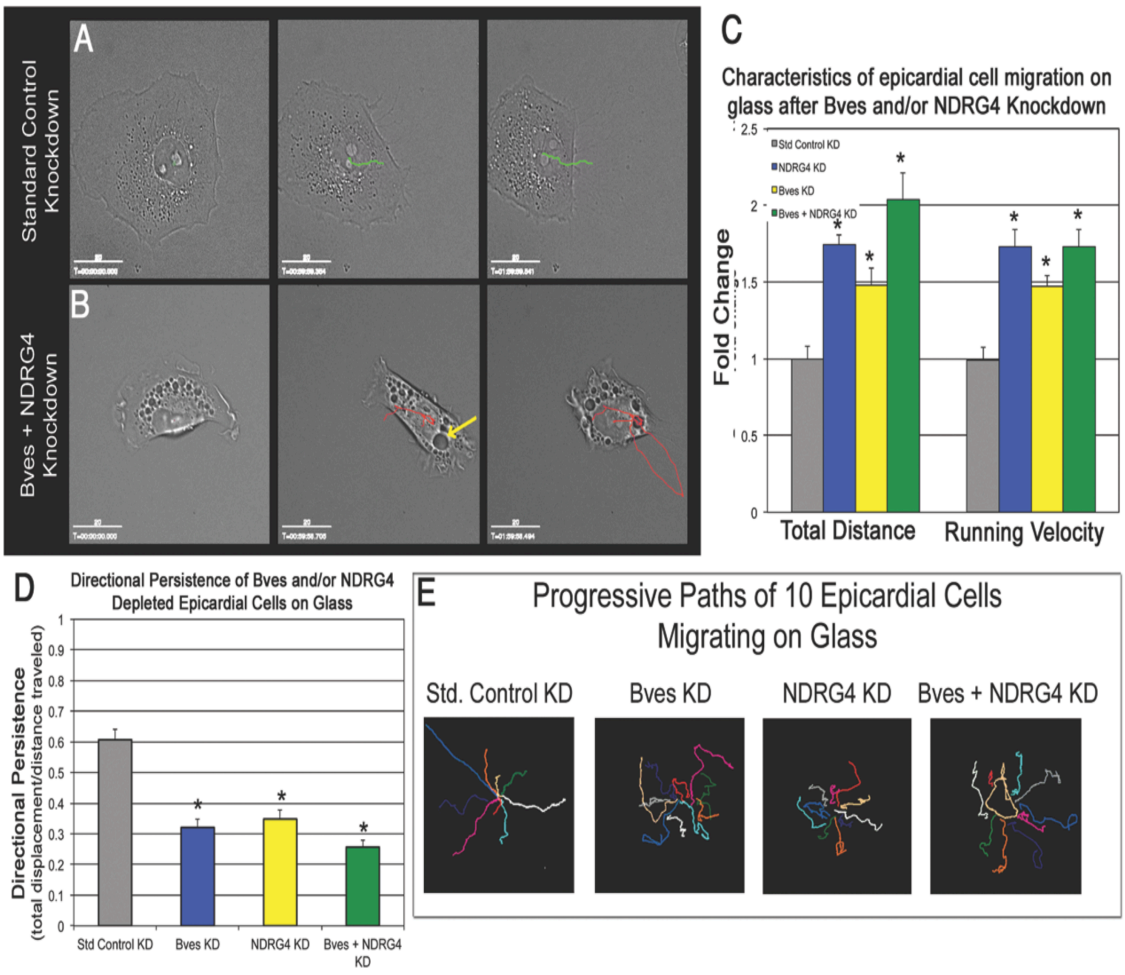

Figure 4.5 Bves and NDRG4 coregulate epicardial cell directional persistence and fibronectin trafficking. (A) Epicardial cells treated with SC siRNA and plated at low density on glass dishes move a short distance with high directionality over the timecourse. In these representative images, the nuclear path of movement is demarcated by the green line (ImageJ manual tracking). (B) Bves/NDRG4 siRNA-depleted epicardial cells have deregulated movement, as cells tracked over the timecourse (purple line) appear to travel further, without directionality compared to controls. Cells also retain large cytoplasmic vacuoles (yellow arrow). (C) Manual tracking quantification indicates that Bves- and/or NDRG4-depletion conditions exhibit accelerated cell movement speed and increased distance traveled, which is highly statistically significant; n≥40 cells per condition; *p≤0.0001. (D) Bves and/or NDRG4-depleted cells had highly significantly impaired directional persistence, (a ratio of the total displacement over the distance traveled, (with 1 being highly directional and 0 being random); n≥40 cells per condition; *p≤0.0001. (E) An overlay of representative tracks of epicardial cells illustrates the impaired directionality and randomized movement exhibited by Bves- and/or NDRG4-depleted cells (10 tracks per condition).

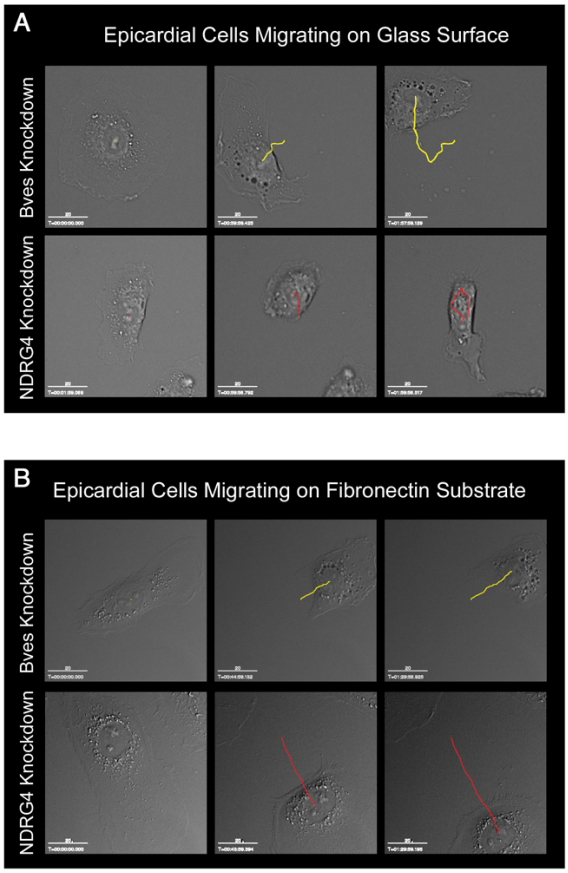

Figure 4.6 Bves or NDRG4-depleted epicardial cells have impaired movement on glass but not fibronectin. (A) Bves or NDRG4 depleted epicardial cells appear to move long distances and have poor directional persistence compared to controls as tracked by ImageJ manual tracking and demarcated by the yellow and red lines, respectively (Figure 4)**.** (B) Plating Bves or NDRG4 depleted epicardial cells on an evenly disbursed fibronectin matrix rescues directional persistence defects on a glass surface (A).

Bves and NDRG4 Coregulate Epicardial Cell Directional Persistence and Fibronectin Trafficking

Disruption of Bves or NDRG4 leads to an increase in random cell motility *in vitro* and Bves-depletion causes a defect in cell homing in whole organisms (Andrée et al, 2002; Nishimoto et al, 2003; Ripley et al, 2006; Lin et al, 2007; Melotte et al, 2009). Still, the molecular and cellular mechanisms underlying

randomized movement are poorly understood. To determine the specific motility defect impaired with loss of function, epicardial cells were treated with Bves and/or NDRG4, or SC siRNA, plated on glass in complete medium, and imaged for two hours at a frame rate of one/min. Distance traveled, velocity and directional persistence were quantitated using Image J. Interestingly, Bves-, NDRG4- or co-depleted cells had strikingly poor directional persistence (Figure 4.5D) calculated by dividing the total displacement traveled by the distance traveled. Directional persistence is measured on a scale of 0 to 1 where 0 is random movement and 1 is movement in a straight line (Harms et al, 2005). Also, depleted cells exhibited faster paced movement and longer path lengths as compared to controls, mirroring *in vivo* results [Figure 4.5A-C, Figure 4.6A, Supplemental Movies 1-4; tracking lines follow cell nuclei; (Ripley et al, 2006)]. An overlay of the progressive paths of 10 representative cells illustrates that disruption of Bves and/or NDRG4 function randomizes and accelerates cell movement (Figure 4.5E).

In addition to impaired cell movements, time-lapse DIC imaging demonstrated that Bves- and/or NDRG4-depleted cells accumulated large cytoplasmic vacuoles (Figure 4.5B, yellow arrow) that originated at the plasma membrane and rapidly traveled toward the cell nucleus (Supplemental Movies 1-4). Since vesicular enlargement is generally associated with membrane trafficking defects, this finding suggested that Bves and NDRG4 are necessary for regulated vesicular transport. Two recent studies demonstrated that endocytic

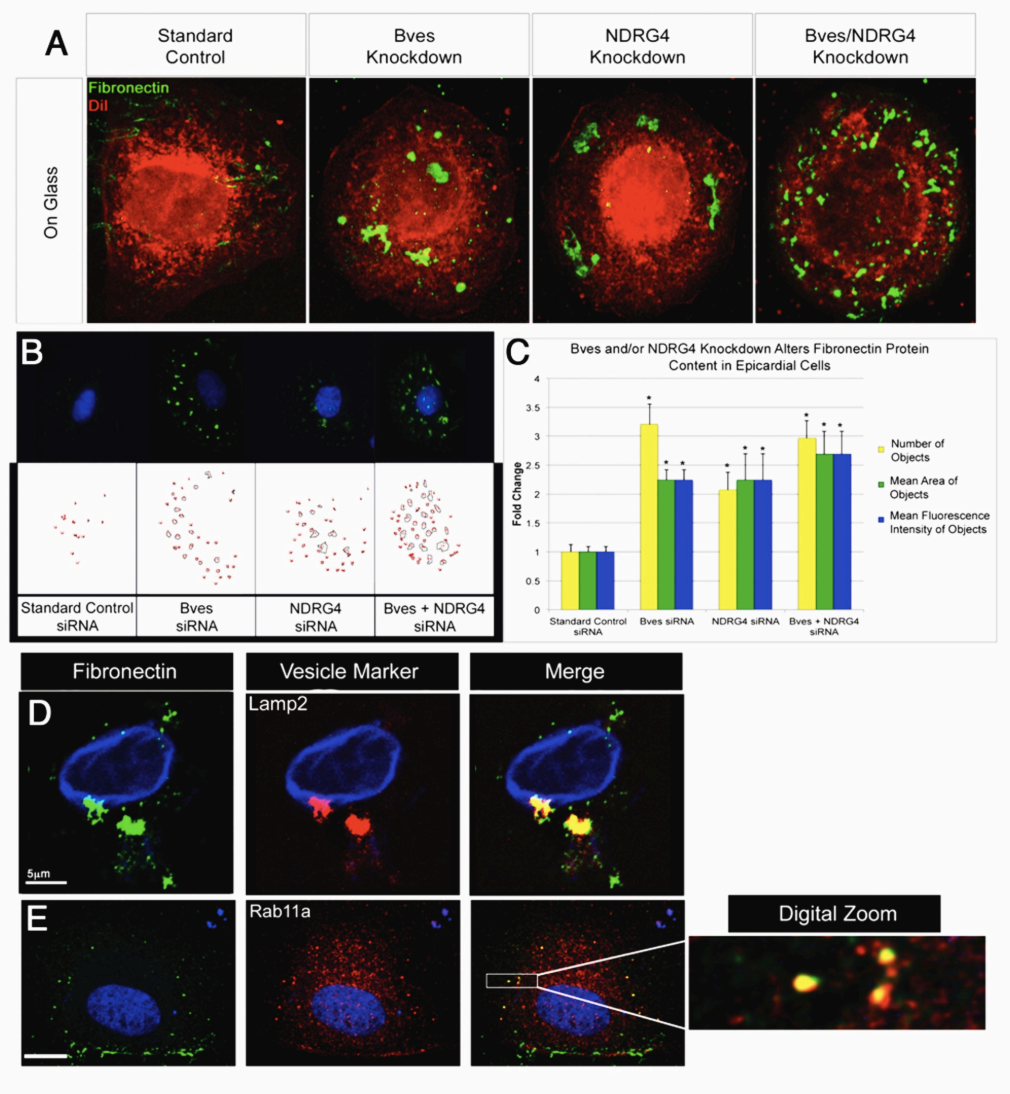

Figure 4.7 Bves/NDRG4-depleted cells contain large fibronectin positive objects in late endosomal/lysosomal and recycling endosome compartments. (A) Epicardial cells marked with DiI (Red; to mark the membranes) and labeled with Fibronectin antibody indicate that Bves- and/or NDRG4-depleted epicardial cells retain vesicles of cytoplasmic fibronectin. (B) Fibronectin positive objects were identified and measured using ImageJ thresholding and particle analysis (top original image, bottom overlay of included particles). (C) Quantification with ImageJ indicates that there are significantly more fibronectin positive objects that are larger with stronger fluorescence intensity compared to controls; *p≤0.001 n≥50 cells/condition. (D) Bves/NDRG4-depleted epicardial cells labeled for Fibronectin (green) and Lamp2 (red) indicate that cytoplasmic fibronectin traffics in late endosomal/lysosomal compartments; scale bar is 5µm, optical slices are 1 Airy Unit. (E) Bves/NDRG4-depleted epicardial cells labeled with a Fibronectin antibody (green) and Rab11a (red) indicate that fibronectin also traffics through recycling endosomes; scale bar is 10µm.

trafficking of exogenous fibronectin present in the environment regulates cell movement (Lobert et al, 2010; Sung et al, 2011). Given prior data and our current phenotype of randomized cell movement and large intracellular vesicles, we tested whether fibronectin accumulates intracellularly in Bves- and/or NDRG4-depleted cells. As shown in Figure 4.7A, immunofluorescence confocal microscopy revealed that large fibronectin-positive structures are indeed present in the cytoplasm of these cells. Quantification by object analysis in ImageJ revealed that Bves and/or NDRG4-depleted cells exhibited a 2-3-fold increase in the number, mean area, and intensity of fibronectin-positive structures, compared with controls (Figure 4.7B-C). Colocalization of these structures with LAMP2 demonstrated fibronectin accumulation within late endosomal/lysosomal compartments (Figure 4.7D), as previously reported (Sung et al, 2011). In addition, there was colocalization of fibronectin in small Rab11a-positive endosomes (Figure 4.7D-E). Together, these data suggest that disruption of Bves and NDRG4 function impairs endocytic trafficking of fibronectin.

Fibronectin Substrate Rescues Bves and NDRG4 Migration and Trafficking Defects

We have previously shown that a cytoskeletal protein, cortactin, facilitates resecretion of internalized fibronectin from a late endosomal/lysosomal compartment to promote adhesion assembly, lamellipodial stability and effective cell migration (Sung et al, 2011). In this previous study, migration defects in

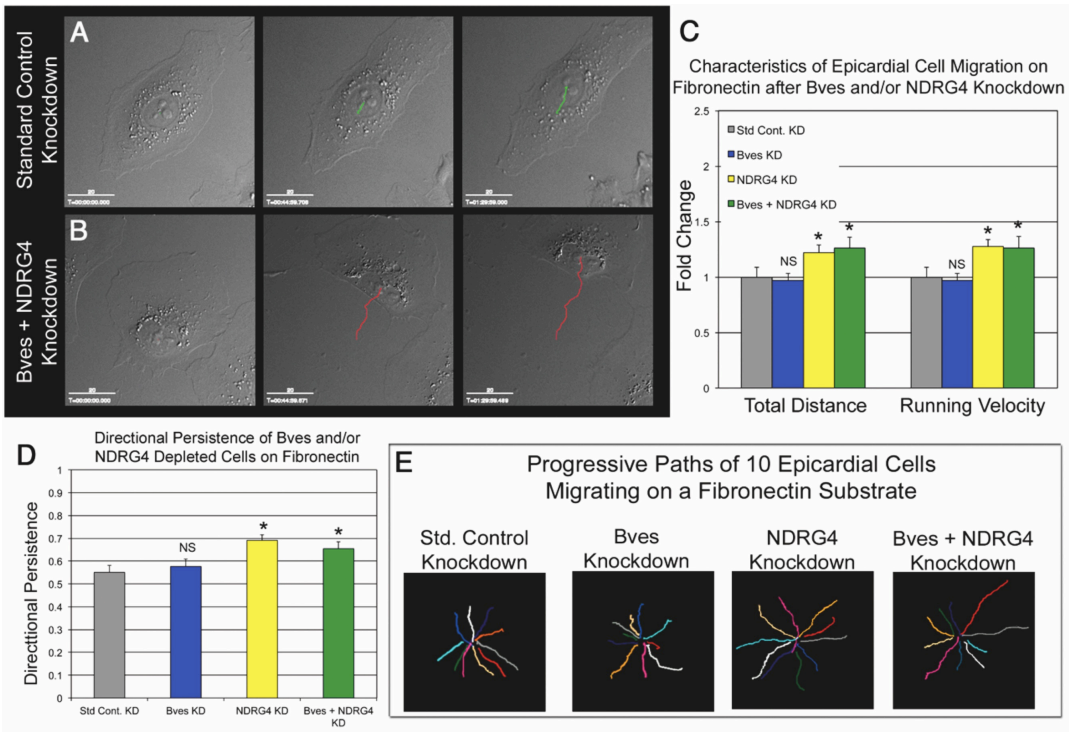

Figure 4.8 Fibronectin substrate rescues Bves and NDRG4 migration and trafficking defects. (A) Control epicardial cells on an evenly-distributed fibronectin matrix exhibit a high amount of directional movement over the timecourse. (B) Bves/NDRG4 co-depleted epicardial cells plated as described in (A) also exhibit a high level of directionality over the timecourse. (C) ImageJ manual tracking analysis indicates that migration distance and velocity are partially restored on fibronectin substrate; *p≤0.05, n≥44 cells/condition, NS=not significant compared to SC. (D) Strikingly, Bves-depleted cell directionality is fully rescued, and NDRG4/co-depleted cells have significantly better directionality than controls; *p≤0.05, n≥44 cells/condition, NS=not significant compared to SC. (E) Representative tracks of ten cells per condition plated on fibronectin illustrate that directional persistence defects are rescued on fibronectin substrate.

cortactin-depleted cells were fully rescued when cells were plated on substrates coated with high concentrations of exogenous ECM, making this an ideal assay to determine whether genes such as Bves and NDRG4 regulate autocrine ECM secretion.

Bves-, NDRG4- and co-depleted cells were plated on glass coverslips coated with 10 μg/ml fibronectin and assayed by live imaging as in Figure 4. Interestingly, Bves and/or NDRG4-depleted cells now migrated with directional persistence when plated on fibronectin substrate (Figure 4.8D-E, Figure 4.6 and Supplemental Movies 5-8). Image quantification analysis demonstrated that presence of a fibronectin matrix fully rescued directional persistence or improved it beyond control level (Figure 4.8C, compare to data in Fig 4.5C). In contrast to the full rescue of all phenotypes in Bves-depleted cells, distance and velocity measurements in NDRG4-depleted and co-depleted cells were only partially rescued by plating on exogenous fibronectin (Figure 4.8C, compare to Fig 4.5C), suggesting that NDRG4 may have additional functions in cell motility. Overall, exogenously applied fibronectin matrix rescued movement, suggesting that Bves and NDRG4 might regulate autocrine-ECM deposition to facilitate directional movement when cells lack substrate.

Bves and NDRG4 Coregulate Autocrine ECM Deposition

Our data suggest that Bves and NDRG4 regulate cell movement through deposition of ECM. To test the functionality of ECM produced by control and Bves/NDRG4-depleted cells, we isolated autocrine-produced cell-free ECM from each of the cell types by removing confluent cell monolayers with 20 mM ammonium hydroxide (Sung et al, 2011). Fresh Bves/NDRG4-depleted or control cells were then plated on these cell-free matrices and monitored for two hours.

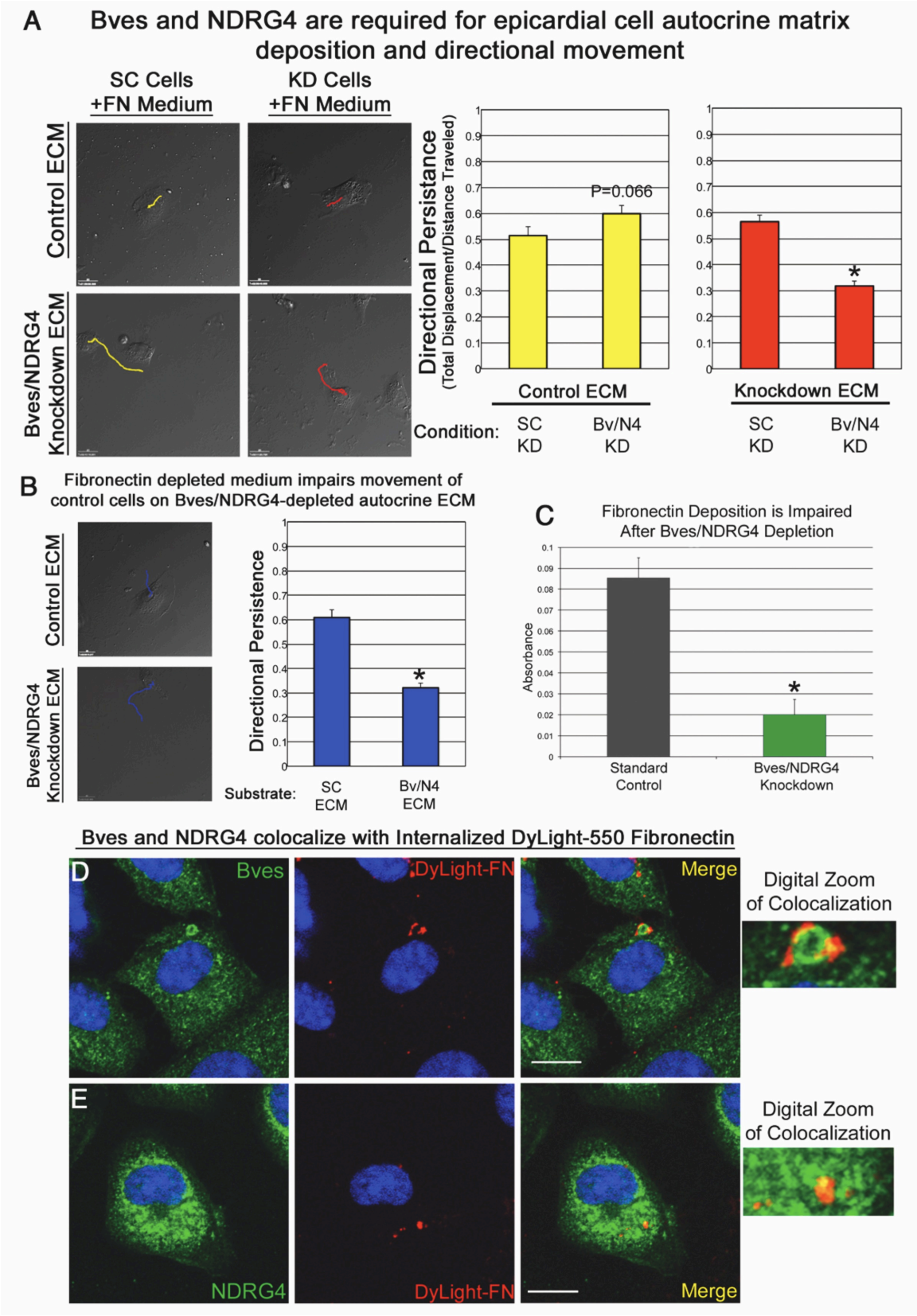
A
Bves and NDRG4 are required for epicardial cell autocrine matrix deposition and directional movement
SC Cells +FN Medium
KD Cells +FN Medium
Control ECM
Bves/NDRG4 Knockdown ECM
Directional Persistance
(Total Displacement/Distance Traveled)
P=0.066
*
Control ECM
Knockdown ECM
Condition:
SC
KD
Bv/N4
KD
B
Fibronectin depleted medium impairs movement of control cells on Bves/NDRG4-depleted autocrine ECM
Directional Persistence
Substrate:
SC ECM
Bv/N4 ECM
C
Fibronectin Deposition is Impaired After Bves/NDRG4 Depletion
Absorbance
Standard Control
Bves/NDRG4 Knockdown
Bves and NDRG4 colocalize with Internalized DyLight-550 Fibronectin
D
Bves
DyLight-FN
Merge
Digital Zoom of Colocalization
E
NDRG4
DyLight-FN
Merge
Digital Zoom of Colocalization

Figure 4.9 Bves and NDRG4 coregulate fibronectin deposition. ECM deposition is probed using a cell-free ECM assay, which removes cells but retains the ECM. Migration of newly-plated cells is then assessed on the previously-produced ECM to test the functionality of the matrix. (A) On control-produced extracellular matrix, control and gene-depleted epicardial cells move directionally. Conversely, on Bves/NDRG4-depleted ECM, control cells move directionally, but Bves/NDRG4-depleted cells have poor directional persistence; $n>50$ cells; $*p\leq0.0001$. (B) When control epicardial cells were fed medium-lacking fibronectin, cells only moved directionally on control ECM. Unlike in (A), control epicardial cells failed to overcome poorly produced ECM, when fibronectin was unavailable in the medium; $n\geq50$ cells, $*p\leq0.001$. (C) Biotin-labeled fibronectin deposition assays indicate that Bves/NDRG4-depleted cells have impaired fibronectin deposition onto a surface compared to controls; $n=7$ assays. (D) Fibronectin-free medium supplemented with DyLight-550 labeled fibronectin (DyLight-FN) is internalized by epicardial cells after one hour. Endogenous Bves colocalizes with DyLight-FN on vesicular structures; optical slices are 1 Airy Unit, scale is 10μm. (E) Internalized DyLight-FN also colocalizes with endogenous NDRG4 on vesicular structures; scale is 10μm.

On ECM produced by control cells, newly-plated epicardial cells moved directionally whether cells were treated with SC or Bves/NDRG4 siRNA (Figur4.9A, Supplemental Movies 9-10). This is similar to results obtained from cells plated on exogenous fibronectin substrates (see Figure 4.8B). In contrast, only control cells moved in a directionally persistent manner on ECM produced by Bves/NDRG4 depleted cells (Figure 4.9A, Supplemental Movies 11-12), while Bves/NDRG4-depleted cells moved randomly, phenocopying their behavior on glass (see Figure 4.5B).

In this previous experiment, soluble fibronectin was present in the medium in both experimental conditions. Thus, a possible explanation for the efficient migration of control cells on matrix produced by Bves/NDRG4-depleted cells is that they can dynamically internalize and resecrete fibronectin present in the medium for use as a motility substrate. To test this hypothesis, cells were replated on matrix deposited by control or Bves/NDRG4-depleted cells. Motility assays were then performed in medium depleted of fibronectin [prepared as described by: (Danen 2002; Sung et al, 2011)]. As expected, control cells moved in a directionally persistent manner on matrix produced by control cells, as dynamic ECM secretion of internalized fibronectin was unnecessary on a well-formed matrix (Figure 4.9B). Conversely, in the absence of soluble fibronectin, control cells were unable to migrate persistently when plated on matrix produced by Bves/NDRG4-depleted cells (Figure 4.9B, Supplemental Movies 13 & 14).

Thus, the presence of fibronectin in the medium is required for control cells to overcome deficiencies in matrix produced by Bves/NDRG4-depleted cells (compare Figures 4.9B and 4.9A). These data demonstrate that fibronectin internalization and resecretion may be necessary for persistent cellular movement of epicardial cells and that loss of cellular Bves and NDRG4 function disrupts this process.

To directly test whether Bves and NDRG4 regulate fibronectin internalization and/or deposition, biotin-labeled fibronectin was added to the medium of control and Bves/NDRG4-depleted epicardial cell sheets after 24 hours of culture in fibronectin-free medium. After 18 hours, cells were removed from the plate with ammonium hydroxide and the amount of biotin-labeled fibronectin present in the resulting autocrine-secreted ECM was quantified by streptavidin-HRP ELISA (see Materials and Methods for details). Absorbance measurement demonstrated that Bves/NDRG4-depleted epicardial cells deposited four-fold less fibronectin than controls (Figure 4.9C). To directly visualize whether epicardial cells internalized fibronectin, DyLight 550 labeled fibronectin was added to cell grown in fibronectin-depleted medium for one hour (Figure 4.9D-E). Under these conditions, internalized DyLight 550 fibronectin localized to vesicular compartments that co-label with Bves and NDRG4 (Figure 4.9D-E, respectively). Taken together, these studies demonstrate that internalization of soluble fibronectin into vesicles proceeds in the absence of

Bves and NDRG4, but re-secretion of this ECM component is dependent on their function to promote directionally persistent migration.

Discussion

In this study we identified an interaction between Bves and a novel binding partner, NDRG4 and demonstrated that the two proteins function together to promote directionally persistent cell movement. We find that Bves and NDRG4 are important for resecretion of fibronectin into the ECM from a late endosomal/lysosomal compartment. Our data further indicate that fibronectin secretion is critical for persistent epicardial cell migration. Thus, in the absence of NDRG4 or Bves, cell motility is randomized when cells are forced to autocrine secrete ECM. This phenotype can be rescued on exogenously applied fibronectin and matrix produced by control cells. Taken together, we propose that Bves is a pivotal regulator of cell migration and adhesion by coordinating subcellular trafficking of intra- and extracellular proteins, and that this function has broad implications for development, repair and cancer.

The Interacting Partners Bves and NDRG4 Regulate Overlapping Cellular and Developmental Behaviors

Using multiple methodologies, we show that Bves and NDRG4 physically interact. The identification of this interaction was of immediate interest as previous studies demonstrated that loss of Bves and NDRG4 function result in

similar cellular phenotypes. For example, morpholino Bves knockdown impairs lamellipodial formation in *Xenopus* head mesoderm and NIH-3T3 cells (Smith et al, 2008; Hager et al, 2010), while expression of antisense NDRG4 RNA inhibits neurite outgrowth in PC12 neuronal cell lines (Ohki et al, 2002). Additionally, Bves and NDRG4 are hypermethylated and downregulated in multiple cancer cell types (Feng et al, 2008; Melotte et al, 2009; Schilling et al, 2009; Kim et al, 2010; Williams et al, 2011) and overexpression of either gene inhibits migration in related cancers, suggesting that the genes may suppress metastasis (Melotte et al, 2009; Williams et al, 2011). These overlapping phenotypes suggest that the Bves/NDRG4 interaction is important for morphogenesis, repair and tumor suppression.

Previous *in vivo* and *in vitro* gene perturbation studies indicate that cell movement is disorganized with loss of Bves function (Ripley et al, 2004; Ripley et al, 2006), but the molecular mechanism underlying these phenotypes has not been determined. Here, using a clonal epicardial cell line, we quantified Bves influence on directional migration for the first time, and demonstrate that NDRG4 depletion, like its binding partner Bves, randomizes cell movement. This loss of directional persistence may explain the errors in morphogenesis and wound healing previously reported above.

While NDRG4 regulates cell migration in cancer and other cell lines (Nishimoto et al, 2003; Melotte et al, 2009; Wang and Hill 2009), the current study is the first illustration of the mechanism by which NDRG4 influences this behavior. Although

NDRG4 has not been previously shown to regulate vesicular trafficking, previous studies on the related family member, NDRG1, have shown that it directs E-Cadherin recycling, as well as myelin sheath maintenance and APO AI/AII lipid trafficking in Schwann cells (Hunter et al, 2005; Berger et al, 2006; Kachhap et al, 2007; King et al, 2011). Also, NDRG2 is necessary for IL-10 secretion (Choi et al, 2010). The present data provide a possible molecular explanation for these phenotypes through NDRG association with Bves. The collective data suggest a global mechanism through which NDRG molecules impact a broad array of cellular behaviors perturbed in multiple cancer types (Melotte et al, 2010).

ECM Secretion Enhances Directional Persistence and may Promote *In Vivo* Morphogenesis Events

Our study demonstrates that fibronectin matrix produced by control cells or simple application of purified protein supports directionally persistent epicardial cell movement. Consistent with our findings, Harms *et al*. reported that fibronectin substrate confers directionally persistent movement in CHO cells (Harms et al, 2005). One possible explanation for the requirement of ECM in promoting persistent motility could be that spontaneous cell polarization facilitating cell migration is frequently unstable but can be stabilized by adhesion formation at the leading edge of cells. Consistent with this idea, Bves inhibition results in lamellipodial and cell polarization defects (Hager and Bader 2009; Hager et al, 2010). At lower matrix concentrations or in a complex ECM environment (e.g. *in*

vivo), direct deposition of ECM at the leading edge of cells might be the most efficient mechanism to stabilize newly formed lamellipodia and thus strengthen cell polarization.

Bves and NDRG4 are Essential for Autocrine ECM Deposition

Bves/NDRG4-dependent fibronectin deposition proceeds through a newly identified trafficking mechanism in which exogenous soluble fibronectin is endocytosed, processed through recycling in late endosomes/lysosomes, and resecreted onto an underlying matrix (Sung et al, 2011). The initial uptake of fibronectin appears to be uninhibited with loss of Bves or NDRG4 function. Indeed, large fibronectin and LAMP2 double-positive late endosomal compartments as well as smaller fibronectin and Rab11 double-positive recycling endosomal compartments are found in the cytoplasm of Bves- and/or NDRG4-depleted cells. The accumulation of fibronectin in those compartments suggests that Bves and NDRG4 may function downstream of internalization to promote fibronectin secretion from either late or recycling endosomes (Sung et al, 2011). Clearly, loss of Bves and NDRG4 results in a reduction in biotin-labeled fibronectin moving from the medium to the insoluble matrix.

Interestingly, we previously found that Bves binds VAMP3, an endosomal v-SNARE that regulates recycling endosome fusion at the plasma membrane for integrin and protease secretion (Proux-Gillardeaux et al, 2005; Hager et al, 2010), and that this interaction was important for β1-integrin trafficking (Hager *et al*, 2010). That finding raises the possibility that fibronectin and its receptors are

recycled in the same endosomal vesicles to promote efficient cell motility. Of note, Lobert *et al*. recently showed that fibronectin binding leads to trafficking of $\alpha 5\beta 1$-integrin into late endosomes, suggesting that they are cotrafficked during the initial part of the pathway (Lobert et al, 2010). In our studies on cortactin, we also found that fibronectin trafficked through a late endosomal/lysosomal compartment before exocytosis. An important future direction will be to determine the exact role of VAMP3 in BVES/NDRG4-mediated fibronectin secretion.

The present study demonstrates that Bves and NDRG4 regulate autocrine ECM production in epicardial cells. While it is known that epicardium makes fibronectin which is abundant in the subepicardial space, and that adhesion of integrin receptors to substrates is critical for coronary artery formation (Manasek 1969; Kalman et al, 1995; Kwee et al, 1995; Yang et al, 1995; Sengbusch et al, 2002; Nahirney et al, 2003), the current study is the first report of a subcellular trafficking mechanism that regulates this process. During embryonic epicardial development, dynamic ECM secretion could support *de novo* fibronectin deposition during epicardial sheet migration and also provide a substrate for myocardial adhesion. Furthermore, combined with the previous data in cancer cells, our finding that fibronectin secretion regulates persistent motility of epicardial cells suggests that autocrine ECM secretion is likely to regulate migration in both developmental systems and disease processes.

Summary

The present data are the first to indicate that Bves, through an interaction with NDRG4, regulates exocytosis of macromolecules to the extracellular matrix. The number and variation in subcellular events regulated by Bves in developmental, reparative, and disease processes is now emerging. It is possible that the trafficking compartment regulated by Bves and its binding partners NDRG4 and VAMP3 shuttles diverse contents depending on cellular context. Thus, we propose a central or unifying theme for its function, namely that Bves is a pivotal interacting protein in the trafficking of diverse molecules for cell movement and adhesion.

CHAPTER V

CONCLUSIONS AND FUTURE DIRECTIONS

Conclusions

Summary

This dissertation presents experiments developed to identify and elucidate regulators of epicardial cell behaviors. First, the present chapter will discuss the findings of Chapter II and the implications of chemical genetic screening to epicardial research. Second, studies performed in Chapter IV identified a novel epicardial cell behavior, autocrine ECM deposition, and two regulators of this mechanism. The relevance of these findings to heart development and repair will be discussed. Third, Chapter III revealed that Bves/VAMP3 interaction regulates cell adhesion through β1-integrin and, possibly, general recycling endosome trafficking. As Chapter IV identified a Bves/NDRG4 interaction that regulates directional migration through autocrine ECM deposition mechanism, these findings suggest that Bves globally regulates cellular trafficking to facilitate adhesion and migration. Thus, this chapter will discuss how studies defining Bves binding interactions have illuminated the understanding of Bves molecular activity. Finally, taking the previous studies collectively, a working model of Bves global function will be proposed.

Chemical Genetic Screens Elucidate Coordination of Epicardial Behaviors

Proepicardial contribution to coronary vasculature has been observed for several decades and is well described (Manasek 1976; Mikawa and Gourdie 1996; Lepilina et al, 2006). Many molecules have been identified that extrinsically regulate specific phases of epicardial development and it is clear that the process employs overlapping signaling mechanisms to regulate multiple behaviors (Olivey and Svensson 2010). Still, how epicardial cells coordinate these signaling mechanisms and subsequent behaviors is largely unknown. One possible reason for this deficit is that most of the studies previously addressing signaling during epicardial development have been approached in a linear fashion, often observing the contribution of single pathways to single behaviors [see Figure 1.4; (Olivey and Svensson 2010)]. While these studies are important for initial identification of signals involved in this process, the scope is only a narrow window of the entire coordinated program; very few detailed cell biological studies examine the regulation of concurrent epicardial behaviors. Chapter II augments previous literature by developing *in vitro* and *ex vivo* methodologies to examine effects of signaling cascade players on multiple epicardial behaviors concurrently, as well as determine the simultaneous influence of multiple signal cascades on a single cellular process.

As proof-of-principle, the present studies resolve a cooperative interaction between TGFβ and BMP signaling in which the hormones coregulate epicardial sheet migration, while other behaviors occurring in unison, including single cell migration, only require TGFβ signaling (process diagrammed in Figure 5.1). As

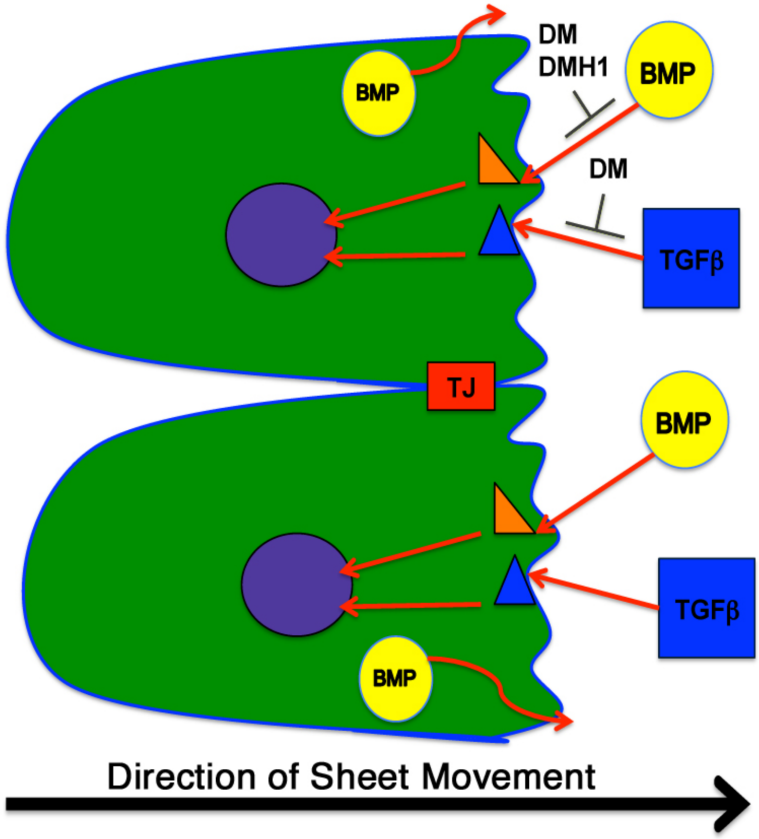

Figure 5.1 TGFβ and BMP signaling cooperatively regulate epicardial sheet movement. Epicardial cells move as sheets to cover the developing heart. During this movement BMP signals are elaborated into the extracellular space. TGFβ and BMP signal cascades then cooperatively regulate sheet movement. Two tools, Dorsomorphin (DM) and DMH1 can broadly or specifically inhibit these pathways.

discussed in detail in the introduction, TGFβ signaling has previously been determined to stimulate EMT, migration and early differentiation of epicardial cells in culture (Olivey and Svensson 2010). Additionally, $TGF\beta_{1\&3}$ regulate *in vivo* murine coronary vessel formation as: *Tgfβr3* null mice produce fewer vessels, ALK5 stimulation promotes EMT, and *Alk5* null murine epicardia fail to adhere to the myocardium and produce small coronary vessels (Zwijsen et al, 2001; Compton et al, 2007; Sridurongrit et al, 2008). Hence, our data are

consistent with previous findings in which TGFβ signaling is a general regulator of many epicardial behaviors *in vitro* and *in vivo.* Alternatively, BMP signaling, while widely expressed throughout the sinus venosus, developing PE and heart, has primarily been identified to stimulate only PE specification and sheet migration (Schlueter et al, 2006; van Wijk et al, 2009; Ishii et al, 2010).

Although these hormones have been individually identified to influence epicardial development; few studies suggest that BMP and TGFβ signaling cooperatively regulate epicardial development, and this conclusion has only been indirectly implied. For example, Inhibitory-Smad6 null mice upregulate BMP-specific Smads 1/5/8, which contributed to impaired coronary vessel formation, similar to the phenotype observed in *Alk5* null mice (Imamura et al, 1997). These data imply that TGFβ and BMP signaling cooperatively co-regulate epicardial development, but neither definitively identify this relationship or elucidate when/how TGFβ and BMP are coordinated. The studies presented here directly examine, at high resolution, simultaneous regulation of single epicardial behaviors by TGFβ and BMP signal cascades, as well as the effect of TGFβ or BMP singling on multiple concurrent behaviors. The cooperative regulatory relationship observed *in vitro* was also applicable to *ex vivo* studies, underscoring the relevance of data observed *in vitro* to organism development. Taken together, the present data provide novel experimental methodologies for the field to either investigate a range of behaviors and pathways or isolate single elements.

To date, regulators of epicardial development have emerged through classic gain- and loss-of-function mutation studies as well as stimulation by

specific growth factors (Olivey and Svensson 2010). The growing field of chemical genetics uses small organic molecule treatments, rather than mutations, to influence protein behaviors in cellular and developmental systems (Stockwell 2004). Small organic molecules tools are valuable for studying complex developmental programs because synthesized molecules can be controlled to specifically influence individual functions of target proteins, while leaving other behaviors intact (Stockwell 2004). Additionally, these chemicals are inexpensive to create, and vast chemical libraries allow for unbiased screening of cellular and developmental behaviors to identify novel players that regulate the process under examination (Stockwell 2004). The studies outlined here are the first to utilize a directed chemical genetic screen to establish simple readouts of epicardial behaviors, and as a result determined that Dorsomorphin (DM) inhibits TGFβ and BMP signaling while DMH1 specifically inhibits BMP (Figure 5.1). These experiments could become a standard for pathway characterization and discovery in the epicardium, as the small organic molecule screening methodologies presented here have readouts that are highly amenable to future unbiased, high-throughput screening. Such future studies could be essential to broadly describe, and eventually mimic, epicardial development during injury repair.

Epicardial Cell Cultures Robustly Recycle and Redeposit Soluble Fibronectin

In early electron microscopy studies identifying the extracardiac origin of the epicardium, a “floccent” material was observed in epicardial cell cytoplasm that was later identified to be fibronectin (Manasek 1969; Manasek 1976). In mice, fibronectin is expressed on the basal surface of PE cells and in patches on the apical sheath covering the naked myocardium (Kalman et al, 1995). Fibronectin expression fluctuates throughout development but is highly enriched in the subepicardial space (Tidball 1992; Bouchey et al, 1996). While *fibronectin* global null mice are embryonic lethal prior to PE formation, the fibronectin plasma membrane binding partner, $\alpha 4\beta 1$-integrin, and another myocardial expressed fibrillar substrate, VCAM-1, are critical for epicardial sheet migration to the heart, adherence and coronary vessel formation (George et al, 1993; Kwee et al, 1995; Yang et al, 1995; Sengbusch et al, 2002). Even before reaching the heart, PE villi interact with extracellular matrix present in the pericardial cavity to initiate sheet migration (Nahirney et al, 2003). Interestingly, several combinations of α and β integrins adhere to and catalyze fibronectin fibrillogenesis in epicardial cells, and disruption of $\alpha 4\beta 1$ integrin impairs fibronectin incorporation into a subepicardial matrix (Pae et al, 2008). Thus, the field has demonstrated that epicardial cells make fibronectin, and that adhesion to this substrate is an essential epicardial process for development, yet no research to date has determined how epicardial cells facilitate subepicardial fibronectin enrichment

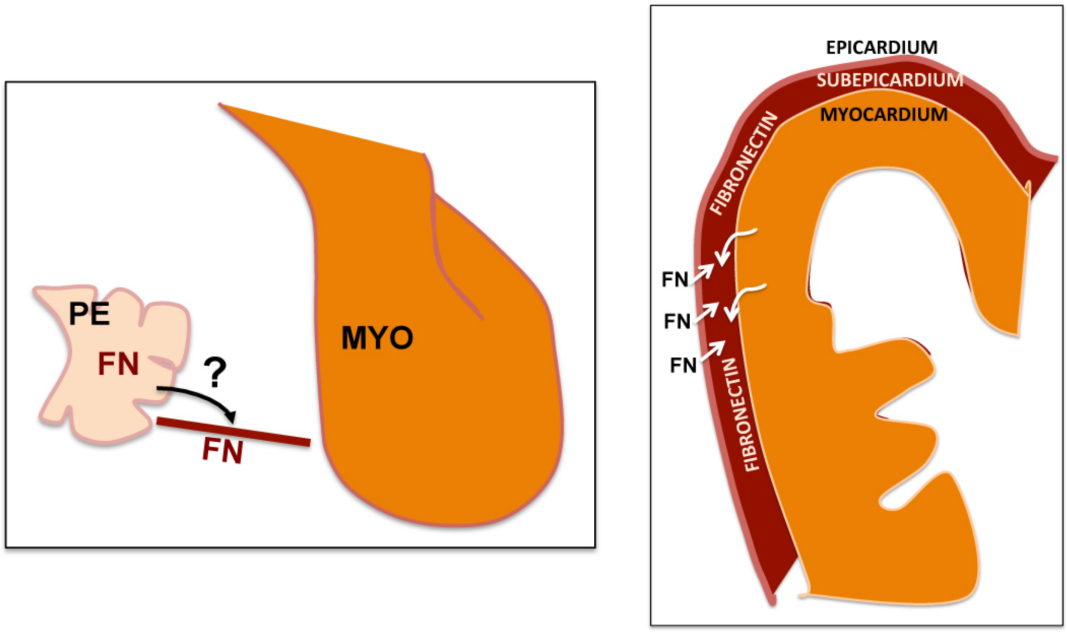

Figure 5.2 Fibronectin deposition is essential for epicardial development. (A) An extracellular matrix bridge between the PE and developing heart adheres to PE cells and is required for sheet migration to the heart (Nahirney 2003). PE cells contain fibronectin (Manasek 1969) and could produce the ECM bridge. (B) Fibronectin is also abundant in the subepicardial space (subepicardium). Both the epicardium and the myocardium contribute to this layer. Epicardial contributions to both sheet movement and adhesion could occur using autocrine ECM deposition (Chapter IV). Images adapted from Winter and Gittenberger-de Groot 2007.

and subsequent adhesion.

In the present studies, epicardial cell culture models are effective tools to recapitulate developmental behaviors. With these tools, we identified a behavior novel to epicardial cells: internalization of soluble exogenous fibronectin for re-deposition onto an underlying surface and subsequent directional movement. While this behavior has not yet been described *in vivo*, these cell biological assays are critical to bridge the information gap between the presence of subcellular fibronectin in epicardium (Manasek 1976) and the essential role for integrin substrates in epicardial adhesion and directed migration [Figure 5.2;

(Kwee et al, 1995; Yang et al, 1995; Sengbusch et al, 2002; Merki et al, 2005; Pae et al, 2008)]. Our experiments address the important question: what mechanism facilitates deposition and enrichment of ECM substrates in the subepicardium and throughout the heart? Manipulation of such a mechanism may become critically important as mounting evidence suggests that EPDCs secrete proteins after MI to condition a niche in which injured cardiac tissue could either undergo fibrosis or regenerate (Poss et al, 2002; Zhou et al, 2011).

Bves and NDRG4 Interact in Epicardial Cells

Bves was first discovered through subtractive screening of the developing heart (Reese et al, 1999; Andrée et al, 2000). Polyclonal antibody labeling techniques determined that Bves has highly enriched expression in the chick PE, migrating PE villi, surface epicardial sheet, in the cytoplasm of subepicardial EPDCs, and around the developing coronary arteries (Reese and Bader 1999; Wada et al, 2001) In cell lines and *in vivo,* Bves exhibits plasma membrane localization in epicardial sheets, while after epicardial delamination Bves localization shifts to the cytoplasm (Wada et al, 2001; Osler et al, 2005). Bves colocalizes with adherens junction markers and functions to sustain epicardial sheet integrity, while blocking Bves function impairs *ex vivo* PE outgrowth and migration (Wada et al, 2001; Osler et al, 2005). Collectively, these studies suggest that Bves influences both cell-cell and cell-matrix adhesion in epicardial tissue, yet Bves protein function remains unidentified in the epicardium. Likewise, while NDRG4 is enriched in heart tissue and regulates cardiomyocyte

proliferation, expression of NDRG4 or a function for this protein in epicardial cells has not been identified (Qu et al, 2002; Qu et al, 2008).

Cell biology assays allowed the identification of Bves and NDRG4 interaction in epicardial cells. Protein-depletion and dominant negative interference of the interaction demonstrated that, as suggested by antibody labeling and prior loss-of-function studies (Nishimoto et al, 2003; Hager and Bader 2009; Melotte et al, 2010), Bves and NDRG4 regulate epicardial cell migration. Cell tracking and image analyses of Bves- and NDRG4-depleted epicardial cell migration indicated that these proteins influence epicardial directional persistence by regulating trafficking of internalized fibronectin for deposition. While identifying a novel epicardial cell process, the present data also provide two regulators of this behavior. Indeed, these data are the first to describe a function for Bves in epicardial tissue, despite its identification as dynamically expressed therein over ten years ago. Furthermore, the data presented in this dissertation link NDRG4 to a novel molecular pathway and thus provide a framework for future studies on this protein in developmental and disease systems.

Bves Facilitates Diverse Behaviors Through Binding Partner Interactions

Despite the well-described roles for Bves in epithelial sheet maintenance and cell migration, establishing molecular function of Bves, which shares no known homologous domains, has been difficult. Initially, it was suggested that Bves is a novel transmembrane adhesion protein, functioning similar to occludin

and E-Cadherin but subsequent biochemistry refuted this theory, as the putative adhesive domain was, in fact, intracellular (Wada et al, 2001; Knight et al, 2003). Furthermore, Bves was subsequently demonstrated to have broader affects, as regulated migration also requires Bves (Ripley et al, 2006). Bves is enriched in heart tissue, but is expressed at low levels in most other cell types and thus few clues to function could be derived from expression patterns. Similarly, subcellular Bves expression is both cytoplasmic and plasma membrane localized, with intensity in either domain dependent upon cell morphology and/or adhesive properties (from a sheet to a single mobile unit). Many signal cascades and protein players localize in these domains and are associated with such large-scale cellular alterations, and hence these data failed to provide a definitive protein function for Bves.

Studies on Bves regulation of epithelial sheet maintenance began to define a function for this protein. Osler et al. (2006) demonstrated that Bves is required for localization of junction proteins to the cell surface, which confers sheet integrity. Additionally, Bves C-terminus was sufficient to pulldown complexes that include ZO-1 protein. These data were corroborated by recent studies demonstrating that aberrant expression of Bves C-terminus interferes with pulldowns of ZO-1 complexes, and also interferes with activity of tight junction-dependent RhoA signaling through mislocalization of GEF-H1 (Russ et al, 2010; Russ et al, 2011). Importantly, cells expressing Bves mutated at the KK residues essential for dimerization failed to localize junction molecules to the cell surface. Collectively, these data suggest that Bves supports epithelial integrity

and intercellular adhesion by shuttling proteins to intercellular junctions, yet the molecular pathway through which Bves moves these proteins was entirely unknown. To elucidate Bves function at higher resolution required two-hybrid screening to identify direct binding partners.

Initial screens identified interaction between Bves and GEFT, an activator of the RhoGTPases Rac1 and Cdc42 (Guo et al, 2003; Smith and Bader 2006). RhoGEF and RhoGTPase molecules control myriad behaviors, are well-described local regulators of lamellipodial extension as well as intercellular adhesion, and thus participate in many subcellular pathways regulating diverse cellular behaviors (Nobes and Hall 1995; Kuroda et al, 1999). Smith *et al.* (2008) demonstrated that overexpression of Bves-C terminus inhibited Rac1 and Cdc42 activity as well as lamellipodial extension and migration, and that Bves interaction within the Dbl Homology domain of GEFT, [the segment that binds to the target RhoGTPase nucleotide binding pocket to stimulate GDP release (Rossman et al, 2002)]. These data suggest that Bves could physically inhibit GEFT binding and thus regulate activation of downstream RhoGTPase targets. Additionally, Rac1 and Cdc42 activities are regulated based on GEF localization at plasma membrane active sites, the site of Bves and GEFT colocalization, suggesting that Bves regulates GEFT via localization (Etienne-Manneville and Hall 2002; Smith et al, 2008). Finally, as RhoGTPase signaling and GEFT activity regulate many behaviors from neurite extension to myogenesis, Bves-GEFT interaction provides the first data to suggest that Bves could operate through a single mechanism to regulate disparate cellular functions. However, further identification of other direct

binding partners is required to illuminate the global pathway through which Bves operates.

Using split-ubiquitin two-hybrid screening we demonstrated that Bves directly binds to VAMP3 (Chapter III), an endosomal v-SNARE that regulates recycling of multiple subcellular factors including transferrin and notably, β1-integrin. We demonstrated that Bves influences recycling of two VAMP3 cargos and that Bves simultaneously colocalizes with internalized β1-integrin and VAMP3 (Chapter III). We further demonstrated that VAMP3-dependent cell spreading and lamellipodial formation are impaired *in vitro* and in *Xenopus laevis* head mesoderm cells, which may explain the drastic morphological defects exhibited with Bves disruption in previous studies (Wada et al, 2001; Osler et al, 2005). These data indicate that β1 integrin turnover requires Bves and are the first to demonstrate a subcellular pathway through which Bves influences cell-surface adhesion. Additionally, a Bves/VAMP3 interaction could explain how Bves loss-of-function affects diverse cellular behaviors. It has been demonstrated that VAMP3 facilitates a range of subcellular trafficking events, from delivering endomembranes to protruding pseudopods (Bajno et al, 2000), to secretion of matrix metalloproteases in fibrosarcoma cells (Kean et al, 2009), to transport of myelin in oligodendrocytes (Feldmann et al, 2011). As Bves regulates recycling of multiple VAMP3-dependent cargoes, the data suggest that Bves is a general mediator of cell surface trafficking and in this capacity regulates a variety of cellular behaviors.

VAMP3 shuttles vesicles to and from the cell surface where it binds with t-SNARE molecules on the receiving membrane to form trans-SNARE complexes and draw the membranes into proximity for fusion (Hu et al, 2007). To execute these binding events SNARE proteins have highly specialized structures containing transmembrane residues and a long α-helical domain that binds with compatible SNARE molecules to form end-to-end oriented helical bundles (see Figure 1.13). This orientation draws the transmembrane domains close together, allowing for membrane fusion and delivery of cargos such as transferrin receptors and β1-integrin (Leabu 2006). As SNARE molecules are highly specialized, they may rely upon other molecules for targeting to sites of activity (Leabu 2006). Bves colocalizes with both VAMP3 and its cargo β1-integrin on vesicles and also on the cell surface, making it a candidate regulator of VAMP3 localization. Bves could bind VAMP3 on the vesicular membrane and then dimerize with existing Bves on the plasma membrane to pull VAMP3 into proximity with t-SNARE molecules. Additionally, Bves already localized on the plasma membrane could directly bind to VAMP3. Using multiple cooperative binding events could tether VAMP3 at the targeted docking site while leaving it free to interact with t-SNARE molecules. The role of VAMP3-Bves interaction in the general Bves mechanism will be discussed in detail below.

Data presented in this dissertation additionally elucidate an interaction between Bves and NDRG4 (Chapter IV). Bves and NDRG4 interact in the C-terminus of Bves at residues 207-216 that are part of a novel domain outside of the conserved Popeye sequence (see Figure 1.7). The Bves/NDRG4 interaction

was the most frequent hit in the split-ubiquitin screen of the heart library from which it was identified, suggesting the importance of this interaction in heart tissue. Additionally, manipulation of Bves or NDRG4 expression exhibited similar cellular phenotypes, alluding to a common function for these proteins (Hager and Bader 2009; Melotte et al, 2010). As NDRG4 has not been linked to a subcellular pathway, the interaction with Bves provides the first molecular underpinnings for the influence of NDRG4 on cellular behaviors. Also, being involved with recycling endosome trafficking could explain how NDRG4 regulates diverse behaviors cell-specifically (Melotte et al, 2010); cells use many of the same subcellular trafficking components to context-dependently interact with the environment (Ulrich and Heisenberg 2009; Scita and Di Fiore 2010). Thus, the interaction with Bves illuminates the subcellular function of NDRG4.

Some clues to NDRG4 function in the Bves mechanism can be gleaned from studies performed on other NDRG family proteins. The NDRG family are highly conserved cytoplasmic proteins that contain an α/β hydrolase domain, but are missing the expected catalytic motifs to function in this capacity [see Figure 1.16; (Shaw et al, 2002; Bhaduri et al, 2003)]. Despite this, the NDRG proteins regulate many overlapping behaviors, supporting the important and redundant subcellular function of these proteins. For example, all NDRG proteins are critical for tumor suppression in normal epithelia, and gain- or loss-of-function of any NDRG4 protein affects a variety of cellular behaviors from proliferation, to migration, to maintenance of differentiation (Melotte et al, 2010). Interestingly, a pattern has recently emerged that could unify NDRG protein function. NDRG1

regulates trafficking of myelin and apolipoproteins I/II to the cell surface in Schwann cells (Berger et al, 2004; Hunter et al, 2005; King et al, 2011). These data together explain how NDRG1 mutation causes the demyelinating neuropathy, hereditary motor and sensory neuropathy-Lom (HMSNL). Similarly, NDRG2 regulates secretion of IL-10 from differentiated dendrite cell models (Choi et al, 2010). Importantly, like Bves, NDRG1 also regulates recycling of E-Cadherin to and from intercellular junctions (Kachhap et al, 2007). This study also elucidates how NDRG proteins functionally participate in subcellular trafficking. In addition to defining NDRG1 regulation of E-Cadherin, Kachhap *et al* (2008) illustrated that NDRG1 is a peripheral membrane protein bound to phosphotidylinositol 4-phosphate that additionally associates with membrane bound Rab4a-GTPase. NDRG1 fails to bind Rab4a-GDP and, like Bves, it influences recycling kinetics of the canonical recycling endosome cargo, transferrin (Kachhap et al, 2007). These data reveal that NDRG1 proteins are RabGTPase effectors that facilitate recycling endosome transport. As all NDRG proteins similarly influence subcellular behaviors and exhibit redundancy, we speculate that NDRG4 is also a Rho or RabGTPase effector. In this way, through interaction with Bves, NDRG4 also influences subcellular trafficking and migration.

Bves may Orient Effector Proteins to Facilitate Subcellular Cargo Delivery of Adhesion Components

When considering the collective data on interacting partners and pathways associated with Bves, a working model of Bves function begins to resolve. In our recent studies we have defined interactions between Bves and GEFT, VAMP3, NDRG4 and Bves itself, and found that these interactions regulate similar cellular behaviors in multiple experimental models. This suggests that the proteins are players functioning together in a joint mechanism to facilitate common cellular effects. Indeed, Bves regulation of both β1-integrin and fibronectin, presented here, is supported by recent studies in which co-internalization of β1-integrin and fibronectin is essential for regulated cellular movement (Lobert et al, 2010; Dozynkiewicz et al, 2011). Bves colocalizes with vesicles labeled with both β1-integrin and VAMP3, and thus β1-integrin and fibronectin could be trafficked together in VAMP3 labeled vesicles (Chapter III). As discussed above, VAMP3 may use binding partners to facilitate targeting (Leabu 2006), and Bves may be the targeting molecule available to bind to VAMP3 both on the vesicles and from the plasma membrane, as well as perform Bves homodimerization between vesicular and plasma membrane Bves. The sum of these binding events could tether vesicles at docking sites and pull them toward targets, while leaving VAMP3 available for its specialized function (Figure 5.3). Additionally and importantly, our description of NDRG4 and Bves regulation of fibronectin deposition (Chapter IV) mirrors a recent study in which internalized fibronectin is resecreted from late endosome/lysosomal compartments to facilitate migration in

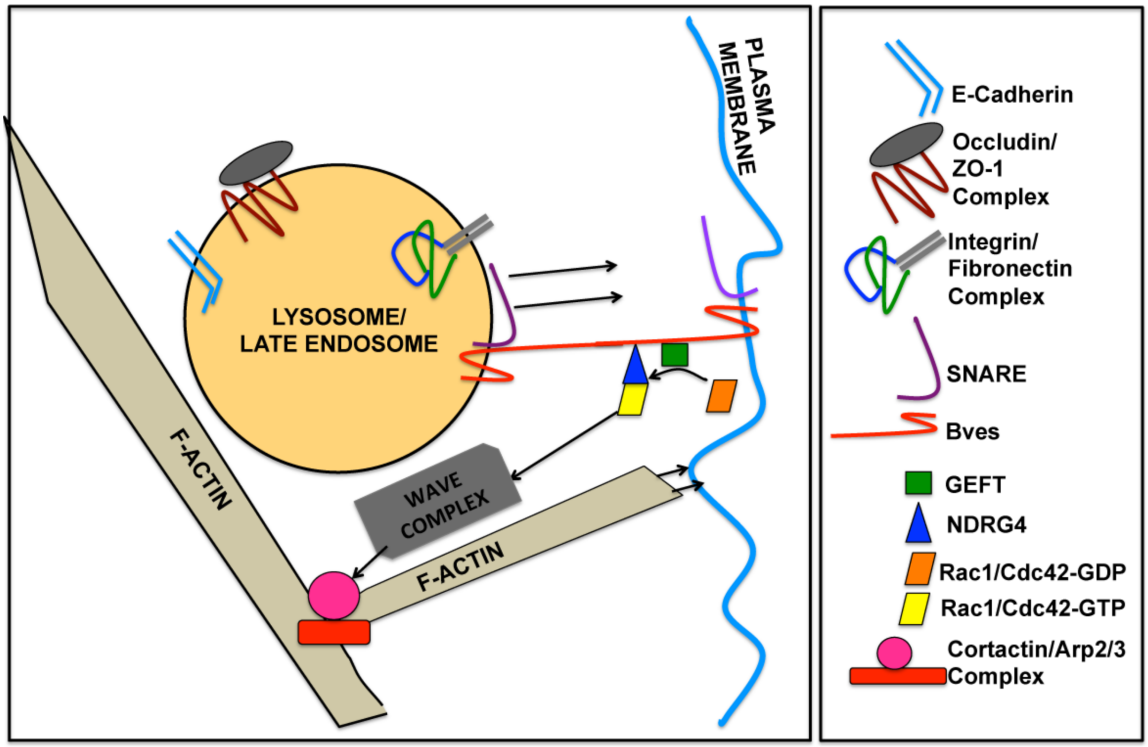

Figure 5.3 Working Model: Bves orients binding partners to facilitate endosome fusion. Endosomes utilize F-actin polymerization for movement to the plasma membrane (Ridley 2006). Branched actin polymerization requires cortactin binding to F-actin and the Arp2/3 complex (Sung 2011). First, Bves positions GEFT at the plasma membrane where it activates Rac1/Cdc42-GDP to Rac2/Cdc42-GTP (Smith 2008). Bves may also position NDRG4 for binding to activated Rac1/Cdc42-GTP. Rac1/Cdc42 would activate the WAVE complex to mediate Arp2/3-cortactin nucleation of branched actin polymerization. These events would move endosomes toward the plasma membrane. Next, at the plasma membrane, Bves bound to v-SNARE proteins VAMP2/3 could bind to Bves and SNARE proteins on the plasma membrane. These interactions would bring SNARE complexes in close apposition while leaving the SNARE residues available for membrane fusion. Fusion of these vesicles could deliver cell-cell or cell-substrate adhesion molecules to the plasma membrane for cell migration or intercellular adhesion. Bves functions as a scaffold to localize these players.

cancer cells (Sung et al, 2011). These authors demonstrated that cortactin, a regulator of the actin-nucleating factor, Arp2/3, is essential for autocrine ECM deposition. Overexpression of the Arp2/3-interacting and actin-binding domains of cortactin exclusively rescued motility defects caused by cortactin depletion,

suggesting that actin polymerization is essential for fibronectin deposition (Sung et al, 2011). It is well understood that movement of vesicles to the membrane requires RhoGTPase-stimulated actin polymerization (Ridley 2001), and Sung et al. (2011) suggest that cortactin facilitates this process. As a transmembrane protein, Bves is trafficked to the plasma membrane along with its binding partner GEFT. GEFT could be positioned by Bves to stimulate RhoGTPase activity for cortactin-mediated branched actin polymerization through WAVE activation of Arp2/3 nucleating factors (Figure 5.3). This could facilitate movement of vesicles to the plasma membrane. Finally, as discussed above, NDRG4 may be a Rho- or RabGTPase binding effector that stimulates actin polymerization (Kachhap et al, 2007). NDRG4 colocalizes with Bves on vesicles but also in the cell cortex at points of protrusion. NDRG4 binding to Bves is within the residues of Bves that could extend the furthest into the cell cytoplasm, and Bves may present NDRG4 as a substrate for RabGTPase or RhoGTPase, (activated by GEFT bound to Bves closer to the membrane) to actin polymerization (Figure 5.3). Additionally, NDRG1 regulation of both E-Cadherin and transferrin, two other Bves-recycled cargoes suggests that this mechanism could universally apply to all Bves cargoes and NDRG proteins (Figure 5.3). Thus, we propose that Bves is a plasma membrane scaffolding molecule that moves players to docking sites at the cell surface. Bves positions these players to participate in a complex that facilitates vesicle fusion and cargo delivery (Figure 5.3). In this way Bves is a pivotal regulator of cell cortex, plasma membrane and secretory trafficking to promote cell-cell and/or cell-surface adhesion.

Future Directions

Bves and NDRG4 Global Function in the Mouse

NDRG4 and Bves Regulate Murine Gut Development

The studies outlined in Chapter III elucidate Bves and NDRG4 function in adult epicardial cell lines. To solidify the relevance of these findings these studies must be extended to animal models systems. In murine development this has been hindered by the occurrence of compensation from other protein family members. For example, *Bves* knockout mice develop normally, but exhibit impaired skeletal muscle regrowth after injury (Andrée et al, 2000). In these studies, experimental intervention provoked defects, suggesting that deficiencies are present in Bves depleted animals but low level Bves expression or compensation may be sufficient to assuage developmental phenotypes. Likewise, NDRG4 phenotypes may be tempered by compensation-based phenotype rescue, as murine models with complete NDRG1 deficiency have intensified phenotypes compared to NDRG1 hypomorphic mutant mice (Okuda et al, 2004; King et al, 2011). Similarly, NDRG4$^{-/-}$ murine models exhibit delayed development but overall appear structurally normal (Figure 5.4B). Thus, we attempted to exacerbate NDRG4 and Bves developmental phenotypes by breeding an NDRG4$^{-/-}$; Bves$^{-/-}$ mouse.

The double knockout mice exhibit a striking phenotype in which mice are smaller and most die around 24 days old (Figure 5.4D). Interestingly, the cause of death appears to be a necrotic gut, which does not occur in the

single knockout littermates (Figure 5.4C). This phenotype is of particular interest as both NDRG4 and Bves are colorectal cancer tumor suppressor proteins (Melotte et al, 2009; Williams et al, 2011). Thus, future studies in this model system are warranted to describe the defects and determine the cause of death.

First, the adult and embryonic gut must be analyzed by H&E staining for gross morphological defects. With this technique, the structures of the villi will be examined to determine whether the subcellular junctions between the villi remain intact. These studies will be coupled with antibody labeling of frozen sections with tight and adherens junction markers, as well as markers of gut cell types (e.g. PAS staining for goblet cells). Additionally, fibronectin is abundantly expressed in the basement membrane of intestinal epithelia and $\alpha 5\beta 1$ integrin protects intestinal epithelial cells from apoptosis (Quaroni et al, 1978; Lee and Juliano 2000). Thus, impaired fibronectin and $\beta 1$-integrin distribution and aberrant apoptosis could explain the disintegration of NDRG4$^{-/-}$; Bves$^{-/-}$ murine intestines and will be compared to single knockout and heterozygote littermates using antibody labeling techniques and TUNEL stains. Finally, NDRG4-depleted mice exhibit neural phenotypes including impaired spatial learning defects (Yamamoto et al, 2011), thus it is important to inspect the development of Auerbach's plexus using a neural stain such as Holmes silver nitrate. Data gathered from these studies will suggest followup functional studies to be performed in intestinal epithelial cell lines (e.g. Caco2 cells) or isolated primary cells, which could include the fibronectin and integrin trafficking/deposition and adhesion assays performed in this dissertation. Together these studies solidify

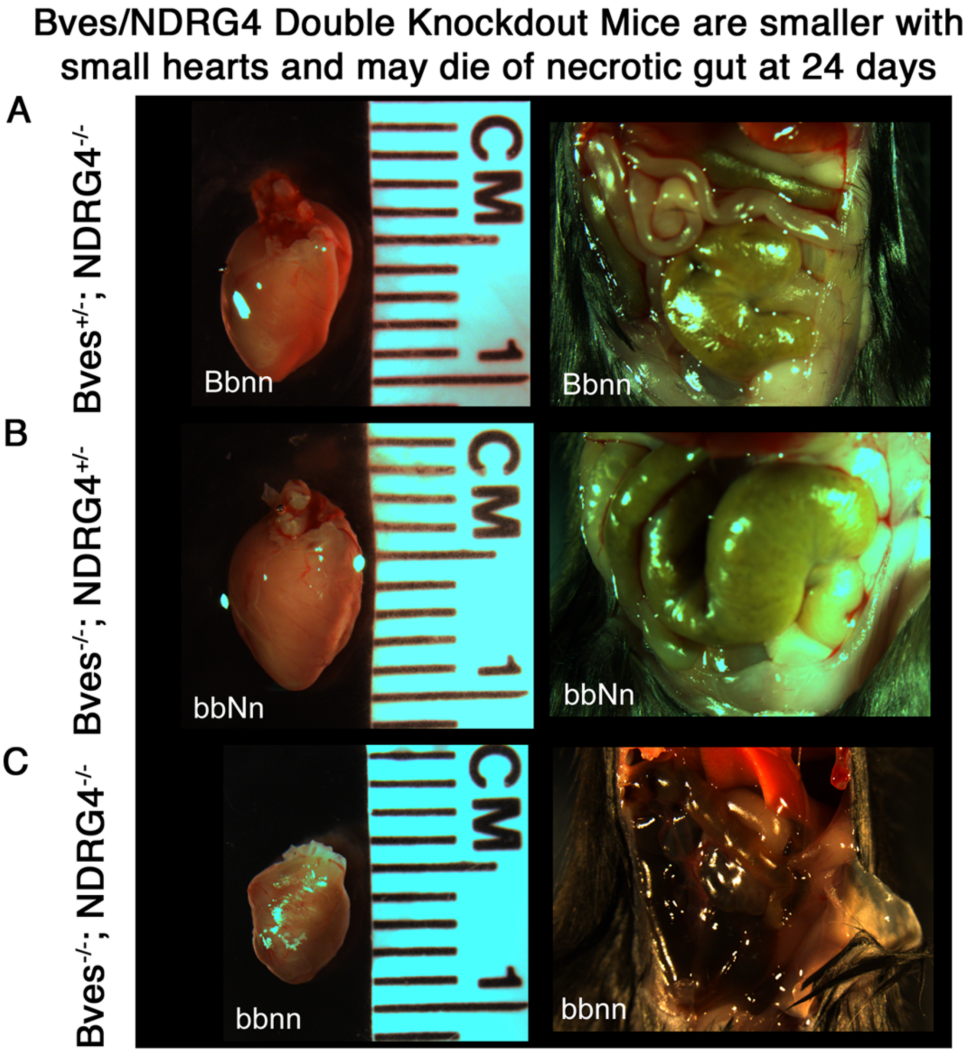

49 pups	B-N-	bbN-	B-nn	bbnn
Number	24	14	4	7
Average Weight (24 days)	11.71	8.83	9.52	6.62
Died	0	0	0	4

Figure 5.4 NDRG4$^{-/-}$; Bves$^{-/-}$ murine models have developmental defects. (A) Bves or (B) NDRG4 single knockdown murine heart and gut development occurs without obvious defects. (C) NDRG4$^{-/-}$; Bves$^{-/-}$ murine models exhibit smaller hearts and necrotic guts at 24 days of age. (D) NDRG4$^{-/-}$; Bves$^{-/-}$ mice are smaller overall and many die around 24 days of age.

the relevance of Bves and NDRG4 during embryonic development, and additionally elucidate the specific mechanism through which Bves and NDRG4 could influence both organism development and colorectal cancer.

NDRG4 and Bves in Murine Heart Development and Epicardial Migration

As illustrated in Figure 5.4, NDRG4$^{-/-}$; Bves$^{-/-}$ murine models also exhibit smaller hearts. This phenotype could be due to the overall smaller size of the mice from nutritional defects caused by a necrotic gut. However, the data presented in this dissertation demonstrate that Bves and NDRG4 coregulate epicardial cell migration and could influence myriad heart developmental processes from PE protrusion to epicardial sheet adhesion to coronary vessel formation. Indeed, a preliminary study suggests that NDRG4$^{-/-}$ isolated epicardial cells migrate further and faster with impaired directional persistence than NDRG4$^{+/-}$ littermates (Figure 5.5). While these data require substantiation, they suggest that impaired epicardial movement could contribute to the small heart phenotype observed in NDRG4$^{-/-}$; Bves$^{-/-}$ adult mice. Defects in heart function could also contribute to mortality around 24 days of age.

Thus, NDRG4$^{-/-}$; Bves$^{-/-}$ knockout hearts will be compared to single knockout and heterozygous littermates with H&E staining to determine gross morphological differences during development and as an adult, such as cardiomyocyte thickness and number/size of coronary vessels. The PE and epicardium will be visually compared with immunostaining or *in situ* hybridization for markers such as WT1 or Tbx18. Also, fibronectin deposition, which fluctuates

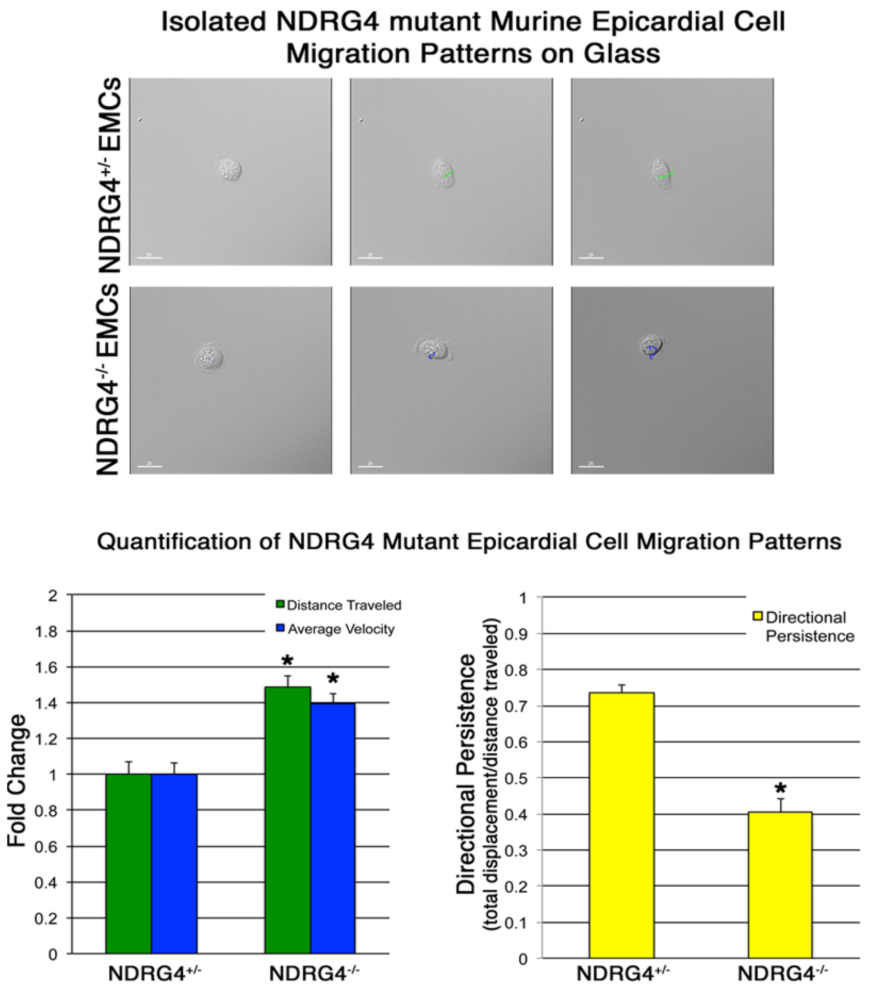

Figure 5.5 NDRG$^{-/-}$ epicardial cells migrate faster with poor directional persistence compared to NDRG4$^{+/-}$ littermates. NDRG4$^{-/-}$ and NDRG4$^{+/-}$ murine epicardial cell migration was monitored for one hour. NDRG4$^{-/-}$ migration was faster with poor directionality compared to NDRG4$^{+/-}$ littermates. These data reflect studies performed in cell lines in Chapter IV.

during development but is highly enriched in the subepicardial space (Tidball 1992), will be compared with antibody labeling of cryosections. Similarly, localization and expression of β1-integrin will be compared. Developmental timepoints will be collected to evaluate progression of PE cells to and over the heart. Additionally, as demonstrated in the preliminary study, isolated embryonic NDRG4$^{-/-}$; Bves$^{-/-}$ epicardial single cellular migration will be examined as well as

β1 integrin recycling and fibronectin deposition. *Ex vivo* epicardial sheet expansion and fibronectin deposition could also be compared, as performed in Chapters II and IV. Preliminary studies and previous work predict that NDRG4$^{-/-}$; Bves$^{-/-}$-depleted murine epicardia would exhibit impaired fibronectin deposition, de-regulated integrin localization and overall disorganized movement. As a consequence of migration defects it would be expected that murine models present with impaired coronary vessel formation and possibly thin cardiomyocyte wall thickness, as previously demonstrated in integrin and VCAM-1 depletion models (Kwee et al, 1995; Yang et al, 1995; Sengbusch et al, 2002). Additionally, these models could be used to test function of Bves/NDRG4 in the epicardial response to induced Myocardial Infarction. It would be anticipated that NDRG4$^{-/-}$; Bves$^{-/-}$ murine models exhibit impaired healing and fibrotic scar formation, as EPDC fibroblasts contribute to the healing process, as discussed in Chapter I (Zhou et al, 2011). Taken together, these studies would elucidate the role of Bves and NDRG4 during *in vivo* epicardial development and would solidify the relevance of our findings in Chapter IV.

The murine models may fail to exhibit heart phenotypes due to redundancy. In this case, alternative experiments would be performed to assess Bves and NDRG4 influence on *Xenopus laevis (X. laevis)* heart development. *X. laevis* is a common model for studies on heart development (Warkman and Krieg 2007), and many gene depletion and reconstitution techniques are optimized in this system. While redundancy could still be an issue, as all NDRG family genes are expressed in this organism (NCBI), lack of Bves redundancy may provide a

more accurate phenotype and present novel findings regarding Bves and NDRG4 effect on heart development. Also, *X. laevis* is very useful for mosaic analysis of gene function to avoid embryonic lethality, and would provide a valuable *in vivo* model system to microinjection of Bves/NDRG4 minimal binding domain plasmids (Chapter IV) and test the relevance of Bves/NDRG4 interaction during overall embryonic development. For example, overexpression of the Bves/NDRG4 dominant negative in A1 blastomeres and subsequent LacZ tracing would determine whether this interaction contributes to organized cellular movement and overall morphologic development previously attributed to Bves alone (Ripley et al, 2006). The successful completion of these studies would highlight the relevance of the Bves/NDRG4 interaction during heart and overall embryonic development.

Bves and NDRG4 Globally Regulate Trafficking

The data presented here demonstrate that Bves and NDRG4 traffic fibronectin for epicardial cell substrate deposition. However, studies on both Bves and NDRG family proteins suggest that these molecules are global regulators of cell surface trafficking and, as such, will participate in trafficking of many subcellular components in a variety of tissues. Figure 5.5 presents preliminary data suggesting that Bves and NDRG4 participate in autocrine ECM deposition *in vivo*. NDRG4 is expressed in the heart, but is also expressed in embryos missing cardiac tissue (Figure 5.6A; H-heart; E-whole embryo), suggesting that NDRG4, possibly through interaction with Bves, could perform a global function. In cross

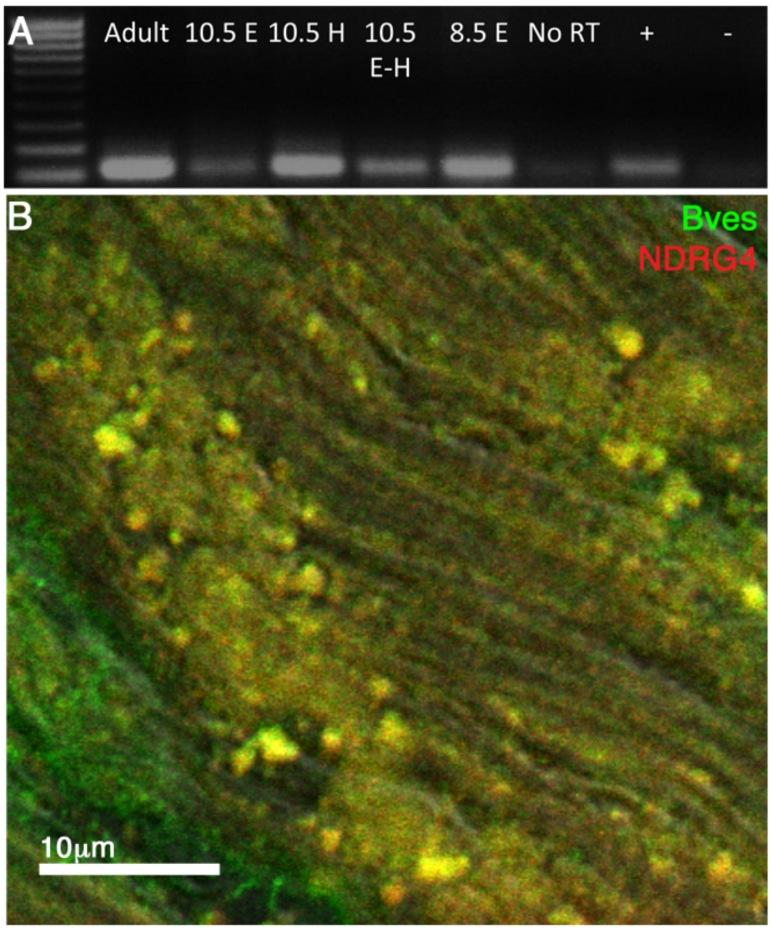

Figure 5.6 NDRG4 is highly enriched in heart tissue and colocalizes with Bves in puncta in cardiomyocyte tissue. (A) NDRG4 mRNA is expressed in murine heart tissue and other parts of the embryo; E-embryo, H-Heart , E-H embryo without heart. (B) In wildtype E14.5 murine ventricular cardiomyocytes, Bves and NDRG4 colocalize in vesicular structures.

section of E14.5 murine ventricular tissue, Bves and NDRG4 are highly expressed and, similar to epicardial tissue, colocalized at subcellular puncta (Figure 5.6B). Previous work indicates that Bves localization in cardiomyocytes shifts from the cytoplasm to the plasma membrane junctions (intercalated discs), suggesting a trafficking function in these cells (Smith and Bader 2006). Our preliminary data visually support this hypothesis and suggest that the Bves/NDRG4-regulated trafficking mechanism is additionally functioning in

cardiomyocytes. Based on these previous studies and our preliminary data, it would be of interest to determine whether intercalated disc formation is affected by Bves and NDRG4 depletion. Initial studies would label transverse sections through murine ventricular tissue of adult NDRG4$^{-/-}$; Bves$^{-/-}$ hearts with intercalated disc markers such as N-Cadherin and Connexin 43 (Zuppinger et al, 2000). It would be expected that Bves/NDRG4 disruption would impair cardiomyocyte adhesion and intercalated disc formation. Echocardiograms will be performed to compare ventricular dimension, cardiac output, and to test for abnormal beat synchrony in Bves/NDRG4 depleted hearts. Additionally, cardiomyocytes will be isolated and tested with patch-clamp analysis to compare conduction efficiencies. If gap junction formation is deregulated in NDRG4$^{-/-}$; Bves$^{-/-}$ hearts then it would be expected that cardiomyocyte conduction and beating would be impaired.

Additional preliminary data presented in Figure 5.7 demonstrate that Bves and NDRG4 colocalize in puncta in sections through adult murine brain tissue. These puncta are reminiscent of vesicular structures observed in epicardial cells and ventricular cardiomyocytes, and suggest that Bves and NDRG4 universally participate in cellular trafficking events. Our initial studies would determine the type of cells in which Bves and NDRG4 colocalize. NDRG4 has previously been detected in many types of brain cells such as the neurons of the cerebrum and the Purkinje cells of the cerebellum (Okuda et al, 2008). Additionally, NDRG4 is expressed in rat PC12 neurons where it is essential for neurite extension (Ohki et al, 2002), a process requiring integrin adhesion to ECM components

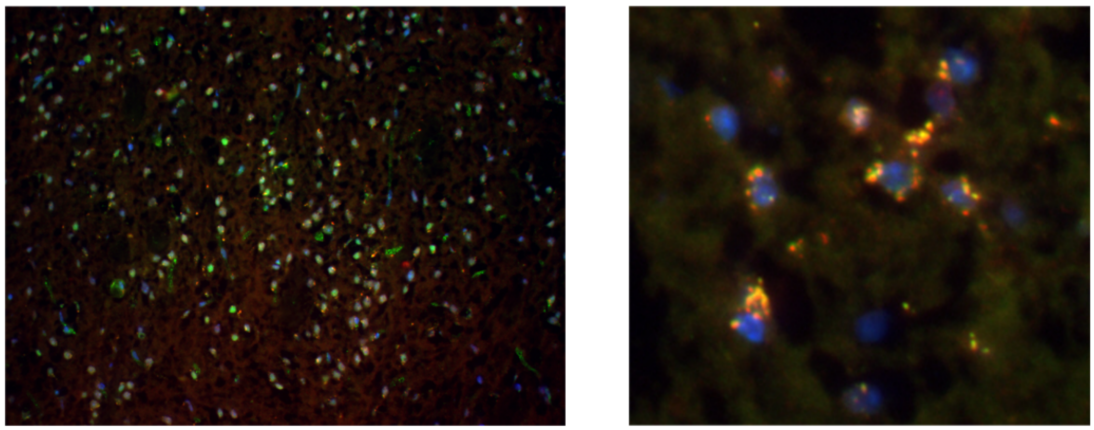

Figure 5.7. Bves and NDRG4 colocalize in murine brain tissue. Bves (green) and NDRG4 (red) are both expressed in puncta around the nuclei and cell body of brain cells, presumably neurons, in E14.5 murine developing brain tissue.

(Buck and Horwitz 1987; Powell et al, 1997). ECM is critical in the brain for cell signaling and general adhesion; some neurodegeneration disorders result from ECM deficiencies (Bonneh-Barkay and Wiley 2009). NDRG4 is downregulated in the neurodegenerative disorder, Alzheimers Disease (Zhou et al, 2001). Thus, neurite extension would be quantified and ECM deposition/cellular adhesion tested in Bves/NDRG4 siRNA-depleted, or dominant negative-disrupted PC12 neurons, using assays outlined in Chapters III and IV. Additionally, *in vivo* studies on brain structure and development would be pursued on NDRG4$^{-/-}$; Bves$^{-/-}$ versus single knockout or heterozygote littermate brain structure with H&E staining, Golgi Stain and NeuN antibody labeling (to mark neurons). NeuroSilver Staining Kits will be used to identify amyloid plaques and degenerating neurons in NDRG4$^{-/-}$; Bves$^{-/-}$ knockout murine models. The motor phenotype, previous studies, and current data predict that NDRG4$^{-/-}$; Bves$^{-/-}$ mice will exhibit changes in brain morphology accompanied with elevated plaque formation and PC12

neurons will fail to extend processes and deposit ECM components after Bves/NDRG4 interference.

Successful completion of these future studies would further enhance current work by demonstrating that Bves and NDRG4 regulate subcellular trafficking *in vivo*. These data would solidify the observations presented here in culture. Collectively, these studies would broaden the global relevance of Bves/NDRG4 regulated trafficking by demonstrating its effect on multiple tissue types and the imperative nature of the interaction to protect from subcellular trafficking-related diseases.

Elucidating Bves and NDRG4 Protein Activities

Classical scaffold molecules bind to several signaling components simultaneously, do not contain enzymatic activity, and are highly diverse, as they have evolved to facilitate a variety of signaling processes and events including Rho GTPase signaling and exocytosis (Zeke et al, 2009; Good et al, 2011). From the data presented in this dissertation I developed a working model of Bves function in which it is a scaffold that localizes effector molecules of vesicle membrane fusion to deliver cargoes for cell-cell and cell-substrate adhesion. Testing Bves role as a scaffold that mediates vesicle fusion requires in depth understanding of the coordinated relationships between Bves and its binding partners, the exact function of each of binding protein, and the ability cells to perform fusion in the absence of Bves.

Developing a Map of Bves Binding Relationships

Previous data have demonstrated that Bves (358 residues) interacts in the C-terminus with GEFT, NDRG4, VAMP3 and Bves molecules. It is known that Bves binds to NDRG4 between residues 307-316, to Bves at the KK residues (272-273), and to GEFT within the Popeye Domain [Figure 1.7 binding map; (Kawaguchi et al, 2008; Smith et al, 2008)]. To elucidate the structure of the Bves complex the minimal binding domain of all binding partners will be determined with SPOTs analysis. Additionally, competition assays for the binding proteins, western blotting and tagged/endogenous pulldowns will be utilized to determine if the molecules form a complex. Using fluorescent-labeled proteins, the spatial relationships of Bves binding partners will be visualized in real time (to follow cells undergoing process extension and adhesion). Additionally, the model postulates that Bves binds to other Bves proteins situated on an apposing membrane (Figure 5.3). To determine whether this spatial orientation occurs, separate *in vitro* transcription and translation procedures with CFP and YFP tagged Bves proteins in the presence of microsomes will be performed. The microsomes will be mixed to determine if Bves interacts with apposing Bves proteins based on FRET output. Finally, in the model fibronectin, β1-integrin, and possibly other cargoes (e.g. E-Cadherin) are co-trafficked in VAMP3 labeled endosomes. Antibody labeling and application of pre-labeled molecules would be inspected with fixed and real time imaging to confirm these trafficking relationships. Together, these data would elucidate whether Bves binding

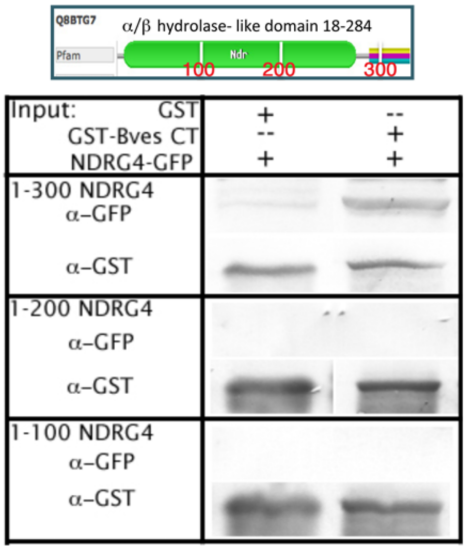

Figure 5.8 NDRG4 residues 200-300 are required for Bves binding. NDRG4 is a 352 AA cytoplasmic protein with an α/β hydrolase domain that spans the majority of the protein, but is thought to be nonfunctional. Pulldowns of Bves C-terminus and NDRG4-GFP trunctations indicate that NDRG4 residues 200-300, within the hydrolase domain, are required for Bves binding; diagram adapted from PFAM.

partners function in common or separate pathways to mediate cargo delivery.

Our previous work indicate that in addition to localizing GEFT, Bves also binds to the RhoGTPase activation domain, and thus could normally function to restrict or regulate GEFT signaling (Smith et al, 2008). To broaden the Bves scaffold map, it will be determined whether Bves influences protein activities, localization, or both characteristics of its binding partners. After identifying the minimal binding residues of the binding partners, dominant negative peptides to the binding domains will be applied and fluorescent-tagged binding partner localizations will be monitored after interfering with the Bves interaction. In the case of GEFT, to test whether Bves inhibits GEFT activation of Cdc42/Rac1 *in vitro* transcription/translation of GEFT and either Bves-full length, or Bves mutated in the GEFT binding domain will be performed. Modified PAK1 pulldown

assays would be performed to determine whether Bves binding affects Cdc42 and Rac1 activation *in vitro*. This would remove the localization constraints that occur in cell line models. If Bves only regulates GEFT protein activity, it would be predicted that mutated Bves would have a high level of GEFT activity, while full length Bves would be less active. If Bves regulates GEFT by localization alone, GEFT activation in the presence of full length Bves should remain comparable to mutated Bves. Experiments such as these could demonstrate whether Bves regulates binding partner proteins based on localization alone, or also regulates protein activities.

Determining the molecular function of NDRG4

Preliminary data indicate that Bves binds to NDRG4 within residues 200-300, which is a sequence within the NDRG4 α/β hydrolase domain (Figure 5.8). This suggests that any putative molecular activity for NDRG4 could require or be restricted by Bves binding. NDRG4 could function, like NDRG1, as a RhoGTPase or RabGTPase effector protein when, for example, Cdc42, is bound to GTP (Kachhap et al, 2007). Our preliminary data indicate that NDRG4 colocalizes with actin (polymerized by RhoGTPases) at possible sites of vesicular export (Figure 5.9A). Thus, it is of interest to determine whether NDRG4 is a RhoGTPase or RabGTPase binding effector that facilitates actin polymerization. This will be tested using overexpression Co-IP studies of NDRG4 and constitutively active Rho and RabGTPases such as Cdc42, Rac1, RhoA, and Rab4a. We would also test constitutively inactivated RhoGDPases. It would be

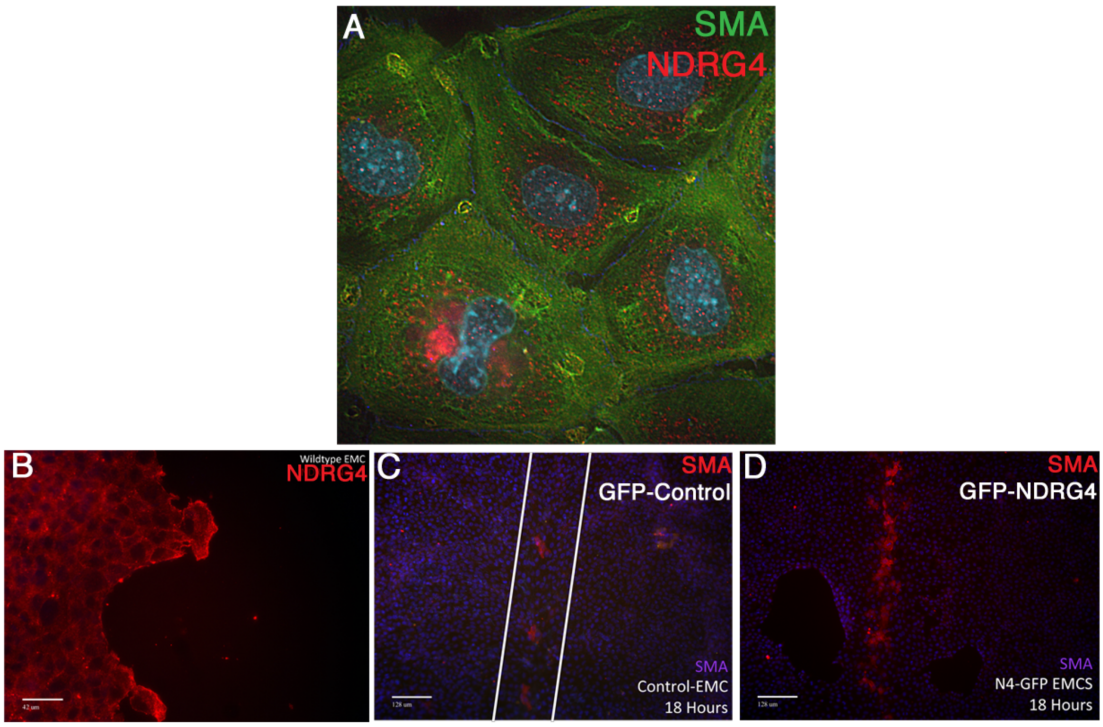

Figure 5.9 NDRG4 colocalizes with actin and may stimulate actin accumulation in injured epicardial cell sheets (A) Epicardial cells express NDRG4 (red) which colocalizes with a-Smooth Muscle Actin (green) at possible plasma membrane localized sites of secretion. (B) Scratch wounded epicardial cells become enriched in NDRG4 containing puncta at the cell surface. (C) Scratch wounded epicardial cell sheets enrich for αSMA at the site of the wound. (D) This phenomenon is exacerbated by overexpression of GFP-NDRG4.

predicted that NDRG4 is an effector for RhoGTPase molecules responsible for actin-based vesicle fusion such as Cdc42, or RhoA and that, like NDRG1, NDRG4 will specifically bind to RhoGTPase proteins in their active conformation. α-SMA stress fiber formation occurs at sites of epithelial wounding (Darby et al, 1990), and NDRG4 overexpression may upregulate this process (Figure 5.9B). Thus, it would be additionally interesting to test whether NDRG4 disruption affects actin polymerization and vesicle trafficking dynamics. Finally, as Bves may regulate activity of NDRG4 as well as localization, we will perform *in vitro*

RhoGTPase activity assays (as described above for GEFT) in the presence of full length Bves, or Bves mutated in the NDRG4 binding residues. Successful completion of these experiments will provide a map of Bves binding interactions, elucidate protein-binding dynamics and determine whether Bves directly modulates binding partner activities.

Identifying a Role for Bves and NDRG4 in Vesicle Fusion

The data illustrated in the working model suggest that Bves and NDRG4 mediate vesicle fusion for cargo delivery. It is imperative to test whether vesicle fusion relies on these proteins. This experiment can be approached using TIRF microscopy. Briefly, epicardial cells would be depleted for Bves/NDRG4, fibronectin starved, then pulsed with DyLight Fibronectin. The basolateral surface of the epicardial cells will be monitored for fibronectin binding as a readout of vesicle fusion. Other vesicle markers could also be assessed, or fluorescence vesicle tracking systems such as GFP-tagged insulin granules could be applied and followed (Ohara-Imaizumi et al, 2004). Additionally, applying a dominant negative peptide against the KK domain could test whether Bves homodimerization regulates vesicle fusion, which could be confirmed in cell lines stably expressing truncated Bves using similar methodology. Collectively, these studies will provide evidence for Bves function as a regulator of vesicle fusion and will establish a molecular framework for Bves-mediated vesicular delivery of cell-cell and cell-matrix components.

REFERENCES

Aijaz, S, F D'Atri, S Citi, MS Balda and K Matter (2005). Binding of GEF-H1 to the tight junction-associated adaptor cingulin results in inhibition of Rho signaling and G1/S phase transition. *Developmental cell* **8**(5): 777-786.

Alberts, B (2002). *Molecular biology of the cell*. New York, Garland Science.

Andrée, B, A Fleige, H-H Arnold and T Brand (2002). Mouse Pop1 is required for muscle regeneration in adult skeletal muscle. *Mol Cell Biol* **22**(5): 1504-1512.

Andrée, B, T Hillemann, G Kessler-Icekson, T Schmitt-John, H Jockusch, HH Arnold and T Brand (2000). Isolation and characterization of the novel popeye gene family expressed in skeletal muscle and heart. *Dev Biol* **223**(2): 371-382.

Ausoni, S and S Sartore (2009). From fish to amphibians to mammals: in search of novel strategies to optimize cardiac regeneration. *The Journal of Cell Biology* **184**(3): 357-364.

Austin, A, L Compton, J Love, C Brown and J Barnett (2008). Primary and immortalized mouse epicardial cells undergo differentiation in response to TGFβ. *Dev. Dyn.* **237**(2): 366-376.

Austin, A, L Compton, J Love, N Sanchez, C Brown and J Barnett (2010). Migration and differentiation of epicardial cells stimulated by TGFβ1, TGFβ2, or BMP-2 do not require the Type III Transforming Growth Factor β receptor. *FASEB J.* **24**(180.6).

Bajno, L, XR Peng, AD Schreiber, HP Moore, WS Trimble and S Grinstein (2000). Focal exocytosis of VAMP3-containing vesicles at sites of phagosome formation. *J Cell Biol* **149**(3): 697-706.

Berger, P, A Niemann and U Suter (2006). Schwann cells and the pathogenesis of inherited motor and sensory neuropathies (Charcot-Marie-Tooth disease). *Glia* **54**(4): 243-257.

Berger, P, EE Sirkowski, SS Scherer and U Suter (2004). Expression analysis of the N-Myc downstream-regulated gene 1 indicates that myelinating Schwann cells are the primary disease target in hereditary motor and sensory neuropathy-Lom. *Neurobiology of disease* **17**(2): 290-299.

Bhaduri, A, L Krishnaswamy, GR Ullal, MM Panicker and R Sowdhamini (2003). Fold prediction and comparative modeling of Bdm1: a probable alpha/beta hydrolase associated with hot water epilepsy. *J Mol Model* **9**(1): 3-8.

Bhattacharya, S, BA Stewart, BA Niemeyer, RW Burgess, BD McCabe, P Lin, G Boulianne, CJ O'Kane and TL Schwarz (2002). Members of the synaptobrevin/vesicle-associated membrane protein (VAMP) family in Drosophila

are functionally interchangeable in vivo for neurotransmitter release and cell viability. *Proceedings of the National Academy of Sciences of the United States of America* **99**(21): 13867-13872.

Bishop, AL and A Hall (2000). Rho GTPases and their effector proteins. *The Biochemical journal* **348 Pt 2**: 241-255.

Bonneh-Barkay, D and CA Wiley (2009). Brain extracellular matrix in neurodegeneration. *Brain pathology* **19**(4): 573-585.

Borisovska, M, Y Zhao, Y Tsytsyura, N Glyvuk, S Takamori, U Matti, J Rettig, T Sudhof and D Bruns (2005). v-SNAREs control exocytosis of vesicles from priming to fusion. *The EMBO journal* **24**(12): 2114-2126.

Bouchey, D, CJ Drake, AM Wunsch and CD Little (1996). Distribution of connective tissue proteins during development and neovascularization of the epicardium. *Cardiovasc Res* **31 Spec No**: E104-115.

Brand, T (2005). The Popeye domain-containing gene family. *Cell Biochem Biophys* **43**(1): 95-103.

Breton, S, NN Nsumu, T Galli, I Sabolic, PJ Smith and D Brown (2000). Tetanus toxin-mediated cleavage of cellubrevin inhibits proton secretion in the male reproductive tract. *American journal of physiology. Renal physiology* **278**(5): F717-725.

Brunger, AT (2005). Structure and function of SNARE and SNARE-interacting proteins. *Quarterly Reviews of Biophysics* **38**(1): 1-47.

Bryan, B, V Kumar, LJ Stafford, Y Cai, G Wu and M Liu (2004). GEFT, a Rho family guanine nucleotide exchange factor, regulates neurite outgrowth and dendritic spine formation. *The Journal of biological chemistry* **279**(44): 45824-45832.

Bryan, BA, Y Cai and M Liu (2006). The Rho-family guanine nucleotide exchange factor GEFT enhances retinoic acid- and cAMP-induced neurite outgrowth. *Journal of neuroscience research* **83**(7): 1151-1159.

Bryan, BA, DC Mitchell, L Zhao, W Ma, LJ Stafford, B-B Teng and M Liu (2005). Modulation of muscle regeneration, myogenesis, and adipogenesis by the Rho family guanine nucleotide exchange factor GEFT. *Mol Cell Biol* **25**(24): 11089-11101.

Bryant, DM and JL Stow (2004). The ins and outs of E-cadherin trafficking. *Trends in Cell Biology* **14**(8): 427-434.

Buck, CA and AF Horwitz (1987). Integrin, a transmembrane glycoprotein complex mediating cell-substratum adhesion. *Journal of cell science. Supplement* **8**: 231-250.

Cai, C-L, J Martin, Y Sun, L Cui, L Wang, K Ouyang, L Yang, L Bu, X Liang, X Zhang, et al. (2008). A myocardial lineage derives from Tbx18 epicardial cells. *Nature* **454**(7200): 104-108.

Cai, H, K Reinisch and S Ferro-Novick (2007). Coats, tethers, Rabs, and SNAREs work together to mediate the intracellular destination of a transport vesicle. *Dev Cell* **12**(5): 671-682.

Caswell, P and J Norman (2008). Endocytic transport of integrins during cell migration and invasion. *Trends in Cell Biology* **18**(6): 257-263.

Caswell, PT and JC Norman (2006). Integrin trafficking and the control of cell migration. *Traffic* **7**(1): 14-21.

Chen, D, M Zhao and G Mundy (2004). Bone morphogenetic proteins. *Growth Factors* **22**(4): 233-241.

Chen, JK, J Taipale, MK Cooper and PA Beachy (2002). Inhibition of Hedgehog signaling by direct binding of cyclopamine to Smoothened. *Genes & Development* **16**(21): 2743-2748.

Chen, TH, TC Chang, JO Kang, B Choudhary, T Makita, CM Tran, JB Burch, H Eid and HM Sucov (2002). Epicardial induction of fetal cardiomyocyte proliferation via a retinoic acid-inducible trophic factor. *Developmental biology* **250**(1): 198-207.

Choi, S-C, KD Kim, J-T Kim, S-S Oh, SY Yoon, EY Song, HG Lee, Y-K Choe, I Choi, J-S Lim, et al. (2010). NDRG2 is one of novel intrinsic factors for regulation of IL-10 production in human myeloid cell. *Biochem Biophys Res Commun* **396**(3): 684-690.

Compton, L, D Potash, N Mundell and J Barnett (2005). Transforming growth factor-β induces loss of epithelial character and smooth muscle cell differentiation in epicardial cells. *Dev. Dyn.* **235**(1): 82-93.

Compton, LA, DA Potash, CB Brown and JV Barnett (2007). Coronary vessel development is dependent on the type III transforming growth factor beta receptor. *Circulation research* **101**(8): 784-791.

Cross, EE, RT Thomason, M Martinez, CR Hopkins, CC Hong and DM Bader (2011). Application of small organic molecules reveals cooperative TGFbeta and BMP regulation of mesothelial cell behaviors. *ACS chemical biology* **6**(9): 952-961.

Cuny, G, P Yu, J Laha, X Xing, J-F Liu, C Lai, D Deng, C Sachidanandan, K Bloch and R Peterson (2008). Structure-activity relationship study of bone morphogenetic protein (BMP) signaling inhibitors. *Bioorg Med Chem Lett* **18**(15): 4388-4392.

Cuny, GD, PB Yu, JK Laha, X Xing, J-F Liu, CS Lai, DY Deng, C Sachidanandan, KD Bloch and RT Peterson (2008). Structure-activity relationship study of bone morphogenetic protein (BMP) signaling inhibitors. *Bioorg Med Chem Lett* **18**(15): 4388-4392.

Danen, EHJ (2002). The fibronectin-binding integrins alpha5beta1 and alphavbeta3 differentially modulate RhoA-GTP loading, organization of cell matrix adhesions, and fibronectin fibrillogenesis. *The Journal of Cell Biology* **159**(6): 1071-1086.

Darby, I, O Skalli and G Gabbiani (1990). Alpha-smooth muscle actin is transiently expressed by myofibroblasts during experimental wound healing. *Lab Invest* **63**(1): 21-29.

Daro, E, P van der Sluijs, T Galli and I Mellman (1996). Rab4 and cellubrevin define different early endosome populations on the pathway of transferrin receptor recycling. *Proceedings of the National Academy of Sciences of the United States of America* **93**(18): 9559-9564.

Davidson, LA, M Marsden, R Keller and DW Desimone (2006). Integrin alpha5beta1 and fibronectin regulate polarized cell protrusions required for Xenopus convergence and extension. *Current Biology* **16**(9): 833-844.

Deak, F, OH Shin, ET Kavalali and TC Sudhof (2006). Structural determinants of synaptobrevin 2 function in synaptic vesicle fusion. *Journal of Neuroscience* **26**(25): 6668-6676.

DeMali, KA, K Wennerberg and K Burridge (2003). Integrin signaling to the actin cytoskeleton. *Current Opinion in Cell Biology* **15**(5): 572-582.

Desclozeaux, M, J Venturato, FG Wylie, JG Kay, SR Joseph, HT Le and JL Stow (2008). Active Rab11 and functional recycling endosome are required for E-cadherin trafficking and lumen formation during epithelial morphogenesis. *Am J Physiol Cell Physiol* **295**(2): C545-556.

DeSimone, DW, L Davidson, M Marsden and D Alfandari (2005). The Xenopus embryo as a model system for studies of cell migration. *Methods in Molecular Biology* **294**: 235-245.

Dettman, RW, W Denetclaw, Jr., CP Ordahl and J Bristow (1998). Common epicardial origin of coronary vascular smooth muscle, perivascular fibroblasts, and intermyocardial fibroblasts in the avian heart. *Developmental biology* **193**(2): 169-181.

DiAngelo, JR, TK Vasavada, W Cain and MK Duncan (2001). Production of monoclonal antibodies against chicken Pop1 (BVES). *Hybrid Hybridomics* **20**(5-6): 377-381.

Dokic, D and R Dettman (2006). VCAM-1 inhibits TGFbeta stimulated epithelial-mesenchymal transformation by modulating Rho activity and stabilizing intercellular adhesion in epicardial mesothelial cells. *Developmental Biology* **299**(2): 489-504.

Dozynkiewicz, MA, NB Jamieson, I Macpherson, J Grindlay, PV van den Berghe, A von Thun, JP Morton, C Gourley, P Timpson, C Nixon, et al. (2011). Rab25 and CLIC3 Collaborate to Promote Integrin Recycling from Late Endosomes/Lysosomes and Drive Cancer Progression. *Developmental cell*.

Duan, J, C Gherghe, D Liu, E Hamlett, L Srikantha, L Rodgers, JN Regan, M Rojas, M Willis, A Leask, et al. (2011). Wnt1/βcatenin injury response activates the epicardium and cardiac fibroblasts to promote cardiac repair. *EMBO J*.

Dünnwald, M, A Varshavsky and N Johnsson (1999). Detection of transient in vivo interactions between substrate and transporter during protein translocation into the endoplasmic reticulum. *Mol Biol Cell* **10**(2): 329-344.

Etienne-Manneville, S and A Hall (2002). Rho GTPases in cell biology. *Nature* **420**(6916): 629-635.

Fackler, OT and R Grosse (2008). Cell motility through plasma membrane blebbing. *Journal of Cell Biology* **181**(6): 879-884.

Feldmann, A, J Amphornrat, M Schonherr, C Winterstein, W Mobius, T Ruhwedel, L Danglot, KA Nave, T Galli, D Bruns, et al. (2011). Transport of the major myelin proteolipid protein is directed by VAMP3 and VAMP7. *The Journal of neuroscience : the official journal of the Society for Neuroscience* **31**(15): 5659-5672.

Feng, Q, SE Hawes, JE Stern, L Wiens, H Lu, ZM Dong, CD Jordan, NB Kiviat and H Vesselle (2008). DNA methylation in tumor and matched normal tissues from non-small cell lung cancer patients. *Cancer Epidemiol Biomarkers Prev* **17**(3): 645-654.

Fields, IC, E Shteyn, M Pypaert, V Proux-Gillardeaux, RS Kang, T Galli and H Folsch (2007). v-SNARE cellubrevin is required for basolateral sorting of AP-1B-dependent cargo in polarized epithelial cells. *Journal of Cell Biology* **177**(3): 477-488.

Galli, T, T Chilcote, O Mundigl, T Binz, H Niemann and P De Camilli (1994). Tetanus toxin-mediated cleavage of cellubrevin impairs exocytosis of transferrin receptor-containing vesicles in CHO cells. *Journal of Cell Biology* **125**(5): 1015-1024.

George, EL, EN Georges-Labouesse, RS Patel-King, H Rayburn and RO Hynes (1993). Defects in mesoderm, neural tube and vascular development in mouse embryos lacking fibronectin. *Development* **119**(4): 1079-1091.

Giehl, K and A Menke (2006). Moving on: Molecular mechanisms in TGFbeta-induced epithelial cell migration. *Signal Transduction* **6**: 355-364.

Gittenberger-de Groot, A, M Vrancken Peeters, M Mentink, R Gourdie and R Poelmann (1998). Epicardium-derived cells contribute a novel population to the myocardial wall and the atrioventricular cushions. *Circulation Research* **82**(10): 1043-1052.

Good, MC, JG Zalatan and WA Lim (2011). Scaffold proteins: hubs for controlling the flow of cellular information. *Science* **332**(6030): 680-686.

Grosshans, BL, D Ortiz and P Novick (2006). Rabs and their effectors: achieving specificity in membrane traffic. *Proceedings of the National Academy of Sciences of the United States of America* **103**(32): 11821-11827.

Guo, X, LJ Stafford, B Bryan, C Xia, W Ma, X Wu, D Liu, Z Songyang and M Liu (2003). A Rac/Cdc42-specific exchange factor, GEFT, induces cell proliferation, transformation, and migration. *The Journal of biological chemistry* **278**(15): 13207-13215.

Guo, X and X-F Wang (2009). Signaling cross-talk between TGF-beta/BMP and other pathways. *Cell Res* **19**(1): 71-88.

Hager, HA and DM Bader (2009). Bves: ten years after. *Histol Histopathol* **24**(6): 777-787.

Hager, HA, RJ Roberts, EE Cross, V Proux-Gillardeaux and DM Bader (2010). Identification of a novel Bves function: regulation of vesicular transport. *EMBO J* **29**(3): 532-545.

Hao, J, M Daleo, C Murphy, P Yu, J Ho, J Hu, R Peterson, A Hatzopoulos and C Hong (2008). Dorsomorphin, a selective small molecule inhibitor of BMP signaling, promotes cardiomyogenesis in embryonic stem cells. *PLoS ONE* **3**(8): e2904.

Hao, J, J Ho, J Lewis, K Karim, R Daniels, P Gentry, C Hopkins, C Lindsley and C Hong (2010). In vivo structure-activity relationship study of dorsomorphin analogues identifies selective VEGF and BMP inhibitors. *ACS Chem Biol* **5**(2): 245-253.

Hao, J, JN Ho, JA Lewis, KA Karim, RN Daniels, PR Gentry, CR Hopkins, CW Lindsley and CC Hong (2010). In vivo structure-activity relationship study of dorsomorphin analogues identifies selective VEGF and BMP inhibitors. *ACS Chem Biol* **5**(2): 245-253.

Harms, BD, GM Bassi, AR Horwitz and DA Lauffenburger (2005). Directional persistence of EGF-induced cell migration is associated with stabilization of lamellipodial protrusions. *Biophys J* **88**(2): 1479-1488.

Heldin, CH, K Miyazono and P ten Dijke (1997). TGF-beta signalling from cell membrane to nucleus through SMAD proteins. *Nature* **390**(6659): 465-471.

Hirohashi, S (1998). Inactivation of the E-cadherin-mediated cell adhesion system in human cancers. *American Journal of Pathology* **153**(2): 333-339.

Hitz, MP, P Pandur, T Brand and M Kühl (2002). Cardiac specific expression of Xenopus Popeye-1. *Mech Dev* **115**(1-2): 123-126.

Ho, E and Y Shimada (1978). Formation of the epicardium studied with the scanning electron microscope. *Dev Biol* **66**(2): 579-585.

Holly, SP, MK Larson and LV Parise (2000). Multiple roles of integrins in cell motility. *Experimental Cell Research* **261**(1): 69-74.

Hongo, S, T Watanabe, K Takahashi and A Miyazaki (2006). Ndrg4 enhances NGF-induced ERK activation uncoupled with Elk-1 activation. *J Cell Biochem* **98**(1): 185-193.

Hood, L, J Heath, M Phelps and B Lin (2004). Systems biology and new technologies enable predictive and preventative medicine. *Science* **306**(5696): 640-643.

Hu, C, D Hardee and F Minnear (2007). Membrane fusion by VAMP3 and plasma membrane t-SNAREs. *Experimental cell research* **313**(15): 3198-3209.

Hunter, M, D Angelicheva, I Tournev, E Ingley, DC Chan, GF Watts, I Kremensky and L Kalaydjieva (2005). NDRG1 interacts with APO A-I and A-II and is a functional candidate for the HDL-C QTL on 8q24. *Biochem Biophys Res Commun* **332**(4): 982-992.

Huotari, J and A Helenius (2011). Endosome maturation. *The EMBO journal* **30**(17): 3481-3500.

Huveneers, S, H Truong, R Fassler, A Sonnenberg and EH Danen (2008). Binding of soluble fibronectin to integrin alpha5 beta1 - link to focal adhesion redistribution and contractile shape. *Journal of cell science* **121**(Pt 15): 2452-2462.

Hynes, RO (2002). Integrins: bidirectional, allosteric signaling machines. *Cell* **110**(6): 673-687.

Imamura, T, M Takase, A Nishihara, E Oeda, J Hanai, M Kawabata and K Miyazono (1997). Smad6 inhibits signalling by the TGF-beta superfamily. *Nature* **389**(6651): 622-626.

Inman, G, F Nicolás, J Callahan, J Harling, L Gaster, A Reith, N Laping and C Hill (2002). SB-431542 is a potent and specific inhibitor of transforming growth factor-beta superfamily type I activin receptor-like kinase (ALK) receptors ALK4, ALK5, and ALK7. *Molecular Pharmacology* **62**(1): 65-74.

Inman, GJ, FJ Nicolás, JF Callahan, JD Harling, LM Gaster, AD Reith, NJ Laping and CS Hill (2002). SB-431542 is a potent and specific inhibitor of transforming growth factor-beta superfamily type I activin receptor-like kinase (ALK) receptors ALK4, ALK5, and ALK7. *Molecular Pharmacology* **62**(1): 65-74.

Ishii, Y, R Garriock, A Navetta, L Coughlin and T Mikawa (2010). BMP signals promote proepicardial protrusion necessary for recruitment of coronary vessel and epicardial progenitors to the heart. *Developmental Cell* **19**(2): 307-316.

Iyer, K, L Bürkle, D Auerbach, S Thaminy, M Dinkel, K Engels and I Stagljar (2005). Utilizing the split-ubiquitin membrane yeast two-hybrid system to identify protein-protein interactions of integral membrane proteins. *Sci STKE* **2005**(275): pl3.

Izumi, T (2007). Physiological roles of Rab27 effectors in regulated exocytosis. *Endocrine journal* **54**(5): 649-657.

Jahn, R and RH Scheller (2006). SNAREs--engines for membrane fusion. *Nat Rev Mol Cell Biol* **7**(9): 631-643.

Johnson, KE (1976). Circus movements and blebbing locomotion in dissociated embryonic cells of an amphibian, Xenopus laevis. *Journal of Cell Science* **22**(3): 575-583.

Johnson, KE, T Darribere and JC Boucaut (1993). Mesodermal cell adhesion to fibronectin-rich fibrillar extracellular matrix is required for normal Rana pipiens gastrulation. *Journal of Experimental Zoology* **265**(1): 40-53.

Kachhap, SK, D Faith, DZ Qian, S Shabbeer, NL Galloway, R Pili, SR Denmeade, AM DeMarzo and MA Carducci (2007). The N-Myc down regulated Gene1 (NDRG1) Is a Rab4a effector involved in vesicular recycling of E-cadherin. *PLoS ONE* **2**(9): e844.

Kalaydjieva, L, D Gresham, R Gooding, L Heather, F Baas, R de Jonge, K Blechschmidt, D Angelicheva, D Chandler, P Worsley, et al. (2000). N-myc downstream-regulated gene 1 is mutated in hereditary motor and sensory neuropathy-Lom. *Am J Hum Genet* **67**(1): 47-58.

Kalman, F, S Viragh and L Modis (1995). Cell surface glycoconjugates and the extracellular matrix of the developing mouse embryo epicardium. *Anatomy and embryology* **191**(5): 451-464.

Kawaguchi, M, HA Hager, A Wada, T Koyama, MS Chang and DM Bader (2008). Identification of a Novel Intracellular Interaction Domain Essential for Bves Function. *PLoS ONE* **3**(5): e2261.

Kean, MJ, KC Williams, M Skalski, D Myers, A Burtnik, D Foster and MG Coppolino (2009). VAMP3, syntaxin-13 and SNAP23 are involved in secretion of matrix metalloproteinases, degradation of the extracellular matrix and cell invasion. *Journal of Cell Science* **122**(22): 4089-4098.

Keller, RE (1980). The cellular basis of epiboly: an SEM study of deep-cell rearrangement during gastrulation in Xenopus laevis. *Journal of Embryology and Experimental Morphology* **60**: 201-234.

Kim, M, H-R Jang, K Haam, T-W Kang, J-H Kim, S-Y Kim, S-M Noh, K-S Song, J-S Cho, H-Y Jeong, et al. (2010). Frequent silencing of popeye domain-containing genes, BVES and POPDC3, is associated with promoter hypermethylation in gastric cancer. *Carcinogenesis* **31**(9): 1685-1693.

King, RHM, D Chandler, S Lopaticki, D Huang, J Blake, JR Muddle, T Kilpatrick, M Nourallah, T Miyata, T Okuda, et al. (2011). Ndrg1 in development and maintenance of the myelin sheath. *Neurobiol Dis* **42**(3): 368-380.

Kirschner, KM, N Wagner, KD Wagner, S Wellmann and H Scholz (2006). The Wilms tumor suppressor Wt1 promotes cell adhesion through transcriptional activation of the alpha4integrin gene. *The Journal of biological chemistry* **281**(42): 31930-31939.

Knight, RF, DM Bader and JR Backstrom (2003). Membrane topology of Bves/Pop1A, a cell adhesion molecule that displays dynamic changes in cellular distribution during development. *The Journal of biological chemistry* **278**(35): 32872-32879.

Komiyama, M, K Ito and Y Shimada (1987). Origin and development of the epicardium in the mouse embryo. *Anat Embryol* **176**(2): 183-189.

Koss, L and M Melamed (2006). Koss' diagnostic cytology and its histopathologic bases. *books.google.com* **1**.

Kramer, A, U Reineke, L Dong, B Hoffmann, U Hoffmüller, D Winkler, R Volkmer-Engert and J Schneider-Mergener (1999). Spot synthesis: observations and optimizations. *J Pept Res* **54**(4): 319-327.

Kramer, A and J Schneider-Mergener (1998). Synthesis and screening of peptide libraries on continuous cellulose membrane supports. *Methods Mol Biol* **87**: 25-39.

Kruithof, B, B van Wijk, S Somi, M Kruithof-de Julio, J Pérez Pomares, F Weesie, A Wessels, A Moorman and M van den Hoff (2006). BMP and FGF regulate the differentiation of multipotential pericardial mesoderm into the myocardial or epicardial lineage. *Developmental Biology* **295**(2): 507-522.

Kumano, G and WC Smith (2002). Revisions to the Xenopus gastrula fate map: implications for mesoderm induction and patterning. *Developmental Dynamics* **225**(4): 409-421.

Kuroda, S, M Fukata, M Nakagawa and K Kaibuchi (1999). Cdc42, Rac1, and their effector IQGAP1 as molecular switches for cadherin-mediated cell-cell adhesion. *Biochemical and biophysical research communications* **262**(1): 1-6.

Kwee, L, HS Baldwin, HM Shen, CL Stewart, C Buck, CA Buck and MA Labow (1995). Defective development of the embryonic and extraembryonic circulatory systems in vascular cell adhesion molecule (VCAM-1) deficient mice. *Development* **121**(2): 489-503.

Lanzetti, L (2007). Actin in membrane trafficking. *Current Opinion in Cell Biology* **19**(4): 453-458.

Lavine, KJ, AC White, C Park, CS Smith, K Choi, F Long, CC Hui and DM Ornitz (2006). Fibroblast growth factor signals regulate a wave of Hedgehog activation that is essential for coronary vascular development. *Genes & development* **20**(12): 1651-1666.

Leabu, M (2006). Membrane fusion in cells: molecular machinery and mechanisms. *J Cell Mol Med* **10**(2): 423-427.

Lee, JW and RL Juliano (2000). alpha5beta1 integrin protects intestinal epithelial cells from apoptosis through a phosphatidylinositol 3-kinase and protein kinase B-dependent pathway. *Molecular biology of the cell* **11**(6): 1973-1987.

Lepilina, A, A Coon, K Kikuchi, J Holdway, R Roberts, C Burns and K Poss (2006). A dynamic epicardial injury response supports progenitor cell activity during zebrafish heart regeneration. *Cell* **127**(3): 607-619.

Lie-Venema, H, I Eralp, S Maas, AC Gittenberger-De Groot, RE Poelmann and MC DeRuiter (2005). Myocardial heterogeneity in permissiveness for epicardium-derived cells and endothelial precursor cells along the developing heart tube at the onset of coronary vascularization. *Anat Rec A Discov Mol Cell Evol Biol* **282**(2): 120-129.

Lin, S, D Zhao and M Bownes (2007). Blood vessel/epicardial substance (bves) expression, essential for embryonic development, is down regulated by Grk/EFGR signalling. *Int J Dev Biol* **51**(1): 37-44.

Liu, J and D Stainier (2010). Tbx5 and Bmp signaling are essential for proepicardium specification in zebrafish. *Circulation Research* **106**(12): 1818-1828.

Lobert, VH, A Brech, NM Pedersen, J Wesche, A Oppelt, L Malerød and H Stenmark (2010). Ubiquitination of alpha 5 beta 1 integrin controls fibroblast migration through lysosomal degradation of fibronectin-integrin complexes. *Dev Cell* **19**(1): 148-159.

Luftman, K, N Hasan, P Day, D Hardee and C Hu (2009). Silencing of VAMP3 inhibits cell migration and integrin-mediated adhesion. *Biochem Biophys Res Commun* **380**(1): 65-70.

Manasek, F (1976). Macromolecules of the extracellular compartment of embryonic and mature hearts. *Circulation Research* **38**(5): 331-337.

Manasek, FJ (1969). Embryonic development of the heart. II. Formation of the epicardium. *J Embryol Exp Morphol* **22**(3): 333-348.

Männer, J (1992). The development of pericardial villi in the chick embryo. *Anat Embryol* **186**(4): 379-385.

Männer, J (1993). Experimental study on the formation of the epicardium in chick embryos. *Anat Embryol* **187**(3): 281-289.

Männer, J (1999). Does the subepicardial mesenchyme contribute myocardioblasts to the myocardium of the chick embryo heart? A quail-chick chimera study tracing the fate of the epicardial primordium. *Anat Rec* **255**(2): 212-226.

Männer, J, J Pérez-Pomares, D Macías and R Muñoz-Chápuli (2001). The origin, formation and developmental significance of the epicardium: a review. *Cells Tissues Organs* **169**(2): 89-103.

Mao, Y and JE Schwarzbauer (2005). Fibronectin fibrillogenesis, a cell-mediated matrix assembly process. *Matrix biology : journal of the International Society for Matrix Biology* **24**(6): 389-399.

Marsden, M and DW DeSimone (2001). Regulation of cell polarity, radial intercalation and epiboly in Xenopus: novel roles for integrin and fibronectin. *Development* **128**(18): 3635-3647.

Marsden, M and DW DeSimone (2003). Integrin-ECM interactions regulate cadherin-dependent cell adhesion and are required for convergent extension in Xenopus. *Current Biology* **13**(14): 1182-1191.

Maxfield, FR and TE McGraw (2004). Endocytic recycling. *Nat Rev Mol Cell Biol* **5**(2): 121-132.

McCarthy, M (2006). Allen Brain Atlas maps 21,000 genes of the mouse brain. *Lancet neurology* **5**(11): 907-908.

McDonald, JA (1988). Extracellular matrix assembly. *Annual review of cell biology* **4**: 183-207.

McMahon, HT, YA Ushkaryov, L Edelmann, E Link, T Binz, H Niemann, R Jahn and TC Sudhof (1993). Cellubrevin is a ubiquitous tetanus-toxin substrate homologous to a putative synaptic vesicle fusion protein. *Nature* **364**(6435): 346-349.

Mellgren, A, C Smith, G Olsen, B Eskiocak, B Zhou, M Kazi, F Ruiz, W Pu and M Tallquist (2008). Platelet-derived growth factor receptor beta signaling is required for efficient epicardial cell migration and development of two distinct coronary vascular smooth muscle cell populations. *Circulation Research* **103**(12): 1393-1401.

Mellman, I and WJ Nelson (2008). Coordinated protein sorting, targeting and distribution in polarized cells. *Nat Rev Mol Cell Biol* **9**(11): 833-845.

Melotte, V, MHFM Lentjes, SM van den Bosch, DMEI Hellebrekers, JPJ de Hoon, KAD Wouters, KLJ Daenen, IEJM Partouns-Hendriks, F Stessels, J Louwagie, et al. (2009). N-Myc downstream-regulated gene 4 (NDRG4): a candidate tumor suppressor gene and potential biomarker for colorectal cancer. *J Natl Cancer Inst* **101**(13): 916-927.

Melotte, V, X Qu, M Ongenaert, W van Criekinge, AP de Bruïne, HS Baldwin and M van Engeland (2010). The N-myc downstream regulated gene (NDRG) family: diverse functions, multiple applications. *FASEB J* **24**(11): 4153-4166.

Merki, E, M Zamora, A Raya, Y Kawakami, J Wang, X Zhang, J Burch, SW Kubalak, P Kaliman, JCI Belmonte, et al. (2005). Epicardial retinoid X receptor alpha is required for myocardial growth and coronary artery formation. *Proc Natl Acad Sci USA* **102**(51): 18455-18460.

Mikawa, T, A Borisov, A Brown and D Fischman (1992). Clonal analysis of cardiac morphogenesis in the chicken embryo using a replication-defective retrovirus: I. Formation of the ventricular myocardium. *Dev Dyn* **193**(1): 11-23.

Mikawa, T and D Fischman (1992). Retroviral analysis of cardiac morphogenesis: discontinuous formation of coronary vessels. *Proc Natl Acad Sci USA* **89**(20): 9504-9508.

Mikawa, T and R Gourdie (1996). Pericardial mesoderm generates a population of coronary smooth muscle cells migrating into the heart along with ingrowth of the epicardial organ. *Developmental Biology* **174**(2): 221-232.

Mitchell, D, EG Pobre, AW Mulivor, AV Grinberg, R Castonguay, TE Monnell, N Solban, JA Ucran, RS Pearsall, KW Underwood, et al. (2010). ALK1-Fc inhibits multiple mediators of angiogenesis and suppresses tumor growth. *Molecular cancer therapeutics* **9**(2): 379-388.

Mitchell, DC, BA Bryan, L Liu, XH Hu, XQ Huang, WK Ji, PC Chen, WF Hu, JP Liu, J Zhang, et al. (2011). GEFT, A Rho family guanine nucleotide exchange factor, regulates lens differentiation through a Rac1-mediated mechanism. *Current molecular medicine* **11**(6): 465-480.

Mitchelmore, C, S Büchmann-Møller, L Rask, MJ West, JC Troncoso and NA Jensen (2004). NDRG2: a novel Alzheimer's disease associated protein. *Neurobiol Dis* **16**(1): 48-58.

Molin, DG, U Bartram, K Van der Heiden, L Van Iperen, CP Speer, BP Hierck, RE Poelmann and AC Gittenberger-de-Groot (2003). Expression patterns of Tgfbeta1-3 associate with myocardialisation of the outflow tract and the development of the epicardium and the fibrous heart skeleton. *Developmental dynamics : an official publication of the American Association of Anatomists* **227**(3): 431-444.

Moon, RT, AD Kohn, GV De Ferrari and A Kaykas (2004). WNT and beta-catenin signalling: diseases and therapies. *Nat Rev Genet* **5**(9): 691-701.

Morabito, CJ, RW Dettman, J Kattan, JM Collier and J BRISTOW (2001). Positive and negative regulation of epicardial–mesenchymal transformation during avian heart development. *Developmental Biology* **234**(1): 204-215.

Muñoz-Chápuli, R, D Macías, C Ramos, V de Andrés, A Gallego and P Navarro (1994). Cardiac development in the dogfish (Scyliorhinus canicula): a model for the study of vertebrate cardiogenesis. *Cardioscience* **5**(4): 245-253.

Mutsaers, SE and S Wilkosz (2007). Structure and function of mesothelial cells. *Cancer treatment and research* **134**: 1-19.

Na, J, M Marsden and DW DeSimone (2003). Differential regulation of cell adhesive functions by integrin alpha subunit cytoplasmic tails in vivo. *Journal of Cell Science* **116**(Pt 11): 2333-2343.

Nahirney, P, T Mikawa and D Fischman (2003). Evidence for an extracellular matrix bridge guiding proepicardial cell migration to the myocardium of chick embryos. *Dev Dyn* **227**(4): 511-523.

Nakada, N, S Hongo, T Ohki, A Maeda and M Takeda (2002). Molecular characterization of NDRG4/Bdm1 protein isoforms that are differentially regulated during rat brain development. *Brain Res Dev Brain Res* **135**(1-2): 45-53.

Ng, T, D Shima, A Squire, PI Bastiaens, S Gschmeissner, MJ Humphries and PJ Parker (1999). PKCalpha regulates beta1 integrin-dependent cell motility through association and control of integrin traffic. *The EMBO journal* **18**(14): 3909-3923.

Nieuwkoop, PD and J Faber (1994). *Normal table of Xenopus laevis (Daudin) : a systematical and chronological survey of the development from the fertilized egg till the end of metamorphosis*. New York, Garland Pub.

Nishimoto, S, J Tawara, H Toyoda, K Kitamura and T Komurasaki (2003). A novel homocysteine-responsive gene, smap8, modulates mitogenesis in rat vascular smooth muscle cells. *Eur J Biochem* **270**(11): 2521-2531.

Nobes, CD and A Hall (1995). Rho, rac, and cdc42 GTPases regulate the assembly of multimolecular focal complexes associated with actin stress fibers, lamellipodia, and filopodia. *Cell* **81**(1): 53-62.

Ohara-Imaizumi, M, C Nishiwaki, T Kikuta, S Nagai, Y Nakamichi and S Nagamatsu (2004). TIRF imaging of docking and fusion of single insulin granule motion in primary rat pancreatic beta-cells: different behaviour of granule motion between normal and Goto-Kakizaki diabetic rat beta-cells. *The Biochemical journal* **381**(Pt 1): 13-18.

Ohki, T, S Hongo, N Nakada, A Maeda and M Takeda (2002). Inhibition of neurite outgrowth by reduced level of NDRG4 protein in antisense transfected PC12 cells. *Brain Res Dev Brain Res* **135**(1-2): 55-63.

Okuda, T, Y Higashi, K Kokame, C Tanaka, H Kondoh and T Miyata (2004). Ndrg1-deficient mice exhibit a progressive demyelinating disorder of peripheral nerves. *Mol Cell Biol* **24**(9): 3949-3956.

Okuda, T, K Kokame and T Miyata (2008). Differential expression patterns of NDRG family proteins in the central nervous system. *J Histochem Cytochem* **56**(2): 175-182.

Olivey, H, N Mundell, A Austin and J Barnett (2005). Transforming growth factor-β stimulates epithelial–mesenchymal transformation in the proepicardium. *Dev. Dyn.* **235**(1): 50-59.

Olivey, H and E Svensson (2010). Epicardial-myocardial signaling directing coronary vasculogenesis. *Circulation Research* **106**(5): 818-832.

Osler, ME and DM Bader (2004). Bves expression during avian embryogenesis. *Dev Dyn* **229**(3): 658-667.

Osler, ME, MS Chang and DM Bader (2005). Bves modulates epithelial integrity through an interaction at the tight junction. *J Cell Sci* **118**(Pt 20): 4667-4678.

Osler, ME, TK Smith and DM Bader (2006). Bves, a member of the Popeye domain-containing gene family. *Dev Dyn* **235**(3): 586-593.

Pae, SH, D Dokic and RW Dettman (2008). Communication between integrin receptors facilitates epicardial cell adhesion and matrix organization. *Dev Dyn* **237**(4): 962-978.

Pardali, E, MJ Goumans and P ten Dijke (2010). Signaling by members of the TGF-beta family in vascular morphogenesis and disease. *Trends in cell biology* **20**(9): 556-567.

Parnes, D, V Jacoby, A Sharabi, H Schlesinger, T Brand and G Kessler-Icekson (2007). The Popdc gene family in the rat: molecular cloning, characterization and expression analysis in the heart and cultured cardiomyocytes. *Biochim Biophys Acta* **1769**(9-10): 586-592.

Pennisi, D and T Mikawa (2009). FGFR-1 is required by epicardium-derived cells for myocardial invasion and correct coronary vascular …. *Developmental Biology*.

Pérez-Pomares, J, D Macías, L García-Garrido and R Muñoz-Chápuli (1998). The origin of the subepicardial mesenchyme in the avian embryo: an immunohistochemical and quail-chick chimera study. *Developmental Biology* **200**(1): 57-68.

Peterson, RT (2009). Drug discovery: Propping up a destructive regime. *Nature* **461**(7264): 599-600.

Pfeffer, SR (2007). Unsolved mysteries in membrane traffic. *Annual Review of Biochemistry* **76**: 629-645.

Platta, HW and H Stenmark (2011). Endocytosis and signaling. *Current opinion in cell biology* **23**(4): 393-403.

Polgar, J, SH Chung and GL Reed (2002). Vesicle-associated membrane protein 3 (VAMP-3) and VAMP-8 are present in human platelets and are required for granule secretion. *Blood* **100**(3): 1081-1083.

Poliseno, L, L Salmena, J Zhang, B Carver, W Haveman and P Pandolfi (2010). A coding-independent function of gene and pseudogene mRNAs regulates tumour biology. *Nature* **465**(7301): 1033-1038.

Poss, KD, LG Wilson and MT Keating (2002). Heart regeneration in zebrafish. *Science* **298**(5601): 2188-2190.

Powelka, AM, J Sun, J Li, M Gao, LM Shaw, A Sonnenberg and VW Hsu (2004). Stimulation-dependent recycling of integrin beta1 regulated by ARF6 and Rab11. *Traffic* **5**(1): 20-36.

Powell, EM, S Meiners, NA DiProspero and HM Geller (1997). Mechanisms of astrocyte-directed neurite guidance. *Cell and Tissue Research* **290**(2): 385-393.

Proux-Gillardeaux, V, J Gavard, T Irinopoulou, RM Mege and T Galli (2005). Tetanus neurotoxin-mediated cleavage of cellubrevin impairs epithelial cell migration and integrin-dependent cell adhesion. *Proceedings of the National Academy of Sciences of the United States of America* **102**(18): 6362-6367.

Proux-Gillardeaux, V, R Rudge and T Galli (2005). The tetanus neurotoxin-sensitive and insensitive routes to and from the plasma membrane: fast and slow pathways? *Traffic* **6**(5): 366-373.

Qu, X, H Jia, DM Garrity, K Tompkins, L Batts, B Appel, TP Zhong and HS Baldwin (2008). Ndrg4 is required for normal myocyte proliferation during early cardiac development in zebrafish. *Developmental biology* **317**(2): 486-496.

Qu, X, Y Zhai, H Wei, C Zhang, G Xing, Y Yu and F He (2002). Characterization and expression of three novel differentiation-related genes belong to the human NDRG gene family. *Mol Cell Biochem* **229**(1-2): 35-44.

Quaroni, A, KJ Isselbacher and E Ruoslahti (1978). Fibronectin synthesis by epithelial crypt cells of rat small intestine. *Proceedings of the National Academy of Sciences of the United States of America* **75**(11): 5548-5552.

Ramos, JW and DW DeSimone (1996). Xenopus embryonic cell adhesion to fibronectin: position-specific activation of RGD/synergy site-dependent migratory behavior at gastrulation. *Journal of Cell Biology* **134**(1): 227-240.

Ramos, JW, CA Whittaker and DW DeSimone (1996). Integrin-dependent adhesive activity is spatially controlled by inductive signals at gastrulation. *Development* **122**(9): 2873-2883.

Reefman, E, JG Kay, SM Wood, C Offenhauser, DL Brown, S Roy, AC Stanley, PC Low, AP Manderson and JL Stow (2010). Cytokine secretion is distinct from secretion of cytotoxic granules in NK cells. *Journal of immunology* **184**(9): 4852-4862.

Reese, D, T Mikawa and D Bader (2002). Development of the coronary vessel system. *Circulation Research* **91**(9): 761-768.

Reese, DE and DM Bader (1999). Cloning and expression of hbves, a novel and highly conserved mRNA expressed in the developing and adult heart and skeletal muscle in the human. *Mamm Genome* **10**(9): 913-915.

Reese, DE, M Zavaljevski, NL Streiff and D Bader (1999). bves: A novel gene expressed during coronary blood vessel development. *Dev Biol* **209**(1): 159-171.

Ren, R, M Nagel, E Tahinci, R Winklbauer and K Symes (2006). Migrating anterior mesoderm cells and intercalating trunk mesoderm cells have distinct responses to Rho and Rac during Xenopus gastrulation. *Developmental Dynamics* **235**(4): 1090-1099.

Ridley, AJ (2001). Rho proteins: linking signaling with membrane trafficking. *Traffic* **2**(5): 303-310.

Riley, PR and N Smart (2011). Vascularizing the heart. *Cardiovasc Res* **91**(2): 260-268.

Ripley, AN, MS Chang and DM Bader (2004). Bves is expressed in the epithelial components of the retina, lens, and cornea. *Invest Ophthalmol Vis Sci* **45**(8): 2475-2483.

Ripley, AN, ME Osler, CVE Wright and D Bader (2006). Xbves is a regulator of epithelial movement during early Xenopus laevis development. *Proc Natl Acad Sci USA* **103**(3): 614-619.

Roberts, M, S Barry, A Woods, P van der Sluijs and J Norman (2001). PDGF-regulated rab4-dependent recycling of alphavbeta3 integrin from early endosomes is necessary for cell adhesion and spreading. *Current biology : CB* **11**(18): 1392-1402.

Roberts, MS, AJ Woods, TC Dale, P Van Der Sluijs and JC Norman (2004). Protein kinase B/Akt acts via glycogen synthase kinase 3 to regulate recycling of alpha v beta 3 and alpha 5 beta 1 integrins. *Molecular and cellular biology* **24**(4): 1505-1515.

Rossman, KL, DK Worthylake, JT Snyder, DP Siderovski, SL Campbell and J Sondek (2002). A crystallographic view of interactions between Dbs and Cdc42: PH domain-assisted guanine nucleotide exchange. *The EMBO journal* **21**(6): 1315-1326.

Roth, J (2002). Protein N-glycosylation along the secretory pathway: relationship to organelle topography and function, protein quality control, and cell interactions. *Chemical reviews* **102**(2): 285-303.

Ruoslahti, E and B Obrink (1996). Common principles in cell adhesion. *Experimental cell research* **227**(1): 1-11.

Russ, PK, AI Kupperman, S-H Presley, FR Haselton and MS Chang (2010). Inhibition of RhoA signaling with increased Bves in trabecular meshwork cells. *Invest Ophthalmol Vis Sci* **51**(1): 223-230.

Russ, PK, CJ Pino, CS Williams, DM Bader, FR Haselton and MS Chang (2011). Bves Modulates Tight Junction Associated Signaling. *PLoS ONE* **6**(1): e14563.

Russell, JL, SC Goetsch, NR Gaiano, JA Hill, EN Olson and JW Schneider (2011). A dynamic notch injury response activates epicardium and contributes to fibrosis repair. *Circulation research* **108**(1): 51-59.

Scales, SJ, JB Bock and RH Scheller (2000). The specifics of membrane fusion. *Nature* **407**(6801): 144-146.

Schilling, SH, AB Hjelmeland, DR Radiloff, IM Liu, TP Wakeman, JR Fielhauer, EH Foster, JD Lathia, JN Rich, X-F Wang, et al. (2009). NDRG4 is required for cell cycle progression and survival in glioblastoma cells. *The Journal of biological chemistry* **284**(37): 25160-25169.

Schlueter, J, J Männer and T Brand (2006). BMP is an important regulator of proepicardial identity in the chick embryo. *Developmental Biology* **295**(2): 546-558.

Schmidt, A and A Hall (2002). Guanine nucleotide exchange factors for Rho GTPases: turning on the switch. *Genes Dev* **16**(13): 1587-1609.

Schmierer, B and CS Hill (2007). TGFbeta-SMAD signal transduction: molecular specificity and functional flexibility. *Nature reviews. Molecular cell biology* **8**(12): 970-982.

Schwartz, MA and SJ Shattil (2000). Signaling networks linking integrins and rho family GTPases. *Trends in Biochemical Sciences* **25**(8): 388-391.

Scita, G and PP Di Fiore (2010). The endocytic matrix. *Nature* **463**(7280): 464-473.

Sechler, JL, Y Takada and JE Schwarzbauer (1996). Altered rate of fibronectin matrix assembly by deletion of the first type III repeats. *The Journal of cell biology* **134**(2): 573-583.

Segers, V and R Lee (2008). Stem-cell therapy for cardiac disease. *Nature* **451**(7181): 937-942.

Segev, N (2001). Ypt/rab gtpases: regulators of protein trafficking. *Sci STKE* **2001**(100): RE11.

Selchow, A and R Winklbauer (1997). Structure and cytoskeletal organization of migratory mesoderm cells from the Xenopus gastrula. *Cell Motility and the Cytoskeleton* **36**(1): 12-29.

Sengbusch, JK, W He, KA Pinco and JT Yang (2002). Dual functions of [alpha]4[beta]1 integrin in epicardial development: initial migration and long-term attachment. *The Journal of cell biology* **157**(5): 873-882.

Shaw, E, LA McCue, CE Lawrence and JS Dordick (2002). Identification of a novel class in the alpha/beta hydrolase fold superfamily: the N-myc differentiation-related proteins. *Proteins* **47**(2): 163-168.

Shelton, E and K Yutzey (2008). Twist1 function in endocardial cushion cell proliferation, migration, and differentiation during heart valve development. *Developmental Biology* **317**(1): 282-295.

Shi, F and J Sottile (2008). Caveolin-1-dependent beta1 integrin endocytosis is a critical regulator of fibronectin turnover. *Journal of cell science* **121**(Pt 14): 2360-2371.

Shook, D and R Keller (2003). Mechanisms, mechanics and function of epithelial-mesenchymal transitions in early development. *Mechanisms of Development* **120**(11): 1351-1383.

Sieber, C, J Kopf, C Hiepen and P Knaus (2009). Recent advances in BMP receptor signaling. *Cytokine Growth Factor Rev* **20**(5-6): 343-355.

Singh, P, C Carraher and JE Schwarzbauer (2010). Assembly of fibronectin extracellular matrix. *Annual review of cell and developmental biology* **26**: 397-419.

Skalski, M and MG Coppolino (2005). SNARE-mediated trafficking of alpha5beta1 integrin is required for spreading in CHO cells. *Biochemical and biophysical research communications* **335**(4): 1199-1210.

Smart, N, CA Risebro, JE Clark, E Ehler, L Miquerol, A Rossdeutsch, MS Marber and PR Riley (2010). Thymosin beta4 facilitates epicardial neovascularization of the injured adult heart. *Annals of the New York Academy of Sciences* **1194**: 97-104.

Smith, CL, ST Baek, CY Sung and MD Tallquist (2011). Epicardial-derived cell epithelial-to-mesenchymal transition and fate specification require PDGF receptor signaling. *Circulation research* **108**(12): e15-26.

Smith, JC, K Symes, RO Hynes and D DeSimone (1990). Mesoderm induction and the control of gastrulation in Xenopus laevis: the roles of fibronectin and integrins. *Development* **108**(2): 229-238.

Smith, T and D Bader (2006). Characterization of Bves expression during mouse development using newly generated immunoreagents. *Dev. Dyn.* **235**(6): 1701-1708.

Smith, TK, HA Hager, R Francis, DM Kilkenny, CW Lo and DM Bader (2008). Bves directly interacts with GEFT, and controls cell shape and movement through regulation of Rac1/Cdc42 activity. *Proc Natl Acad Sci USA* **105**(24): 8298-8303.

Somlyo, AP and AV Somlyo (2000). Signal transduction by G-proteins, rho-kinase and protein phosphatase to smooth muscle and non-muscle myosin II. *The Journal of physiology* **522 Pt 2**: 177-185.

Sridurongrit, S, J Larsson, R Schwartz, P Ruiz-Lozano and V Kaartinen (2008). Signaling via the Tgf-beta type I receptor Alk5 in heart development. *Developmental biology* **322**(1): 208-218.

Stockwell, B (2004). Exploring biology with small organic molecules. *Nature* **432**(7019): 846-854.

Sung, Bong H, X Zhu, I Kaverina and Alissa M Weaver (2011). Cortactin Controls Cell Motility and Lamellipodial Dynamics by Regulating ECM Secretion. *Current Biology* **21**(17): 1460-1469.

Svensson, E (2009). Look who's talking: FGFs and BMPs in the proepicardium. *Circulation Research* **105**(5): 406-407.

Symons, M and N Rusk (2003). Control of vesicular trafficking by Rho GTPases. *Current Biology* **13**(10): R409-418.

Tajika, Y, M Sato, T Murakami, K Takata and H Yorifuji (2007). VAMP2 is expressed in muscle satellite cells and up-regulated during muscle regeneration. *Cell and Tissue Research* **328**(3): 573-581.

Tayeb, MA, M Skalski, MC Cha, MJ Kean, M Scaife and MG Coppolino (2005). Inhibition of SNARE-mediated membrane traffic impairs cell migration. *Experimental Cell Research* **305**(1): 63-73.

Tidball, J (1992). Distribution of collagens and fibronectin in the subepicardium during avian cardiac development. *Anatomy and embryology* **185**(2): 155-162.

Tomanek, R (2005). Formation of the coronary vasculature during development. *Angiogenesis* **8**(3): 273-284.

Torlopp, A, SS Breher, J Schlüter and T Brand (2006). Comparative analysis of mRNA and protein expression of Popdc1 (Bves) during early development in the chick embryo. *Dev Dyn* **235**(3): 691-700.

Ulrich, F and C-P Heisenberg (2009). Trafficking and Cell Migration. *Traffic* **10**(7): 811-818.

van Wijk, B, G van den Berg, R Abu-Issa, P Barnett, S van der Velden, M Schmidt, J Ruijter, M Kirby, A Moorman and M van den Hoff (2009). Epicardium and myocardium separate from a common precursor pool by crosstalk between bone morphogenetic protein- and fibroblast growth factor-signaling pathways. *Circulation Research* **105**(5): 431-441.

Vasavada, TK, JR DiAngelo and MK Duncan (2004). Developmental expression of Pop1/Bves. *J Histochem Cytochem* **52**(3): 371-377.

Veale, KJ, C Offenhauser and RZ Murray (2011). The role of the recycling endosome in regulating lamellipodia formation and macrophage migration. *Communicative & integrative biology* **4**(1): 44-47.

Vieira, JM and PR Riley (2011). Epicardium-derived cells: a new source of regenerative capacity. *Heart* **97**(1): 15-19.

Virágh, S and CE Challice (1981). The origin of the epicardium and the embryonic myocardial circulation in the mouse. *Anat Rec* **201**(1): 157-168.

Vrancken Peeters, MP, MM Mentink, RE Poelmann and AC Gittenberger-de Groot (1995). Cytokeratins as a marker for epicardial formation in the quail embryo. *Anatomy and embryology* **191**(6): 503-508.

Wada, A, TK Smith, ME Osler, DE Reese and D Bader (2003). Epicardial/Mesothelial Cell Line Retains Vasculogenic Potential of Embryonic Epicardium. *Circulation Research* **92**(5): 525-531.

Wada, AM, DE Reese and DM Bader (2001). Bves: prototype of a new class of cell adhesion molecules expressed during coronary artery development. *Development* **128**(11): 2085-2093.

Wallingford, JB, BA Rowning, KM Vogeli, U Rothbacher, SE Fraser and RM Harland (2000). Dishevelled controls cell polarity during Xenopus gastrulation. *Nature* **405**(6782): 81-85.

Wang, JF and DJ Hill (2009). Identification and action of N-myc downstream regulated gene 4 A2 in rat pancreas. *J Endocrinol* **201**(1): 15-25.

Warkman, AS and PA Krieg (2007). Xenopus as a model system for vertebrate heart development. *Seminars in cell & developmental biology* **18**(1): 46-53.

Williams, CS, B Zhang, JJ Smith, A Jayagopal, CW Barrett, C Pino, P Russ, SH Presley, D Peng, DO Rosenblatt, et al. (2011). BVES regulates EMT in human corneal and colon cancer cells and is silenced via promoter methylation in human colorectal carcinoma. *J Clin Invest* **121**(10): 4056-4069.

Willis, BC and Z Borok (2007). TGF-beta-induced EMT: mechanisms and implications for fibrotic lung disease. *American journal of physiology. Lung cellular and molecular physiology* **293**(3): L525-534.

Wilm, B (2005). The serosal mesothelium is a major source of smooth muscle cells of the gut vasculature. *Development* **132**(23): 5317-5328.

Winklbauer, R and M Nagel (1991). Directional mesoderm cell migration in the Xenopus gastrula. *Developmental Biology* **148**(2): 573-589.

Winter, E and A Gittenberger-de Groot (2007). Epicardium-derived cells in cardiogenesis and cardiac regeneration. *Cell Mol Life Sci* **64**(6): 692-703.

Wu, M, C Smith, J Hall, I Lee, K Luby-Phelps and M Tallquist (2010). Epicardial spindle orientation controls cell entry into the myocardium. *Developmental Cell* **19**(1): 114-125.

Yamamoto, H, K Kokame, T Okuda, Y Nakajo, H Yanamoto and T Miyata (2011). NDRG4-deficient mice exhibit spatial learning deficits and vulnerabilities to cerebral Ischemia. *The Journal of biological chemistry*.

Yang, JT, H Rayburn and RO Hynes (1995). Cell adhesion events mediated by alpha 4 integrins are essential in placental and cardiac development. *Development* **121**(2): 549-560.

Yap, AS, MS Crampton and J Hardin (2007). Making and breaking contacts: the cellular biology of cadherin regulation. *Current Opinion in Cell Biology* **19**(5): 508-514.

Yu, PB, CC Hong, C Sachidanandan, JL Babitt, DY Deng, SA Hoyng, HY Lin, KD Bloch and RT Peterson (2008). Dorsomorphin inhibits BMP signals required for embryogenesis and iron metabolism. *Nat Chem Biol* **4**(1): 33-41.

Zamora, M, J Manner and P Ruiz-Lozano (2007). Epicardium-derived progenitor cells require beta-catenin for coronary artery formation. *Proceedings of the National Academy of Sciences of the United States of America* **104**(46): 18109-18114.

Zeke, A, M Lukacs, WA Lim and A Remenyi (2009). Scaffolds: interaction platforms for cellular signalling circuits. *Trends in cell biology* **19**(8): 364-374.

Zhou, B, LB Honor, H He, Q Ma, JH Oh, C Butterfield, RZ Lin, JM Melero-Martin, E Dolmatova, HS Duffy, et al. (2011). Adult mouse epicardium modulates myocardial injury by secreting paracrine factors. *The Journal of clinical investigation* **121**(5): 1894-1904.

Zhou, B, LB Honor, Q Ma, JH Oh, RZ Lin, JM Melero-Martin, A von Gise, P Zhou, T Hu, L He, et al. (2012). Thymosin beta 4 treatment after myocardial infarction

does not reprogram epicardial cells into cardiomyocytes. *Journal of molecular and cellular cardiology* **52**(1): 43-47.

Zhou, B, Q Ma, S Rajagopal, S Wu, I Domian, J Rivera-Feliciano, D Jiang, A von Gise, S Ikeda, K Chien, et al. (2008). Epicardial progenitors contribute to the cardiomyocyte lineage in the developing heart. *Nature* **454**(7200): 109-113.

Zhou, G, R Myers, Y Li, Y Chen, X Shen, J Fenyk-Melody, M Wu, J Ventre, T Doebber, N Fujii, et al. (2001). Role of AMP-activated protein kinase in mechanism of metformin action. *J Clin Invest* **108**(8): 1167-1174.

Zhou, RH, K Kokame, Y Tsukamoto, C Yutani, H Kato and T Miyata (2001). Characterization of the human NDRG gene family: a newly identified member, NDRG4, is specifically expressed in brain and heart. *Genomics* **73**(1): 86-97.

Zimmerman, L, J De Jesús-Escobar and R Harland (1996). The Spemann organizer signal noggin binds and inactivates bone morphogenetic protein 4. *Cell* **86**(4): 599-606.

Zuppinger, C, M Eppenberger-Eberhardt and HM Eppenberger (2000). N-Cadherin: structure, function and importance in the formation of new intercalated disc-like cell contacts in cardiomyocytes. *Heart failure reviews* **5**(3): 251-257.

Zwijsen, A, L van Grunsven, E Bosman, C Collart, L Nelles, L Umans, T Van de Putte, G Wuytens, D Huylebroeck and K Verschueren (2001). Transforming growth factor beta signalling in vitro and in vivo: activin ligand-receptor interaction, Smad5 in vasculogenesis, and repression of target genes by the deltaEF1/ZEB-related SIP1 in the vertebrate embryo. *Mol Cell Endocrinol* **180**(1-2): 13-24.